Bulletin

of

The Geological Society of America

VOLUME 66 June 1955 NUMBER 6

CONTENTS

	Pages
Low-angle overthrusting in the central Cumberland Plateau, Tennessee. By Richard G. Stearns	615–628
Pleistocene geology of the southwestern Wind River Mountains, Wyoming. By G. William Holmes and John H. Moss	629–654
Spectrographic analysis by use of mutual standard method. By W. H. Dennen and W. C. Fowler	655–662
Geomorphology of south-central Washington, illustrated by the Yakima East quadrangle. By Aaron C. Waters	663–684
Log of the Senigon well, southern Quebec. By T. H. Clark and Isles Strachan	685–698
Origin of the upland silt near Fairbanks, Alaska. By Troy L. Péwé	699–724
Disconformity between Lower and Middle Ordovician series at Douglas Lake, Tennessee. By Josiah Bridge	725–730
1950 and 1951 eruptions of Mihara Yama, O Shima Volcano, Japan. By Helen L. Foster and Arnold C. Mason	731–762
Short Notes	
Direction of current flow in some Lower Cambrian clastics in Maryland. By John C. Whitaker	763–766
Anomalous uranium-lead ages. By J. L. Kulp and W. R. Eckelmann	767–768
Additional evidence of volcanism on Mars. By Dean B. McLaughlin	769–772
Submarine topography west of Mexico and Central America. By John G. Heacock, Jr., and J. Lamar Worzel	773–776
Gravity anomalies associated with seamounts. By G. Lynn Shurbet and J. Lamar Worzel	777–782
Index to Volume 66 (January–June)	783–788

Subscription $15.00 per year.

Printing Office: Mt. Royal & Guilford Aves., Baltimore 2, Md.

Communications for publications should be addressed to The Geological Society of America, Dr. H. R. Aldrich, Secretary, 419 West 117 Street, New York, N. Y.

Please give notice of change of address 4 weeks in advance. Claims for non-receipt of the Bulletin of a given month must be sent to the Secretary of the Society before the end of the second succeeding month.

Entered as second-class matter at the Post Office at Baltimore, Md., under the Act of Congress of July 16, 1894.
Accepted for mailing at special rate of postage provided for in Section 1103 Act of October 3, 1917, authorized on July 8, 1918.

PAPERS IN PRESS FOR FORTHCOMING ISSUES

Evidence for No Cenozoic Isthmus of Tehuantepec Seaways. By J. Wyatt Durham, A. R. V. Arellano, and J. H. Peck, Jr.

Crustal Structure and Surface-wave Dispersion. Part IV: Atlantic and Pacific Ocean Basins. By Jack E. Oliver, Maurice Ewing, and Frank Press

Seismic-Refraction Profiles in the Submerged Atlantic Coastal Plain near Ambrose Lightship. By R. O. Carlson and M. V. Brown

Monoclines of the Colorado Plateau. By Vincent C. Kelley

Sub-Chattanooga Residuum in Tennessee and Kentucky. By Charles Milton, Louis C. Conant, and Vernon E. Swanson

Cambrian Contacts in Eastern Pennsylvania. By Bradford Willard

Lake Chippewa, a Low Stage of Lake Michigan Indicated by Botton Sediments. By J. L. Hough

Measurement of the Deformation of the Sierra Nevada since Middle Eocene. By F. S. Hudson

Transformation of Indices in Twin Gliding. By A. Pabst

Catoctin Formation near Luray, Virginia. By John C. Reed, Jr.

Isotopic Composition and Distribution of Lead, Uranium, and Thorium in a Precambrian Granite. By George R. Tilton, Claire Patterson, Harrison Brown, Mark Inghram, Richard Hayden, David Hess, and Esper Larsen, Jr.

BULLETIN OF THE GEOLOGICAL SOCIETY OF AMERICA
VOL. 66, PP. 615-628, 5 FIGS. JUNE 1955

LOW-ANGLE OVERTHRUSTING IN THE CENTRAL CUMBERLAND PLATEAU, TENNESSEE

BY RICHARD G. STEARNS

ABSTRACT

The Cumberland Plateau overthrust, a continuous series of thrust and cross faults, extends southwest across the Cumberland Plateau of Tennessee from its junction with the Valley and Ridge thrusts near the north end of the Sequatchie Valley anticline. The strata involved vary in competency and hence control the structural pattern.

The faults mapped bound a low-angle thrust sheet. Associated anticlines are probably due to faulting at depth, as shown by the Big Peavine Mountain anticline which results from 3 miles of thrusting. The thrust forming this anticline outcrops 5 miles to the west as the Cumberland Plateau overthrust; it extends eastward, arches over the Sequatchie Valley anticline, and has its roots in the Valley and Ridge province.

The Cumberland Plateau overthrust is mechanically and regionally similar to the Pine Mountain overthrust to the north. It extends at least 50 miles southwest of its junction with the Valley and Ridge province, and perhaps as far south as Birmingham, Alabama (200 mi.). These relationships support the controversial sole-fault hypothesis of Southern Appalachian Valley and Ridge structure.

CONTENTS

TEXT

	Page
Introduction	615
Regional setting	615
Previous investigations	617
Present investigation	617
Acknowledgments	617
Stratigraphy	618
Structure	618
Sequatchie Valley anticline	618
Belt of thrust and cross faults north and northwest of anticline	621
Thrust faults	621
Cross faults	622
Big Peavine Mountain structure	623
Interpretation	624
General	624
Attitude of fault planes	624
Movement along faults	626
Comparison with the Pine Mountain block	626
Regional significance of Cumberland Plateau overthrust	627
Conclusions	628
References cited	628

ILLUSTRATIONS

Figure	Page
1. Major structural and physiographic features of Southern Appalachian region	616
2. Generalized stratigraphic column of Crab Orchard Mountains area	618
3. Structural features associated with northern end of Sequatchie Valley anticline	619
4. Structure contour map of Crab Orchard Mountains area	620
5. Structural cross sections of Crab Orchard Mountains area	625

INTRODUCTION

Regional Setting

The Cumberland Plateau, underlain by rocks of the Pennsylvanian system, extends in a northeast-southwest direction across eastern Tennessee, from Kentucky into Alabama. Pennsylvanian and older strata dip steeply northwest along its eastern margin, but throughout most of the plateau strata dip gently southeast off the flank of the Nashville dome.

To the east of the Cumberland Plateau lies the Valley and Ridge province which is characterized by imbricate faulting and folding. Steeply dipping strata along the eastern margin of the plateau have formerly been considered the western limit of faults and folds

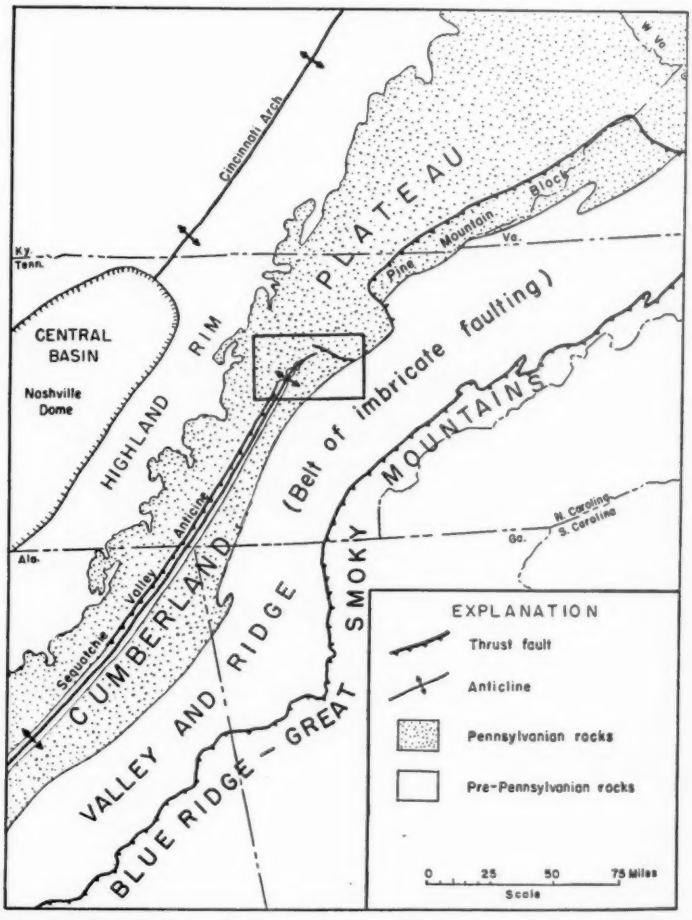

FIGURE 1.—MAJOR STRUCTURAL AND PHYSIOGRAPHIC FEATURES OF SOUTHERN APPALACHIAN REGION
Area of Figure 3 is shown as inset.

of the Valley and Ridge type. The gently dipping strata characterizing the Cumberland Plateau present such a contrast to this complex structure on the east that workers have thought of the plateau as unaffected by mountain-building processes.

Structural features observed within the plateau were considered anomalous and of only local significance. There are, however, areas of considerable structural disturbance within the Cumberland Plateau, seemingly isolated from the Valley and Ridge structures. The most prominent of these features are the Sequatchie Valley anticline and the Pine Mountain thrust block (Fig. 1).

The Sequatchie Valley anticline is an asymmetrical fold overturned to the west and broken along the west side by a thrust fault. This single anticline extends for more than 200 miles northeastward from central Alabama to Cumberland County in east-central Tennessee. Near its northeastern end it forms a line of low anticlinal mountains called the Crab Orchard Mountains (Figs. 1, 3). At the northeast end

of the Crab Orchard Mountains the anticline ends at the Emory River fault zone which strikes southeast nearly at right angles to the anticline, and merges with the Valley and Ridge province.

The Pine Mountain block is a low-angle overthrust sheet bounded on the west by the Pine Mountain thrust fault, which extends for about 120 miles from Campbell County in northeastern Tennessee northeastward across southeastern Kentucky into southwestern Virginia.'It is terminated at each end by cross faults which connect the Pine Mountain fault with the Valley and Ridge province. The Jacksboro fault of Campbell County, Tennessee, forms the southwestern boundary of the Pine Mountain block, and the Russell Fork fault of Dickenson and Buchanan counties, Virginia, forms its northeastern termination.

In the Lantana area, several miles west of the southern end of the Crab Orchard Mountains, is another disturbance which was earlier believed isolated.

Previous Investigations

The earliest reference to the structural geology of this area is by Safford (1869, p. 71), who first defined the Sequatchie Valley anticline and recognized that the Crab Orchard Mountains are its northeastern termination. He also noted the presence of the outlying Lantana disturbances west of the Crab Orchard Mountains.

The Crab Orchard Mountains and part of the Sequatchie Valley were first mapped by Hayes and Keith as parts of the Kingston (Hayes, 1894) and Wartburg (Keith, 1897) folios. They did not map either the Emory River fault or any Lantana faults west of the Sequatchie Valley anticline. Keith (1897, p. 3), mentions several of the faults which he interpreted as minor anticlines.

Jillson (1923, p. 373–378) described the Emory River fault zone. He recognized that the Sequatchie Valley anticline disappears south of the Emory River fault; he also mentioned some structures present where the Emory River fault meets Hatfield Mountain, and concluded that the Emory River fault continues on northwestward beyond this junction. Glenn (1925, p. 334–335) concurred with Jillson and added information on this fault and the Whetstone Mountain fault zone.

Butts and Nelson (1925, Pl. 1) mapped the Lantana faults of the Crossville quadrangle, but were unaware of their true significance.

Rodgers (1950, p. 672–681) also noted this pattern from the literature and from topographic patterns on recent maps. He interpreted topographic features connecting the areas of known faults as anticlines. He concluded that this pattern bounds an incipient thrust sheet similar to the Pine Mountain block whose main manifestation is the Sequatchie Valley anticline; on this basis he outlined the mechanics of its formation.

Present Investigation

This unusual structural pattern attracted the interest of geologists in Tennessee, and the writer was encouraged to begin a detailed study of this pattern. Mapping began in the spring of 1949 in the area which includes portions of the Sequatchie Valley anticline and the seemingly isolated Lantana disturbances. The part of this area mapped in detail includes the Ozone, Hebbertsburg, Dorton, and Fox Creek 7½ minute quadrangles (Fig. 3). For convenience this group of quadrangles will be referred to as the Crab Orchard Mountains area. The writer also made a reconnaissance study of the structural belt beyond the limits of detailed mapping as far as Lantana and Harriman. The detailed study of the structure is being continued by Robert Mitchum, who in the summer of 1951 mapped in detail the Lancing and part of the Camp Austin quadrangles.

Acknowledgments

The project was initiated while H. B. Burwell was State Geologist and continued under H. W. Ferguson. Special thanks are due W. D. Hardeman, present State Geologist of Tennessee, who not only actively aided in field mapping and critically read the manuscript, but aided and encouraged the writer in many ways during all phases of this investigation.

John W. Jewell and Bailey Rascoe mapped the Fox Creek and part of the Dorton quadrangles. The writer is greatly indebted for

their permission to use information derived from the mapping. In addition to this, Mr. Jewell assisted the writer when the field work was begun, and contributed considerable time on many subsequent reconnaissance trips.

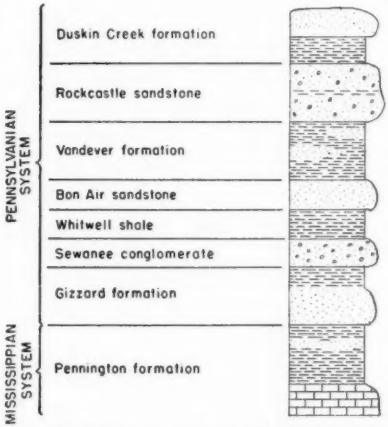

FIGURE 2.—GENERALIZED STRATIGRAPHIC COLUMN OF CRAB ORCHARD MOUNTAINS AREA

The writer is greatly indebted to E. C. Dapples who directed doctorial research at Northwestern University. C. W. Wilson, Jr. first suggested that the writer make this the basic area for a research project. He also critically read the manuscript. Mrs. Alice Clements Ewing drafted maps, sections, and figures.

STRATIGRAPHY

Overlying massive competent limestones of Meramec and early Chester age is the less competent Pennington formation (Fig. 2) which is uppermost Mississippian and is composed of red, green, and olive shales with thin limestones and sandstones.

Pennsylvanian beds overlie the Pennington in a series of competent sandstone beds alternating, in units 100 feet thick, with much less competent coal-bearing shale units. Lowest in the series are the Gizzard sandstones and shales, which are approximately 200 feet thick. The upper portion of the Gizzard is relatively incompetent, consisting of shale and coal, whereas the sandy lower part is more competent.

The massive Sewanee conglomerate, about 100 feet thick, overlies the Gizzard formation and consists of pebbly sandstone. It is overlain by the Whitwell shale, 80 feet thick, which contains a widespread coal seam. Above this weak shale is another strong sandstone, the Bon Air, also 80 feet thick. Above the Bon Air sandstone lie about 200 feet of incompetent shaly beds forming the Vandever formation, which are succeeded by the massive 180-foot-thick Rockcastle sandstone.

Overlying the Rockcastle the shale and sandstone units of the Duskin Creek formation are commonly present, but apparently exerted little influence upon the structure.

STRUCTURE

Sequatchie Valley Anticline

This anticlinal fold extends more than 200 miles from Blount County, Alabama, to Cumberland County, Tennessee, where it terminates as the Crab Orchard Mountains. Throughout its length it is breached by erosion, and in Tennessee it is named for this prominent valley. Massive Pennsylvanian sandstones form a prominent and unbreached anticlinal ridge named the Crab Orchard Mountains. The anticline is broken on its steeper northwest flank by a thrust fault which terminates near the head of the Sequatchie Valley, and does not continue into the Crab Orchard Mountains.

The anticline in the Crab Orchard Mountains area gradually diminishes northeastward (Fig. 4) until it disappears at the Emory River fault in the eastern part of the Lancing quadrangle (Fig. 3). Dips of 5°–20° prevail on the southeast flank of the anticline, but on the northwest flank dips are steep, ranging from 25° to 60°. Flattening of dip is abrupt at the outer edge of the steep northwest flank—from 60° to less than 10° in a distance of about 200 yards. On the southeast flank dip dies out gradually to the southeast.

In the east-central part of the Ozone quadrangle the anticline bifurcates (Fig. 4). The northwest fold (Chesnut Oak Ridge anticline) is relatively minor but continues to the north border of the Ozone quadrangle along the same strike as the main anticline to the southwest.

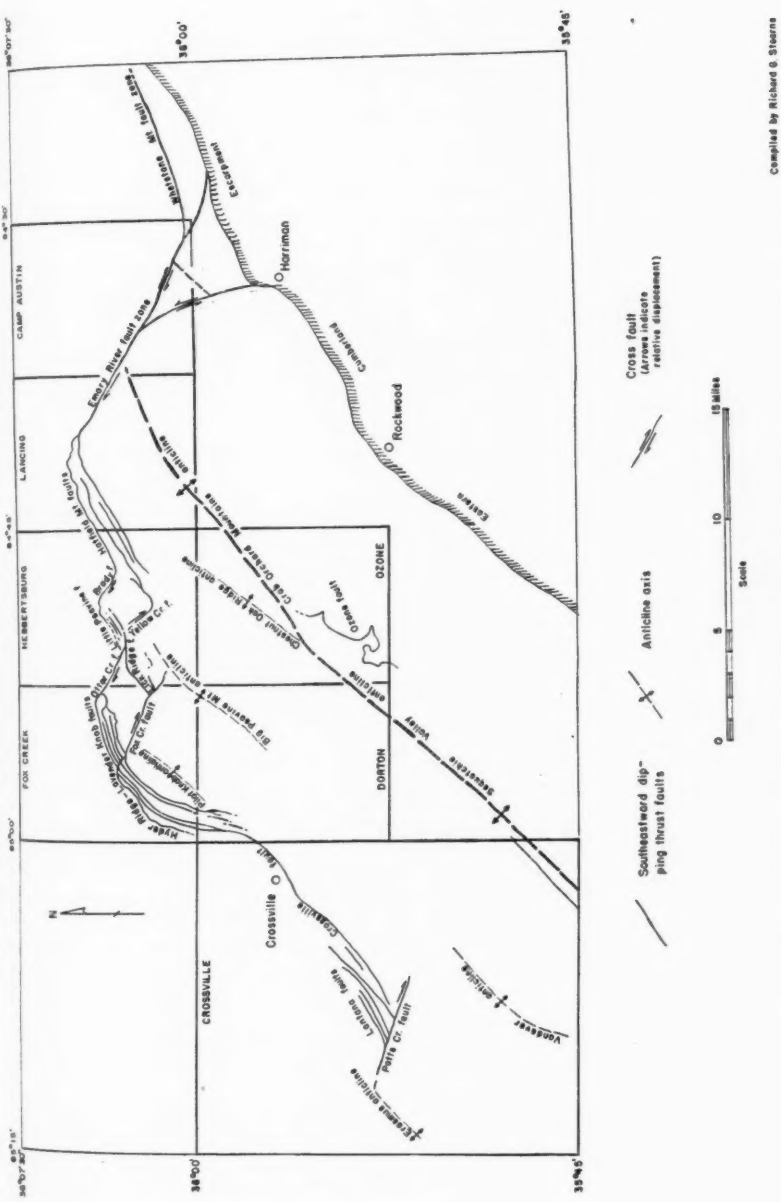

FIGURE 3.—STRUCTURAL FEATURES ASSOCIATED WITH NORTHERN END OF SEQUATCHIE ANTICLINE
This area is shown as inset on Figure 1.

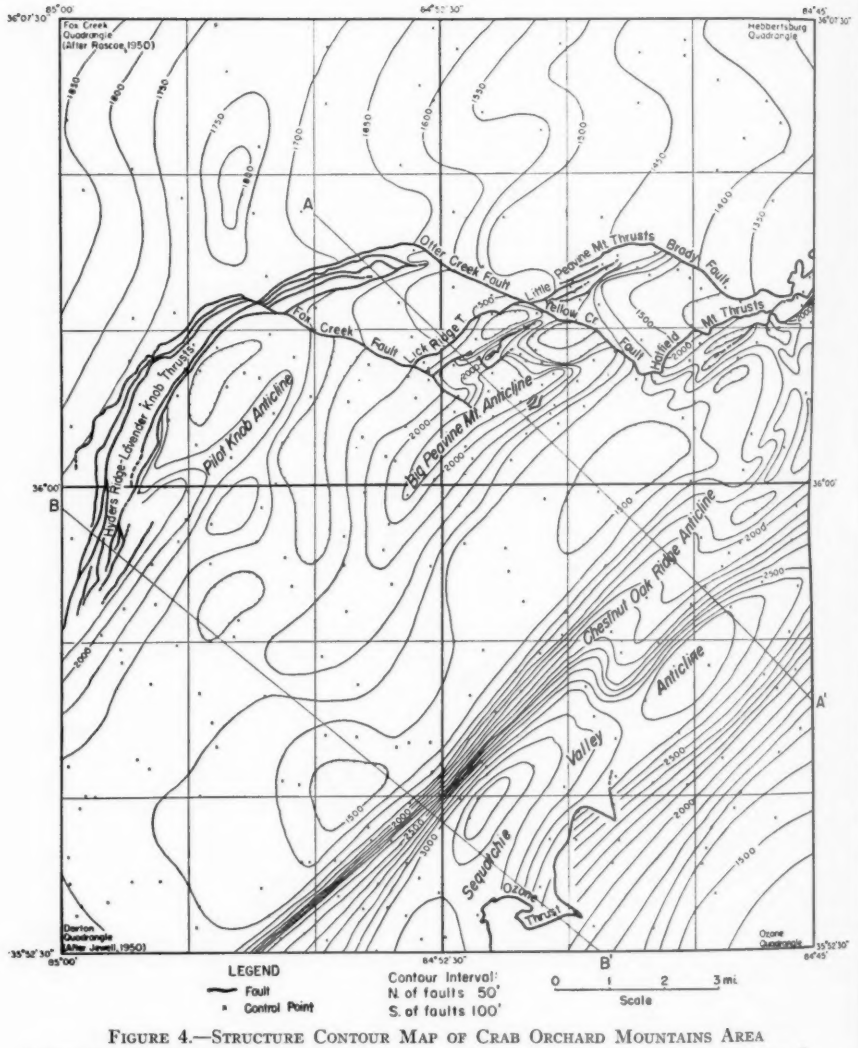

FIGURE 4.—STRUCTURE CONTOUR MAP OF CRAB ORCHARD MOUNTAINS AREA
Datum is top of Rockcastle sandstone. Lines A-A′ and B-B′ are structure sections on Figure 5.

It ends abruptly at the north border of the Ozone quadrangle. The main anticline, however, changes strike and bears more toward the east (Crab Orchard Mountains).

With the exception of local crushing along the steep northwest limb of the Sequatchie Valley anticline, the beds are only slightly deformed. Very intense crushing and tight folding, however, occur in restricted stratigraphic zones on both flanks. For example, in the southeastern part of the Ozone quadrangle, beds of the Gizzard formation are contorted and sheared, whereas overlying and underlying beds have only gentle dips. Farther northeast in this quadrangle the Sewanee conglomerate is so sheared and folded that it is difficult to discern bedding. In each of these instances underlying and overlying strata are not contorted.

A thrust fault, here named the Ozone fault,

occurs on the southeast flank of the Sequatchie Valley anticline at the southern border of the Ozone quadrangle. Although this fault is separated from the fault system west of the anticline, it is important because the fault plane is exposed for 1 mile downdip, and as far as this fault plane is exposed it follows bedding so that stratigraphic throw is slight. The Bon Air sandstone and Whitwell shale are here repeated so that they overlie each other for at least 1 mile. Relative to bedding, about 200 feet of vertical movement is represented. On the hanging wall, beds are intensely crushed and contorted, but below the fault plane only minor fractures in shale and squeezing of coal occur. Thus above the thrust the Bon Air sandstone is strongly contorted, but below the thrust this same sandstone is nearly undisturbed.

Significant relationships shown by this fault are: (1) very low angle of faulting relative to bedding, (2) considerable horizontal movement and small vertical movement, and (3) intense contortion of beds immediately above the fault plane and only slight deformation of beds below. These relationships illustrate on a relatively small scale the type of faulting which is believed to affect the entire region.

Belt of Thrust and Cross Faults North and Northwest of Anticline

Thrust faults.—The thrust faults in the belt strike northeast and their planes dip southeast at angles ranging from less than 10° to about 50°. Most thrust faults occur in zones of restricted width within which there are several faults. Thrusts either merge with cross faults or terminate along strike in small, sharp, asymmetrical anticlines overturned to the northwest. As in the Ozone fault, rocks above the fault planes are characteristically crushed and contorted, but beds below are undisturbed. Where several faults occur close together, however, beds both above and below fault planes may be crushed, if such beds are between two thrust planes.

Thrust zones are generally marked by prominent ridges, owing to dip of resistant sandstone beds. These zones are, from east to west, the Hatfield Mountain faults, Little Peavine Mountain faults, Lick Ridge faults, Lavender Knob faults, Hyders Ridge faults, Crossville fault, Lantana faults, and Erasmus "anticline" (Fig. 3).

HATFIELD MOUNTAIN FAULTS: Three faults make up the easternmost zone which the writer mapped in detail in the Hebbertsburg quadrangle. Along the northwestern fault highly contorted beds of Rockcastle sandstone are thrust over Duskin Creek. Just northeast of Brady Branch this fault turns northwestward and forms the Brady cross fault. The middle fault is associated with steeply dipping beds, and it dips about 50° southeast. Throw is variable along this fault. Rockcastle sandstone is thrust over Duskin Creek formation to the northeast, but to the southwest throw increases until Bon Air sandstone is thrust over Duskin Creek formation. There is a rather abrupt end to this fault as it turns sharply northwest to form the Yellow Creek cross fault. The southeasternmost thrust diminishes abruptly to the southwest and terminates in an asymmetrical anticline. Although the fault extends only a short distance into the Ozone quadrangle, greatest throw occurs here as Sewanee conglomerate is locally thrust over Duskin Creek formation.

LITTLE PEAVINE MOUNTAIN FAULTS: These occur about 2 miles northwest of the Hatfield Mountain fault zone. They lie between the Brady cross fault and the Yellow Creek-Otter Creek cross-fault line (Fig. 3). Slippage along these thrusts appears minor because no single fault in this zone is continuous between the limiting tear faults. Of the five faults making up this zone, three connect with neither tear fault but terminate at each end in sharp anticlines. Through most of this zone the thrust plates consist of successively repeated slices of Rockcastle.

LICK RIDGE FAULT ZONE: This is nearly continuous with the Little Peavine faults (Fig. 3), but is slightly offset to the northwest by the Otter Creek cross fault. Throughout a 2-mile zone one major fault is continuous; this thrust joins the Otter Creek cross fault on the northeast and the Fox Creek cross fault on the southwest. The main Lick Ridge fault thrusts Rockcastle sandstone over Duskin Creek formation at a low angle, judging by the 15° dip of beds on the hanging-wall side. Near its northeast end where it joins the Otter Creek cross fault,

however, dips are much steeper, ranging up to 80° to the southeast.

Only two other thrust faults are known along Lick Ridge, both of them minor. One joins the Fox Creek tear fault, and the other terminates at both ends in minor anticlines. The first locally thrusts beds as old as lower Vandever shale over Duskin Creek formation. It ends in an anticline to the northeast. Along the other minor thrust, Rockcastle sandstone is thrust over Duskin Creek formation, and this fault dies out on either end in anticlines.

LAVENDER KNOB-HYDERS RIDGE FAULTS: These extend southwest from the end of the Otter Creek cross fault across the Fox Creek and Dorton quadrangles (Fig. 3). Five southeast-dipping thrust faults compose the Lavender Knob-Hyders Ridge zone. In the Lavender Knob zone successive sheets of Rockcastle sandstone, and in some cases Duskin Creek formation, are thrust over one another. Beds as old as Sewanee conglomerate are involved in the Hyders Ridge area, but poor exposures make stratigraphic determinations difficult. Three of these thrusts end near the southwest corner of the Fox Creek quadrangle, but two continue into the Dorton quadrangle, where they are involved in a complex area of minor thrust faults. All five thrusts merge with the Otter Creek fault to the northeast.

The Crossville fault was first mapped by Butts and Nelson (1925, Pl. 1) as a normal fault terminating north of Crossville. This fault, which is actually a thrust fault, continues along the southeast outskirts of Crossville and joins the Hyders Ridge fault zone in the Dorton quadrangle.

Beds on the southeast (upthrown) side of the Crossville fault are contorted and dip southeast, forming a continuous prominent ridge. This ridge of southeast-dipping sandstone has been traced southwestward to the Lantana fault zone of Butts and Nelson (1925, Pl. 1).

LANTANA FAULTS: These were interpreted by Butts and Nelson (1925, p. 21) as normal. They stated:

> "the fault planes are assumed to be very steep or nearly vertical as the general surrounding conditions do not appear to indicate any considerable horizontal movement such as would be involved in overthrusts. . . ."

These faults, however, are continuous with the thrusts to the northeast, and display intense crushing. Therefore, they are thrust faults similar to those to the northeast. The Lantana faults end abruptly at a cross fault termed the Potts Creek fault by Butts and Nelson.

ERASMUS DEFORMATIONAL LINE: Butts and Nelson (1925, p. 20) interpreted this as an anticline with gentle dips on its southeast limb and nearly vertical dips on its northwest limb. The present writer observed crushing of heavy sandstone units in this vicinity, and Butts and Nelson reported similar conditions farther to the southwest along this strike. Thus instead of a simple asymmetrical anticline, this feature is probably thrust on the northwest limb giving the appearance of an unnaturally sharp anticlinal crest.

Butts and Nelson (1925, p. 20) report that structural disturbances continue several miles southwestward from this "anticline" along the same strike as far as Spencer, Van Buren County, beyond the area mapped. The writer visited this area and observed intense deformation of both Mississippian Pennington beds and Pennsylvanian sandstones.

Cross faults.—The thrust faults are interrupted and connected by several northwest-trending cross faults, which limit the zones of thrusting and invariably merge with or become at least one thrust of each zone. From east to west these transverse lines of faulting are: the Emory River fault, Brady fault, Otter Creek-Yellow Creek fault, Fox Creek fault, and Potts Creek fault (Fig. 3).

Where a significant throw occurs along these faults, beds on the southwest side are commonly raised relative to those on the northeast side. Commonly there is no appreciable vertical offset on these faults, the movement having been primarily lateral, in which case the faults may be traced by the trends of associated crushed rock.

EMORY RIVER FAULT ZONE: Jillson (1923, p. 373) interpreted this as an overthrust from the southwest. He believed that it extends northwest beyond the Hatfield Mountain area up Clear Creek in the northwestern part of the Lancing quadrangle, and that the southwest had risen relative to the northeast block.

Rodgers (1950, p. 676) correctly suggested that the zone does not cross the Hatfield Mountain "anticline" but swings into this structure.

Although some crowding occurred along the Emory River fault, most movement is attributed to slippage along its strike. Locally, no throw occurs as at Camp Austin. Here, the fault is a zone of crushing in a minor anticline. Throw increases along the fault to the northwest, until a maximum of at least 500 feet occurs where this fault turns and becomes the Hatfield thrust fault zone.

The writer traced this fault as far southeast as the Camp Austin quadrangle. Near Camp Austin the fault zone splits. According to C. W. Wilson, Jr., John W. Jewell, and R. M. Mitchum, Jr. (Personal communication), one split joins the Valley and Ridge structural system just north of Harriman, Tennessee, the other at Elverton Gap.

Northwest of Camp Austin the surface trace of this fault is on the southwest side of the Emory River. Flat-lying beds are exposed on both sides of the stream to within 1 mile southeast of Nemo. At Nemo the river changes direction and crosses and recrosses the fault. Contrary to the pattern suggested by Jillson (1923, p. 376), this fault does not continue up Clear Creek past Hatfield Mountain. It swings abruptly southwestward at Hatfield Mountain and merges with the Hatfield Mountain thrust belt.

BRADY FAULT: This is the next cross fault to the southwest. Most beds adjacent to this fault are poorly exposed, but in the gorge of Daddys Creek excellent exposures occur. Intense compression attended this faulting as is indicated by the massive, folded and crushed Rockcastle beds. In addition to the main fault there are three subsidiary faults, but they are not traced beyond the gorge. Most beds southwest of this fault are elevated above the corresponding beds to the northeast. Vertical offset is about 100 feet near the Hatfield Mountain thrust and nearly 300 feet on the northeast end of Little Peavine Mountain where this fault merges with the Little Peavine thrusts.

YELLOW CREEK FAULT: Its relationships are similar to the Brady fault with certain modifications. This cross fault is formed by one of the Hatfield Mountain thrusts turning northwest and extending toward the area where the Little Peavine Mountain and Lick Ridge thrusts join the Otter Creek cross faults.

Here again, beds southwest of the fault are elevated relative to beds on the northeast side. This offset decreases to the northwest; but even where vertical offset is slight, the fault can be traced by scant exposures and loose blocks of crushed sandstone. Such data indicate that it joins the Otter Creek cross fault.

Excellent exposures of the Yellow Creek cross fault occur in the gorges of Daddys Creek and Yellow Creek. Here it is a steeply dipping fault overthrust from the southwest. In this vicinity Bon Air sandstone is thrust against Rockcastle sandstone at a high angle. The upthrown Bon Air continues unbroken around the turn where the middle of the three Hatfield Mountain thrusts becomes this cross fault.

OTTER CREEK FAULT: This extends from the junction of the Little Peavine and Lick Ridge thrusts northwest into the Fox Creek quadrangle where it merges with the Lavender Knob thrust faults (Fig. 4). It exhibits some slight vertical displacement.

FOX CREEK FAULT: This extends northwest from Peavine Mountain near the west edge of the Hebbertsburg quadrangle (Fig. 4). It terminates in the Hyders Ridge-Lavender Knob thrust faults by offsetting these thrusts about 2000 feet. There is little vertical offset at the Lavender Knob thrusts to the northwest, but the south side is considerably upthrown to the southeast near Big Peavine Mountain. This fault terminates on the southeast at Big Peavine Mountain in intensely contorted beds of the Bon Air sandstone.

The Potts Creek cross fault, mapped by Butts and Nelson (1925), joins the Erasmus "anticline" with the Lantana thrusts. This is the last cross fault mapped to the southwest; continued tracing of the fault system may disclose others.

Big Peavine Mountain Structure

The Big Peavine Mountain structure extends from the southeastern part of the Hebbertsburg quadrangle southwest into the Dorton quadrangle (Fig. 4). Elevations on the Rockcastle sandstone show that it is superficially an anticline. Evidence shows that this structure is not

a conventional anticline, but a consequence of faulting genetically associated with the fault system previously discussed.

On Big Peavine Mountain, the Bon Air sandstone is intensely crushed and contorted, whereas the overlying beds are only gently warped with the dip of the flanks of the anticline. Such relationships suggest faulting beneath the Bon Air. This stratigraphically localized deformation is reminiscent of the Ozone fault to the southeast where the Bon Air is similarly deformed.

Two wells have been drilled on this structure. In both wells a normal stratigraphic sequence was encountered downward from the Rockcastle to the Bon Air, and a normal sequence upward from the Pennington formation to the top of the Sewanee conglomerate. Between the Sewanee below and Bon Air above there are about 800 feet of sandstone in several units separated by only a few feet of shale. Such a thickness of sandstone is many times greater than the normal Sewanee-Bon Air interval, and must be attributed to duplication by faulting. Repetition of lower beds by faulting readily accounts for the anticlinal structural relief in the overlying Rockcastle sandstone, as shown by cross section *A-A'* on Figure 5.

The broad, flat top of the Big Peavine Mountain anticline suggests duplication for a considerable distance across its strike. This would require considerable horizontal movement as would the Ozone fault. The thrust that formed this anticlinal feature does not outcrop in this vicinity, but probably outcrops as the Hyders Ridge-Lavender Knob thrust zone 5 miles to the northwest.

The Hyders Ridge-Lavender Knob thrust fault beneath Big Peavine Mountain must dip gently to the southeast, as does the Ozone fault, probably following bedding for a great distance and changing its stratigraphic position about 200 feet in 5 miles.

Interpretation

General

A continuous belt of thrust and cross faults has been mapped from near Harriman, Roane County, to the Erasmus "anticline" in White County (Fig. 3). Probably this system extends at least 15 miles farther to Spencer in Van Buren County (southwest of area shown in Fig. 3). This series of southeast-dipping thrusts offset by northwest-trending en echelon cross faults is here called the Cumberland Plateau overthrust.

Regionally there is a decided similarity in pattern between this system and the system of faults marking the Pine Mountain thrust block to the northeast (Figs. 1, 3), in the angular relationships of thrust and cross faults, in general dimensions, and in position with reference to the regional structure. The similar patterns suggest that these two structural systems had the same origin and mechanics. To verify this inference, the nature of the Cumberland Plateau overthrust is studied and then compared with the known behavior of the Pine Mountain block.

Attitude of Fault Planes

Thrust faults of this area have southeast-dipping fault planes. No exception to this direction was observed in the Cumberland Plateau. At the surface, the dips of the faults range up to 40°. Evidence suggests that at depth these faults are nearly horizontal. This is displayed by the Ozone thrust and inferred for the Lavender Knob-Hyders Ridge thrust beneath Big Peavine Mountain.

Southeastward from Big Peavine Mountain the faulting follows bedding below the competent Bon Air fairly closely, and probably breaks through the Sewanee conglomerate beneath the Chesnut Oak Ridge anticline. This explains the anomalous, stratigraphically restricted zones of crushing in the Sewanee on the flanks of the Sequatchie Valley anticline just east of Chesnut Oak Ridge. If these crushed zones are actually related to the fault under Peavine Mountain as postulated, this faulting has moved downward only 200 feet in the 7 miles between Peavine Mountain and the Crab Orchard Mountains. Because these zones of crushing are present on both limbs of the Sequatchie anticline, the thrust sheet must also arch over this anticline, which implies that the main fault system is not directly related to the anticline. (*See* Fig. 5.)

Where planes of cross faults may be measured or estimated, they dip steeply to the southwest.

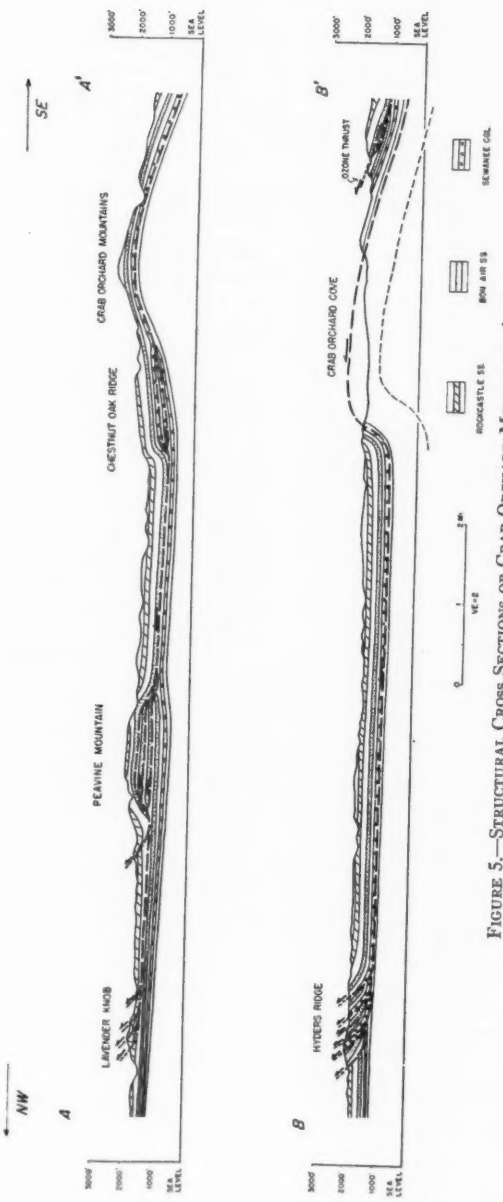

FIGURE 5.—STRUCTURAL CROSS SECTIONS OF CRAB ORCHARD MOUNTAINS AREA
Section lines drawn on Figure 4.

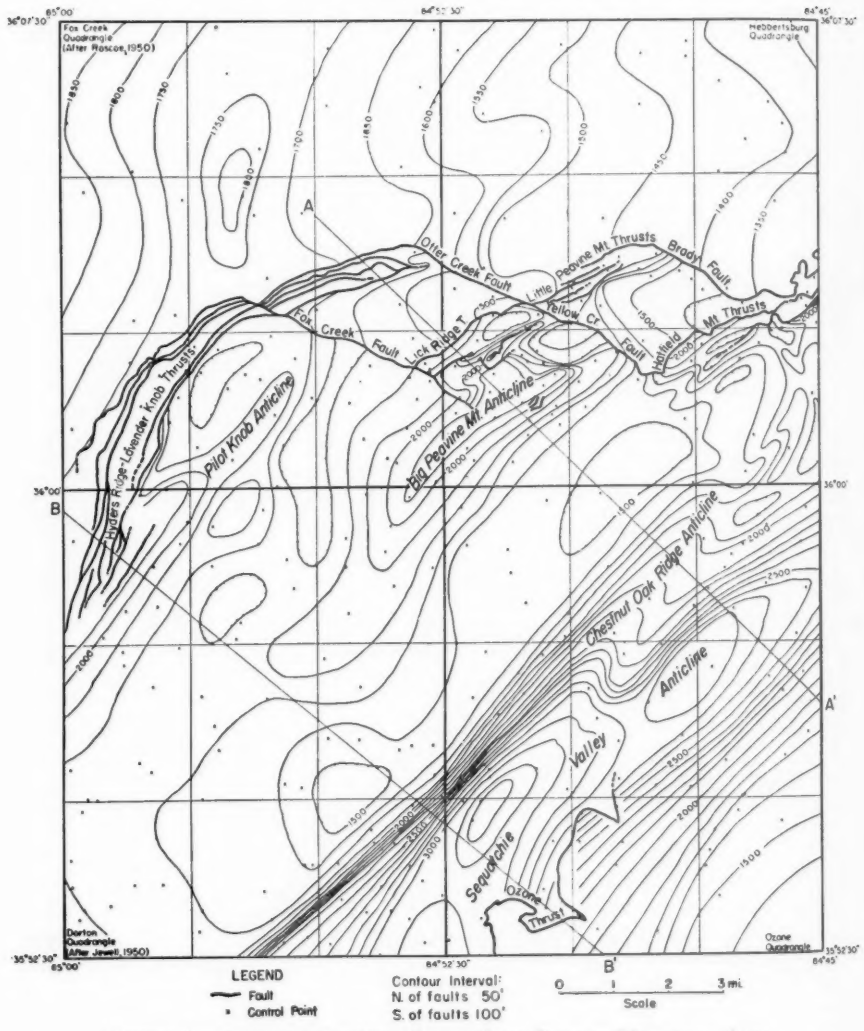

FIGURE 4.—STRUCTURE CONTOUR MAP OF CRAB ORCHARD MOUNTAINS AREA
Datum is top of Rockcastle sandstone. Lines A-A′ and B-B′ are structure sections on Figure 5.

It ends abruptly at the north border of the Ozone quadrangle. The main anticline, however, changes strike and bears more toward the east (Crab Orchard Mountains).

With the exception of local crushing along the steep northwest limb of the Sequatchie Valley anticline, the beds are only slightly deformed. Very intense crushing and tight folding, however, occur in restricted stratigraphic zones on both flanks. For example, in the southeastern part of the Ozone quadrangle, beds of the Gizzard formation are contorted and sheared, whereas overlying and underlying beds have only gentle dips. Farther northeast in this quadrangle the Sewanee conglomerate is so sheared and folded that it is difficult to discern bedding. In each of these instances underlying and overlying strata are not contorted.

A thrust fault, here named the Ozone fault,

occurs on the southeast flank of the Sequatchie Valley anticline at the southern border of the Ozone quadrangle. Although this fault is separated from the fault system west of the anticline, it is important because the fault plane is exposed for 1 mile downdip, and as far as this fault plane is exposed it follows bedding so that stratigraphic throw is slight. The Bon Air sandstone and Whitwell shale are here repeated so that they overlie each other for at least 1 mile. Relative to bedding, about 200 feet of vertical movement is represented. On the hanging wall, beds are intensely crushed and contorted, but below the fault plane only minor fractures in shale and squeezing of coal occur. Thus above the thrust the Bon Air sandstone is strongly contorted, but below the thrust this same sandstone is nearly undisturbed.

Significant relationships shown by this fault are: (1) very low angle of faulting relative to bedding, (2) considerable horizontal movement and small vertical movement, and (3) intense contortion of beds immediately above the fault plane and only slight deformation of beds below. These relationships illustrate on a relatively small scale the type of faulting which is believed to affect the entire region.

Belt of Thrust and Cross Faults North and Northwest of Anticline

Thrust faults.—The thrust faults in the belt strike northeast and their planes dip southeast at angles ranging from less than 10° to about 30°. Most thrust faults occur in zones of restricted width within which there are several faults. Thrusts either merge with cross faults or terminate along strike in small, sharp, asymmetrical anticlines overturned to the northwest. As in the Ozone fault, rocks above the fault planes are characteristically crushed and contorted, but beds below are undisturbed. Where several faults occur close together, however, beds both above and below fault planes may be crushed, if such beds are between two thrust planes.

Thrust zones are generally marked by prominent ridges, owing to dip of resistant sandstone beds. These zones are, from east to west, the Hatfield Mountain faults, Little Peavine Mountain faults, Lick Ridge faults, Lavender Knob faults, Hyders Ridge faults, Crossville fault, Lantana faults, and Erasmus "anticline" (Fig. 3).

HATFIELD MOUNTAIN FAULTS: Three faults make up the easternmost zone which the writer mapped in detail in the Hebbertsburg quadrangle. Along the northwestern fault highly contorted beds of Rockcastle sandstone are thrust over Duskin Creek. Just northeast of Brady Branch this fault turns northwestward and forms the Brady cross fault. The middle fault is associated with steeply dipping beds, and it dips about 50° southeast. Throw is variable along this fault. Rockcastle sandstone is thrust over Duskin Creek formation to the northeast, but to the southwest throw increases until Bon Air sandstone is thrust over Duskin Creek formation. There is a rather abrupt end to this fault as it turns sharply northwest to form the Yellow Creek cross fault. The southeasternmost thrust diminishes abruptly to the southwest and terminates in an asymmetrical anticline. Although the fault extends only a short distance into the Ozone quadrangle, greatest throw occurs here as Sewanee conglomerate is locally thrust over Duskin Creek formation.

LITTLE PEAVINE MOUNTAIN FAULTS: These occur about 2 miles northwest of the Hatfield Mountain fault zone. They lie between the Brady cross fault and the Yellow Creek-Otter Creek cross-fault line (Fig. 3). Slippage along these thrusts appears minor because no single fault in this zone is continuous between the limiting tear faults. Of the five faults making up this zone, three connect with neither tear fault but terminate at each end in sharp anticlines. Through most of this zone the thrust plates consist of successively repeated slices of Rockcastle.

LICK RIDGE FAULT ZONE: This is nearly continuous with the Little Peavine faults (Fig. 3), but is slightly offset to the northwest by the Otter Creek cross fault. Throughout a 2-mile zone one major fault is continuous; this thrust joins the Otter Creek cross fault on the northeast and the Fox Creek cross fault on the southwest. The main Lick Ridge fault thrusts Rockcastle sandstone over Duskin Creek formation at a low angle, judging by the 15° dip of beds on the hanging-wall side. Near its northeast end where it joins the Otter Creek cross fault,

however, dips are much steeper, ranging up to 80° to the southeast.

Only two other thrust faults are known along Lick Ridge, both of them minor. One joins the Fox Creek tear fault, and the other terminates at both ends in minor anticlines. The first locally thrusts beds as old as lower Vandever shale over Duskin Creek formation. It ends in an anticline to the northeast. Along the other minor thrust, Rockcastle sandstone is thrust over Duskin Creek formation, and this fault dies out on either end in anticlines.

LAVENDER KNOB-HYDERS RIDGE FAULTS: These extend southwest from the end of the Otter Creek cross fault across the Fox Creek and Dorton quadrangles (Fig. 3). Five southeast-dipping thrust faults compose the Lavender Knob-Hyders Ridge zone. In the Lavender Knob zone successive sheets of Rockcastle sandstone, and in some cases Duskin Creek formation, are thrust over one another. Beds as old as Sewanee conglomerate are involved in the Hyders Ridge area, but poor exposures make stratigraphic determinations difficult. Three of these thrusts end near the southwest corner of the Fox Creek quadrangle, but two continue into the Dorton quadrangle, where they are involved in a complex area of minor thrust faults. All five thrusts merge with the Otter Creek fault to the northeast.

The Crossville fault was first mapped by Butts and Nelson (1925, Pl. 1) as a normal fault terminating north of Crossville. This fault, which is actually a thrust fault, continues along the southeast outskirts of Crossville and joins the Hyders Ridge fault zone in the Dorton quadrangle.

Beds on the southeast (upthrown) side of the Crossville fault are contorted and dip southeast, forming a continuous prominent ridge. This ridge of southeast-dipping sandstone has been traced southwestward to the Lantana fault zone of Butts and Nelson (1925, Pl. 1).

LANTANA FAULTS: These were interpreted by Butts and Nelson (1925, p. 21) as normal. They stated:

> "the fault planes are assumed to be very steep or nearly vertical as the general surrounding conditions do not appear to indicate any considerable horizontal movement such as would be involved in overthrusts. . . ."

These faults, however, are continuous with the thrusts to the northeast, and display intense crushing. Therefore, they are thrust faults similar to those to the northeast. The Lantana faults end abruptly at a cross fault termed the Potts Creek fault by Butts and Nelson.

ERASMUS DEFORMATIONAL LINE: Butts and Nelson (1925, p. 20) interpreted this as an anticline with gentle dips on its southeast limb and nearly vertical dips on its northwest limb. The present writer observed crushing of heavy sandstone units in this vicinity, and Butts and Nelson reported similar conditions farther to the southwest along this strike. Thus instead of a simple asymmetrical anticline, this feature is probably thrust on the northwest limb giving the appearance of an unnaturally sharp anticlinal crest.

Butts and Nelson (1925, p. 20) report that structural disturbances continue several miles southwestward from this "anticline" along the same strike as far as Spencer, Van Buren County, beyond the area mapped. The writer visited this area and observed intense deformation of both Mississippian Pennington beds and Pennsylvanian sandstones.

Cross faults.—The thrust faults are interrupted and connected by several northwest-trending cross faults, which limit the zones of thrusting and invariably merge with or become at least one thrust of each zone. From east to west these transverse lines of faulting are: the Emory River fault, Brady fault, Otter Creek-Yellow Creek fault, Fox Creek fault, and Potts Creek fault (Fig. 3).

Where a significant throw occurs along these faults, beds on the southwest side are commonly raised relative to those on the northeast side. Commonly there is no appreciable vertical offset on these faults, the movement having been primarily lateral, in which case the faults may be traced by the trends of associated crushed rock.

EMORY RIVER FAULT ZONE: Jillson (1923, p. 373) interpreted this as an overthrust from the southwest. He believed that it extends northwest beyond the Hatfield Mountain area up Clear Creek in the northwestern part of the Lancing quadrangle, and that the southwest had risen relative to the northeast block.

Rodgers (1950, p. 676) correctly suggested that the zone does not cross the Hatfield Mountain "anticline" but swings into this structure.

Although some crowding occurred along the Emory River fault, most movement is attributed to slippage along its strike. Locally, no throw occurs as at Camp Austin. Here, the fault is a zone of crushing in a minor anticline. Throw increases along the fault to the northwest, until a maximum of at least 500 feet occurs where this fault turns and becomes the Hatfield thrust fault zone.

The writer traced this fault as far southeast as the Camp Austin quadrangle. Near Camp Austin the fault zone splits. According to C. W. Wilson, Jr., John W. Jewell, and R. M. Mitchum, Jr. (Personal communication), one split joins the Valley and Ridge structural system just north of Harriman, Tennessee, the other at Elverton Gap.

Northwest of Camp Austin the surface trace of this fault is on the southwest side of the Emory River. Flat-lying beds are exposed on both sides of the stream to within 1 mile southeast of Nemo. At Nemo the river changes direction and crosses and recrosses the fault. Contrary to the pattern suggested by Jillson (1923, p. 376), this fault does not continue up Clear Creek past Hatfield Mountain. It swings abruptly southwestward at Hatfield Mountain and merges with the Hatfield Mountain thrust belt.

BRADY FAULT: This is the next cross fault to the southwest. Most beds adjacent to this fault are poorly exposed, but in the gorge of Daddys Creek excellent exposures occur. Intense compression attended this faulting as is indicated by the massive, folded and crushed Rockcastle beds. In addition to the main fault there are three subsidiary faults, but they are not traced beyond the gorge. Most beds southwest of this fault are elevated above the corresponding beds to the northeast. Vertical offset is about 100 feet near the Hatfield Mountain thrust and nearly 300 feet on the northeast end of Little Peavine Mountain where this fault merges with the Little Peavine thrusts.

YELLOW CREEK FAULT: Its relationships are similar to the Brady fault with certain modifications. This cross fault is formed by one of the Hatfield Mountain thrusts turning northwest and extending toward the area where the Little Peavine Mountain and Lick Ridge thrusts join the Otter Creek cross faults.

Here again, beds southwest of the fault are elevated relative to beds on the northeast side. This offset decreases to the northwest; but even where vertical offset is slight, the fault can be traced by scant exposures and loose blocks of crushed sandstone. Such data indicate that it joins the Otter Creek cross fault.

Excellent exposures of the Yellow Creek cross fault occur in the gorges of Daddys Creek and Yellow Creek. Here it is a steeply dipping fault overthrust from the southwest. In this vicinity Bon Air sandstone is thrust against Rockcastle sandstone at a high angle. The upthrown Bon Air continues unbroken around the turn where the middle of the three Hatfield Mountain thrusts becomes this cross fault.

OTTER CREEK FAULT: This extends from the junction of the Little Peavine and Lick Ridge thrusts northwest into the Fox Creek quadrangle where it merges with the Lavender Knob thrust faults (Fig. 4). It exhibits some slight vertical displacement.

FOX CREEK FAULT: This extends northwest from Peavine Mountain near the west edge of the Hebbertsburg quadrangle (Fig. 4). It terminates in the Hyders Ridge-Lavender Knob thrust faults by offsetting these thrusts about 2000 feet. There is little vertical offset at the Lavender Knob thrusts to the northwest, but the south side is considerably upthrown to the southeast near Big Peavine Mountain. This fault terminates on the southeast at Big Peavine Mountain in intensely contorted beds of the Bon Air sandstone.

The Potts Creek cross fault, mapped by Butts and Nelson (1925), joins the Erasmus "anticline" with the Lantana thrusts. This is the last cross fault mapped to the southwest; continued tracing of the fault system may disclose others.

Big Peavine Mountain Structure

The Big Peavine Mountain structure extends from the southeastern part of the Hebbertsburg quadrangle southwest into the Dorton quadrangle (Fig. 4). Elevations on the Rockcastle sandstone show that it is superficially an anticline. Evidence shows that this structure is not

a conventional anticline, but a consequence of faulting genetically associated with the fault system previously discussed.

On Big Peavine Mountain, the Bon Air sandstone is intensely crushed and contorted, whereas the overlying beds are only gently warped with the dip of the flanks of the anticline. Such relationships suggest faulting beneath the Bon Air. This stratigraphically localized deformation is reminiscent of the Ozone fault to the southeast where the Bon Air is similarly deformed.

Two wells have been drilled on this structure. In both wells a normal stratigraphic sequence was encountered downward from the Rockcastle to the Bon Air, and a normal sequence upward from the Pennington formation to the top of the Sewanee conglomerate. Between the Sewanee below and Bon Air above there are about 800 feet of sandstone in several units separated by only a few feet of shale. Such a thickness of sandstone is many times greater than the normal Sewanee-Bon Air interval, and must be attributed to duplication by faulting. Repetition of lower beds by faulting readily accounts for the anticlinal structural relief in the overlying Rockcastle sandstone, as shown by cross section *A-A'* on Figure 5.

The broad, flat top of the Big Peavine Mountain anticline suggests duplication for a considerable distance across its strike. This would require considerable horizontal movement as would the Ozone fault. The thrust that formed this anticlinal feature does not outcrop in this vicinity, but probably outcrops as the Hyders Ridge-Lavender Knob thrust zone 5 miles to the northwest.

The Hyders Ridge-Lavender Knob thrust fault beneath Big Peavine Mountain must dip gently to the southeast, as does the Ozone fault, probably following bedding for a great distance and changing its stratigraphic position about 200 feet in 5 miles.

Interpretation

General

A continuous belt of thrust and cross faults has been mapped from near Harriman, Roane County, to the Erasmus "anticline" in White County (Fig. 3). Probably this system extends at least 15 miles farther to Spencer in Van Buren County (southwest of area shown in Fig. 3). This series of southeast-dipping thrusts offset by northwest-trending en echelon cross faults is here called the Cumberland Plateau overthrust.

Regionally there is a decided similarity in pattern between this system and the system of faults marking the Pine Mountain thrust block to the northeast (Figs. 1, 3), in the angular relationships of thrust and cross faults, in general dimensions, and in position with reference to the regional structure. The similar patterns suggest that these two structural systems had the same origin and mechanics. To verify this inference, the nature of the Cumberland Plateau overthrust is studied and then compared with the known behavior of the Pine Mountain block.

Attitude of Fault Planes

Thrust faults of this area have southeast-dipping fault planes. No exception to this direction was observed in the Cumberland Plateau. At the surface, the dips of the faults range up to 40°. Evidence suggests that at depth these faults are nearly horizontal. This is displayed by the Ozone thrust and inferred for the Lavender Knob-Hyders Ridge thrust beneath Big Peavine Mountain.

Southeastward from Big Peavine Mountain the faulting follows bedding below the competent Bon Air fairly closely, and probably breaks through the Sewanee conglomerate beneath the Chesnut Oak Ridge anticline. This explains the anomalous, stratigraphically restricted zones of crushing in the Sewanee on the flanks of the Sequatchie Valley anticline just east of Chesnut Oak Ridge. If these crushed zones are actually related to the fault under Peavine Mountain as postulated, this faulting has moved downward only 200 feet in the 7 miles between Peavine Mountain and the Crab Orchard Mountains. Because these zones of crushing are present on both limbs of the Sequatchie anticline, the thrust sheet must also arch over this anticline, which implies that the main fault system is not directly related to the anticline. (*See* Fig. 5.)

Where planes of cross faults may be measured or estimated, they dip steeply to the southwest.

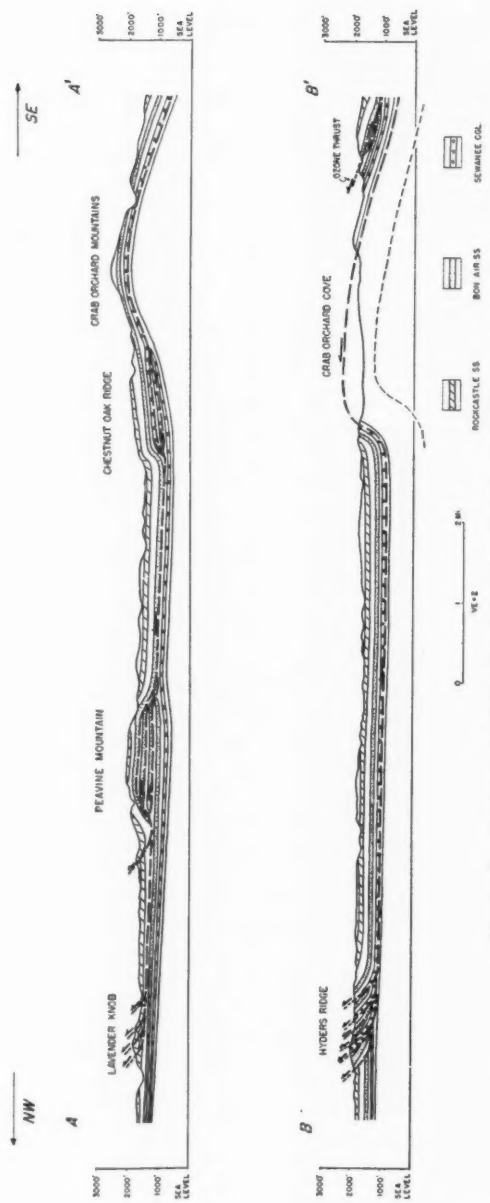

FIGURE 5.—STRUCTURAL CROSS SECTIONS OF CRAB ORCHARD MOUNTAINS AREA
Section lines drawn on Figure 4.

Because these faults turn and merge with or become thrusts at the surface, their dip must flatten where they merge with the low-angle fault planes at depth.

The best illustration of this relation is the junction of the Yellow Creek tear fault and the Hatfield Mountain thrust zone. Here the beds associated with both faults may be traced continuously around the transition from thrust to cross fault. Such a gradual turn with no discontinuity in the upthrown side shows that these two faults formed simultaneously. Therefore the amount of strike slip on the cross fault is equal to the amount of heave on the thrust fault.

The Emory River fault merges with the low-angle extension of the Hatfield Mountain thrust to the southwest. At Harriman and Elverton, branches of the Emory River fault merge with or disappear under the Chattanooga fault of the Valley and Ridge province (Rodgers, 1953, Pls. 7, 8).

Movement along Faults

Strike slip along cross faults must be equal to heave on the associated thrusts. This is, of course, true only for the Emory River, Brady, Otter Creek, and Potts Creek faults that limit the fault system to the northeast. Those extending southeastward into the thrust sheet have strike slip depending on the relative movement of adjacent thrust blocks. In some thrusts there is no way to establish from surface mapping the horizontal extent of duplication and maximum movement can not be estimated.

In the case of Big Peavine Mountain, however, subsurface data give the amount of duplication, of which surface mapping gives the approximate horizontal extent. Such information suggests that this apparent anticline is the result of approximately three miles of thrusting. The Lavender Knob thrust and the whole en echelon series of cross faults and tear faults must represent the same amount of movement.

Duplicated beds were mapped for 1 mile across the strike on the Ozone thrust. Since none of the Little Peavine thrusts is continuous between the limiting cross faults, this zone probably represents only about 1000 feet of movement. The Fox Creek cross fault extends into the overthrust mass. Strike slip of about 2000 feet is estimated for this fault by offset of the Hyders Ridge-Lavender Knob faults.

Comparison with the Pine Mountain Block

Previous investigations (Wentworth, 1921, p. 351–353; Butts. 1927, p. 8–9; Rich, 1934, p. 1584–1589) established that the thrust- and cross-fault pattern outlines a low-angle thrust sheet which has moved several miles to the northwest relative to underlying rocks. On the northwest this sheet is limited by the Pine Mountain thrust, which is terminated at both ends by cross faults—the Russell Fork fault in Virginia and the Jacksboro fault in Tennessee.

Two longitudinal divisions occur within the block—the Middlesboro syncline to the northwest, adjacent to the Pine Mountain thrust fault, and the Powell Valley anticline to the southeast. The Powell Valley anticline is broad and flat-topped, but becomes narrow and less significant to the northeast. Fensters on this anticline expose Silurian beds underlying the Cambro-Ordovician (Butts, 1927, p. 1–6). Such fensters mark the position of the thrust plane nearly 20 miles southeast of its outcrop along Pine Mountain.

Duplication of pre-Pennsylvanian beds during the thrusting developed the Powell Valley anticline; as the anticline diminishes in width northeastward, the amount of horizontal movement along the causal fault decreases. This block rotated about its northeast end. Only slight movement is reported at its northeast end (Wentworth, 1921, p. 365), but more than 10 miles near its southwest end (Rich, 1934, p. 1558).

The low-angle fault basal to this thrust sheet follows mainly two incompetent layers—shales in the Lower and Middle Cambrian Rome and Conasauga formations, and the Chattanooga shale. Breaks in these incompetent beds are connected by a more steeply dipping fracture across the intervening competent beds (Rich, 1934, p. 1590).

The Pine Mountain fault, like thrust faults of the Cumberland Plateau overthrust, dips comparatively steeply southeastward on the

outcrop, but flattens with depth to become a bedding fault. Also, where duplicated beds are not removed by erosion, the overlying strata show anticlinal features both in the case of the Pine Mountain overthrust (Powell Valley anticline) and the Cumberland Plateau overthrust (Peavine Mountain anticline). The primary attitude of the major fault plane is flat in both cases. The many en echelon cross faults of the Cumberland Plateau thrust are the counterpart of the single Jacksboro fault at the southwest end of the Pine Mountain thrust block. In both cases the cross faults, which are primarily strike-slip faults, have undergone some thrusting because of crowding.

Comparison of the pattern of these two fault systems strongly supports the inference that they have identical relationships and mechanics of formation. Judging from the cross faults, the northeast end of the Cumberland Plateau overthrust is a mirror image of the southeast end of the Pine Mountain block. The swing of the Emory River fault into the en echelon cross faults and thrusts corresponds mechanically with the turn of the Jacksboro fault into the Pine Mountain thrust.

Although these two major thrust sheets are similar in width across the strike from their western outcrops to the Cumberland Mountain front, it is not certain that they have the same length. The Pine Mountain block is about 125 miles long, but faults outlining the Cumberland Plateau thrust sheet have only been mapped for about 35 miles southwest of the Emory River. However, faulting does occur 15 miles southwest of this point where it involves beds of the Pennington shale.

Since the last known exposure was in the Pennington, this fault may extend farther southwestward, hidden in the soft, incompetent Pennington shale. In logging cores taken from drill holes in Franklin County, Tennessee, (about 20 miles west of the Sequatchie Valley near the Alabama border) Pennington shales were observed to be considerably sheared and contorted. It is possible that most of the Pennsylvanian of south Tennessee has been thrust northwestward even though there are no surficial indications of such movement. It is also possible, however, that this fault system dies out southwestward and does not affect the plateau in southern Tennessee.

Rich (1934, p. 1595) and Rodgers (1950, p. 677) have suggested that the Sequatchie Valley anticline itself is a result of a low-angle thrust. If so, the thrusting occurred later, since the Cumberland Plateau thrust is here folded (Fig. 5). The Cumberland Plateau thrusts terminate at the Emory River, at the end of the Sequatchie Valley anticline. This coincidence suggests that the southwest end of the Cumberland Plateau thrust may also coincide with the southwest end of the Sequatchie Valley anticline in Blount County, Alabama. If this is correct, then in areal dimensions the Cumberland Plateau thrust sheet is even more extensive than the Pine Mountain Block, although the horizontal movement and thickness of beds involved was probably much less.

Regional Significance of Cumberland Plateau Overthrust

There are two concepts of Appalachian structure, characterized by Rodgers as the "thick-skinned" and "thin-skinned" schools of thought. He states (1949, p. 1653):

> "The thick-skinned geologists . . . have reasoned from the broad low folds of the (Appalachian) plateau to the hypothesis that the folds and faults of the Valley and Ridge province are the main manifestation of the Appalachian orogeny and that each continues separately to the basement. The thin-skinned geologists . . . have reasoned from the great low-angle thrust faults . . . , especially the Pine Mountain fault, to the hypothesis that the Paleozoic rocks of the unmetamorphosed part of the Appalachians, caught on the margin of intense deformation on the southeast, were stripped completely off the basement and piled up against the unyielding plateau in great rootless folds and imbricate thrust sheets underlain by a few bedding-plane faults of immense displacement."

Proponents of the "thick-skinned" concept, notably Ver Wiebe (1936), point to the Pine Mountain overthrust as an exception, a structural anomaly having no bearing on the essential structural pattern of the Appalachian region. Proponents of the "thin-skinned" concept use this low-angle thrust as main proof of their contentions. This nearly horizontal thrust sheet involving rocks of the Cumberland Plateau led some geologists (Rich, 1934, p. 1596; Miller, 1945, p. 1183) to question the classic interpretation of the attitude of the other Appalachian faults at depth. They

thought the younger sedimentary rocks were sheared from the underlying crystalline basement along an extensive horizontal basal fault, the observed steeply dipping faults merged with the sole fault at depth, and the underlying basement rocks remained undisturbed.

The Cumberland Plateau overthrust markedly modifies the evidence. Along much, if not all of the Southern Appalachian fault system, low-angle thrusting is the terminal structure to the west. This new evidence, in conjunction with previously known facts, further supports the thin-skinned concept of Southern Appalachian Valley structure.

Conclusions

The system of thrust and cross faults, herein named the Cumberland Plateau overthrust, extends southwest from the Emory River fault and bounds a low-angle thrust sheet fundamentally similar to the Pine Mountain block. From the fault outcrop the fracture extends southeastward at a shallow depth, primarily along bedding planes of shales through undisturbed Pennsylvanian and upper Mississippian beds, and has its roots in the faults of the Valley and Ridge province. Thus, discordance between the Cumberland Plateau and the Valley and Ridge province to the southeast is not so sharp as has been supposed, and outlying structures of the Plateau are in fact genetically related to the structure of the Valley and Ridge.

This thrust sheet may extend southwestward to Birmingham, Alabama, at the southern end of the Sequatchie Valley anticline, a distance of well over 200 miles. Pennsylvanian, and perhaps some upper Mississippian beds, underlying the whole Cumberland Plateau south of Van Buren County, Tennessee, may have been thrust northwestward along the basal low-angle fault. It is also possible that upper beds in the Black Warrior coal field of Alabama have experienced similar, less-extensive movement.

This thrust, and the previously known Pine Mountain thrust, indicate a western marginal belt of low-angle thrusts along nearly the entire length of the Southern Appalachian Valley. Discovery of the Cumberland Plateau overthrust therefore lends additional support to the thin-skinned concept of Southern Appalachian Valley structure.

References Cited

Butts, C., and Nelson, W. A., 1925, Geology and mineral resources of the Crossville quadrangle: Tenn. Div. Geol. Bull. 33-D.

—— 1927, Fensters in the Cumberland overthrust block of southwest Virginia: Va. Geol. Survey Bull. 28.

Glenn, L. C., 1925, The northern Tennessee coal field: Tenn. Div. Geol. Bull. 33-B.

Hayes, C. W., 1894, Kingston, Tennessee: U. S. Geol. Survey Geol. Atlas, folio 4.

Jillson, W. R., 1923, Emory River overthrust of east Tennessee: Pan-Am. Geologist, v. 39, p. 373–378.

Keith, A., 1897, Wartburg, Tennessee: U. S. Geol. Survey Geol. Atlas, folio 40.

Miller, R. L., 1945, Relation of overthrust faults in southwest Virginia: Geol. Soc. America Bull., v. 56, p. 1182–1183.

Rich, J. L., 1934, Mechanics of low-angle overthrust faulting as illustrated by Cumberland thrust block, Virginia, Kentucky and Tennessee: Am. Assoc. Petroleum Geologists Bull., v. 18, p. 1584–1596.

Rodgers, John, 1949, Evolution of thought on structure of middle and southern Appalachians: Am. Assoc. Petroleum Geologists Bull., v. 33, p. 1643–1654.

—— 1950, Mechanics of Appalachian folding as illustrated by Sequatchie anticline, Tennessee and Alabama: Am. Assoc. Petroleum Geologists Bull., v. 34, p. 672–681.

—— 1953, Geologic map of East Tennessee with explanatory text: Tenn. Div. Geol. Bull. 58, pt. II.

Safford, J. M., 1869, Geology of Tennessee: S. C. Mercer, Nashville, 550 p.

Ver Wiebe, W. A., 1936, Geosynclinal boundary faults: Am. Assoc. Petroleum Geologists Bull., v. 20, p. 910–938.

Wentworth, C. K., 1921, Russell Fork fault of southwest Virginia: Jour. Geology, v. 29, p. 351–369.

Division of Geology, State of Tennessee, Nashville, Tenn.

Manuscript Received by the Secretary of the Society, January 22, 1954.

known Pine
rn marginal
rly the en-
ppalachian
nd Plateau
nal support
uthern Ap-

Geology and
quadrangle:

d overthrust
Geol. Survey

nnessee coal
.
essee: U. S.
.
verthrust of
gist, v. 39,

U. S. Geol.

thrust faults
oc. America

-angle over-
Cumberland
and Ten-
Geologists

thought on
ppalachians:
Bull., v. 33,

n folding as
e, Tennessee
oleum Geol-

nnessee with
Geol. Bull.

essee: S. C.

l boundary
ogists Bull.,

rk fault of
gy, v. 29,

TENNESSEE,

CRETARY OF

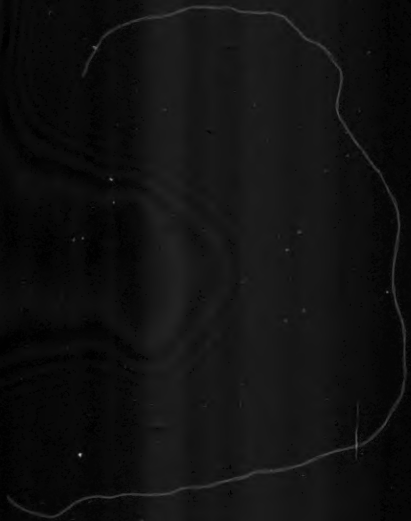

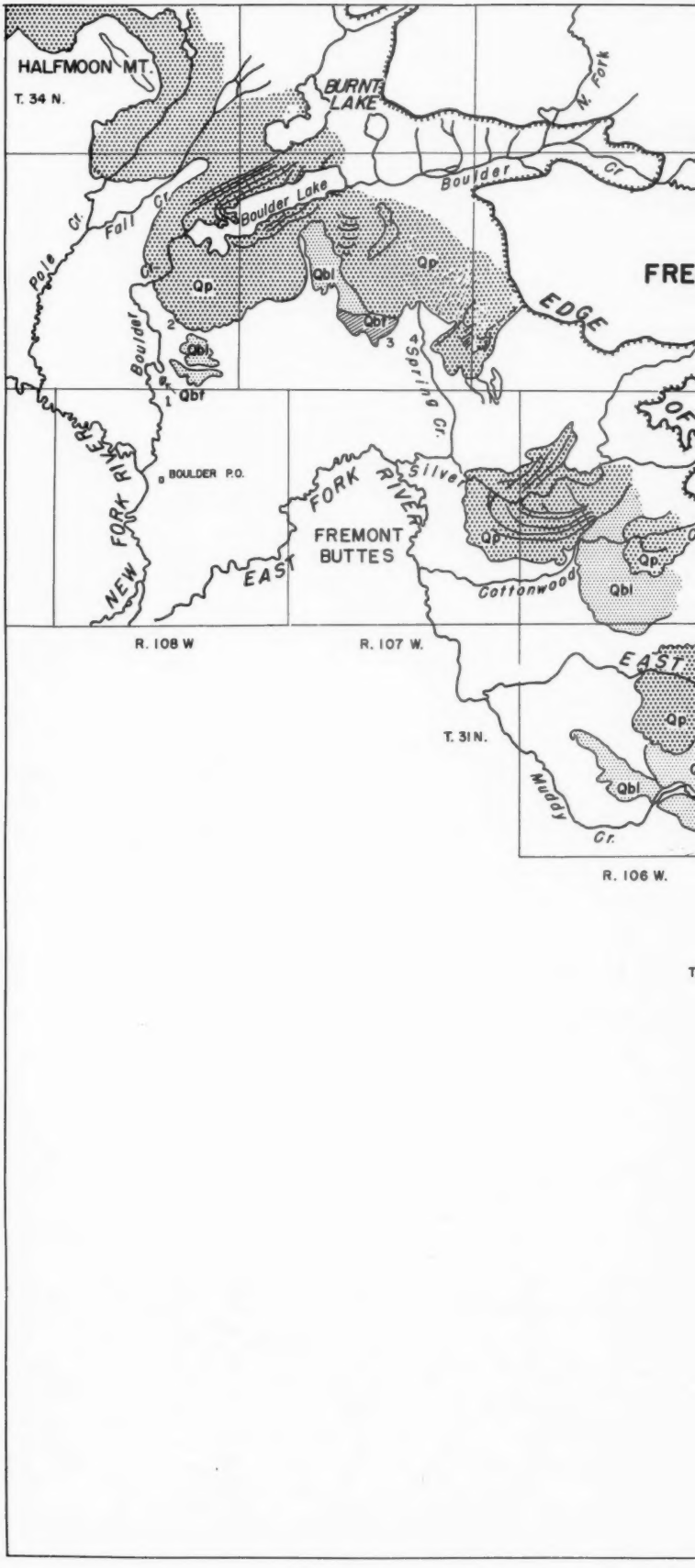
HALFMOON MT.
T. 34 N.
BURNT LAKE
N. Fork
Boulder Cr.
Boulder Lake
Fall Cr.
Pole Cr.
Qp
Qbl
Qbf
FRE
EDGE
Boulder
NEW FORK RIVER
BOULDER P.O.
Spring Cr.
Silver
FORK RIVER
EAST
FREMONT BUTTES
Cottonwood
R. 108 W
R. 107 W.
T. 31 N.
EAST
Muddy Cr.
R. 106 W.

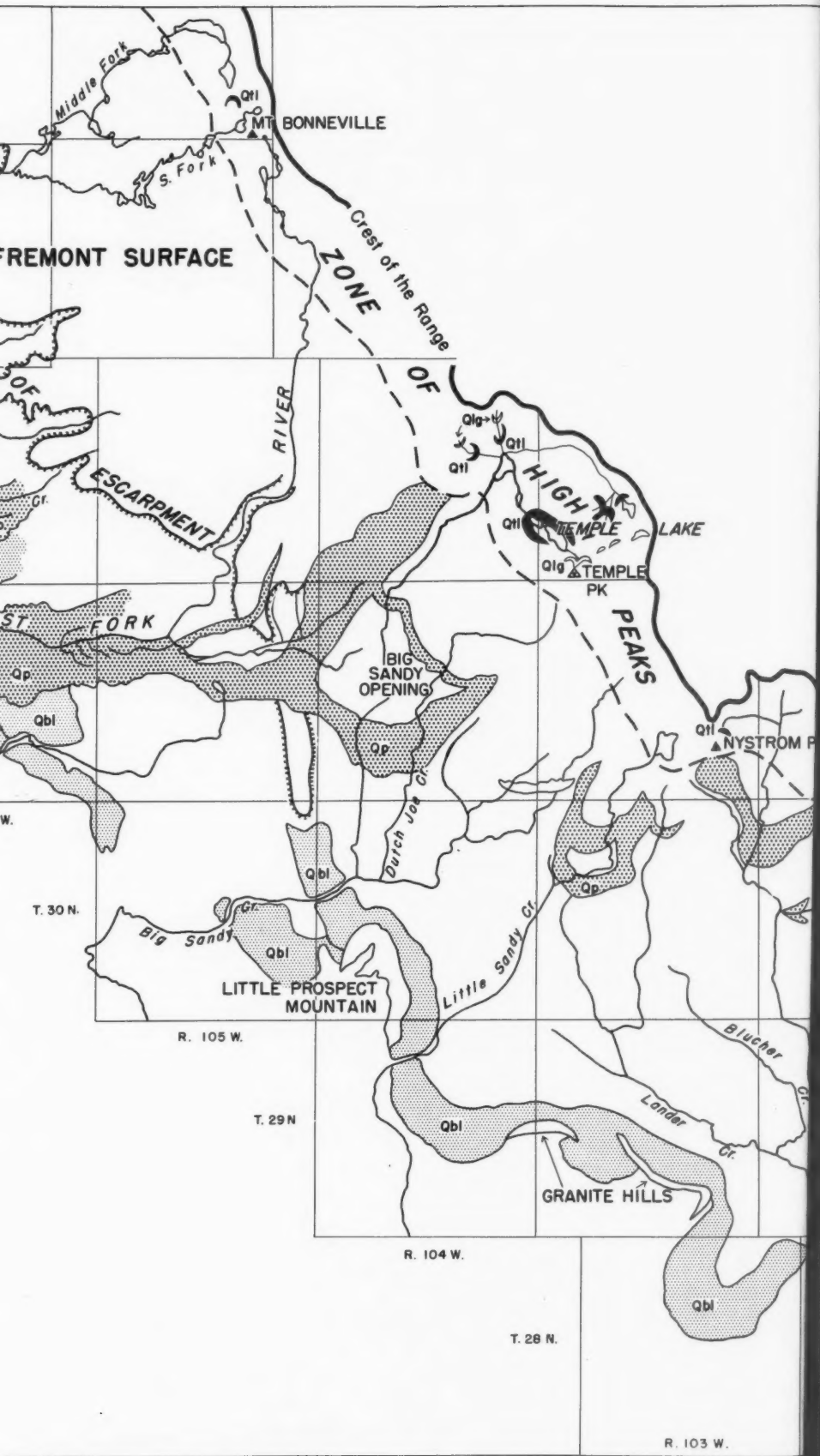

MORAINES OF THE SOUTHWESTERN WIND RIVER RANGE AND BRIDGER BASIN
Mapped by G. William Holmes and John Hall Moss

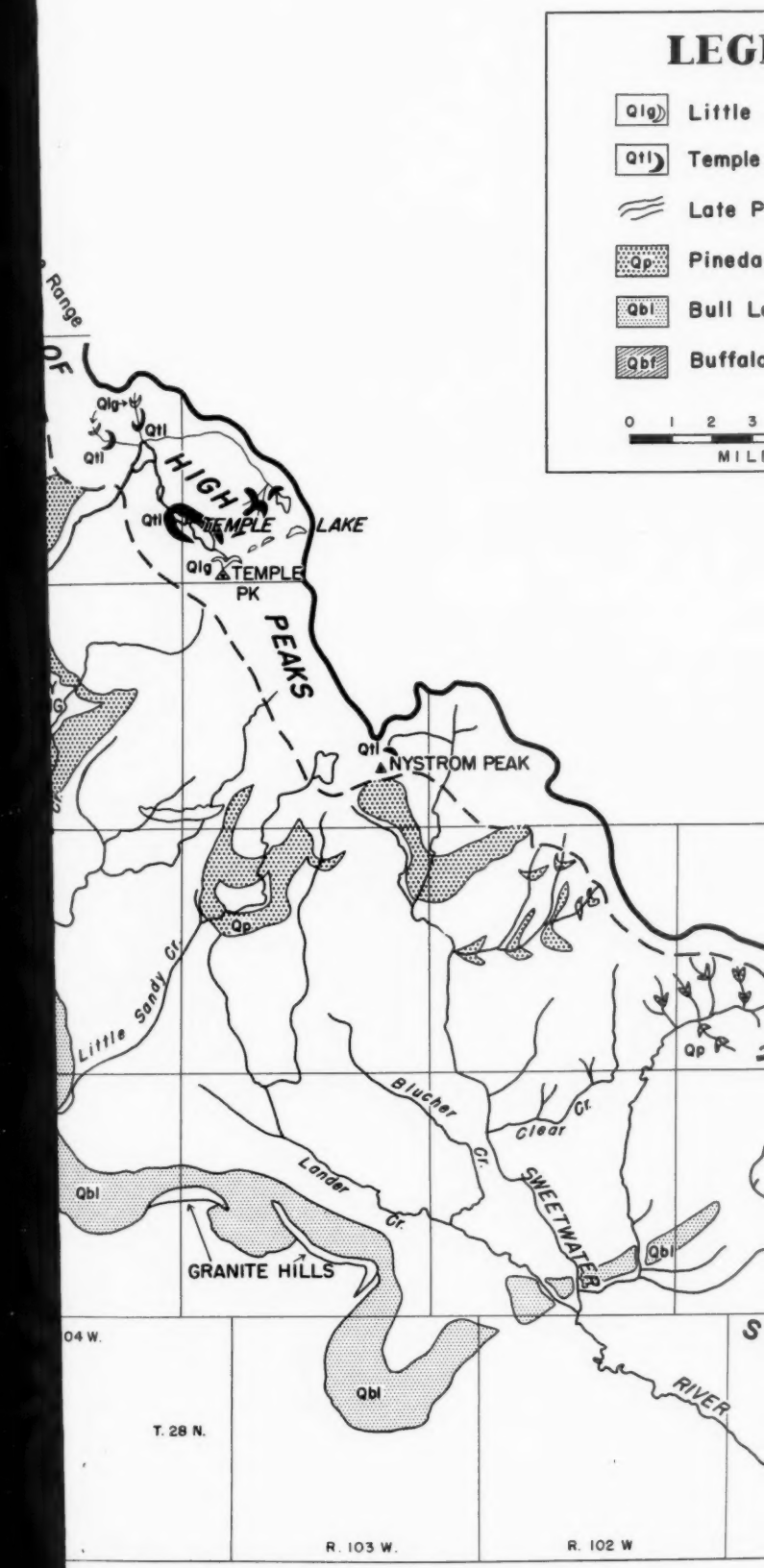

RIVER RANGE AND BRIDGER BASIN
es and John Hall Moss

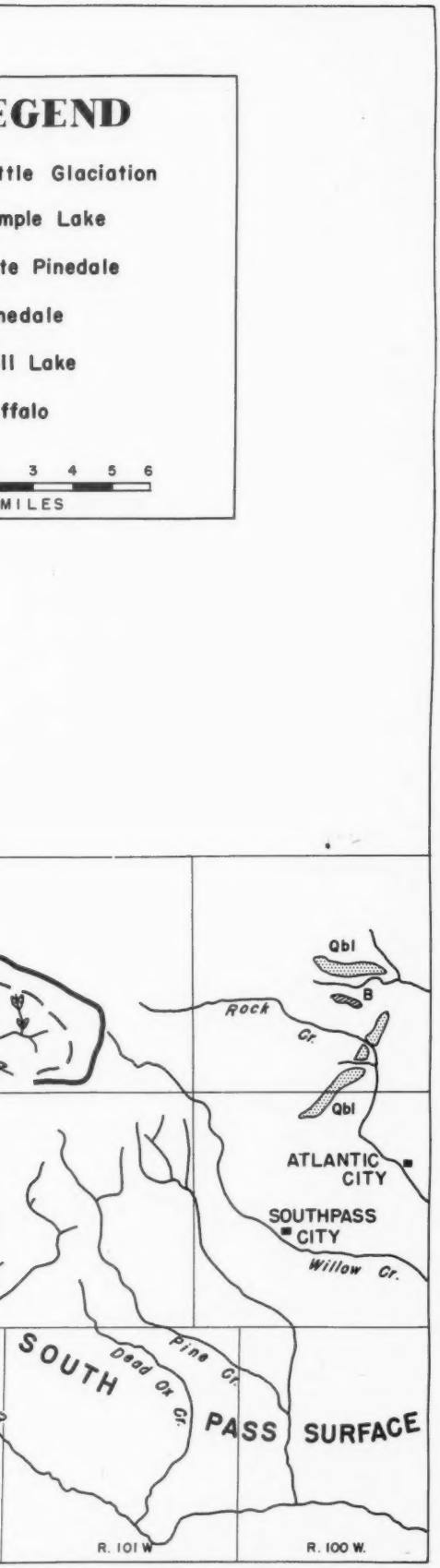
EGEND
ttle Glaciation
mple Lake
te Pinedale
nedale
ll Lake
ffalo
3 4 5 6
MILES
Qbl
B
Rock
Cr.
Qbl
ATLANTIC
CITY
SOUTHPASS
CITY
Willow Cr.
SOUTH
Dead Ox Cr.
Pine Cr.
PASS
SURFACE
R. 101 W.
R. 100 W.

BULLETIN OF THE GEOLOGICAL SOCIETY OF AMERICA
VOL. 66, PP. 629-654, 2 FIGS., 3 PLS. JUNE 1955

PLEISTOCENE GEOLOGY OF THE SOUTHWESTERN WIND RIVER MOUNTAINS, WYOMING

BY G. WILLIAM HOLMES AND JOHN H. MOSS

ABSTRACT

Patches of Buffalo till record the earliest glaciation in the southwestern Wind River Mountains. In places, these rest in youthful valleys cut in high gravel terrace. Two other younger and lower terraces are both topographically and stratigraphically associated with Buffalo till, which may indicate that the Buffalo advance was compound. The pattern of well-preserved moraines shows that during both Bull Lake and Pinedale time the west-central portion of the range was covered by a mountain icecap from which piedmont glaciers flowed to the floor of the Bridger Basin. In the southern part of the range the glaciers were confined to valleys. Bull Lake stage is clearly double; two large, weathered, and modified moraines are present in several valleys. Each is associated with an extensive outwash plain and valley train.

The Pinedale stage is recorded by massive, fresh, slightly modified moraines behind which are many recessional moraines. Extensive outwash aprons lead outward from the massive Pinedale moraines, and a small lower terrace can be traced through the main Pinedale moraine to the recessional loops. In several upper valleys well-formed slightly weathered small moraines of the Temple Lake stage occur within 2 miles of cirque headwalls. A terrace below the younger Pinedale outwash is correlated with the Temple Lake stage. In sheltered cirques, small very fresh moraines, probably from the Little Ice Age, occur upstream from the Temple Lake moraines and a few yards from existing small glaciers. The sequence of glacial deposits in this region is typical of many ranges in the Rocky Mountain region.

Outwash terraces of the Bull Lake, Pinedale, and Temple stages have been traced down the Big Sandy valley nearly to the Green River and down the Sweetwater valley to the North Platte. Thus the Green-Colorado and Platte-Missouri drainages are linked across the Continental Divide by means of traceable outwash deposits. Eolian action was pronounced in the Eden valley during Bull Lake, Pinedale, and post-Pinedale time, and in the East Fork valley during Pinedale time. Frost action features record two phases of intensity in areas formerly covered by Pinedale glaciers: an earlier phase synchronous with the Temple Lake advance, a later during the Little Ice Age. Pollen profiles in the Eden valley show a climatic change during post-Pinedale time, notably a grass maximum which was probably contemporaneous with the Temple Lake advance and the occupation of the Finley site by Early Man.

CONTENTS

TEXT

	Page
Introduction	630
Acknowledgments	631
Geologic and geomorphic setting	632
Glacial erosion	633
Glacial deposition	633
General	633
Toboggan terrace	634
Buffalo till	634
Buffalo (?) and Faler terraces	635
Bull Lake complex	638
Pinedale complex	640
Temple Lake advance	641
Little Ice Age advance	642
Relative chronology of glacial advances	643
Frost action and mass movement	643
Sand dunes	644
Vegetation	645
Early Man	645
Regional pattern of glaciation	645
General	645

Page
Classification 650
Summary 651
Correlation with the Middle West 651
References cited 651

ILLUSTRATIONS

Figure Page
1. Location map 631
2. Terrace profiles 636–637
Plate Facing page
1. Moraines of the southwestern Wind River Range and Bridger basin 629
Facing page
2. Moraines and terraces of the Boulder area .. 634
3. Pinedale moraine around Boulder Lake 640

TABLES

Table Page
1. Characteristics of the moraines 634
2. Sedimentary characteristics of till particles less than 4 mm 635
3. Height of terraces above stream in middle course 638
4. Summary of Pleistocene events 644
5. Typological classification of representative Rocky Mountain glacial deposits 646

Introduction

The Wind River Mountains are located in west-central Wyoming about 100 miles southeast of Yellowstone Park (Fig. 1). The range forms a part of the Continental Divide, extending southeastward for about 110 miles from Togwotee Pass (Lat. 43°45′N.) to South Pass (Lat. 42°20′N.). This massive barrier separates the Wind River Basin on the northeast from the Bridger Basin on the southwest. It consists of a jagged backbone of intensely glaciated peaks over 12,000 feet high which rise above dissected remnants of extensive erosion surfaces. Gannett Peak, altitude 13,785 feet, is the highest mountain in Wyoming and is surrounded by numerous glaciers (Wentworth and Delo, 1931, p. 620–625; M. L. Meier, 1951, M. A. thesis, State Univ. of Iowa). Because of its great height the Wind River Range is ideally suited for the study of Pleistocene mountain glaciation. An icecap and numerous individual mountain glaciers several times covered the area and emplaced a distinctive complex of glacial and glaciofluvial deposits.

The area covered in this investigation includes the southwest portion of the Wind River Range between Boulder Lake and South Pass as well as the valleys of Big Sandy Creek and the Sweetwater River. Although only a few of the summit elevations of the southern half of the range exceed 13,000 feet, relief in this area is great and glaciation was severe. A border escarpment separates the crystalline rocks of the mountains from the sedimentary rocks of the basin, and ranges in height from a few hundred feet in the Big Sandy drainage to over 3000 feet near Green River Lakes. Mountain streams cut the escarpment in deep gorges which during glacial periods provided avenues for ice descent.

Four important drainage systems have their origin in the Wind River Mountains. The Wind-Bighorn system, tributary to the Missouri, is fed by streams flowing down the northeastern flank. The Green River, tributary to the Colorado, originates in a glacier west of Gannett Peak and is augmented by many streams flowing down the southwestern slope. The Sweetwater River, tributary to the North Platte, drains the southeastern end of the range. Tributaries of the Snake River rise in the extreme northwest portion of the mountains.

The area covered in this report lies in the upper reaches of the Green and North Platte Drainages. The northern part of the area is drained by tributaries of New Fork River and Big Sandy Creek which drain into the Green River in the Bridger Basin. The southern part is drained by the Sweetwater River which, after flowing southward toward the Bridger Basin, cuts back eastward through the range and meanders across the southern part of the Wind River Basin to join the North Platte at Pathfinder Reservoir.

During the summers of 1946 and 1947 the authors independently mapped bedrock and Pleistocene deposits in two areas on the southwest flank of the Wind River Range: Moss studied the Big Sandy drainage from Eden to the headwaters; Holmes mapped the southwestern half of the Mt. Bonneville quadrangle and the adjacent portion of the basin around the village of Boulder. In 1949 and 1950, Moss and Holmes jointly mapped the inter-

vening area and extended the study eastward to the mouth of the Sweetwater River and northwestward into the Fremont quadrangle and the Pinedale area. The general sequence

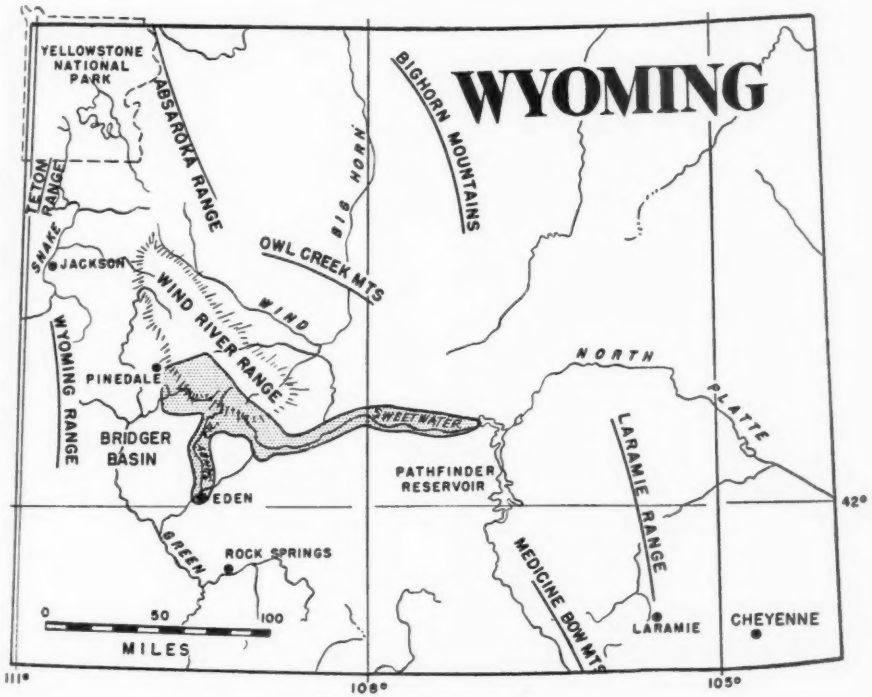

FIGURE 1.—LOCATION MAP
Showing Sweetwater, Big Sandy, and upper Green River drainages.

was established during the first two seasons. The later work—partly on a reconnaissance scale—demonstrated the variety of form taken by the glacial deposits, and established correlations with deposits in adjacent areas. During the 1950 season the writers jointly studied outwash deposits and moraines in the southern part of the range. Terraces were traced to the mouth of Sweetwater River, which extended the correlation of outwash deposits from the Green River across the Continental Divide to the North Platte River.

Although previous reports mentioned evidence for glaciation in the Wind River Range, the first extensive investigation was made in 1915 by Blackwelder. Blackwelder's study furnished the chronological framework for the present inquiry, although it did not include the area here described. In recent years reports on glaciation in other sections of the range have appeared: W. de Laguna (1938, Ph.D. thesis, Harvard University); Branson and Branson (1941; 1945); Miner and Delo (1943); Richmond (1945; 1948); Baker (1946); Miner and Apfel (1946); Blackwelder (1950). Investigations of adjacent ranges, particularly pertinent to this report, were made by Fryxell (1930) in the Teton Range and Horberg (1938) in the Gros Ventre Range.

ACKNOWLEDGMENTS

The authors are deeply indebted to the late Professor Kirk Bryan of Harvard University, a great source of encouragement and inspiration. He generously gave of his energy and time and faithfully visited the field camps each year. Immediately prior to his untimely death

in Cody, Wyoming, he was in Moss's camp in the southern Wind River Mountains.

The writers gratefully acknowledge financial support from the Wennergren Foundation for Anthropological Research, the Penrose Bequest of The Geological Society of America, the Curtis Publishing Company, and the Sheldon Fund of Harvard University. The American Geographical Society, the Union Pacific Railroad, Beloit College, and Franklin and Marshall College lent surveying instruments. Thanks are due the numerous field assistants, notably Margaret Moss, Sheila Holmes, George Biemsderfer, Dr. Alice James, John James, H. B. Stewart, Jr., Kirk Bryan, Jr., Frank Wright, Joseph Hartshorn, Robert Barrel, Sylvester Ludington, Donald Kuhlman, William O. Williams, Robert R. Williams, Richard Donley, Donald Wise, Ervin Brown, Martha Brown, and Jack Zwalley.

The writers are extremely grateful for the help and kindness of Wyoming residents, particularly Miss Ellen Carpenter, Atlantic City; Mr. Fred Stratton, South Pass City; Mr. and Mrs. John Coppes, Farson; Mr. and Mrs. Leonard Priebe, Boulder; Mr. Ed Cazier and Mr. and Mrs. Harold Faler, Pinedale. Special thanks are due Mr. and Mrs. Dennis Mitchell of Boulder for excellent guide service, advice, hospitality, and many other kindnesses. Dr. L. R. Wilson, Dr. Sheldon Judson, and Dr. Herbert E. Wright critically read the manuscript and made valuable suggestions.

Geologic and Geomorphic Setting

The bedrock complex from which glaciers in the southwestern Wind River Mountains derived their materials is markedly simpler than that in other glaciated segments of the range. The complex includes Precambrian crystalline rocks of the mountain core, Paleozoic sedimentary formations of the few small hogback remnants on the flank, and Cenozoic sediments of the Bridger Basin.

The mountain core is composed of metamorphic and igneous rocks. In the South Pass area the Precambrian complex is quartzite, phyllite, schist, greenstones, amphibolite, and altered tuff, cut by quartz veins, mafic dikes, and a granodiorite batholith (W. de Laguna, 1938, Ph.D. thesis, Harvard Univ.). The metamorphic rocks can be traced northwestward toward the upper reaches of the Sweetwater River, where they pass into gneiss and gneissic granites. Farther northwest, in the drainage of Big and Little Sandy Creeks, granitoid rocks are more abundant. From Big Sandy Opening to Mt. Bonneville two distinct granitoid units have been mapped: the Geikie, a pink porphyritic quartz monzonite; and the Raid, of similar composition, but gray and medium-grained. North of Mt. Bonneville the Raid quartz monzonite passes into striped gneisses. In the transition zone between these units are many angular blocks of gabbro surrounded by granitic material. Raid quartz monzonite and small bodies of Geikie quartz monzonite can be traced along the border zone and are presumably in contact with the striped gneisses in the axial portion of the range in the Fremont quadrangle (C. Oftedahl, Personal communication). The moraines along the southwest flank, composed predominantly of crystalline rocks, reflect the pattern of the Precambrian rocks in the mountain core.

Paleozoic strata are nearly absent in the southwest quarter of the range, except for small hogbacks which rise above the outwash deposits in the Boulder area. The glaciers covered a very small area of Paleozoic rocks which contributed only locally to the till and outwash.

The Tertiary sediments lie unconformably on Paleozoic beds in the Boulder area and against the Precambrian complex elsewhere along the western escarpment. They can be divided into two units which were both locally incorporated into the tills. The most extensive is a variegated clay, probably the equivalent of the Hiawatha formation (Nace, 1939, p. 15) south of the Sweetwater River. The upper 10 feet of these beds consists of yellow sand containing scattered iron concretions. The second unit includes scattered patches of white sandy tuffaceous sediments in the "Tertiary outlier" near Leckie's ranch and a similar but more widespread deposit between the headwaters of Sweetwater River and South Pass. This tuffaceous deposit is probably Oligocene in age (Nace, 1939, p. 31–32).

A third group of Cenozoic sediments is composed of granitic, mafic, and quartzitic cobbles

which veneer mesas and buttes in the basin. These beds antedate the oldest till in the area, but may represent earlier glacial stages.

To a great extent the topography governed the glaciation on the southwest flank. The axial portion of the range consists of sharp peaks and ridges separated by short, structurally controlled canyons. Southwest of this area are two high-level erosion surfaces, the Fremont surface on the north and the South Pass surface on the south. The Fremont surface ends abruptly on the southwest in the great border escarpment which is indented by deep canyons. The South Pass surface passes into the Bridger Basin across soft Oligocene beds and is only slightly dissected.

The geologic and topographic features with the most bearing on the glacial history are: (1) the granitic and metamorphic source rocks in the mountains, (2) the Paleozoic and Cenozoic sediments in the basin, (3) the structurally controlled cirques and high valleys, (4) the extensive erosion surfaces, and (5) the great western border escarpment and its canyons.

Glacial Erosion

Several generations of glaciers produced magnificant alpine scenery in the Wind River Range. Many cirques and deep U-shaped valleys were cut in the axial portion of the range by individual valley glaciers. The Big Sandy Lake area, for example, is a great compound cirque, with a characteristic U-shaped valley extending westward in the form of a glacial staircase. Mt. Bonneville is a typical arete, and Pyramid Peak is a horn. Cols are numerous, but few are low enough to provide easy access across the divide (Pl. 1).

Downstream from the cirques glacial erosion assumed two phases. North of Big Sandy Opening the glaciers spread westward on the Fremont surface and formed a large mountain icecap at least 1000 feet thick that covered Twin Buttes in the Mt. Bonneville quadrangle. Here the direction of flow of the icecap was controlled by the general southwesterly slope of the erosion surface, modified locally by the preglacial valleys. On the Fremont surface the icecap produced subdued topography, characterized by many rock-basin lakes, swamps, roches moutonnées, disrupted drainage, and broad areas of polished and striated bedrock. As the icecap grew, it flowed southwestward over the edge of the escarpment, controlled largely by the canyons on the west edge of the high erosion surface.

Southeast of Big Sandy Opening no icecap formed. Here the ice was confined to the valleys and emerged in the basin as piedmont glaciers, the largest of which in the southern portion of the area moved several miles across the Bridger Basin but was partly blocked by the Granite Hills. Three tongues of this glacier extended through saddles in the Granite Hills and formed moraines to the southwest (Pl. 1). In general, glacial erosion was less pronounced south of Big Sandy Opening than elsewhere because of the lower altitude of catchment basins and gentle valley gradients.

Glacial Deposition

General

Each glacial episode produced a characteristic complex of glacial and glaciofluvial deposits. These are unusually well preserved in and around the Wind River Mountains because (1) the materials are largely crystalline rocks highly resistant to weathering, (2) the original volume of the deposits was large, and (3) many were laid down on flat erosion surfaces, wide valley bottoms, or basin floors where postdepositional erosion has not been great.

Both the moraine and outwash facies of the several glacial advances are preserved in this area. Their relationship is clear in the younger stages, but in the older stages the moraines are poorly preserved, and the relationship to their outwash is obscure. However, outwash deposits of all stages are well enough preserved to reconstruct the sequence of meltwater deposition and erosion. The glacial terraces retain their topographic and lithologic identities for scores of miles down the main streams; however, their height above the stream is not uniform, especially in the first few miles downstream from the moraine. Near the moraines, stream gradients are steep, the bedrock is not homogenous, and trenching of the valleys below the outwash has been deep. Therefore, comparative terrace heights in the following description refer to the middle and lower portions

of the streams where the stream gradients and relative terrace heights are generally uniform.

Toboggan Terrace

A high gravel terrace located between Fremont Buttes and Boulder Lake (Pl. 2) antedates known deposition of till in this area since Buffalo till lies in valleys cut in these gravels. The largest remnant of this terrace, due north of the summit of Fremont Buttes, covers more than 2 square miles; the other segment, located west of Spring Creek, is approximately 1 square mile. The southern tip of the western segment is 300 feet above East Fork River; the local relief of the eastern segment is 160 feet above Spring Creek. This height approximates that of several extensive benches near Pinedale, which are covered by granitic, volcanic, and sedimentary cobbles. This bench is here named the Toboggan Terrace for a small creek east of these terraces.

Buffalo Till

Blackwelder (1915, p. 328) named the oldest till in western Wyoming the Buffalo from deposits of deeply weathered till along the Buffalo Fork of the Snake River. According to him and others it typically occurs in low mounds on flat-topped divides which are commonly underlain by soft shales or volcanic rocks and are separated by canyons 200–1000 feet deep. The surface of the type Buffalo deposits is generally smooth, almost devoid of boulders, and exhibits no vestige of glacial morphology. Blackwelder holds that Buffalo till was deposited before the deep canyons were formed and its period of weathering and erosion was exceptionally long. He states, however, that tills resembling Buffalo drift may have been the result of more than one glacial stage.

TABLE 1.—CHARACTERISTICS OF MORAINES

Characteristic	Buffalo	Bull Lake		Pinedale		Temple Lake	Little Ice Age
		I	II	Main	Recessional		
Depth of staining (Inches)	72 (Deepest exposure)	132	132	24–36	24–36	8–12	0
Compaction	Very compact	Compact	Compact	Loose	Loose	Loose	Loose
Trenching of terminal moraine	No moraine	Broad valleys	Broad valleys	Narrow channel	Narrow channel	Slight trenching	No channel
Wastage of moraine	Nearly complete	Moderate	Moderate	Slight; hummocky	Slight	Very slight	None
Boulders on moraine	Weathered to dark colors	Moderately weathered	Moderately weathered	Slightly weathered	Slightly weathered	Perceptibly weathered	Very fresh
Boulders within moraine	Rotted	A few rotted; most stained	A few rotted most stained	Fresh	Fresh	Fresh	Fresh
Size of moraine (feet)	Low, broad 10–30	Low to massive 110–500	Low to massive 100–500	Massive 160–400	Small 30–75	Small 50–90	Very small 30–50

Such till occurs at the following localities (Pl. 1): (1) On the west side of a small Paleozoic hogback about 2½ miles north of Boulder, partly below the surface of the Bull Lake I outwash plain, 80–135 feet above Boulder Creek, deeply weathered till exhibits the local influence of the Paleozoic limestone on which it lies, but is composed largely of granitic materials from the mountains. (2) 4 miles north of Boulder along the main irrigation canal, Bull Lake till lies unconformably against Buffalo till. (3) 4 miles north of Fremont Buttes, Buffalo till lies against the eroded face of the Toboggan Terrace which clearly antedates Buffalo time. Downstream from this till is the beginning of a widespread gravel deposit, which, because of its position, is regarded as Buffalo outwash. (4) On the west bank of Spring Creek adjacent to Pennock's fish ponds, excavating machinery exposed Buffalo drift nearly at stream level. At this locality, two distinct outwash terraces occur which may have been associated with Buffalo glaciation. The higher is in contact with Buffalo till, and

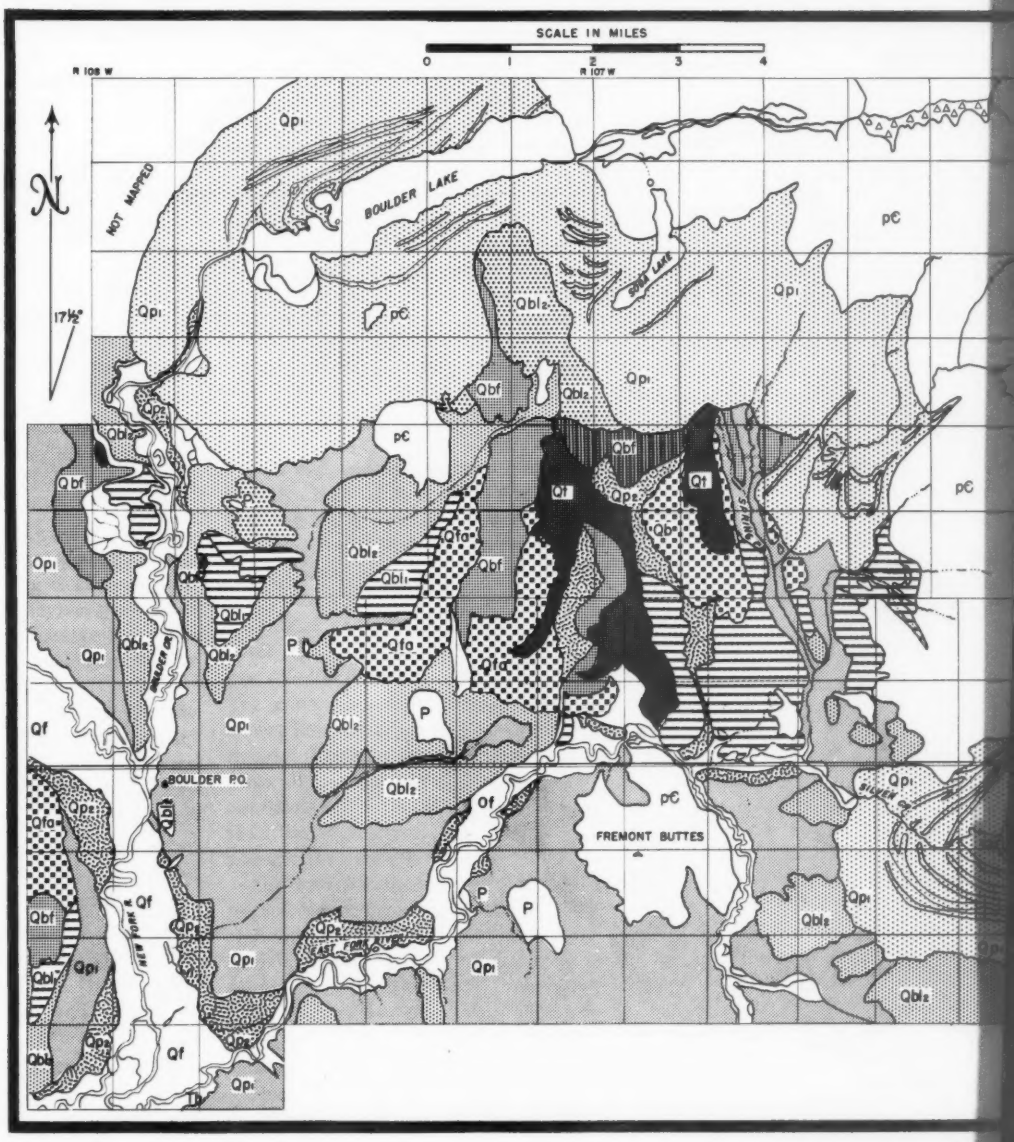

MORAINES AND TERRACES OF THE BOULDER AREA
West-central sector of the Wind River Mountains.
Mapped by G. William Holmes, Sheila Holmes, Joseph Hartshorn, and Robert

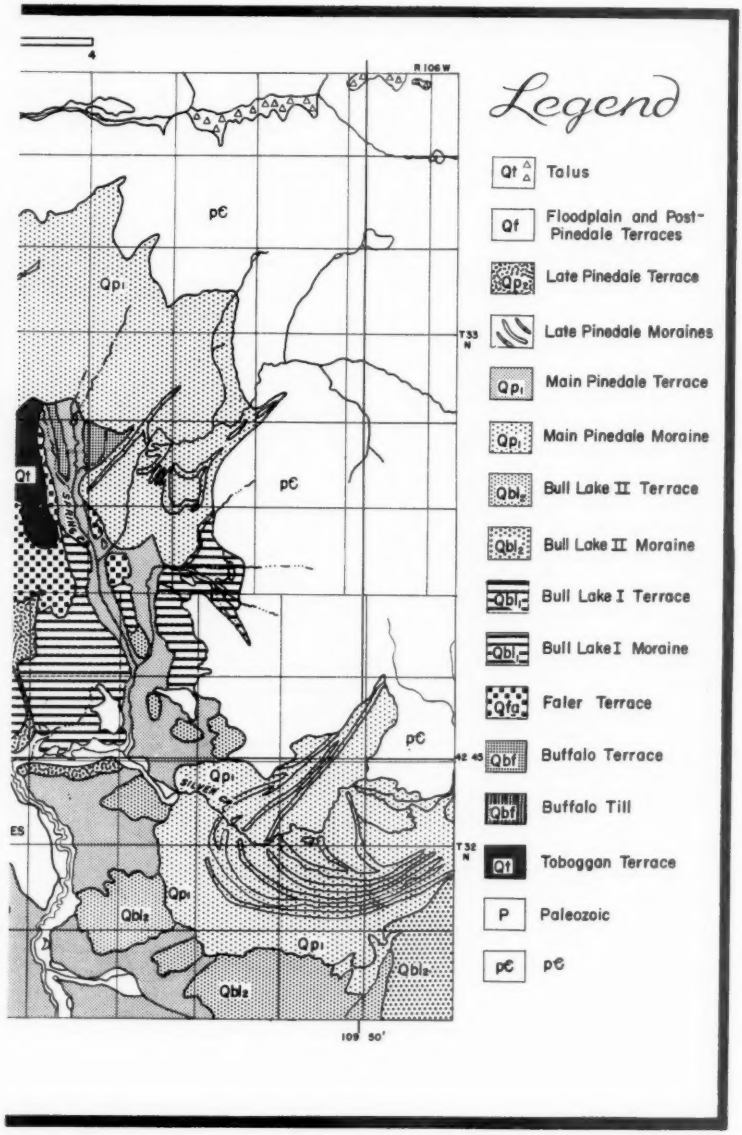

ES OF THE BOULDER AREA
the Wind River Mountains.
Holmes, Joseph Hartshorn, and Robert Barrell

is named the Buffalo terrace. The lower is named the Faler terrace. (5) Chocolate-colored Buffalo till occurs on a hill about 2 miles southwest of the junction of Lander Creek and the Sweetwater River.

firmed the field observations that Buffalo till was derived essentially from the granitoid rocks of the mountains, and has suffered a relatively long period of weathering, alteration, and erosion.

TABLE 2.—SEDIMENTARY CHARACTERISTICS OF TILL PARTICLES LESS THAN 4 MM

Characteristic	Buffalo	Bull Lake		Pinedale	
		I	II	Main	Recessional
Median size (mm)	0.38	0.38	0.44	0.43	0.31
Sorting coefficient	4.20	2.86	5.02	4.13	3.96
Per cent of clay size	5.1	3.5	6.1	5.8	4.1
Liquid limit per cent	50	62	55	30	....
Volume per cent of altered minerals	60	40	30	4	....
Thermal analysis	Some clay	Little clay	Little clay	No clay	....

These exposures demonstrate that buffalo till was emplaced, after the deposition and youthful dissection of the Toboggan terrace, no more than 135 feet above the present streams, and in one place (locality 4) nearly at stream level, which indicates exceptionally little subsequent downcutting of streams; that Buffalo till is associated with two gravel terraces, suggesting that this advance was compound; and that Bull Lake ice and meltwater flowed over Buffalo till.

This till in low, formless mounds, is sparsely dotted by deeply weathered and stained boulders, is itself stained and weathered to the base of a 6 foot exposure, and undoubtedly has been altered by ground water to a much greater depth. It is light gray, except where stained brown or red around the rotted boulders. Mechanical analysis reveals that the size distribution of the component grains does not differ significantly from the particle-size distribution of the younger tills. However, the Atterberg liquid limit test and differential thermal analysis show that it is distinctly plastic and contains clay minerals, indicating long periods of weathering (Table 2). More significant is the high percentage of altered and nearly opaque hornblende and biotite grains in the heavy mineral fraction, which suggests a prolonged period of chemical alteration by descending water. All laboratory tests con-

Buffalo(?) and Faler Terraces

Two high outwash terraces which are near the large body of Buffalo till 4 miles north of Fremont Buttes (locality 3) were deposited in the Toboggan-Bull Lake interval. These terraces, dissected by late Pleistocene streams, can be traced downstream to the New Fork River and up New Fork River and Boulder Creek (Pl. 2). The upper terrace (Buffalo?) lies 130–190 feet above the present streams. The gravels are more than 30 feet thick on Spring Creek, but are only a few feet thick on Boulder Creek where they veneer Tertiary clays. On Spring Creek (Fig. 2) this upper (Buffalo?) terrace buries Buffalo till, and thus must be regarded as interfingering with or younger than Buffalo moraine.

The lower terrace, here named the Faler terrace, is older than both of the Bull Lake terraces and is not physically associated with Buffalo till. It is 100–135 feet above the present streams. The Buffalo(?) and Faler terraces are equally extensive (Pl. 2) and each are separated from younger and older terraces by a substantial and persistent height interval.

Since the Buffalo(?) and Faler terraces lie in valleys cut in Toboggan gravels, and because Bull Lake and younger terraces were deposited in valleys cut in Faler gravels, these gravels were apparently emplaced in the Toboggan-Bull Lake interval. These terraces could be

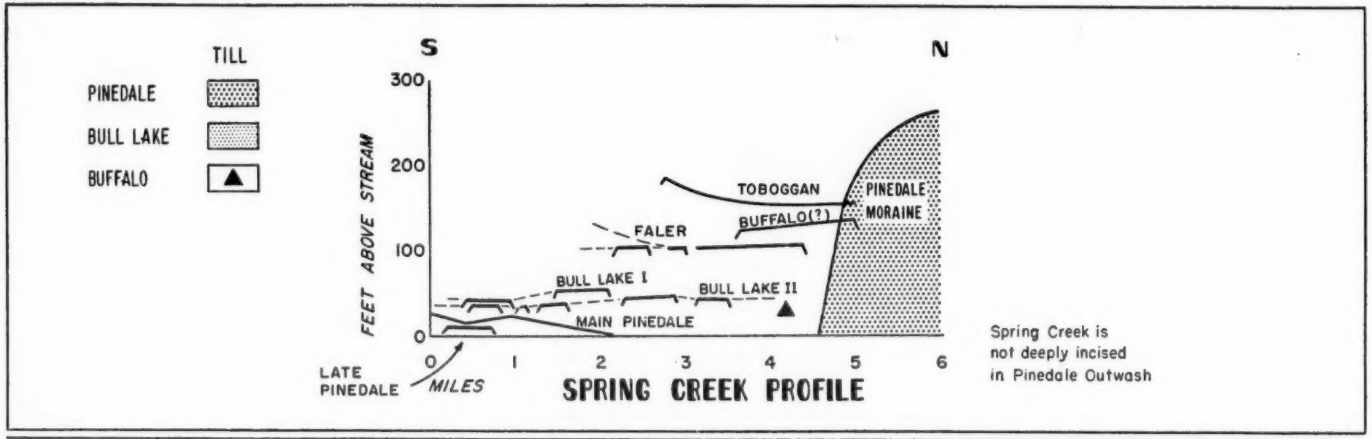
TILL
PINEDALE
BULL LAKE
BUFFALO
S
N
300
200
100
0
FEET ABOVE STREAM
TOBOGGAN
PINEDALE MORAINE
BUFFALO(?)
FALER
BULL LAKE I
BULL LAKE II
MAIN PINEDALE
LATE PINEDALE
0 1 2 3 4 5 6
MILES
SPRING CREEK PROFILE
Spring Creek is not deeply incised in Pinedale Outwash

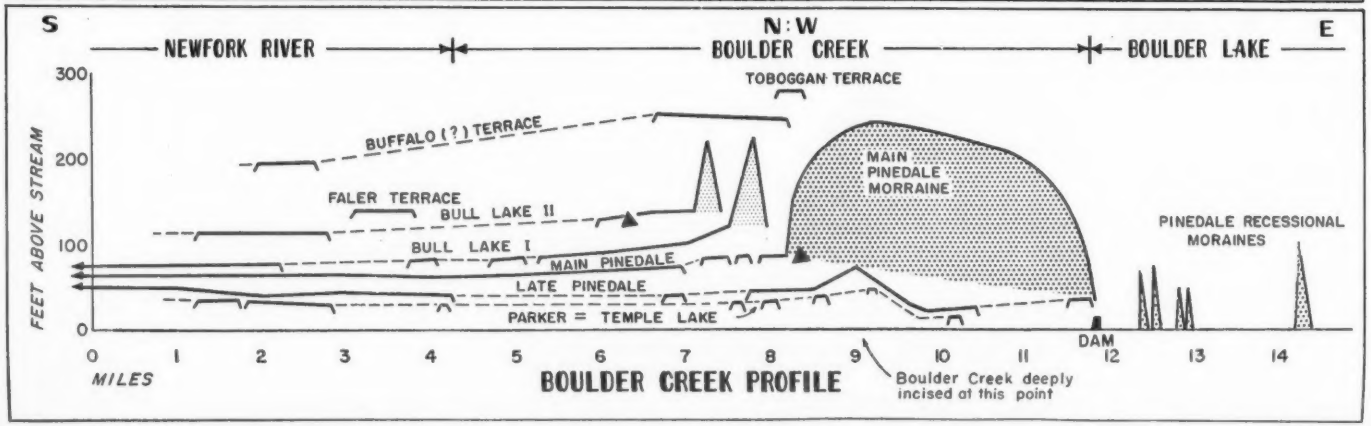
S
N:W
E
NEWFORK RIVER
BOULDER CREEK
BOULDER LAKE
300
200
100
0
FEET ABOVE STREAM
TOBOGGAN TERRACE
BUFFALO (?) TERRACE
FALER TERRACE
BULL LAKE II
BULL LAKE I
MAIN PINEDALE
LATE PINEDALE
PARKER = TEMPLE LAKE
MAIN PINEDALE MORRAINE
PINEDALE RECESSIONAL MORAINES
DAM
0 1 2 3 4 5 6 7 8 9 10 11 12 13 14
MILES
BOULDER CREEK PROFILE
Boulder Creek deeply incised at this point

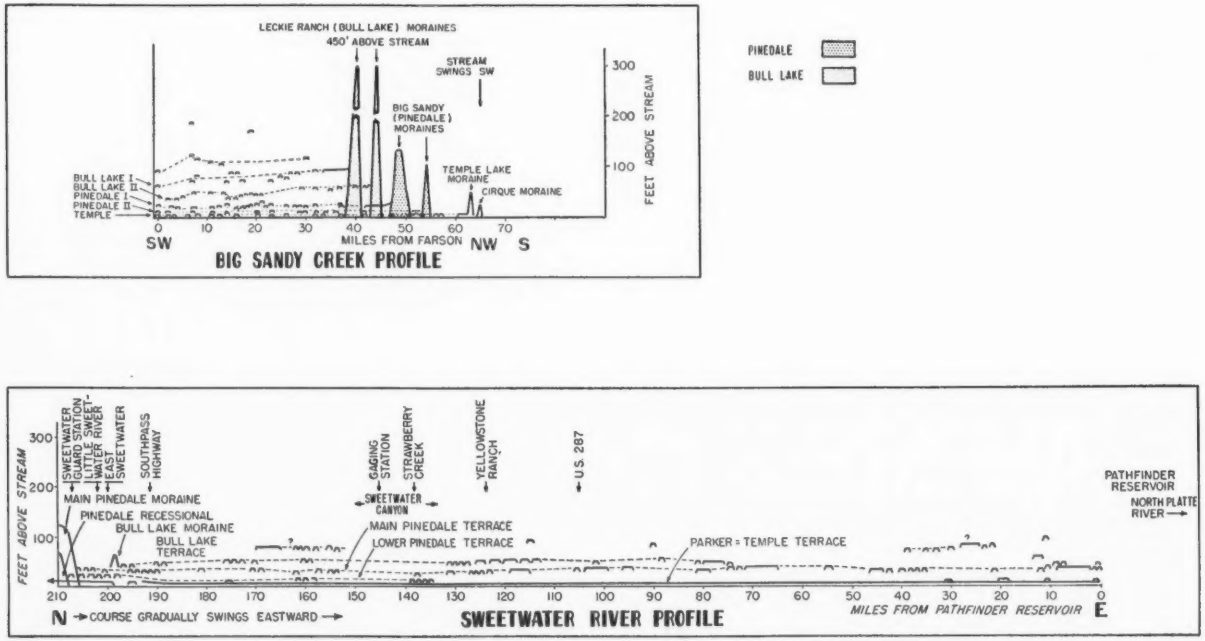

FIGURE 2.—TERRACE PROFILES

Traced along Spring and Boulder creeks in the Boulder area, along Big Sandy Creek from Temple Lake to Eden, and along the Sweetwater River from the Pinedale moraine to Pathfinder Reservoir.

the result of glaciation, uplift of the Wind River Range, or a combination of these two events.

The Buffalo glaciers were probably as large as, if not larger than younger glaciers, and unthroughout the Rocky Mountains for a major uplift during the Pleistocene in the interval that corresponds to the Buffalo-Bull Lake interstadial. This uplift did not affect the

TABLE 3.—HEIGHT OF TERRACES** ABOVE STREAM IN MIDDLE COURSE
(In feet)

Stream system	Toboggan	Buffalo	Faler	Bull Lake		Pinedale		Parker (Temple)	Little Ice Age (Floodplain)	Remarks
				I	II	Main	Recessional			
Boulder Creek	....	195	135*	105	75	65	45	32	0–5	.....
Newfork										
East Fork										
Main stream	300	...	.....	85	60	33	20	.....	0–5	.....
Spring Creek	160*	130	100	50	32	20	10	.....	...	Minor tributary with well-preserved older terraces
Big Sandy Creek	....	?	?							No Buffalo moraines on Sandy Creek
		175	100 Camp	73 High Eden	44 Low Eden	20 Upper Farson	10 Lower Farson	4* Parker	...	
Sweetwater river	Several high, well-preserved terrace remnants in lower course			55		35	12	5	...	Terraces east of Sweetwater canyon best preserved

* Type area.
** Altitude above present grade of smooth line drawn through plotted terrace remnants.

doubtedly provided abundant detritus to their meltwater streams. These outwash gravels probably have not been completely destroyed, for even older gravels (Toboggan terrace) have withstood the meltwater erosion of subsequent glaciations. Because the upper terrace buries Buffalo till, this terrace is contemporaneous with or older than the Buffalo advance. In the absence of other gravels in the area which occupy the Buffalo stratigraphic interval, the upper terrace is tentatively correlated with the Buffalo advance.

The lower of these two gravel benches, the Faler terrace, does not differ lithologically or morphologically from younger or older terraces, and offers no hint of its origin. There is no evidence in the area as to whether the Faler terrace is the result of a recessional phase of Buffalo glaciation, a separate ice advance, or uplift of the mountains. Blackwelder (1915) suggested that the Buffalo stage may be a double glaciation, and Richmond (1948, p. 1401) attributes two terraces in the northwest Wind River Range to Buffalo glaciation. On the other hand, there is widespread evidence

portion of the Bridger basin here described, although it is possible that the Wind River Range proper rose at this time, and gravels were deposited at its foot in the basin.

Bull Lake Complex

Blackwelder (1915, p. 325) named the Bull Lake stage on the basis of well-preserved but erosionally modified moraines on the east side of the range near Bull Lake, which he believed related to the Circle terrace. The degree of erosion, the position of the moraines in the valleys, outwash relationships, and weathering of the tills and surface boulders demonstrate that the Bull Lake moraines are younger than the Buffalo stage but older than Pinedale. Similar moraines are prominent features in many valleys of the southwestern Wind River Mountains (Pl. 1). In many valleys there are two separate but topographically similar Bull Lake moraines, noticeable especially in Big Sandy valley, where the paired moraines escaped the full force of Pinedale ice and meltwater.

Because the South Pass surface flanks the

range in this area, Bull Lake ice was able to move 14–20 miles from the cirques with little obstruction and without descending below 8000 feet. The ice moved as a piedmont glacier across the "Tertiary outlier" to the Granite Hills where it pushed narrow tongues through low saddles and constructed moraines on the slopes leading to the Bridger basin. These moraines, which are especially well developed on the Boulder-Big Sandy Opening road west of Leckie's Ranch, are easily differentiated from the later Pinedale deposits which lie 8–10 miles upstream.

Southeast of the Granite Hills the ice penetrated farthest into the basin, crossing the Continental Divide between Sweetwater River and Pacific Creek. Lack of topographic obstructions and the steep southerly slope of the Pacific-Sweetwater divide aided in this crossing.

In addition to forming massive moraines in the Big Sandy-Sweetwater area, Bull Lake ice deposited vast quantities of ground moraine which buried the maturely dissected pre-Bull Lake landscape. Subsequent erosion of glacial deposits is exhuming the ancient bedrock topography of the "Tertiary outlier."

North of Big Sandy Creek, Bull Lake glaciers were deployed on the basin floor in the valley of Muddy Creek and Boulder Creek, but descended only to the foot of the escarpment in Cottonwood and Scab Creek valleys (Pl. 1). The paired Bull Lake moraines are stratigraphically distinct, as demonstrated by: (1) Bull Lake I moraines are farther downstream from Bull Lake II moraines in Boulder, Muddy, and Big Sandy valleys; (2) Bull Lake II outwash was deposited in the valleys below the level of Bull Lake I outwash, signifying that a period of trenching followed deposition of Bull Lake I outwash; (3) composition differs, for example, in Boulder valley, Bull Lake II till contains mustard-yellow clay and sand, and cobbles of fossil wood and quartzite, whereas Bull Lake I till does not. The stratigraphic and topographic position of Bull Lake drift clearly shows that Bull Lake is a compound stage, younger than Buffalo but older than Pinedale.

In contrast to the formless Buffalo deposits, Bull Lake tills occur in recognizable moraines and are notably less weathered. In Big Sandy and Sweetwater valleys the end moraines have a relief of 200–500 feet, owing in part to their position on bedrock ridges. The combined width of the two moraines is ordinarily 3–4 miles, the older being wider than the younger. The moraines have moderately steep fronts, but are noticeably dissected and have no undrained hollows. Moderately weathered crystalline boulders are abundant on the surface. Many boulders and cobbles beneath the surface crumble readily under a hammer blow. As is Buffalo till, Bull Lake till is compact and difficult to excavate. Depth of oxidation was not readily determinable owing to lack of deep cuts. An 11-foot auger hole, however, failed to reach unoxidized till. Near the south end of the range, oxidized Bull Lake till is yellow brown, whereas oxidized Buffalo till is chocolate-colored. Near Boulder, Bull Lake II till is locally mustard yellow and Bull Lake I yellow brown (Table 2). Both are similar to the other tills (Table 2) but locally contain more Tertiary material. Bull Lake till stands intermediate between Pinedale and Buffalo tills in respect to degree of weathering as expressed by soil and staining depth, percentage of opaque and altered minerals, and number of boulders on the surface. Samples of Bull Lake II till analyzed differ somewhat from samples of Bull Lake I. However, these differences are small compared to the differences between Bull Lake tills and Buffalo or Pinedale tills.

Although Bull Lake outwash has been considerably modified by erosion, its relationship to the Bull Lake moraines can be seen. Well-developed outwash plains extend downstream from the two Bull Lake moraines as a pair of river terraces, the lower 20–40 feet below the upper. Near the Big Sandy bridge downstream from Leckie's ranch, dissected outwash gravel interfingers with the outer Bull Lake moraine. This outwash extends down Big Sandy Creek as the gravel veneer of the highest terrace on the west side of the stream. Remnants of this gravel terrace, found about 80 feet above the creek at the bridge, have been traced to Eden 40 miles south. The lower Bull Lake terrace, which rises about 60 feet above the stream, is correlated with the small outwash plain of the younger Bull Lake moraine immediately west of Leckie's ranch.

Extensive Bull Lake terraces are preserved in the Boulder area, where they occur again at two distinct levels. They are sharply delineated

from the higher Buffalo terraces, which occur several miles from the main streams, and can easily be distinguished from the widespread Pinedale outwash plains, which lie within the cut banks of the Bull Lake II valley train (Fig. 2). The older, higher Bull Lake outwash plain is in contact with the outer Bull Lake moraine, and the lower Bull Lake terrace can be traced around the remnant of the older Bull Lake outwash plain and moraine and to the younger moraine which lies a few hundred yards upstream.

Two high terraces, approximately 60 and 90 feet above the Sweetwater River, are probably the outwash facies of Bull Lake glaciation (Fig. 1). However, most of the meltwater from the Bull Lake glaciers in the upper reaches of the Sweetwater was channeled into the Bridger Basin to the southwest, and only a small lobe crossed the main valley of the Sweetwater River (Pl. 1). Pinedale outwash can be traced upstream through the Bull Lake moraine on Sweetwater River, but the 60- and 90-foot terrace fragments extend only to the Bull Lake moraine (Fig. 2). It is likely that at least the 60 foot terrace is Bull Lake outwash. Although the terrace-moraine relationships on the Sweetwater are less clear than in other drainages, the persistence of probable Bull Lake terrace remnants to the mouth of the river suggests that the regime of the stream was affected in Bull Lake time.

Pinedale Complex

The moraines of the Pinedale stage were described by Blackwelder (1915, p. 324) in many valleys and in particular "around each of the large lakes near Pinedale and on the southwest of the Wind River Range." One of the lakes is undoubtedly Boulder Lake (Pl. 1). He describes Pinedale moraines as being very rough, covered with slightly weathered boulders and mostly undissected.

Such moraines, present in every major valley (Pl. 1), generally lie upvalley from the Bull Lake moraines. In the Boulder Lake and Silver Creek Basins, however, Pinedale ice overrode some of the Bull Lake deposits. Pinedale terminal ramparts are commonly higher, more extensive, and greater in cross section than older moraines. On Boulder, Spring, Silver, and Cottonwood creeks, tongues from the icecap on the Fremont surface pushed down the gorges in the border escarpment and built vast arcuate moraines on the floor of the Bridger Basin. These moraines, with relief of 200–400 feet, are 18–20 miles from the cirques, at elevations averaging 7600 feet. In the Big Sandy and Sweetwater drainages, Pinedale moraines are at elevations of 8500–9500 feet and are only 8–10 miles from the cirques.

In most valleys Pinedale moraines are compound; in contrast to those of the Bull Lake stage, component Pinedale moraines are distinctly unequal in size. In some valleys, such as Boulder Lake basin, at least seven recessional moraines lie within the massive terminal moraine (Pls. 2, 3). Big Sandy valley, on the other hand, has two prominent Pinedale moraines 3 miles apart, plus several small eroded remnants representing recessional halts. In Little Sandy and Sweetwater valleys, Pinedale morainal ridges are smaller and lie farther upstream.

The compound nature of the inner recessionals on the Pinedale moraines is well exhibited in Silver Creek basin and on the steep shores of Boulder Lake (Pl. 3). The minimum slope of the ice front during the early part of the Pinedale retreat is suggested by the slope of these minor lateral ridges. In Boulder Lake basin, the crests of these ridges are progressively steeper in the direction of glacial recession. The individual ridges range from 25 to 60 feet in height. The recessional moraines are commonly interspersed with outwash deposited between the ice and the valley side, or between the recessional moraine and the ice. Possibly in some instances a trough between the morainic ridges was deepened by meltwater.

Because of similarities in weathering characteristics, no long time interval is believed to separate deposition of the successive Pinedale recessional moraines. No significant pattern of the several Pinedale recessionals can be traced from valley to valley.

Pinedale moraines display more pronounced glacial topography and less evidence of weathering than Bull Lake and Buffalo deposits. The moraines are steep-fronted and little dissected. They are heavily strewn with boulders, which show signs of only slight weathering.

PINEDALE MORAINE AROUND BOULDER LAKE
Showing outwash deposits in front of the moraine, the hummocky topography of the main Pinedale moraine, and the many recessionals along the steep lake shores.

The moraine surface is hummocky and pitted with kettle holes. The till is composed almost entirely of crystalline rocks, except for the moraines in the New Fork River drainage which contain a small admixture of Tertiary sand and clay. The unoxidized till is light gray. Mechanical analysis shows that in respect to size distribution Pinedale till does not differ significantly from the other tills (Table 2).

Liquid limit, X-ray, and differential thermal analysis revealed no significant amount of clay minerals. Thus particles finer than .0039 mm, which constitute about 2 per cent of the till, consist essentially of finely pulverized granitic minerals. Limonite staining extends downward 24–36 inches. The till is loosely packed and can be easily excavated. All the characteristics of Pinedale morainic deposits indicate that it has endured a short period of weathering, notably less than that to which Bull Lake drift has been exposed.

Pinedale outwash is abundant in all major valleys. Fresh, barely dissected outwash plains merge with moraines in the Sweetwater, Little and Big Sandy, Muddy, East Fork, Silver, and Boulder valleys (Fig. 2; Pl. 2). Two separate valley trains are usually associated with the Pinedale advance. The more extensive is a continuation of the broad outwash plains which are in contact with the outer, massive, steep-fronted morainal loops. This broad outwash deposit represents the long period of stable conditions during which the enormous Pinedale ramparts were constructed. It is most prominent in the vicinity of Boulder Post Office, where it is 4 miles long and 3 miles wide. In every valley, the upper or main Pinedale terrace is the most conspicuous, rising 20–75 feet above the stream.

Below the main Pinedale terrace is a less extensive gravel deposit, which passes through the narrow channel cut in the Pinedale moraine and merges with one or more of the small outwash plains of the recessional loops. Actually a composite terrace representing several recessional halts, it rises 10–50 feet above the present streams. It is everywhere distinct from the main Pinedale outwash, against whose cut face it was deposited. This lower terrace, in spite of its narrow width, retains its identity for at least 40 miles in the Big Sandy valley. The lower terrace was formed subsequent to the trenching of the Pinedale moraines and outwash and in Boulder Basin was penecontemporaneous with wave erosion on the shores of a proglacial lake. The lower Pinedale terrace is constructional near the recessional moraines but is essentially erosional through the main Pinedale moraine. It is, at least in part, a depositional feature immediately downstream from the main Pinedale moraine. For example, in Boulder valley below the moraine the lower Pinedale terrace is strewn with huge boulders, probably emplaced by ice-rafting. The two Pinedale terraces do not have the same significance as the two Bull Lake terraces because (1) the Bull Lake moraine systems consist of two massive, equally developed moraines, whereas the Pinedale system is composed of the outer massive moraine and two to seven minor inner moraines, clearly recessional in character; (2) Bull Lake I and Bull Lake II outwash plains are approximately equal in area, which indicates a long period between the Bull Lake I and Bull Lake II maxima during which a broad valley was cut in the Bull Lake I valley train. The lower Pinedale terrace, in contrast, is narrow, indicating a short period between deposition of upper Pinedale valley train and the lower Pinedale gravels. The designation "Pinedale I" and "Pinedale II" should not be used in a sense which implies they are distinctly separate and equal advances.

In addition to outwash plains and terrace, numerous kames and kettles are present in the Pinedale complex. These occur in Big Sandy Opening and peripheral to and within the great Boulder Lake moraine.

Temple Lake Advance

In a report of the Big Sandy drainage, Hack (Howard and Hack, 1943, p. 239–240) reported a prominent moraine and outwash plain north of Temple Lake and Temple Peak. On the basis of this moraine and a study of the terraces along Big Sandy Creek, he postulated the Temple Lake stage. Later work by Richmond (1948, p. 1400), G. W. Holmes (1949, Ph.D. thesis, Harvard Univ.), and Moss (1951) has shown that in many valleys small but distinct moraines, similar to Temple Lake moraines, occur 10–20 miles upstream from the Pinedale moraines within a few miles of

cirque headwalls (Pl. 1). Stratigraphic position of the Temple Lake phase is most clearly shown by the location of the moraines and the weathering of the till. Moreover, the outwash where recognized also demonstrates a distinct period of alluviation after the late Pinedale recessional phase and before the Little Ice Age and the formation of the modern flood plain.

North of Temple Lake at an altitude of 10,700 feet, a bouldery crescent-shaped moraine blocks the valley leading from the north-facing cirque of Temple Mountain. The front of the moraine consists principally of a wall of gigantic angular blocks up to 40 feet in diameter interspersed with patches of sandy till. The west lateral moraine is capped with angular blocks; the east lateral moraine is grass-covered. Extending downvalley from the moraine is a grassy outwash plain which continues as a low terrace down Big Sandy Creek.

Similar steep-fronted moraines occur at the same altitude in front of north-facing cirques in the Deep Lake and Black Joe valleys near Temple Lake. Arrowhead and Bluelakes are also dammed by Temple Lake stage moraines formed by south-flowing ice. Other moraines of this stage occur in Middle Fork canyon (north of Mt. Bonneville) and at the headwaters of the Sweetwater River in the Nystrom Peak cirque. All the Temple Lake moraines occur above timberline in sheltered, north-facing cirques (Pl. 1).

Temple Lake moraines are steep-fronted, rise 50–90 feet above the outwash plain, and ordinarily are about 200 feet broad. The surface is strewn with large, angular, lichen-covered and slightly oxidized boulders. Between the boulders a thin, grass-covered soil, 4–6 inches deep, mantles the till. Limonite staining of the till extends to a depth of 12 inches, in contrast to an average of 30 inches in Pinedale till. The boulders on the lateral moraines commonly merge with old, stable talus piles which rest on the canyon sides. Mechanical analysis of Temple Lake till from the Middle Fork of Boulder Creek shows that the particle-size distribution of the fraction less than 10 mm in diameter does not differ markedly from the older tills deposited in Boulder valley (Table 2). This is remarkable, as here Temple Lake ice moved less than a mile from the headwall. It suggests that a substantial amount of very fine particles is produced in the cirques and during the first mile of glacial advance. The general characteristics of the Temple moraines indicate that considerable time separated this advance from both the Pinedale maximum and the Little Ice Age of historic time.

Although the terraces below the Pinedale outwash are narrow, they are remarkably persistent. The terrace immediately below the lower Pinedale terrace, here named the Parker Terrace, is well developed in the lower Boulder, East Fork, Sandy, and Sweetwater valleys and can be traced upstream through all the Pinedale moraines. The outwash is also preserved in the upper valleys and is in contact with the Temple Lake moraines. In some canyons the Temple Lake terrace is poorly preserved. The persistence of the Temple Lake outwash is notable in the lower Sweetwater canyon, where it is the best-preserved valley train. In most places the terrace is about 5 feet above the stream, but in the middle Boulder valley modern trenching has left the Temple Lake terrace 35 feet above the stream. This terrace is composed of sand and silt, a reflection of the weakness of the Temple Lake advance.

Little Ice Age Advance

In the upper Sandy drainage, about 10,800 feet, fresh moraines and protalus ramparts enclose the cirques. The best example of these virtually unweathered moraines lies a few feet from the end of Temple glacier (Pl. 1). Elsewhere in the range, similar fresh moraines are associated with the presently retreating glaciers. These are so clearly of recent date that the writers regard them as expressions of the Little Ice Age of Matthes (1942; 1950). Boulders, many precariously balanced, are gray and exhibit neither surface staining nor lichens; no soil has developed on the till. The moraines are commonly 30–50 feet high. Mechanical analysis (Table 2) shows that they contain only 2–3 per cent silt and clay size particles. The ice probably retreated from these moraines within the last century or two.

The lowest surface in most valleys is a grass-covered flat of silt and fine sand, 2–5 feet above the stream grade, commonly referred to

as the "flood plain." Because of recent downcutting, most floods in the basin do not inundate this flat, but, near the mountains, high water occasionally covers it as well as several higher terraces. It is believed to have been formed concurrently with the Little Ice Age.

Relative Chronology of Glacial Advances

Estimates of the length of time between glacial advances are inexact but may aid in intermontane correlation. The Toboggan terrace, composed of large crystalline cobbles, was deposited shortly before the deposition of Buffalo till, as indicated by the presence of Buffalo till in youthful valleys cut in Toboggan gravels. The origin of these gravels is problematical; they may represent a late and substantial uplift of the mountains or they could be the outwash of a glacial advance.

The interval between the Buffalo and Bull Lake I advance is probably very long. Within this period Buffalo moraines probably lost most of their constructional topographic details. Although in other parts of the Rocky Mountains deep canyons were excavated between Buffalo and Bull Lake maxima, here there was only moderate trenching of the outwash during this interval.

Between Bull Lake I and Bull Lake II advances a short interval is suggested by the topographically similar moraines. The period between Bull Lake II and Pinedale advances was moderately long, but considerably shorter than that between Buffalo and Bull Lake I. The interval between the main Pinedale and its recessional moraines was very short. A somewhat longer period probably separated the deposition of the recessional Pinedale moraines in the basin and the readvance of the Temple Lake glaciers. The period between the Temple Lake and the Little Ice Age advances was short in relation to earlier interstadial intervals but was significantly longer than the period since the advance of the Little Ice Age, which probably occurred within the last two centuries. These estimates are summarized on Table 4.

Frost Action and Mass Movement

During glaciation the general conditions were ideal for intensive frost action in the cool, moist alpine zone. Specific conditions for maximum development of frost phenomena are well-jointed rock or permeable soil, saturation of the rock or soil interstices, frequent freezing and thawing, steep slopes, and deep seasonal frosts or permafrost. The area studied offers evidence of at least two generations of frost action.

An earlier phase is recorded in the area covered by the Pinedale ice sheet. On the valley sides, particularly on the north-facing slopes, great accumulations of talus boulders composed of massive angular blocks derived from the valley sides, mantle the scoured bedrock. The boulders are covered with lichens, and are weathered to faint pink and brown shades. Trees grow around and among the large boulders, indicating that, except for minor exfoliation and frost shattering, the talus accumulations are stable. Above 11,000 feet there are summit felsenmeers of angular but distinctly weathered boulders, sod-encroached stone stripes, and stabilized stone rings. On the west side of East Fork canyon, Mt. Bonneville quadrangle, a large weathered talus pile merges with a weathered protalus rampart, which formerly marked the western extent of a prominent nivation cirque. The degree of weathering, and the lichen cover of these old talus fans, protalus ramparts, felsenmeer and stone rings, suggest that the older generation was contemporaneous with the Temple Lake stage, whose moraines are weathered to a similar degree.

A second and recent generation of frost action is indicated by small fresh talus fans, which in the Middle Fork canyon lie unconformably against the older talus cones. These young talus piles occur only in areas most favorable for frost action, and are similar to, and probably correlatable with, the small moraines of the Little Ice Age advance. Secondary evidence for continuing frost action consists of the innumerable palsen or earth hummocks, which are developed in moist, fine, ground moraine of the alpine meadows. Modern nivation hollows are numerous, occurring as low as 8000 feet. However, it is difficult to separate these hollows from nivation depressions of an earlier generation.

Sand Dunes

In the New Fork, Big Sandy, and Sweetwater drainages, scattered sand dunes occur on the outwash from the lowest terrace to on a Pinedale terrace at 6600 feet. Eastward the dunes are constricted by two groups o buttes to a narrow band less than 2 miles wide The dune field crosses the Continental Divide at 7400 feet, and extends at least 40 miles into

Table 4.—Summary of Pleistocene Events

Moraine deposition	Terrace deposition	Frost action and mass movement	Eolian action	Vegetation	Early man	Interval of weathering and erosion
Little Ice Age moraines	"Floodplain"	Younger talus; palsen		Chenopods and composites		Very short
Temple Lake moraines	Parker terrace	Older talus; felsenmeer and polygonboden		Grass maximum	Occupation Finley site	Short
						Short
Recessional Pinedale moraines	Lower Pinedale terrace	Periglacial frost action likely during glaciation	Widespread eolian action leeward of outwash	Fir		Very short
Main Pinedale moraine	Upper Pinedale terrace					
Bull Lake II moraines	Bull Lake II terrace		Possibly some eolian action in Eden valley			Moderately long
Bull Lake I morine	Bull Lake I terrace					Short
Buffalo till	Faler (?) terrace Buffalo (?) terrace					Very long
	Toboggan terrace					Short

Bull Lake I terrace. Although some sand moves on extremely windy days, the dunes are stabilized. Near the mountains north of Big Sandy Creek, dunes up to 20 feet high rest on the Bull Lake terraces. In the Boulder area, sand sheets, 1–3 feet thick, cover the main Pinedale terrace on the south and east banks of the East Fork River. Here the area of sand accumulation, in respect to prevailing winds, was leeward of the extensive outwash plains.

The largest dune area is the Kilpecker dune field, named by Hack (Howard and Hack, 1943). The dunes extend eastward for about 60 miles from the Eden Valley. The western edge of the dune belt is 6 miles wide, and lies the Red Desert (Howard and Hack, 1943, p. 235).

At present there is no large source of sand. In Bull Lake and Pinedale time, however, Big Sandy, Little Sandy, and Pacific creeks carried large quantities of sand during the diurnal and annual floods. In winter and during the daily periods of slack water, the prevailing winds blew the sand from the exposed flats to the dune field. This same mechanism is believed to be important in the formation of the small sand sheets in the New Fork drainage. The great concentration of sand in the Kilpecker dunes is due to the location of the Eden valley at the junction of three creeks and the

presence of a topographic funnel to the east which concentrated the blowing sand. (*See* Moss, 1951, p. 95–98, for full discussion of eolian stratigraphy in Eden valley.)

Vegetation

The climatic shift of the Pleistocene would be expected to cause a vertical shifting of the vegetation zones in the mountains and basin. However, dendrochronologic studies of spruce trees around Big Sandy Lake show no important climatic changes in the last 250 years. It is possible that because of their location the trees were not well suited to this type of study (Schulman, Personal communication).

Analysis of pollen from two sedimentary columns in a bog in the Bridger Basin 40 miles from the mountains, representing accumulation from Pinedale time to the present, reveals the following changes: A decrease in fir pollen upward; a rise of grass to a maximum midway in the profile; an increase in chenopods and composites (sage brush and sedges) after the grass maximum (Hansen, *in* Moss, 1951, p. 113–117). It is possible but not probable that the increase in grass at the expense of fir is due to decimation of the mountain forests by fire or pestilence. In the Pacific northwest, a somewhat similar sequence of changes is recorded in 70 sedimentary columns and unquestionably has climatic significance. The climatic interpretation of the Bridger Basin profiles indicates an amelioration of the glacial climate after the Pinedale maximum, an increase in precipitation during the grass maximum, a swing towards drier conditions after the grass maximum, and a cooler but not notably moister climate in more recent time (Hansen, *in* Moss, 1951, p. 113–117).

Early Man

The presence of Early Man in the Bridger Basin to near Eden is well known from artifacts found both on the surface and *in situ*. Of principal importance was the discovery of the Finley site in 1940. Here "Yuma" artifacts associated with bison bones were found in a buried soil zone in a sand dune on the edge of the Kilpecker dune field (Howard, Satterthwaite, and Bache, 1941, p. 70–74; Howard, 1943, p. 224–234). The special significance of this find is the unusual variety of "Yuma" points at one locality, the complete absence of Folsom points, and the unique location of the site between the two principal migration routes of Early Man from Alaska and Canada.

Geologic studies, aimed at determining the antiquity and environment of Early Man in the Eden valley, revealed that the artifacts were emplaced during an episode of moist climate late in the interval between the Pinedale maximum and the Climatic Optimum, (Moss *et al.*, 1951). It is possible that this cool interval corresponds to the period of climatic stress represented by the Temple Lake substage in the mountains. In any case, it seems extremely likely that Yuma culture in the Eden valley is younger than Folsom culture at the Lindenmeier site.

Regional Pattern of Glaciation

General

Climatologists and meteorologists generally hold that the fundamental changes in the atmosphere which brought about glaciation operated over areas which were regional, continental, or possibly world-wide in scope. Although meteorological evidence and radio carbon studies support this premise, the regional sequences cannot be correlated without proof of a regional pattern of glacial deposits.

In the Rocky Mountains stratigraphic correlation of glacial deposits is difficult because of the discontinuous nature of moraines, the lack of published data on outwash deposits, the extreme differences in local geology and topography, and the possibility that the individual mountain ranges were elevated at different times during the late Cenozoic.

A review of the extensive published studies of mountain glaciation shows that the glacial deposits can be classified on the basis of (1) topographic and stratigraphic position, (2) geomorphology, and (3) degree of weathering the drift. These criteria were used to analyze published studies of several hundred valleys (Table 5). These studies range in thoroughness from broad reconnaissance of several mountain ranges to detailed scrutiny of a single valley.

TABLE 5.—TYPOLOGICAL CLASSIFICATION OF REPRESENTATIVE ROCKY MOUNTAIN GLACIAL DEPOSITS

Area	Authority	Formless mounds of weathered drift, some on high divides ("Buffalo Type")	Moderately weathered and eroded moraines, some with double laterals ("Bull Lake Type")	Slightly weathered, large hummocky, steep moraines ("Pinedale Type")	Very slightly weathered, small upper valley moraines ("Temple Type")	Very fresh cirque moraines or protalus ramparts ("Little Ice Age Type")
Northern Rocky Mountains						
Glacier Park	Campbell, 1914					Grinnell Glacier moraine; Blackfoot Glacier moraine.
Montana piedmont	Alden, 1932	pre-Wisconsin: Nebr. or Kansan?	Wisconsin moraines			
Watertown, Alberta	Horberg, 1942	Kennedy drift	Early Wisconsin Iowan-Tazewell)	Late Wisconsin (Cary)		Cirque moraines
Castle Mt. Mining District	Weed and Pirsson, 1896		Older, weathered lateral moraines	Younger terminal moraines with knob and sink topography		
Bitterroot and Clearwater mountains	Lindgren, 1904			Massive moraine with little ridges and shallow ponds		Moraine-dammed lake in cirque ?
Custer Co., Idaho	Umpleby, 1913			Knob and kettle moraine at 6300 ft.		
Bitterroot Mountains	Stearns, Bryan, and Crandall, 1939	Buffalo till at 5300 ft.	"Wisconsin" drift above 8000 ft. ?			
Sawtooth Mountains	Umpleby, Westgate and Ross, 1930	"Earlier" stage: erratics 500–700 ft. above stream	"Wisconsin" stage; little modified by erosion; original topography		Recessionals ?	
Salmon River area	Ross, 1929, 1934, 1937	Early Pleistocene glacial deposits on ridges	Small laterals at 8000 ft. on Rock Creek ?	'Wisconsin" glaciation ?		
Middle Rocky Mountains						
Yellowstone Valley Beartooth Mountains	Horberg, 1940 Bevan, 1946	Buffalo High level morainic drift	Bull Lake Broad lobate glacial deposits	Pinedale Canyon moraines in Boulder and Stillwater canyons		
Absaroka Mountains	Parsons, 1939		Large moraine with swell and swale topography in lower	Hummocky, uneven moraine above Sunlight Basin. "Late	Rock glaciers and moraines near Sunlight Glacier ?	

			water canyons			
Absaroka Mountains	Parsons, 1939		Large moraine with swell and swale topography in lower Sunlight valley.	Hummocky, uneven moraine above Sunlight Basin "Late Wisconsin"	Rock glaciers and moraines near Sunlight Glacier	?
Bighorn Mountains	Salisbury and Blackwelder, 1903	Boulders up to 25 ft. in diameter, decayed to center resting on Bald Mountain	Well-formed lateral moraines modified by erosion; no lakes, no terminals.	Long, sharp-ridged lateral and stout terminal moraines; fresh drift, little erosion, many lakes		
Western Wyoming	Blackwelder, 1915	Buffalo	Bull Lake	Pinedale		
Grand Tetons	Fryxell, 1930, and personal communication; Edmund, 1938, 1940, and personal communication.	Buffalo	Bull Lake, possibly double	Pinedale	Possibly older cirque moraines	Little Ice Age moraines in cirques
Gros Ventre and Hoback mountains	Horberg, 1938, and personal communication; Nelson and Church, 1943	Buffalo	Bull Lake (possibly double)	Pinedale		
Northern Wind River Mountains	Miner and Delo, 1943; Miner and Apfel, 1946	Buffalo	Bull Lake	Pinedale		
	Baker, 1946		Older moraines	Younger moraines, with two recessionals		
	Richmond, 1948	Buffalo-Prairie Divide	Bull Lake I-Twin Lakes	Pinedale I-Corral Creek	Pinedale III-Long Draw	Modern glaciers-Sprague
			Bull Lake II-Home	Pinedale II		
Wasatch Mountains	W. W. Atwood, Sr., 1909		Outer, eroded compound lateral moraines	Inner, fresh compound terminal moraines		
	Calkins and Butler, 1943		Early moraines "pre-Wisconsin"	Hummocky moraines "Wisconsin"		
	W. W. Atwood, Sr., 1909	Possible earliest stage	Earlier	Later		
	Bradley, 1936	Little Dry-Buffalo	Blacks Fork-Bull Lake	Smith Fork-Pinedale		

TABLE 5.—*Continued*

Area	Authority	Formless mounds of weathered drift, some on high divides ("Buffalo Type")	Moderately weathered and eroded moraines, some with double laterals ("Bull Lake Type")	Slightly weathered, large hummocky, steep moraines ("Pinedale Type")	Very slightly weathered, small upper valley moraines ("Temple Type")	Very fresh cirque moraines or protalus ramparts ("Little Ice Age Type")
Colorado Plateaus						
Wasatch Plateau	Spieker and Billings, 1940			Unweathered, large, hummocky, compound moraines	Well-developed recessional moraines in cirques	
Boulder Mountain, Utah	Gould, 1939			Fresh moraines containing lakes formed by outlet tongues of plateau glaciers	?	
Southern Rocky Mountains						
Medicine Bow Range	W. W. Atwood, Jr., 1937		Centennial moraine: rolling topography, more severely weathered	Libby moraine		
	Horberg, personal communication		Centennial moraine	Libby moraine	Plateau moraine, 2 miles in front of cirque at 10500 ft and 11000 ft.	Cirque moraines
Park Range	W. W. Atwood, Jr., 1937	Possibly earlier till	"pre-Wisconsin" moraines; eroded, modified	"Wisconsin" fresh moraines		
Never Summer Range and North Park	Eschman, 1952	Owl Mountain drift	Gould moraine	Silver Creek moraine	American Lakes moraine	Protalus ramparts
Cache La Poudre Valley	Bryan and Ray, 1940	Prairie Divide	Home moraine	Corral Creek moraine: fresh compound	Long Draw moraine	Protalus rampart
Rocky Mountain National Park area	Jones and Quam, 1944		Old weathered moraine remnants	Park border moraines; enclose "parks"; concentric lateral ridges	Upper valley moraines with recessional ridges	

Southern Rocky Mountains—*Continued*

Southern Rocky Mountains—*Continued*

Rocky Mountain National Park area	Ray, 1940 (illustrative valley) Fenneman, 1902		Moraine Park moraine at 8000 ft.	Fern Lake moraine at 9500 ft.	Odessa Lake moraine at 11800 ft.	Type Sprague moraine Arapahoe Glacier moraine; fresh morainic ridges
Central City area	Bastin and Hill, 1917	? "Pre-Wisconsin" till on valley sides	? Large "Wisconsin" moraines near Nederland; moraine near Alice containing lake at 10,200 ft.			
Boulder Co., Colorado	Wahlstrom, Ph.D. Thesis, Harvard Univ., 1939	Old weathered till on divides = ? Cerro	Two valley stages = ? Wisconsin			
Beaver-Tarryall area, Park Co., Colo.	Singewald, 1942		Older eroded lateral moraines	Younger moraines with recessionals		
Aspen area	Ray, 1940		Aspen moraine	Moraine at 9000 ft.		
Georgetown Quadrangle	Ray, 1940		Moraines at 8500 ft. and 7900 ft.	Moraine on Chicago Creek at 8900 ft.; on W. Chicago Creek at 9200 ft.	Chicago Lakes moraine at 10,500 ft.	
Arkansas River-Twin Lakes area	Westgate, 1905		Lateral moraines with rolling topography, disintegrated boulders	Rugged, steep, fresh unweathered moraines with inner recessionals		
	Capps, 1909		Eroded, weathered outer moraine	Double, hummocky fresh sharp-crested moraines		
San Juan Mountains	Atwood and Mather, 1932	Cerro: deeply weathered formless masses of drift; profoundly modified	Durango: irregular surface, a few depressions	"Wisconsin" original kettle and knob topography; fresh boulders; recessionals		
	Smith, 1934	Cerro drift on high divides				

The list is by no means exhaustive, but does demonstrate the regional pattern of glaciation.

Classification

On the basis of position, geomorphology, and weathering of the drift, the till deposits conform to several distinct descriptive groups. Geologic evidence cannot as yet prove that this system has chronological significance. Names for these categories were drawn from Blackwelder's study (1915). These are purely descriptive names, and for the present their use does not imply intermontane correlation.

BUFFALO TYPE DRIFT: Deposits of this descriptive type occur in deeply weathered and severely eroded mounds, which ordinarily rest on high ridges or plateaus. The oldest tills have been recognized in as many as 22 localities. Besides the normal effects of alpine erosion, these old deposits have endured a major canyon cutting cycle and intense periglacial frost action. The position of the Buffalo type tills on high benches (in some instances over 1000 feet above the streams), the wide extent of the tills, and the smoothness of the surface on which they rest, show, as Atwood and Atwood (1938, p. 244) have pointed out, that the physiography of the Rocky Mountains during their deposition was substantially different from the present. The ranges must have been broad, high table-lands on which large mountain icecaps developed. The Bridger basin is apparently an exception to this general condition, although the Wind River Range itself may not be.

It is not impossible that while these general physiographic conditions prevailed, ice formed more than once and spread across the high plateau-mountains to emplace more than one drift. Alden (1932, p. 32–38, 69) describes two separate drifts, the "early Pleistocene Mountain drift" and the buried "Illinoian or Iowan drift". Blackwelder (1915) mentions that Buffalo till may actually represent more than one stage, and Richmond (1948, p. 1400) correlates two separate valley trains with pre-Bull Lake glaciation in the Wind River Mountains. Clearest examples of the Buffalo type tills are Atwood and Mather's (1932, p. 82) Cerro tills.

BULL LAKE TYPE DRIFT: Bull Lake type tills are the oldest deposits having recognizable morainal form. They occur in at least 29 localities (Table 5). These moraines, which are ordinarily smooth and lack the details of original ice-constructed topography, commonly occur only as lateral ramparts. In most valleys, streams have removed the terminal sector of the moraine. Moraines of this group rarely attain great size. In a few instances the Bull Lake type moraines are clearly compound, with paired moraines and outwash. The inner moraine is indicative of a substage possibly more important than a recessional pause. Moraines which illustrate this group are Capps' (1909, p. 58) outer moraines below Twin Lakes, Atwood's (1909, p. 68) "earlier," Bradley's (1936, p. 194) Black's Fork, and Jones' and Quam's (1944, p. 218) "old moraine remnants."

PINEDALE TYPE DRIFT: Recognition of Pinedale type moraines is simplified by their fresh appearance, great size, effect on drainage, and textbook morainal topography. Thirty-two localities are listed on Table 5. These moraines are commonly associated with numerous lakes and swamps, narrow, steep stream channels which transect their terminal segments, several small recessional moraines on the inner flank, and well-preserved and extensive outwash facies. Examples of Pinedale type deposits are Capps (1909, p. 57) "later" stage, containing Twin Lakes, or the "Wisconsin" moraines of Atwood and Mather (1932, p. 135).

TEMPLE LAKE TYPE DRIFT: These moraines occur several miles upstream from the massive Pinedale type terminal ramparts, but commonly a few miles from cirques. The Temple type moraines are small, and in some valleys are mantled by trees. Data on these moraines are limited, probably because their significance is not understood. Some investigators have considered them as unimportant recessionals. These moraines, small, practically uneroded, commonly covered by a thin soil, lichen-covered boulders, or possibly by forests, appear to be separated in time from the Pinedale type moraines, and also seem significantly older than the Little Ice Age moraines. Whether they represent a late recessional pause or a completely separate advance from the cirques cannot be ascertained. Examples of this group are the "upper valley" moraines of Jones and Quam (1944, p. 222).

LITTLE ICE AGE TYPE DEPOSITS: These small, exceedingly fresh moraines or protalus ramparts are easily recognized in the cirques. They commonly dam tarns, or may be separated by a few hundred feet from modern glaciers. These tills are as fresh as the talus which forms at the present time in the cirques, but they are the product of glaciers somewhat larger than the present ice masses. It is possible that these cirque moraines could be compound, reflecting more than one very recent advance. Examples occur in Glacier Park (Campbell, 1914, p. 24, 29, 50), and Rocky Mountain National Park (Ray, 1940, p. 1865).

Summary

On the basis of simple, descriptive criteria, it is apparent that the reported glacial deposits in the Rocky Mountains fall into a distinct pattern. In the southwestern Wind River Mountains the till deposits fit into this classification, not only in general but in detail. Divergences exist in some valleys, but consideration of the entire area reveals a complete record. On the basis of the correlation principle of "like sequence of strata" and meteorological evidence, synchroneity of the glacial advances throughout the Rocky Mountains is strongly suggested.

CORRELATION WITH THE MIDDLE WEST

Three principal periods of ice advance are recorded in the southwestern Wind River Mountains: Buffalo, Bull Lake, and Pinedale. For the Bull Lake and Pinedale, and less positively for the Buffalo, there is evidence that each period was compound, consisting of more than one episode of moraine building. The longest time interval between stages separates the Buffalo and Bull Lake. The interval between Bull Lake and Pinedale is substantial and greater than the interval between Bull Lake I and Bull Lake II or between any of the oscillations of the Pinedale.

No direct correlation between the mountain glaciation in the Middle Rocky Mountains and the continental glaciation in the Midwest is presently possible. On the basis of equivalence of topographic expression and degree of weathering, the authors believe the Bull Lake and Pinedale complexes to be Wisconsin in age and the Buffalo to be pre-Wisconsin. The Wisconsin in this area, therefore, consists of two complex episodes separated by a significant time interval.

If further work in the Midwest substantiates the view that the Brady, or Tazewell-Cary, interval is the most pronounced break in the Wisconsin continental glacial sequence, the Brady must correspond to the pronounced Bull Lake-Pinedale interval in the southwestern Wind River Mountains. Since both the Bull Lake and Pinedale are compound advances characterized by more than one moraine-building episode, the former may be a correlate of the Iowan and Tazewell and the latter the Cary and Mankato. The Temple Lake moraines are believed to be either late Mankato or an early pulsation of the Little Ice Age after the "thermal maximum."

Support for this correlation is found in the Waterton Region, Alberta, Canada, where drift of the continental ice interfingers with deposits laid down by mountain glaciers from the northern Rocky Mountains (Horberg, 1954, p. 1140). Horberg concludes that drift which resembles the Pinedale is Cary in age, and drift similar to the Bull Lake may well correlate with the Iowan, Tazewell, and possibly Farmdale. Horberg believes that the Mankato is either restricted or absent in the northern Rockies. In the southwestern Wind Rivers Mountains where a more complete record of glacial activity after the Pinedale maximum has been preserved, one of the periods of moraine building between the Pinedale maximum and the Temple Lake maximum may correlate with the Mankato. Solution of this phase of the glacial problem awaits discovery of materials in the middle Rockies datable by carbon-14 and further work in the Midwest and East to determine the relative importance of the Mankato and the Two Creeks interval in the Wisconsin glacial sequence.

REFERENCES CITED

Alden, W. C., 1932, Physiography and glacial geology of eastern Montana and adjacent areas: U. S. Geol. Survey Prof. Paper 174, 133 p.

Atwood, W. W., 1909, Glaciation of the Uinta and Wasatch Mountains: U. S. Geol. Survey Prof. Paper 61, 96 p.

Atwood, W. W., and Atwood, W. W., Jr., 1938, Opening of the Pleistocene in the Rocky Mountains of the United States: Jour. Geology, v. 46, p. 239–247.

Atwood, W. W., and Mather, K. F., 1932, Physiography and Quaternary geology of the San Juan Mountains, Colorado: U. S. Geol. Survey Prof. Paper 166, 171 p.

Baker, C. L., 1946, Geology of the northwestern Wind River Mountains, Wyoming: Geol. Soc. America Bull., v. 57, p. 565–596.

Ball, S. H., *in* Spurr and Garrey, 1908, Geology of the Georgetown quadrangle, Colorado, p. 29–96: U. S. Geol. Survey Prof. Paper 63, 422 p.

Bastin, E. S., and Hill, J. M., 1917, Economic geology of Gilpin county and adjacent parts of Clear Creek and Boulder counties, Colorado: U. S. Geol. Survey Prof. Paper 94, 379 p.

Bevan, A., 1946, Three stages of Pleistocene glaciation, Beartooth Mountains, Montana: Geol. Soc. America Bull., v. 57, p. 1178–1179.

Blackwelder, E., 1915, Post Cretaceous history of the mountains of central western Wyoming: Jour. Geology, v. 23, p. 97–117; 193–217; 307–340.

—— 1950, Pleistocene geology of the Green River Basin, Wyoming: Wyo. Geol. Assoc. Fifth Ann. Field Conf., Southwestern Wyo., Casper, Wyo. 196 p.

Bradley, W. A., 1936, Geomorphology of the north flank of the Uinta Mountains: U. S. Geol. Survey Prof. Paper 185-I, p. 163–204.

Branson, E. B., and Branson, C. C., 1941, Geology of the Wind River Mountains, Wyoming: Am. Assoc. Petroleum Geologists Bull., v. 25, p. 120–151.

—— 1945, Glaciation in southern part of the Wind River Mountains and their foothills: Geol. Soc. America Bull., v. 56, p. 1148–1149.

Bryan, K., and Ray, L., 1940, Geologic antiquity of the Lindenmeier site: Smithsonian Misc. Coll., v. 99, no. 2, 76 p.

Calkins, F. C., and Butler, B. S., 1943, Geology and ore deposits of the Cottonwood-American Fork area, Utah: U. S. Geol. Survey Prof. Paper 201, 152 p.

Campbell, M. R., 1941, The Glacier National Park: U. S. Geol. Survey Bull. 600, 54 p.

Capps, S. R., 1909, Pleistocene geology of the Leadville quadrangle, Colorado: U. S. Geol. Survey Bull. 386, 99 p.

Cary, M., 1917, Life zone investigations in Wyoming: North Am. Fauna Ser. no. 42, U. S. Dept. Agriculture, Bureau of Biol. Survey, Wash., D. C., 95 p.

Flint, R. F., 1946, Glacial geology and the Pleistocene Epoch: N. Y., John Wiley and Sons, 589 p.

Eschman, D. F., 1952, Glaciation of the Michigan River Basin, North Park, Colorado: Geol. Soc. America Bull., v. 63, p. 1379–1380.

Fenneman, N. M., 1902, The Arapahoe Glacier in 1902: Jour. Geology, v. 10, p. 839–851.

Fryxell, Fritiof, 1930, Glacial features of Jackson Hole, Wyoming: Augustana Coll. Libr., Pub. no. 13.

Gould, L. M., 1939, Glacial Geology of Boulder Mountain, Utah: Geol. Soc. America Bull., v. 50, p. 1371–1380.

Horberg, L., 1938, The structural geology and physiography of the Teton Pass area, Wyoming: Augustana Coll. Libr. Pub. no. 16, 85 p.

—— 1940, Geomorphic problems and glacial geology of the Yellowstone Valley, Park County, Montana: Jour. Geology, v. 48, p. 275–303.

—— 1952, Interrelations of Rocky Mountain and continental glacial drifts in the Watertown region, Alberta (Abstract): Geol. Soc. America Bull., v. 63, p. 1382.

—— 1954, Rocky Mountain and Continental Pleistocene deposits in the Waterton region, Alberta, Canada: Geol. Soc. America Bull., v. 65, p. 1093–1150.

Howard, E. B., and Hack, J. T., 1943, The Finley site: Am. Antiquities, v. 8, p. 224–241.

Howard, E. B., Satterthwaite, L., Jr., and Bache, C., 1941, Preliminary report on a buried Yuma site in Wyoming: Am. Antiquities, v. 7, p. 70–74.

Jones, W. D., and Quam, L. D., 1944, Glacial land forms in Rocky Mountain National Park: Jour. Geology, v. 52, p. 217–234.

Lindgren, W., 1904, A geological reconnaissance across the Bitterroot Range and Clearwater Mountains in Montana and Idaho: U. S. Geol. Survey Prof. Paper 27, 123 p.

Matthes, F. E., 1942, Report on Committee on glaciers: Am. Geophys. Union Trans., 1941–1942, p. 374–393.

—— 1950, The incomparable valley (Fritiof Fryxell, editor): Berkeley, Univ. of Calif. Press, 160 p.

Miner, N. A., and Apfel, E. T., 1946, Three stages of glaciation identified in Wind River valley, Wyoming: Geol. Soc. America Bull., v. 57, p. 1218–1219.

Miner, N. A., and Delo, D. M., 1943, Glaciation of the Du Noir valley, Fremont County, Wyoming: Jour. Geology, v. 51, p. 131–137.

Moss, J. H., *et al.*, 1951, Early Man in the Eden Valley: Univ. Pa. Mus. Mon., 124 p.

Nace, R. L., 1939, Geology of the northwest part of the Red Desert, Sweetwater and Fremont counties, Wyoming: Wyo. Geol. Survey Bull., v. 27, 51 p.

Nelson, V. E., and Church, V., 1943, Critical structures of the Gros Ventre and northern Hoback ranges, Wyoming: Jour. Geology, v. 51, p. 143–166.

Parsons, W. H., 1939, Glacial geology of the Sunlight area, Wyoming: Jour. Geology, v. 47, p. 737–747.

Ray, L. L., 1940, Glacial chronology of the southern Rocky Mountains: Geol. Soc. America Bull., v. 51, p. 1851–1918.

Richmond, G. M., 1945, Geology of the northwest end of the Wind River Mountains, Sublette County, Wyoming: U. S. Geol. Survey Oil and Gas Inv., Prelim. Map no. 31.

—— 1948, Modification of Blackwelder's sequence of Pleistocene glaciation in the Wind River Mountains, Wyoming: Geol. Soc. America Bull., v. 59, p. 1400–1401.

Ross, C. P., 1929, Pleistocene glaciation in Idaho: U. S. Geol. Survey Prof. Paper 158, p. 123–128.

—— 1934, Geology and ore deposits of the Casto quadrangle, Idaho: U. S. Geol. Survey Bull. 854, 135 p.

Ross, C. P., 1937, Geology and ore deposits of the Bayhorse region, Custer County, Idaho: U. S. Geol. Survey Bull. 877, 161 p.

Ruhe, R. V., 1950, Graphic analysis of drift topographies: Am. Jour. Sci., v. 248, p. 435–443.

Salisbury, R. D., and Blackwelder, E., 1903, Glaciation in the Bighorn Mountains: Jour. Geology, v. 11, p. 216–223.

Singewald, G. D., 1942, Stratigraphy, structure and mineralization in the Beaver-Tarryall area, Park County, Colo.: U. S. Geol. Survey Bull 928A, 44 p.

Smith, H. T. U., 1936, Periglacial landslide topography of Canjilon Divide, Rio Arriba County, New Mexico: Jour. Geology, v. 44, p. 836–860.

Spieker, E. M., and Billings, M. P., 1940, Glaciation in the Wasatchplateau, Utah: Geol. Soc. America Bull., v. 51, p. 1173–1198.

Stearns, H. T., Bryan, L. L., and Crandall, L., 1939, Geology and water resources of the Mud Lake region, Idaho: U. S. Geol. Survey Water-Supply Paper 818, 125 p.

Umpleby, J. B., 1913, Geology and ore deposits of Lemi County, Idaho: U. S. Geol. Survey Bull. 528, 182 p.

Umpleby, J. B., Westgate, L. G., and Ross, C. P., 1930, Geology and ore deposits of the Wood River region, Idaho: U. S. Geol. Survey Bull., 814, 250 p.

U. S. Dept. of Agriculture, 1941, Climate and man: Year-book of Agriculture, Wash., D. C. 1248 p.

Weed, W. H., and Pirsson, L. V., 1896, Geology of Castle Mountain Mining district, Montana: U. S. Geol. Survey Bull. 139, 164 p.

Wentworth, C. K., and Delo, D. M., 1931, Dinwoody glaciers, Wind River Mountains, Wyoming, with a brief survey of existing glaciers in the United States: Geol. Soc. America Bull., v. 42, p. 605–620.

Westgate, L. G., 1905, The Twin Lakes glaciated area, Colorado: Jour. Geology, v. 13, p. 285–312.

U. S. Geological Survey, Washington 25, D. C.; Franklin and Marshall College, Lancaster, Pa.

Manuscript Received by the Secretary of the Society, July 22, 1953

BULLETIN OF THE GEOLOGICAL SOCIETY OF AMERICA
VOL. 66, PP. 655-662, 5 FIGS. JUNE 1955

SPECTROGRAPHIC ANALYSIS BY USE OF MUTUAL STANDARD METHOD

By W. H. Dennen and W. C. Fowler

Abstract

The mutual standard method utilizes the inter-relationship of spectral-line intensities and element concentrations to analyse simultaneously all the major rock-forming constituents, and to determine some minor elements. A relative deviation (per cent standard deviation) of 10 per cent results. Analytical time is less than 2 hours per triplicate analysis.

CONTENTS

TEXT

Page
Introduction ... 655
Choice of procedure ... 655
General ... 655
Principles ... 656
Operating procedure ... 658
Precision and accuracy ... 662
Applications ... 662
Conclusions ... 662
References cited ... 662

ILLUSTRATIONS

Figure Page
1. Mutual standard working curve for CaO ... 656
2. Mutual standard working curve for K_2O ... 657
3. Geochemical logs of major constituents of Antrim shale ... 660
4. Geochemical logs of minor elements of Antrim shale ... 661
5. Variation in composition as a result of weathering ... 661

TABLES

Table Page
1. Usable concentration ranges for analysis lines ... 658
2. Standard deviation in per cent of intensity ratios from replicate arcings of *G*-1 and *W*-1 ... 658
3. Comparison of chemical and spectrochemical analyses ... 659

Introduction

Rapid methods of rock analysis are increasingly in demand, and since classical gravimetric methods of silicate analysis are inherently slow, the analyst has turned to instrumental procedures. Three principal instruments have been successfully applied to rock analysis in the past few years—the colorimeter, flame photometer, and emission spectrograph—and a number of analytical procedures have been developed by combining several of these instruments. Shapiro and Brannock (1952, p. 7–17) describe a colorimetric-flame photometric technique of high precision; Leininger and Taylor (1954, p. 436) have developed a combination of these instruments with spectrographic techniques. Other workers have used purely spectrographic techniques. Methods of spectrochemical analysis for major constituents described prior to 1953 are reviewed by Ahrens (1954), precision and accuracy are evaluated by Dennen *et al.* (1951, p. 26–30).

Most spectrographic methods for the determination of the major elements require the addition of internal standards and several separate arcings for complete analysis. However, this time-consuming process is not desirable in some instances.

Choice of Procedure

General

Quantitative spectrographic methods use an internal standard which may be added to the sample or may already be a constituent, which case would eliminate the need for weighing or mixing of materials. A constituent in the

sample may be used in the method of variable internal standardization, for which the standard concentration must be found independently, or in the method of mutual standardization wherein the concentration of the standard is found by difference. The mutual standard method has the advantage over other spectrochemical procedures of simplified sample preparation and concomitant analysis for all major constituents.

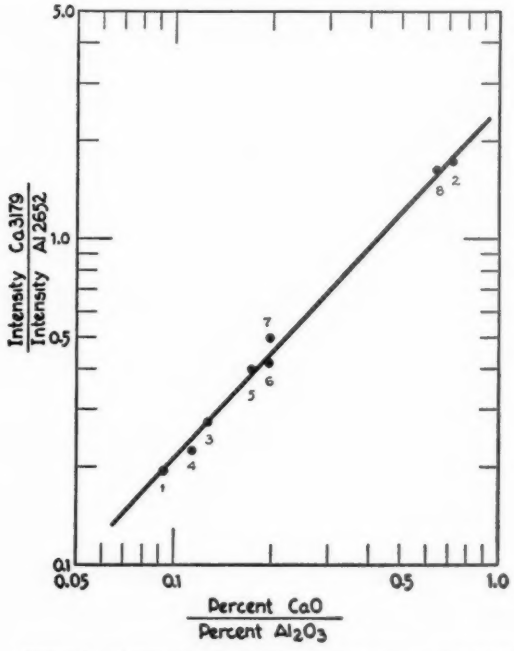

FIGURE 1.—MUTUAL STANDARD WORKING CURVE FOR CaO

1. G-1, standard granite (Fairbairn *et al.*, 1951)
2. W-1, standard diabase (Fairbairn *et al.*, 1951)
3. Bur. Stds. No. 93, boro-silicate glass
4. RGP
5. RA 135
6. EL 316
7. EL 34-167
8. FBSS 459

Igneous rocks from E. S. Larsen, Jr., F. A. Gonyer, Analyst

Spectrochemical analysis by mutual standardization has been used to determine the impurities in steel (Coulliette, 1943, p. 732) and has more recently been applied to the analysis of aluminous ores for alumina, silica, iron, and titania by Churchill and Russell (1945, p. 25), to the analysis of alumina, lime, magnesia, silica, and manganese in steel-making slags by Rosza (1947, p. 394), and to the analysis of these constituents plus iron, phosphorus, and titania in similar matrices by Carlsson and Yü, (1950, p. 276). Lime, magnesia, silica, iron, alumina, and titania in limestone were determined by Leininger (1950, p. 804) who used this method. A.C. arcs and spark sources have been used almost exclusively, although Rosza and Leininger make effective use of D.C. arc excitation.

Principles

The principles of mutual standardization have been discussed by Coulliette (1943, p. 732), Churchill and Russell (1945, p. 25),

Rosza (1947, p. 594), and Carlsson and Yü (1950, p. 276). In brief, the method is based on the assumptions that (1) the intensity ratio of two spectral lines is a function only of the concentration ratio of the two emitting elements, and that (2) the elements sought comprise essentially all of the sample, an assumption made also in gravimetric analysis.

Computation is based on the fact that if

$$A + C + D + \ldots . X = 100$$

then, dividing by A,

$$\frac{A}{A} + \frac{C}{A} + \frac{D}{A} + \cdots\cdots \frac{X}{A} = 100$$

and

$$A = \frac{100}{1 + \frac{B}{A} + \frac{C}{A} + \cdots\cdots \frac{X}{A}}.$$

These conditions do vary of course. The intensity-concentration relationship is affected by variation in the sample matrix, erratic illumination, and miscellaneous errors common to all spectrographic analysis. Constituents not readily determinable by spectrographic means (H_2O, CO_2, organic material, etc.) in amounts greater than ~5 per cent by weight must be determined independently.

Aluminum is chosen as the variable internal standard because of its ubiquity; this gives the formula:

$$\%Al_2O_3 = \frac{100}{1 + \frac{\%SiO_2}{\%Al_2O_3} + \frac{\%TiO_2}{\%Al_2O_3} + \frac{\text{Tot. Fe as } \%Fe_2O_3}{\%Al_2O_3} + \frac{\%MnO}{\%Al_2O_3} + \frac{\%MgO}{\%Al_2O_3} + \frac{\%CaO}{\%Al_2O_3} + \frac{\%Na_2O}{\%Al_2O_3} + \frac{\%K_2O}{\%Al_2O_3}}.$$

The ratios $\%SiO_2/\%Al_2O_3$, $\%TiO/\%Al_2O_3$, and others are obtained from plots (working curves) of intensity ratio versus concentration ratio drawn from data determined by measurements on chemically analyzed standards. Figure 1 is a typical working curve. Intensity ratios are determined by opacity measurements of spectral lines, and the equivalent concentration ratios from the working curves

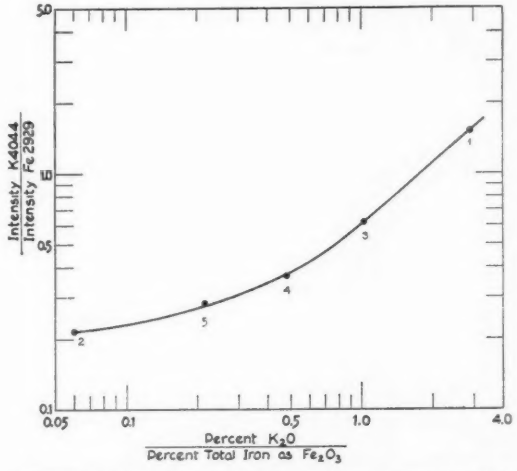

FIGURE 2.—MUTUAL STANDARD WORKING CURVE FOR K_2O
1. G-1, standard granite (Fairbairn *et al.*, 1951)
2. W-1, standard diabase (Fairbairn *et al.*, 1951)
3. G-1 3 parts, W-1 1 part by weight
4. G-1 1 part, W-1 1 part by weight
5. G-1 1 part, W-1 3 parts by weight

are substituted in the equation above, which is then solved for $\%Al_2O_3$. Multiplication of the appropriate concentration ratio by the $\%Al_2O_3$ value then gives the concentration of the other oxides.

TABLE 1.—USABLE CONCENTRATION RANGES FOR ANALYSIS LINES

Line	Concentration range (per cent)
Si2970	50–100
2987	20–80
Al2652	3–20
Ti3088	0.005–1
3242	0.1–2
Fe2912	0.1–10
2929	1–10
Mn2801	0.001–0.1
Ca3006	10–50
3158	0.05–15
3179	0.01–10
Na3302	0.2–10
K4044	0.5–10

this background is obtained by using a working curve based on

$$\frac{\text{Log Intensity K}}{\text{Log Intensity Fe}} \text{ vs. } \frac{\text{Log } \%K_2O}{\text{Log } \% \text{ Total Iron as } Fe_2O_3}.$$

Figure 2 illustrates this working curve.

If the concentration of any constituent in the sample is known prior to analysis, the numerator of the equation should be reduced accordingly, and the appropriate concentration ratio eliminated from the denominator. The mutual standard method may be coupled with any other analytical procedure by this simple modification of the basic formula.

Operating Procedure

Samples are reduced to −100 mesh, dried at 110°C, and packed firmly with a small cylindrical ram into pure carbon electrodes. Samples may be mixed with one part of carbon powder to insure smooth burning. Electrodes an eighth of an inch in diameter with a cavity 1 mm in diameter and 3 mm deep, are used.

TABLE 2.—STANDARD DEVIATION IN PER CENT OF INTENSITY RATIOS FROM REPLICATE ARCINGS OF *G*–1 AND *W*–1

	Si2987/Al2652	Ti3088/Al2652	Fe2912/Al2652	Mn2801/Al2652	Mg2779/Al2652	Ca3179/Al2652	Na3302/Al2652	K4044/Al2652
G–1	8.9	12.0	10.0	6.2	7.6	11.1	9.6	6.8
W–1	10.8	9.7	5.2	8.8	14.0	9.2	13.9	4.6

Better working curves result from widespread concentration ratios. It is advisable to take the ratios of the more variable constituents (titanium, magnesium, calcium, manganese and iron) to aluminum, and the ratios of the more constant constituents (silicon, sodium, and potassium) to iron. The latter ratios may then be transformed into ratios to aluminum by multiplication by the known ratio

$$\frac{\% \text{ Total Iron as } Fe_2O_3}{\%Al_2O_3}.$$

In the present work the ratio of potassium to iron is used because there is a background contribution at the potassium line from an adjacent iron line, and automatic correction for

The sample is excited as the anode and is arced to completion at 6 amperes.

All observations have been made on a large Hilger prism instrument over the wave-length range of 2630Å–4100Å. Slow plates are preferable because of inconveniently high density on more sensitive plates; Eastman *N*-1 plates were used.

A rotating-step sector placed in front of the slit and transmitting $\frac{1}{32}$, $\frac{1}{64}$, and $\frac{1}{128}$ of the incident light provides sufficient selection of line intensities, and facilitates plate calibration.

The spectral lines which may be used satisfactorily in the mutual standard method, in common with spectral lines used in all major element determinations, are relatively insensitive and show little or no self-absorption

TABLE 3.—COMPARISON OF CHEMICAL AND SPECTROCHEMICAL ANALYSES

	Chem.	Spec	Bias	% Bias
SAMPLE 1				
SiO_2	71.14	69.9	1.24	1.7
TiO_2	.29	.27	.02	6.9
Al_2O_3	14.92	15.7	.78	5.2
Total iron as Fe_2O_3	3.23	2.80	.43	13.3
MnO	.05*	.02	..	..
MgO	.85	.74	.11	13.0
CaO	2.94	3.30	.36	12.2
Na_2O	3.50	4.16	.66	18.9
K_2O	2.90	3.38	.48	16.6
Total	99.82	100.27		
SAMPLE 2				
SiO_2	74.68	74.90	.22	0.3
TiO_2	.15	.11	.04	26.7
Al_2O_3	13.80	13.62	.18	1.3
Total iron as Fe_2O_3	2.04	2.52	.48	23.5
MnO	.03	.04	.01	33.3
MgO	.21*	.48	..	..
CaO	2.26	2.38	.12	5.3
Na_2O	4.10	3.40	.70	17.1
K_2O	2.01	2.45	.44	21.9
Total	99.28	99.90	..	..
SAMPLE 3				
SiO_2	62.28	60.3	1.98	3.2
TiO_2	.72	.72	0	0
Al_2O_3	16.68	17.70	1.02	6.1
Total iron as $Fe\,O_3$	6.66	7.10	.44	6.6
MnO	.07	.07	0	0
MgO	2.33	2.66	.33	14.2
CaO	5.72	5.68	.04	0.7
Na_2O	3.50	3.82	.32	9.2
K_2O	1.49	2.02	.53	35.6
Total	99.45	100.07	..	..
SAMPLE 4				
SiO_2	72.58	73.1	.52	0.7
TiO_2	.30	.31	.01	3.3
Al_2O_3	14.12	13.55	.57	4.2
Total iron as Fe_2O_3	3.27	4.20	.93	28.4
MnO	.02*	.05	..	..
MgO	.70	.74	.04	5.7
CaO	2.44	2.17	.27	12.4
Na_2O	3.91	3.59	.32	8.9
K_2O	2.84	2.44	.40	16.4
Total	100.18	100.15	..	..

TABLE 3.—*Continued*

	Chem.	Spec	Bias	% Bias
SAMPLE 5				
SiO_2	59.28	59.3	.02	0
TiO_2	.85	.87	.02	2.3
Al_2O_3	17.86	17.95	.09	0.5
Total iron as Fe_2O_3	7.00	6.29	.71	10.1
MnO	.07	.07	0	0
MgO	3.21	2.96	.25	7.8
CaO	6.46	6.56	.10	1.5
Na_2O	3.39	3.41	.02	0.6
K_2O	1.53	1.55	.02	1.3
Total	99.65	98.96	..	..
SAMPLE 6				
SiO_2	62.70	65.4	2.7	4.1
TiO_2	.66	.61	.05	8.2
Al_2O_3	14.40	13.25	1.15	8.7
Total iron as Fe_2O_3	6.47	6.42	.05	0.8
MnO	.095	.086	.009	10.5
MgO	3.06	3.46	.40	13.1
CaO	6.12	5.43	.69	12.7
Na_2O	2.69	2.76	.07	2.5
K_2O	3.10	3.02	.08	2.7
Total	99.30	100.44	..	..

* Chemical determination uncertain

Sample 1.—*El*-316
Sample 2.—*RA*106
Sample 3.—*El*38-28
Sample 4.—*RA*135
Sample 5.—*El*38-134

Igneous rock samples from E. S. Larsen, Jr., F. A. Gonyer analyst

Sample 6.—Mixture of equal parts of *G*-1 and *W*-1 (Fairbairn *et al.*, 1951)

over the concentration ranges of rock analysis. The lines used in this work, together with their usuable ranges are given in Table 1.

Chemically analyzed materials to be used as standards should approximate the unknown samples in both chemical and mineralogical content, and a standard powder should be exposed with each group of unknowns.

Sensitive lines of some less common elements also lie in this wave-length region, and these elements may be determined in the same operation. Sensitive lines of cobalt, copper, lead, gallium, lanthanum, molybdenum, nickel, silver, vanadium, zinc, and zirconium lie within the wave-length region photographed.

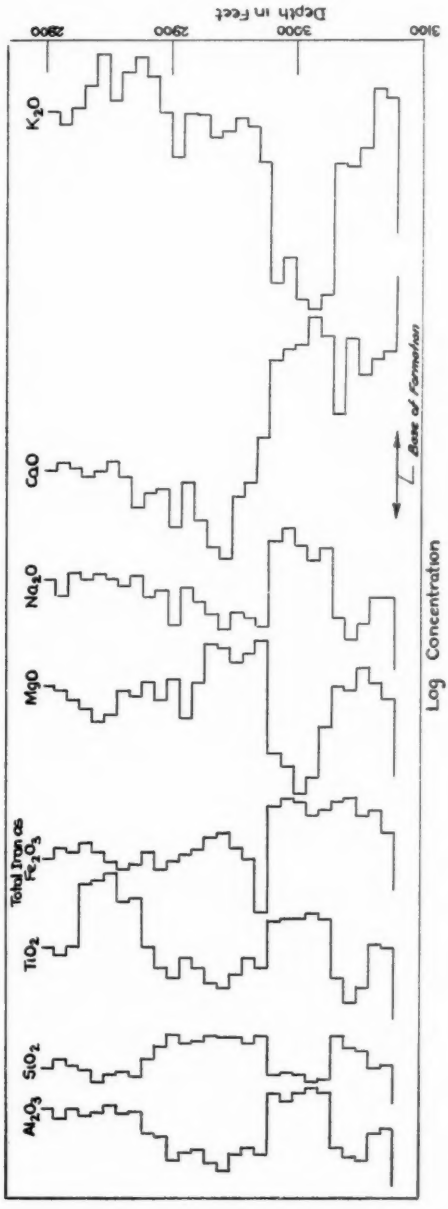

FIGURE 3.—GEOCHEMICAL LOGS OF MAJOR CONSTITUENTS OF ANTRIM SHALE
Variation with depth

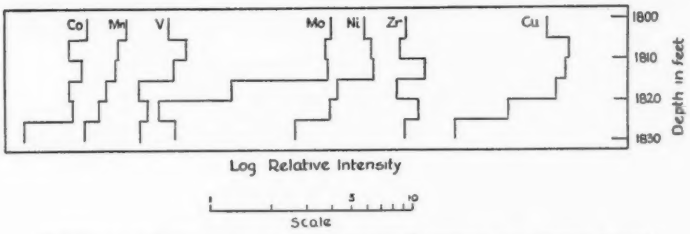

FIGURE 4.—GEOCHEMICAL LOGS OF MINOR ELEMENTS OF ANTRIM SHALE
Variation with depth

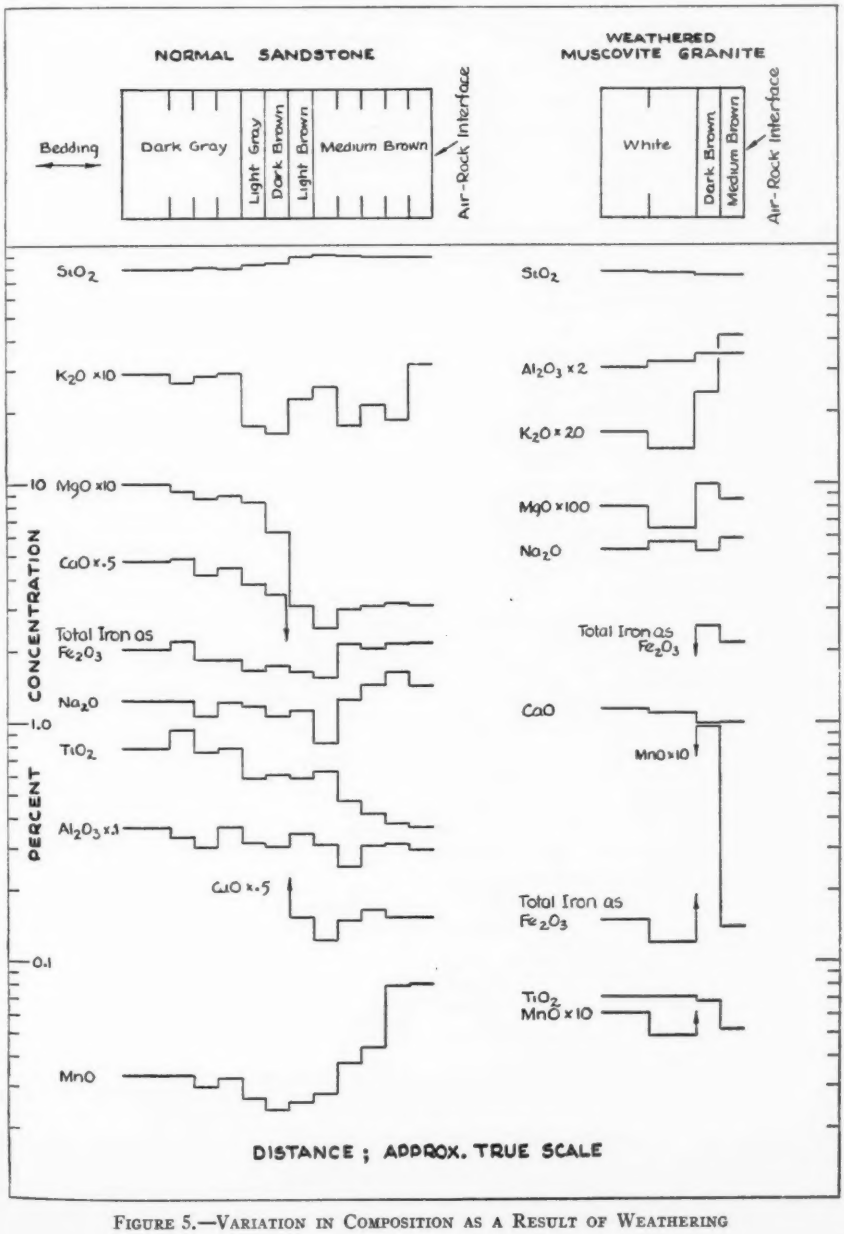

FIGURE 5.—VARIATION IN COMPOSITION AS A RESULT OF WEATHERING

sample may be used in the method of variable internal standardization, for which the standard concentration must be found independently, or in the method of mutual standardization wherein the concentration of the standard is found by difference. The mutual standard method has the advantage over other spectrochemical procedures of simplified sample preparation and concomitant analysis for all major constituents.

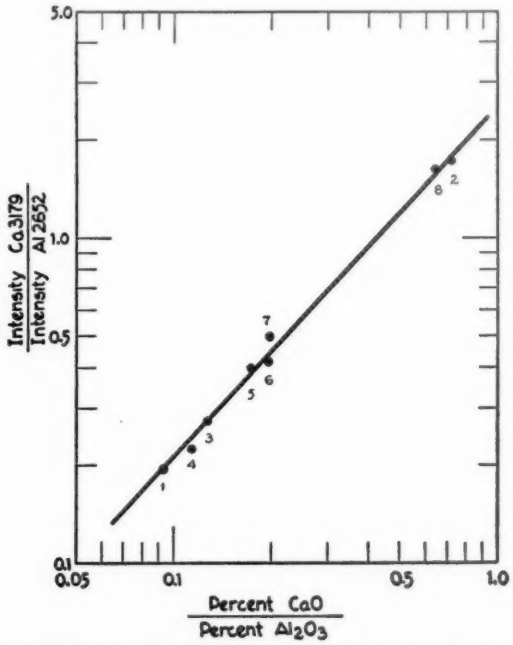

FIGURE 1.—MUTUAL STANDARD WORKING CURVE FOR CaO

1. G-1, standard granite (Fairbairn *et al.*, 1951)
2. W-1, standard diabase (Fairbairn *et al.*, 1951)
3. Bur. Stds. No. 93, boro-silicate glass
4. RGP
5. RA 135
6. EL 316
7. EL 34-167
8. FBSS 459

Igneous rocks from E. S. Larsen, Jr., F. A. Gonyer, Analyst

Spectrochemical analysis by mutual standardization has been used to determine the impurities in steel (Coulliette, 1943, p. 732) and has more recently been applied to the analysis of aluminous ores for alumina, silica, iron, and titania by Churchill and Russell (1945, p. 25), to the analysis of alumina, lime, magnesia, silica, and manganese in steel-making slags by Rosza (1947, p. 394), and to the analysis of these constituents plus iron, phosphorus, and titania in similar matrices by Carlsson and Yü, (1950, p. 276). Lime, magnesia, silica, iron, alumina, and titania in limestone were determined by Leininger (1950, p. 804) who used this method. A.C. arcs and spark sources have been used almost exclusively, although Rosza and Leininger make effective use of D.C. arc excitation.

Principles

The principles of mutual standardization have been discussed by Coulliette (1943, p. 732), Churchill and Russell (1945, p. 25),

Rosza (1947, p. 594), and Carlsson and Yü (1950, p. 276). In brief, the method is based on the assumptions that (1) the intensity ratio of two spectral lines is a function only of the concentration ratio of the two emitting elements, and that (2) the elements sought comprise essentially all of the sample, an assumption made also in gravimetric analysis.

Computation is based on the fact that if

$$A + C + D + \ldots . X = 100$$

then, dividing by A,

$$\frac{A}{A} + \frac{C}{A} + \frac{D}{A} + \cdots\cdots \frac{X}{A} = 100$$

and

$$A = \frac{100}{1 + \frac{B}{A} + \frac{C}{A} + \cdots\cdots \frac{X}{A}}.$$

These conditions do vary of course. The intensity-concentration relationship is affected by variation in the sample matrix, erratic illumination, and miscellaneous errors common to all spectrographic analysis. Constituents not readily determinable by spectrographic means (H_2O, CO_2, organic material, etc.) in amounts greater than ~5 per cent by weight must be determined independently.

Aluminum is chosen as the variable internal standard because of its ubiquity; this gives the formula:

$$\%Al_2O_3 = \frac{100}{1 + \frac{\%SiO_2}{\%Al_2O_3} + \frac{\%TiO_2}{\%Al_2O_3} + \frac{\text{Tot. Fe as } \%Fe_2O_3}{\%Al_2O_3} + \frac{\%MnO}{\%Al_2O_3} + \frac{\%MgO}{\%Al_2O_3} + \frac{\%CaO}{\%Al_2O_3} + \frac{\%Na_2O}{\%Al_2O_3} + \frac{\%K_2O}{\%Al_2O_3}}.$$

The ratios $\%SiO_2/\%Al_2O_3$, $\%TiO/\%Al_2O_3$, and others are obtained from plots (working curves) of intensity ratio versus concentration ratio drawn from data determined by measurements on chemically analyzed standards. Figure 1 is a typical working curve. Intensity ratios are determined by opacity measurements of spectral lines, and the equivalent concentration ratios from the working curves

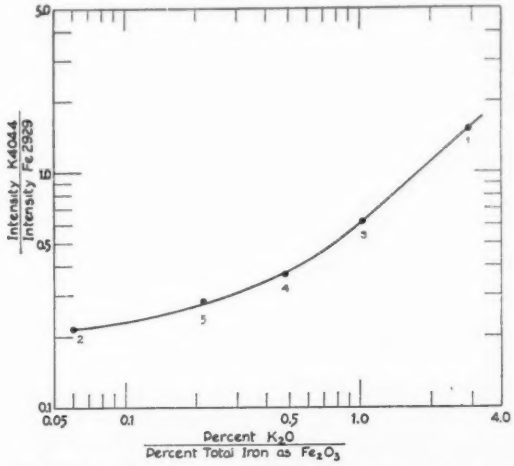

FIGURE 2.—MUTUAL STANDARD WORKING CURVE FOR K_2O
1. G-1, standard granite (Fairbairn *et al.*, 1951)
2. W-1, standard diabase (Fairbairn *et al.*, 1951)
3. G-1 3 parts, W-1 1 part by weight
4. G-1 1 part, W-1 1 part by weight
5. G-1 1 part, W-1 3 parts by weight

are substituted in the equation above, which is then solved for $\%Al_2O_3$. Multiplication of the appropriate concentration ratio by the $\%Al_2O_3$ value then gives the concentration of the other oxides.

TABLE 1.—USABLE CONCENTRATION RANGES FOR ANALYSIS LINES

Line	Concentration range (per cent)
Si2970	50–100
2987	20–80
Al2652	3–20
Ti3088	0.005–1
3242	0.1–2
Fe2912	0.1–10
2929	1–10
Mn2801	0.001–0.1
Ca3006	10–50
3158	0.05–15
3179	0.01–10
Na3302	0.2–10
K4044	0.5–10

Better working curves result from widespread concentration ratios. It is advisable to take the ratios of the more variable constituents (titanium, magnesium, calcium, manganese and iron) to aluminum, and the ratios of the more constant constituents (silicon, sodium, and potassium) to iron. The latter ratios may then be transformed into ratios to aluminum by multiplication by the known ratio

$$\frac{\%\ \text{Total Iron as } Fe_2O_3}{\%Al_2O_3}.$$

In the present work the ratio of potassium to iron is used because there is a background contribution at the potassium line from an adjacent iron line, and automatic correction for this background is obtained by using a working curve based on

$$\frac{\text{Log Intensity K}}{\text{Log Intensity Fe}} \text{ vs. } \frac{\text{Log } \%K_2O}{\text{Log } \%\text{ Total Iron as } Fe_2O_3}.$$

Figure 2 illustrates this working curve.

If the concentration of any constituent in the sample is known prior to analysis, the numerator of the equation should be reduced accordingly, and the appropriate concentration ratio eliminated from the denominator. The mutual standard method may be coupled with any other analytical procedure by this simple modification of the basic formula.

Operating Procedure

Samples are reduced to −100 mesh, dried at 110°C, and packed firmly with a small cylindrical ram into pure carbon electrodes. Samples may be mixed with one part of carbon powder to insure smooth burning. Electrodes an eighth of an inch in diameter with a cavity 1 mm in diameter and 3 mm deep, are used.

TABLE 2.—STANDARD DEVIATION IN PER CENT OF INTENSITY RATIOS FROM REPLICATE ARCINGS OF *G*-1 AND *W*-1

	Si2987/Al2652	Ti3088/Al2652	Fe2912/Al2652	Mn2801/Al2652	Mg2779/Al2652	Ca3179/Al2652	Na3302/Al2652	K4044/Al2652
G-1	8.9	12.0	10.0	6.2	7.6	11.1	9.6	6.8
W-1	10.8	9.7	5.2	8.8	14.0	9.2	13.9	4.6

The sample is excited as the anode and is arced to completion at 6 amperes.

All observations have been made on a large Hilger prism instrument over the wave-length range of 2630Å–4100Å. Slow plates are preferable because of inconveniently high density on more sensitive plates; Eastman *N*-1 plates were used.

A rotating-step sector placed in front of the slit and transmitting $\frac{1}{32}$, $\frac{1}{64}$, and $\frac{1}{128}$ of the incident light provides sufficient selection of line intensities, and facilitates plate calibration.

The spectral lines which may be used satisfactorily in the mutual standard method, in common with spectral lines used in all major element determinations, are relatively insensitive and show little or no self-absorption

TABLE 3.—COMPARISON OF CHEMICAL AND SPECTROCHEMICAL ANALYSES

	Chem.	Spec	Bias	% Bias
SAMPLE 1				
SiO_2	71.14	69.9	1.24	1.7
TiO_2	.29	.27	.02	6.9
Al_2O_3	14.92	15.7	.78	5.2
Total iron as Fe_2O_3	3.23	2.80	.43	13.3
MnO	.05*	.02	..	..
MgO	.85	.74	.11	13.0
CaO	2.94	3.30	.36	12.2
Na_2O	3.50	4.16	.66	18.9
K_2O	2.90	3.38	.48	16.6
Total	99.82	100.27		
SAMPLE 2				
SiO_2	74.68	74.90	.22	0.3
TiO_2	.15	.11	.04	26.7
Al_2O_3	13.80	13.62	.18	1.3
Total iron as Fe_2O_3	2.04	2.52	.48	23.5
MnO	.03	.04	.01	33.3
MgO	.21*	.48	..	..
CaO	2.26	2.38	.12	5.3
Na_2O	4.10	3.40	.70	17.1
K_2O	2.01	2.45	.44	21.9
Total	99.28	99.90	..	..
SAMPLE 3				
SiO_2	62.28	60.3	1.98	3.2
TiO_2	.72	.72	0	0
Al_2O_3	16.68	17.70	1.02	6.1
Total iron as $Fe\,O_3$	6.66	7.10	.44	6.6
MnO	.07	.07	0	0
MgO	2.33	2.66	.33	14.2
CaO	5.72	5.68	.04	0.7
Na_2O	3.50	3.82	.32	9.2
K_2O	1.49	2.02	.53	35.6
Total	99.45	100.07	..	..
SAMPLE 4				
SiO_2	72.58	73.1	.52	0.7
TiO_2	.30	.31	.01	3.3
Al_2O_3	14.12	13.55	.57	4.2
Total iron as Fe_2O_3	3.27	4.20	.93	28.4
MnO	.02*	.05	..	..
MgO	.70	.74	.04	5.7
CaO	2.44	2.17	.27	12.4
Na_2O	3.91	3.59	.32	8.9
K_2O	2.84	2.44	.40	16.4
Total	100.18	100.15	..	..

TABLE 3.—*Continued*

	Chem.	Spec	Bias	% Bias
SAMPLE 5				
SiO_2	59.28	59.3	.02	0
TiO_2	.85	.87	.02	2.3
Al_2O_3	17.86	17.95	.09	0.5
Total iron as Fe_2O_3	7.00	6.29	.71	10.1
MnO	.07	.07	0	0
MgO	3.21	2.96	.25	7.8
CaO	6.46	6.56	.10	1.5
Na_2O	3.39	3.41	.02	0.6
K_2O	1.53	1.55	.02	1.3
Total	99.65	98.96	..	..
SAMPLE 6				
SiO_2	62.70	65.4	2.7	4.1
TiO_2	.66	.61	.05	8.2
Al_2O_3	14.40	13.25	1.15	8.7
Total iron as Fe_2O_3	6.47	6.42	.05	0.8
MnO	.095	.086	.009	10.5
MgO	3.06	3.46	.40	13.1
CaO	6.12	5.43	.69	12.7
Na_2O	2.69	2.76	.07	2.5
K_2O	3.10	3.02	.08	2.7
Total	99.30	100.44	..	..

* Chemical determination uncertain

Sample 1.—*El*-316
Sample 2.—*RA*106
Sample 3.—*El*38–28
Sample 4.—*RA*135
Sample 5.—*El*38–134

Igneous rock samples from E. S. Larsen, Jr., F. A. Gonyer analyst

Sample 6.—Mixture of equal parts of *G*-1 and *W*-1 (Fairbairn *et al.*, 1951)

over the concentration ranges of rock analysis. The lines used in this work, together with their usuable ranges are given in Table 1.

Chemically analyzed materials to be used as standards should approximate the unknown samples in both chemical and mineralogical content, and a standard powder should be exposed with each group of unknowns.

Sensitive lines of some less common elements also lie in this wave-length region, and these elements may be determined in the same operation. Sensitive lines of cobalt, copper, lead, gallium, lanthanum, molybdenum, nickel, silver, vanadium, zinc, and zirconium lie within the wave-length region photographed.

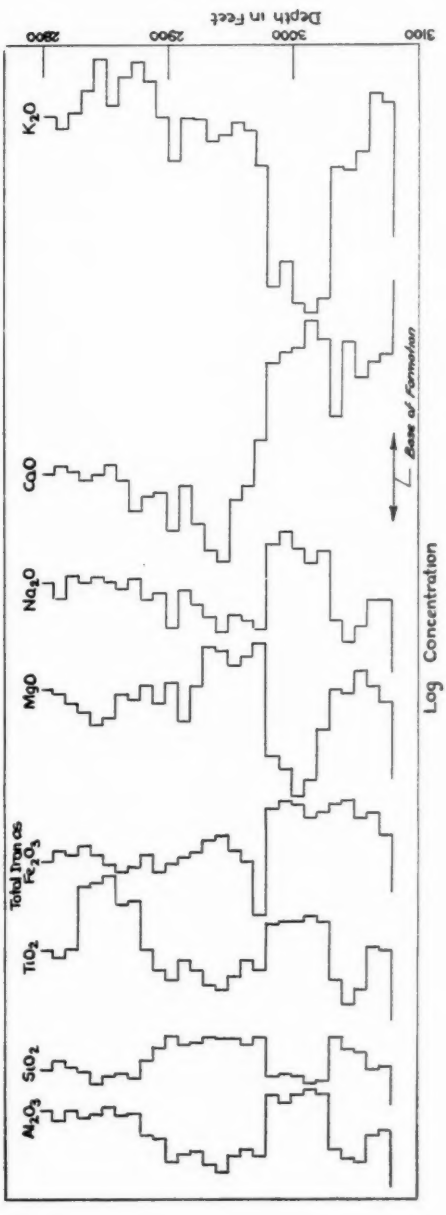

FIGURE 3.—GEOCHEMICAL LOGS OF MAJOR CONSTITUENTS OF ANTRIM SHALE
Variation with depth

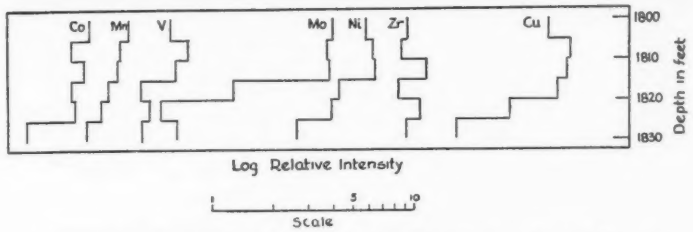

FIGURE 4.—GEOCHEMICAL LOGS OF MINOR ELEMENTS OF ANTRIM SHALE
Variation with depth

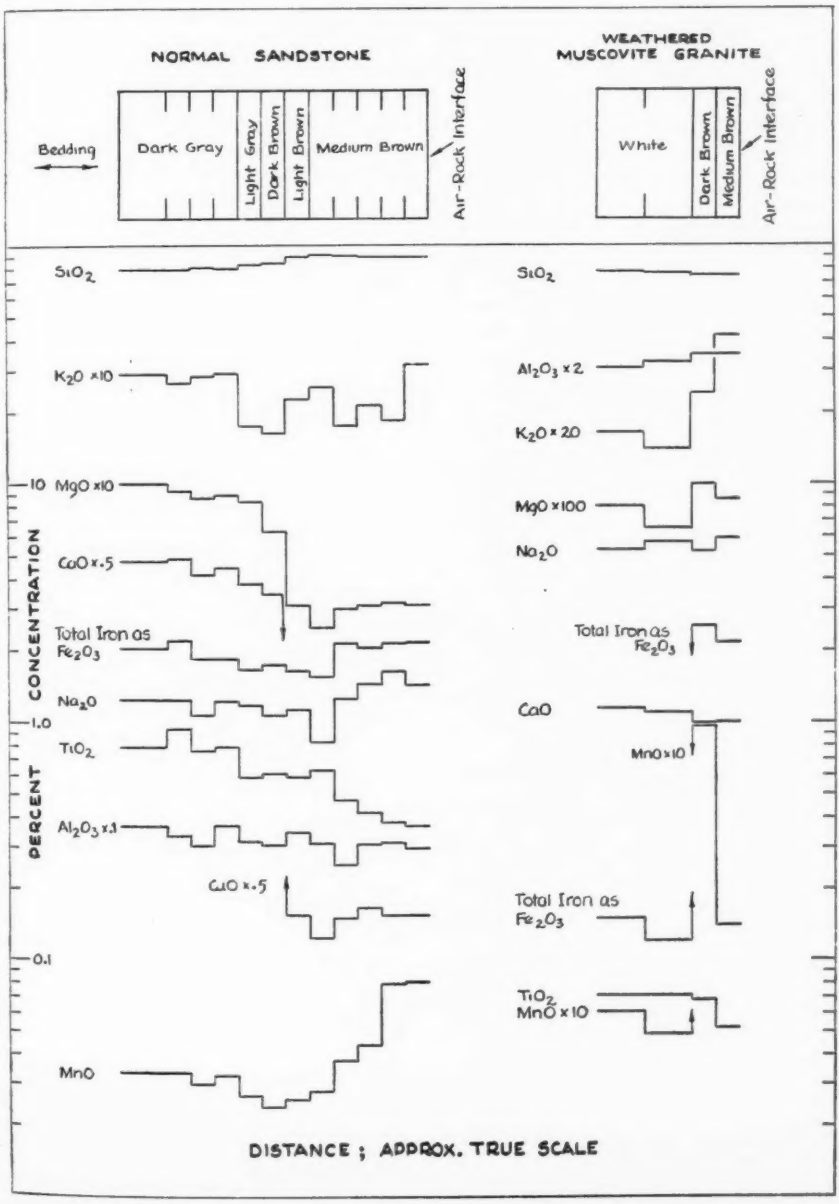

FIGURE 5.—VARIATION IN COMPOSITION AS A RESULT OF WEATHERING

Precision and Accuracy

The precision of the method was evaluated by replicate arcings of *G*-1 and *W*-1 (Fairbairn *et al.*, 1951, p. 2–4), the standard granite and diabase. Most intensity ratios of the spectral lines to A12652 (Table 2) have a relative deviation (per cent standard deviation) of about 10 per cent.

Since spectrographic operations are carried out in duplicate or triplicate, the values in Table 1, which represent the expected percentage deviation of a single determination, would be reduced by $1/\sqrt{n}$ where n is the number of arcings.

This method was checked by comparing chemically determined analyses with results obtained spectrographically (Table 3). The per cent bias of the determinations follows the trend noted by Fairbairn (1952, p. 144–145) for the precision of chemical analyses.

Applications

The method applies in the analysis of abundant samples or investigations of the relative changes in chemistry within or between bodies of rock, such as fractionation, weathering, and contact phenomena.

The mutual standard method was used in analyzing well cuttings of the Antrim shale. (*See* Fig. 3.) The analyses are uncorrected for water, carbon dioxide, and organic material. The geochemical log is illustrated in Figure 3. Such logs are useful for correlation, determination of internal chemical variation, and calculation of average composition.

Figure 4 illustrates the relative variation in concentration of some minor rock constituents from another group of Antrim shale well cuttings, as determined from plates exposed primarily for the analysis of major constituents.

The study of closely spaced samples across a critical zone is often useful. Mutual standard analyses by Miss A. C. Wilfert across such a zone (Fig. 5) show the chemical changes taking place in a narrow strip of weathered rock between apparently fresh material and the surface.

Conclusions

Most other spectrographic methods for the determination of the major elements require the addition of internal standards and several separate arcings for complete analysis. In the method described here, SiO_2, TiO_2, Al_2O_3, total iron as Fe_2O_3, MnO, MgO, CaO, Na_2O, and K_2O are determined in a single operation. The relative deviation of the results is about 10 per cent and the analytical time required is less than 2 hours per triplicate analysis. Many minor elements are also readily determined from the plates.

Spectrochemical determination of this nature may easily be coupled with flame photometric, colorimetric, or other spectrographic procedures to the advantage of each technique.

References Cited

Ahrens, L. H., 1954, Quantitative spectrochemical analysis of silicates: Pergamon Press Ltd., London, 119 p.

Carlsson, C. G., and Yü, J. T. M., 1950, Spectrochemical analysis of steelmaking slags: Iron and Steel Inst. Jour., v. 166, p. 273–280.

Churchill, J. R., and Russell, R. G., 1945, Analysis of aluminous ores by means of spark spectra: Ind. and Eng. Chemistry Anal. Ed., v. 17, p. 24–27.

Coulliette, J. H., 1943, Determination of nickel and chromium in stainless steel: Ind. and Eng. Chemistry Anal. Ed., v. 15, p. 732–734.

Dennen, W. H., Ahrens, L. H., Fairbairn, H. W., 1951, A cooperative investigation of precision and accuracy in chemical, spectrochemical, and modal analysis of silicate rocks, pt. 3, Spectrochemical analysis of major constituent elements in rocks and minerals: U. S. Geol. Survey Bull. 980, p. 25–45.

Fairbairn, H. W., 1952, Precision and accuracy of chemical analysis of silicate rocks: Geochim. et Cosmochim. Acta, v. 4, p. 143.

Fairbairn, H. W., Schlect, W. G., Stevens, R. E., Dennen, W. H., Ahrens, L. H., and Chayes, F., 1951, A cooperative investigation of precision and accuracy in chemical, spectrochemical, and modal analysis of silicate rocks: U. S. Geol. Survey Bull. 980, 71 p.

Leininger, R. K., 1950, Spectrochemical determination of major constituents of limestone (Abstract): Opt. Soc. Am. Jour., v. 40, p. 104.

Leininger, R. K. and Taylor, R., 1954, Scheme of analysis of silicate rocks. Spectrographic methods (Abstract): Anal. Chemistry, v. 26, p. 436.

Rozsa, J. T., 1947, Slag control by routine spectrographic analysis: Metal Progress, v. 51, p. 593–597.

Shapiro, L., and Brannock, W. W., 1952, Rapid analysis of silicate rocks: U. S. Geol. Survey Circ. 165, 17 p.

Cabot Spectrographic Laboratory, Department of Geology and Geophysics, Massachusetts Institute of Technology, Cambridge 39, Mass.

Manuscript Received by the Secretary of the Society, November 20, 1953.

EXPLANATION

QUATERNARY

Recent

Qla

Landslides

Qal

Alluvium

Chiefly alluvial fans and flood-plain deposits, some loess

UNCONFORMITY

Pleistocene

Qt

Silt, sand, and gravel

Chiefly stream terrace deposits

UNCONFORMITY

Ql

Pediment surfaces

Covered with gravel and loess

UNCONFORMITY

TERTIARY

Pliocene and Miocene

Ellensburg formation

Te

Undifferentiated

Chiefly pumiceous andesitic silts, sands and gravels

Teb

Basalt conglomerate

Basalt flows in the Ellensburg formation

Tew

Sediments below the Wenas basalt flow

Tem

Elephant Mountain flow

Ts

Selah Butte flow

Tw

Wenas flow

Ty

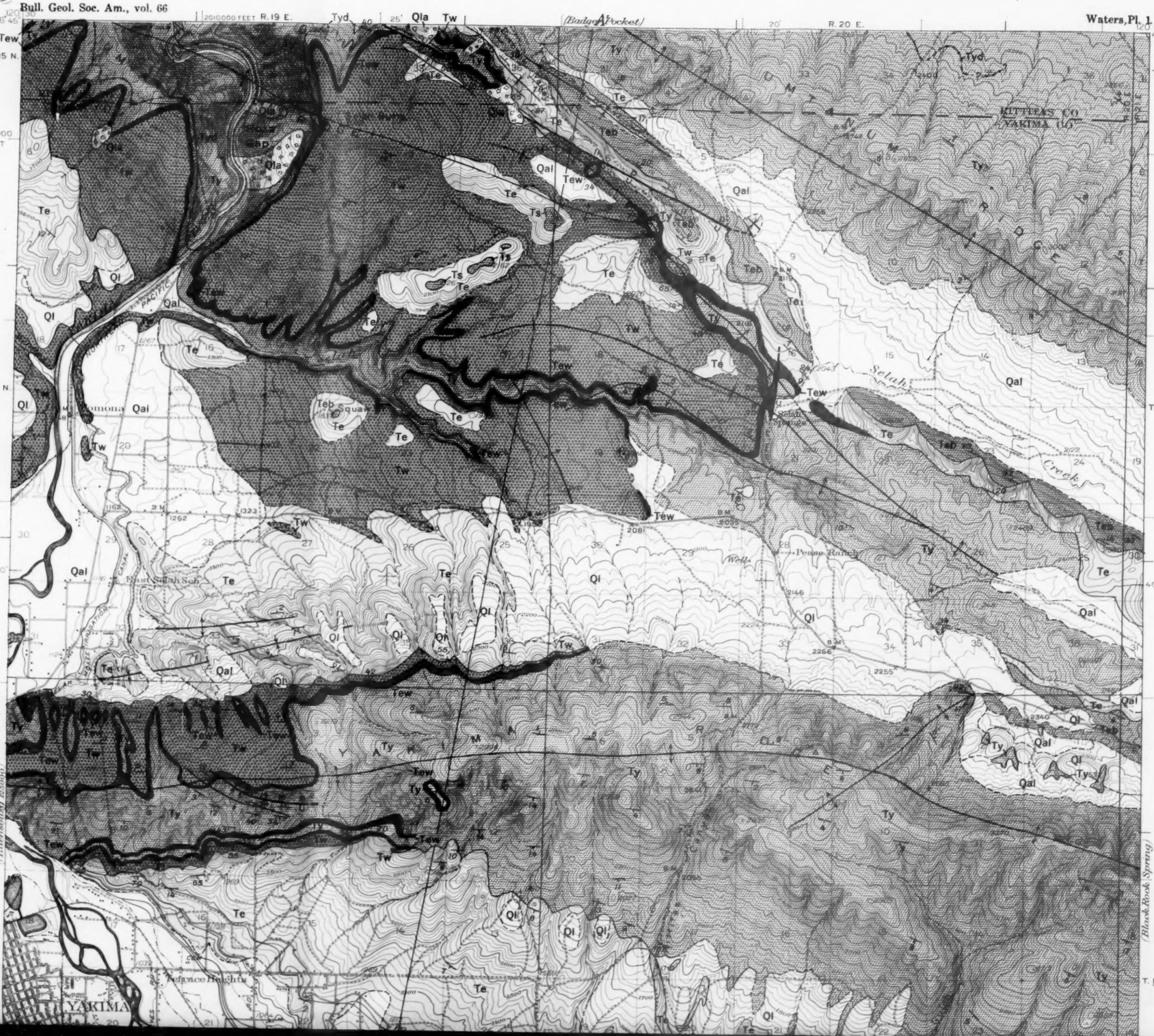

EXPLANATION

Recent	Qla	Landslides	QUATERNARY
Recent	Qal	Alluvium *Chiefly alluvial fans and flood-plain deposits; some loess*	QUATERNARY
		UNCONFORMITY	
Pleistocene	Qt	Silt, sand, and gravel *Chiefly stream terrace deposits*	QUATERNARY
		UNCONFORMITY	
Pleistocene	Ql	Pediment surfaces *Covered with gravel and loess*	QUATERNARY
		UNCONFORMITY	
Pliocene and Miocene — Ellensburg formation	Te	Undifferentiated *Chiefly pumiceous andesitic silts, sands and gravels*	TERTIARY
Pliocene and Miocene — Ellensburg formation	Teb	Basalt conglomerate	TERTIARY
Pliocene and Miocene — Ellensburg formation	Tew	Sediments below the Wenas basalt flow	TERTIARY
Pliocene and Miocene — Basalt flows in the Ellensburg formation	Tem	Elephant Mountain flow	TERTIARY
Pliocene and Miocene — Basalt flows in the Ellensburg formation	Ts	Selah Butte flow	TERTIARY
Pliocene and Miocene — Basalt flows in the Ellensburg formation	Tw	Wenas flow	TERTIARY
Pliocene and Miocene — Basalt flows in the Ellensburg formation	Ty		TERTIARY

Pliocene and Miocene — TERTIARY

Basalt flows in the Ellensburg formation

Tew — Sediments below the Wenas basalt flow

Tem — Elephant Mountain flow

Ts — Selah Butte flow

Tw — Wenas flow

Yakima basalt

Ty — Yakima basalt
Plateau basalt, pillow lava, palagonite tuff

Tyd — Diatomite
Diatomite and silt interbedded with the Yakima basalt

U / D — Fault
U, *upthrown side*; D, *downthrown side*

15 — Strike and dip of beds

Anticline

Syncline

Geology by A. C. Waters

GEOLOGIC MAP AND SECTION OF YAKIMA EAST QUADRANGLE, WASHINGTON

Scale 1:62,500

1 0 4 Miles

Contour interval 25 feet
Datum is mean sea level

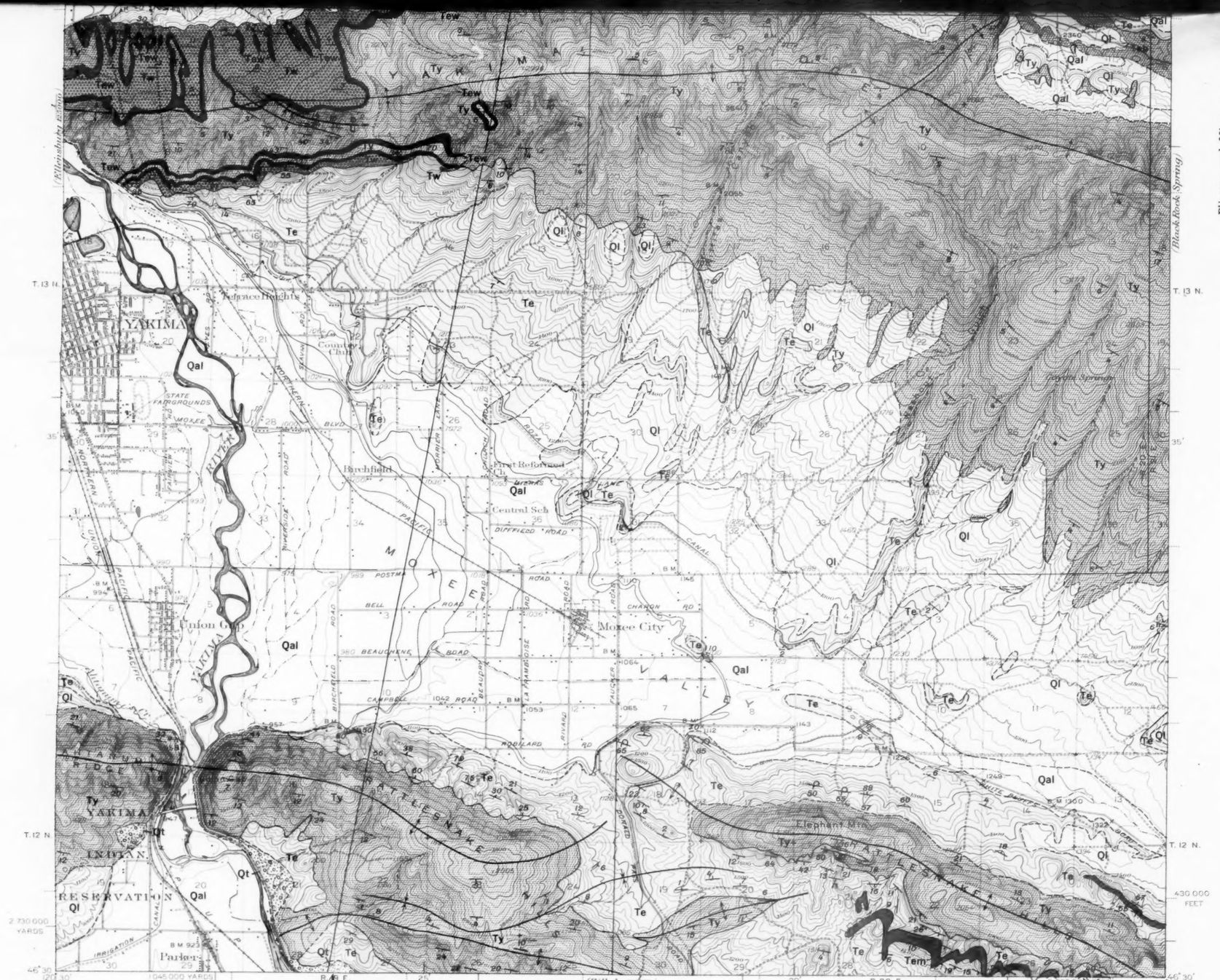

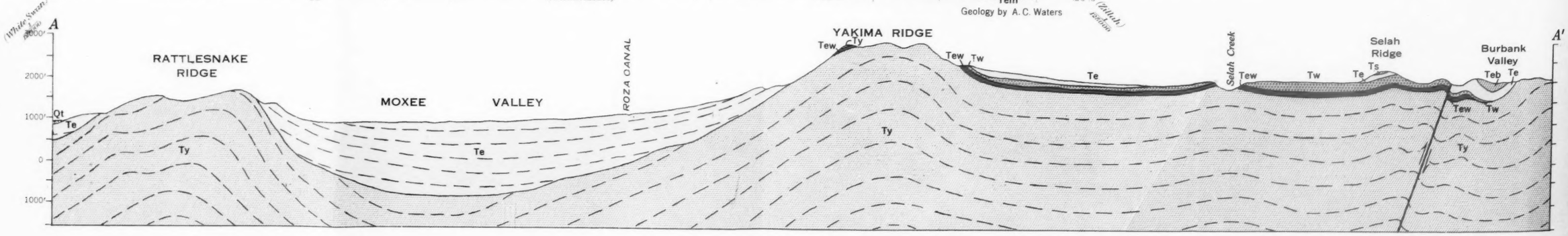

Sediments below the Wenas basalt flow

Elephant Mountain flow

Selah Butte flow

Wenas flow

Yakima basalt
Plateau basalt, pillow lava, palagonite tuff

Diatomite
Diatomite and silt interbedded with the Yakima basalt

Pliocene and Miocene — Basalt flows in the Ellensburg formation — Yakima basalt — TERTIARY

U / D
Fault
U, *upthrown side;* D, *downthrown side*

15
Strike and dip of beds

Anticline

Syncline

APPROXIMATE MEAN DECLINATION, 1936

Geology by A. C. Waters

GEOLOGIC MAP AND SECTION OF YAKIMA EAST QUADRANGLE, WASHINGTON

Scale 1:62,500

1 0 4 Miles

Contour interval 25 feet
Datum is mean sea level

BULLETIN OF THE GEOLOGICAL SOCIETY OF AMERICA
VOL. 66, PP. 663-684, 3 FIGS., 2 PLS. JUNE 1955

GEOMORPHOLOGY OF SOUTH-CENTRAL WASHINGTON, ILLUSTRATED BY THE YAKIMA EAST QUADRANGLE

By Aaron C. Waters

Abstract

Geologic mapping of the Yakima district has been neglected since publication of the Ellensburg and Mount Stuart folios (G. O. Smith, 1903a; 1904; *see also* Calkins, 1905). Reports on other parts of the Columbia River plateau, however, pose new problems and call for revision of some interpretations. This paper presents the results of extending Smith's mapping eastward into the adjacent Yakima East quadrangle, and of considerable reconnaissance work in adjoining areas. The new mapping shows that to the east and south the lower part of the Ellensburg formation interfingers with the Yakima basalt. It also indicates that local diastrophism and volcanism continuously modified and interrupted deposition of the Ellensburg formation.

Smith's conclusions that the great topographic ridges are growing anticlines, not fault blocks, and that the major rivers are antecedent to these folds, are confirmed. The anticlines appear to have grown in a single epoch of deformation instead of in two orogenic episodes separated by a period of peneplanation. The "Cascade lowland" is a local pediment formed on the flanks of a growing anticline, not a remnant of a widespread peneplain.

The new data do not support Warren's hypothesis of defeat and diversion of Columbia River by rise of the Horse Heaven uplift, nor Flint's hypothesis of the cutting of Wallula Gap by a river thus diverted.

CONTENTS

TEXT

	Page
Introduction	664
Acknowledgments	666
Unsolved problems	666
Ellensburg-basalt stratigraphic relations	666
Ellensburg correlation problem	666
Anticlines versus fault blocks	666
Question of a Cascade peneplain	667
Stages in rise of the anticlinal ridges	667
Antecedent, superimposed, or subsequent streams	667
Diversion of Columbia River	668
Contemporaneous volcanism, sedimentation, diastrophism, and erosion	668
Yakima East quadrange	668
Scope and purpose of study	668
Yakima basalt	669
Sedimentary intercalations	670
Contact between the Yakima basalt and the Ellensburg formation	670
Physical conditions, Yakima-Early Ellensburg time	672
Basalt flows interstratified with the Ellensburg formation	673
Wenas flow	673
Selah Butte flow	673
Elephant Mountain flow	673
Post-Wenas part of the Ellensburg formation	673
Unconformities within the Ellensburg formation	674
Structure	675
Anticlinal folds	675
Faults	675
Deformation at shallow depths	676
Geomorphology	676
Surfaces stripped to the Wenas and Yakima basalts	676
Erosion surfaces discordant to structure	676
Type locality of the "Cascade Peneplain"	678
Antecedent Yakima River and Columbia River	679
Diversion of Columbia River	681
Summary and conclusions	683
References cited	684

ILLUSTRATIONS

Figure	Page
1. Map showing anticlinal mountain ridges of south-central Washington	665
2. Profiles of dissected pediments	677
3. Spur east of Kelley Hollow, type locality of the "Cascade peneplain"	679

Plate	Facing page
1. Geologic map and cross section of the Yakima East quadrangle	663
2. Erosion surfaces discordant to structure	676

TABLE

Table	Page
1. Section along Roza Canal and Tunnel, south flank of Roza Gap	671

Introduction

The basic features of the geology of south-central Washington were outlined near the beginning of this century in two folios of the United States Geological Survey (Smith, 1903a; 1904). In these and supplementary papers, G. O. Smith (1901; 1903b; 1903c) and Frank C. Calkins (1905) have described a region of extraordinary structural and geomorphic interest. Their principal conclusions may be summarized as follows:

Between the towns of Ellensburg and Yakima are several high and broad anticlinal ridges which trend approximately east-west (Fig. 1). The ridges are separated by wider, comparatively flat-floored synclinal valleys. Yakima River, the master stream of the region, flows south, crossing the anticlinal ridges in spectacular steep-walled canyons that contrast with its low banks on the flat-floored valleys.

The oldest rocks are a series of plateau basalts, a part of the widespread Columbia River basalt (Merriam, 1901, p. 303). Smith (1903a, p. 3) proposed the name Yakima basalt for the local section of basaltic lava in the Ellensburg-Yakima region. Above the Yakima basalt lies a varied series of sedimentary rocks which Smith (1903a, p. 2) named the Ellensburg formation. This formation consists chiefly of torrentially stratified beds composed of partially devitrified glass shards and pumice lapilli. Lenses of conglomerate containing pebbles of pyroxene and hornblende andesites are common. These materials indicate that the Ellensburg formation was deposited by streams that headed in a growing range of andesitic volcanoes on the west. Extensive remnants of this volcanic range are exposed in the present Cascade Mountains.

Smith (1903a, p. 4) described a thin basalt member, which he named the Wenas basalt, intercalated in the lower part of the Ellensburg formation. He regarded this as a final recrudescence of the volcanic activity that gave rise to the Yakima basalt.

The extrusion of the Yakima and Wenas basalts and the deposition of the Ellensburg formation were first dated as Miocene (Smith, 1903a, p. 2–3), on the basis of fossil plants and of *Hipparion* teeth found in the Ellensburg formation. These age assignments have been modified slightly upward by new fossil finds; much or all of the Ellensburg and its associated intercalated basalt flows is now regarded as Pliocene, although the bulk of the Yakima basalt may be Miocene.[1]

Following deposition of the Ellensburg, the area was warped into broad anticlines and synclines. Although the anticlines formed by this folding are coincident with the present topographic ridges, Smith believed that two distinct periods of folding produced the present topography. Following the first folding (Smith, 1903a, p. 2):

> The streams, with increased grade, began at once their attack on the uplifted rocks, so that erosion took the place of deposition. First the Miocene (Ellensburg) sands and gravels were cut away until these soft beds were wholly removed from the crests of the arches, and thereafter erosion continued until even the hard basalt was taken away in considerable amount.
>
> The degradation of the land by the activity of the streams was continued with no apparent cessation until the whole region was reduced to a lowland. Its relief now became relatively insignificant, the reduction of the approximately level plain, or peneplain, having reached such a degree of perfection that the resistant basalt was leveled off equally with the soft sandstone.
>
> The peneplain resulting from this effectual erosion was next affected by orogenic forces. Along lines for the most part coincident with those of the earlier folding, the level surface was arched and at the same time the whole region was uplifted. This process was an extremely slow one, but it eventually gave considerable relief to what had been a featureless plain. The streams that had meandered over the old lowland now began to entrench themselves, and where the arches of the warped plain slowly rose athwart them the larger rivers performed the task of maintaining their channels. The deep water gaps where Yakima River cuts through these uplifted ridges afford unmistakable evidence of the success with which the river accomplished this task of keeping its right of way. The valleys between the ridges furnished natural routes for surface waters, and thus many of the

[1] Mr. B. L. Foxworthy, of the United States Geological Survey, is preparing a report on water resources of Ahtanum Valley which will contain data on new fossil finds in the Yakima district. Fresh-water mollusks have been recovered from sedimentary beds associated with the upper part of the Yakima basalt in Ahtanum Valley, and vertebrates were found in the lower part of the Ellensburg formation in an irrigation tunnel driven through Yakima Ridge. Both the mollusks and vertebrates have tentatively been assigned to the Pliocene.

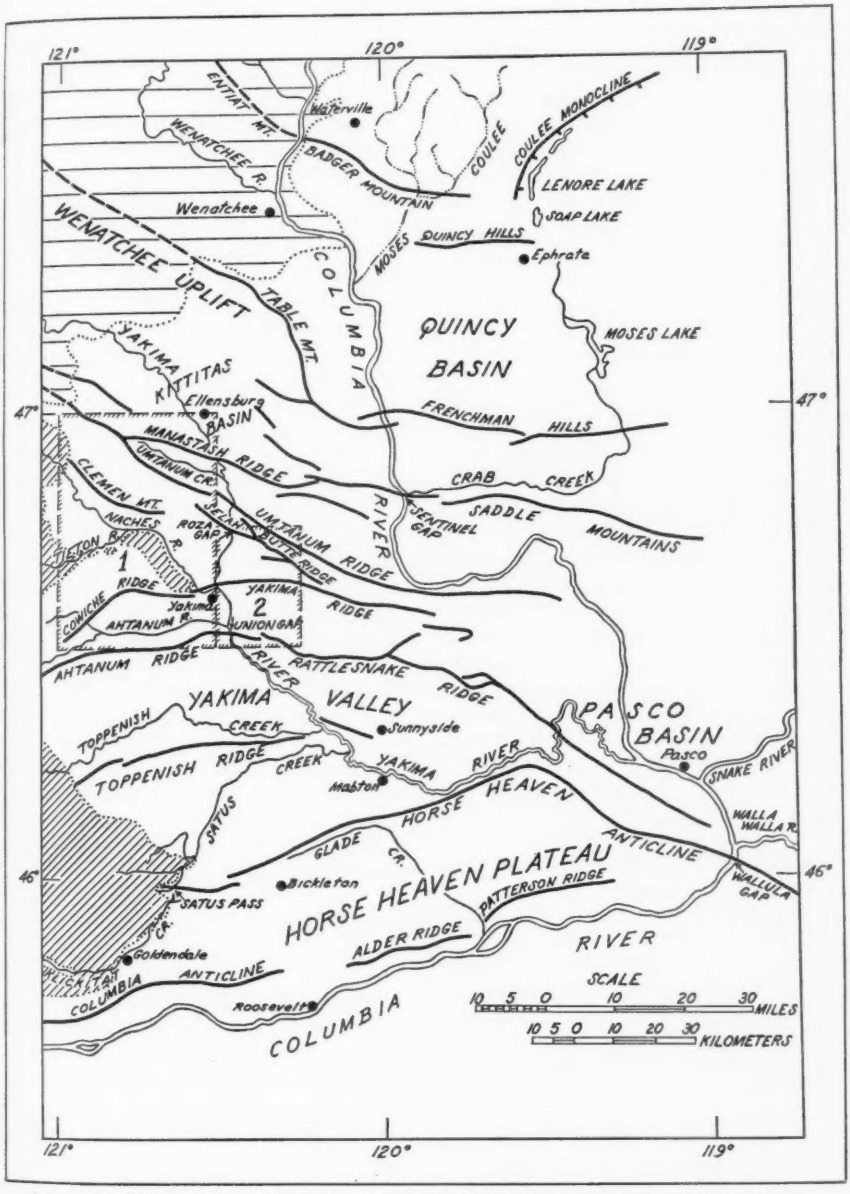

FIGURE 1.—MAP SHOWING ANTICLINAL MOUNTAIN RIDGES OF SOUTH-CENTRAL WASHINGTON

The main anticlinal ridges are shown by heavy lines, dashed where extended into areas underlain by rocks older than the Yakima basalt (horizontal ruled area), and omitted from areas underlain by Quaternary alluvial basalt and andesite (obliquely ruled area).

1 = Ellensburg quadrangle; 2 = Yakima East quadrangle.

tributaries of Yakima River have courses consequent upon the warped hollows of the peneplain.

Smith (1903a, p. 2) fixed the date of the peneplain as Pliocene and considered that its subsequent warping and uplift continued into the Pleistocene. Other events that he attributed to the Pleistocene are widespread canyon cutting, the partial filling of the Naches and Tieton valleys with young flows of hypersthene andesite, the alluviation of some valleys with coarse basaltic gravel (Cowiche gravel and equivalents) or with fine silts, and, finally, the glaciation of the headwaters of the Yakima River and its tributaries.

Acknowledgments

This paper is a by-product of work on the Columbia River basalts financed in part by a grant from the Penrose Bequest of The Geological Society of America.

Special thanks are due Professor J. Hoover Mackin of the University of Washington and Mr. Bruce Foxworthy of the United States Geological Survey. They critically read the manuscript and made many worthwhile suggestions, and they also volunteered important unpublished information on parts of the area. Mr. Philip Choquette assisted in the preparation of the illustrations.

Unsolved Problems

Ellensburg-Basalt Stratigraphic Relations

Since Smith and Calkins' work, geologic studies have brought out a number of unsolved problems, as well as some variants or outright differences in interpretation. Smith considered that extrusion of the basalts was essentially completed before the beginning of deposition of the Ellensburg formation, though he recognized a minor recurrence of volcanic activity in the Early Ellensburg to give rise to the Wenas basalt. But the exact relation of the Ellensburg sediments to the Yakima basalt, when traced east and south of the Yakima-Ellensburg area toward the center of the basalt plateau, is not clear. Do they lie on top of the basalt, or do they interfinger with successively younger basalt flows to the east?

A marginal belt of sedimentary rocks which interfingers with the Columbia River basalt has been recorded at several localities (Pardee and Bryan, 1926, p. 7–8; Fuller, 1931, p. 294–295; Berry, 1931, p. 31; Piper, 1932, p. 119; Waters, 1939, p. 639). These marginal sediments were laid down in shallow lakes, deltas, and fans, as the lower courses of the streams draining the adjacent highlands were dammed by the advancing floods of basalt. Perhaps in the Yakima-Ellensburg region, tracing of the Ellensburg formation to the east might show that it also is interbedded with the basalt in a marginal relationship, and is not a distinctly younger formation as Smith and Calkins had supposed.

Ellensburg Correlation Problem

A related problem is the exact correlation of the lavas and sediments mapped by Smith and Calkins in the Ellensburg quadrangle with analogous basalt-sediment assemblages in other parts of the basalt plateau. Of especial interest is its relation to the Columbia River basalt-Mascall formation sequence of the John Day region (Merriam, 1901), to the Yakima basalt-Dalles formation and the Yakima basalt-Hood River formation sequences of the Columbia gorge (Piper, 1932; Buwalda and Moore, 1930), and to basalt-sedimentary sequences along the junction of the basalt plateau with the crystalline rocks of the Okanogan highlands (Pardee and Bryan, 1926; Fuller, 1931; Berry, 1931; Waters, 1939).

Anticlines Versus Fault Blocks

In an early reconnaissance across central Washington, I. C. Russell (1893, p. 28–31) described the bold east-west ridges of the area as fault blocks, analogous to the tilted lava blocks he had seen in southern Oregon and northwestern Nevada. Smith (1903a; 1903b; 1903c) vigorously contested this interpretation, insisting that the ridges were anticlinal, and that they owed nothing of their straightness and abruptness to faulting. Smith's argument is well documented, and superb cross sections of the anticlines are displayed in the water gaps where Columbia and Yakima Rivers cross the ridges. Therefore it is surprising to find

that one writer has returned to the fault block theory (Hodge, 1931).

Question of a Cascade Peneplain

Smith concluded that, after folding of the basalt and Ellensburg sedimentary rocks, a long period of erosion reduced the anticlinal upwarps to a featureless peneplain. A recurrence of folding along the same axes warped the peneplain surface into the present anticlinal ridges. The chief evidence for the peneplain is found at Kelley Hollow on the Ellensburg quadrangle where erosion has beveled both the relatively unconsolidated Ellensburg pumiceous sediments and the hard basalt flows to a common level (Smith, 1903a, p. 5; 1903c, p. 27).

Smith outlined this interpretation of the geomorphic history in a joint contribution with Bailey Willis (Smith, 1903c). Willis (1903) had studied the Wenatchee-Chelan district farther north where he found evidence of three erosion surfaces. The oldest, named the *Methow plain*, he regarded as correlative with the erosion surface at Kelley Hollow designated the *Cascade lowland* by Smith. In the Wenatchee-Chelan area, however, this supposed peneplain surface is developed largely across the metamorphic and plutonic rocks of the northern Cascades. Willis also recognized a mature land surface, the *Entiat stage*, incised below the Methow plain, or "Cascade lowland". A final stage of canyon cutting (*Twisp stage*) greatly oversteepened the old valleys on the Entiat surface, forming the rugged canyons that now characterize the region.

Pardee (1918, p. 45), working in the area immediately east of Willis, found no evidence of peneplanation of the basalts. He concluded that an old erosion surface on the crystalline rocks north of the basaltic plateau must have been formed prior to extrusion of the basalts. Waters (1939) restudied the Wenatchee-Chelan area and showed that the Entiat erosion surface does not cut the basalts but is actually a much older erosion surface developed on the crystalline rocks, and then buried under the basalt and its associated marginal sediments. Near the Columbia River this old buried surface has been uncovered by the stripping off of the sediments and of the interfingering basalt flows. Willis (1939) reviewed the evidence in the field and agreed with Waters' reinterpretation.

Since the Methow plain of the Wenatchee-Chelan district is older than the Entiat surface, it also antedates the extrusion of the Columbia River basalts. Therefore the supposed correlation of the Methow plain with the "Cascade lowland" which cuts the basalt at Kelley Hollow cannot hold. What is the real nature and extent of the surface at Kelley Hollow, and what bearing does it have on the hypothesis of peneplanation of the Cascade Range and Columbia plateau after initial anticlinal folding and broad uplift?

Stages in Rise of the Anticlinal Ridges

The uncertainties about the extent of the "Cascade lowland" raise another problem. If it can be shown that erosion of the basalt and Ellensburg sediments to a common surface at Kelley Hollow is a local effect and not a widespread peneplain, it is possible that the anticlinal ridges of the Yakima district were formed in one general stage of folding instead of in two, separated by a period of peneplanation, as Smith proposed.

Antecedent, Superimposed, or Subsequent Streams

Smith believed that Yakima River maintained its course across the growing anticlinal ridges during the second (post-Cascade peneplain) period of uplift. Warren (1941a; 1941b), however, believed that growth of the Horse Heaven anticlinal uplift defeated the much more powerful Columbia River, and that Yakima River, also, has been diverted to a synclinal position in the lower part of its course.

Flint (1938a, p. 226) suggested that a pseudo-antecedent relationship has been brought about at Wallula Gap, where the Columbia crosses the Horse Heaven uplift. He thought the Columbia was dammed by uplift to the northwest and that the ponded water escaped over Wallula Gap, the lowest point on the anticlinal ridge. Downcutting at this low structural pass incised the stream into the anticline producing discordant relations that suggest antecedence.

Both Smith (1903a, p. 3) and Calkins (1905, p. 41) had considered this idea of ponding fol-

lowed by overspilling and downcutting of the lowest point on a rising anticlinal ridge. For the Yakima area, however, they rejected the hypothesis and called attention to the common occurrence of deep water gaps only a few miles from much lower structural passes across anticlinal axes.

Diversion of Columbia River

From Spokane to Wenatchee the course of the lower Spokane River and of the Columbia River is at, or close to, the margin of the basalt plateau. Evidently the river followed the crease where the northward- and westward-flowing lavas of the plateau formed a shoreline against the highlands of crystalline rock that margined the basaltic accumulations on the north and west (Willis, 1887, p. 7). At Wenatchee, however, the Columbia turns eastward from its marginal position and flows in a somewhat crooked and circuitous course to the approximate center of the basalt plateau at Pasco.

Chappell (1936) considered the diversion at Wenatchee to be due to eruptive activity in the Wenatchee Mountains to the west. He believed that volcanic materials from these local centers spread eastward, whereas the flows in the main part of the plateau advanced to the north and west. According to Chappell, the Columbia followed the crease between the two sets of flows. He rejected the counter hypothesis of deflection of the Columbia River from its marginal course by rise of the Wenatchee Mountains anticlinal fold. In support of Chappell's conclusion it may be pointed out that the river does not simply detour around the end of the anticline; it is incised on the sloping flank of the fold for a considerable distance, then turns and crosses the uplift in a magnificent water gap many miles west of the lowest point on the uplift (Fig. 1).

In the Satus Pass region, far south of the Wenatchee Mountains, Warren (1941a; 1941b) also studied the problem of the diversion of the Columbia River to the east. He thought that rise of the Horse Heaven uplift defeated the Columbia, diverting it to Wallula Gap 80 miles farther east (Fig. 1). Warren considered, but rejected, the idea that diversion was caused by lava flows, or by a growing fan of water-stratified volcanic materials. Field evidence gathered for this report, however, suggests that volcanism and sedimentation closely following deposition of the lower part of the Ellensburg formation may have been much more important in the diversion than was uplift of the Horse Heaven fold.

Contemporaneous Volcanism, Sedimentation, Diastrophism, and Erosion

The answers to the problems listed above depend, at least in part, on whether eruption of lavas and pyroclastics, warping of basins, erosion of anticlinal arches, and filling of structural troughs were contemporaneous, or whether the outpouring of the Yakima basalt and the deposition of the Ellensburg sediments preceded deformation as Smith and most later authors have assumed. The Ellensburg formation, especially its upper part, is confined largely to synclinal troughs and broad structural basins. In most places only the Yakima basalt is exposed along the crests of the anticlines, though here and there the basal parts of the Ellensburg formation, with interbedded flows such as the Wenas basalt, also appear. The synclinal basins, on the other hand, generally contain 1000 feet or more of Ellensburg sediments, and the larger basins, such as the Pasco basin, Umatilla basin, and the basin between Tygh Ridge and the Mutton Mountains in Oregon, also contain thick and widespread sediments and lava flows that are younger than the Ellensburg formation.

These relations may be due to removal of most or all of the Ellensburg formation and younger deposits from the tops of the anticlines subsequent to uplift, but the alternative proposal that the Ellensburg and younger sediments accumulated chiefly in subsiding basins merits consideration.

Yakima East Quadrangle

Scope and Purpose of Study

The writer is engaged in a study of the Columbia River basalt and its relation to the broader problems of Tertiary volcanism in the Pacific Northwest. Stratigraphic sections of the basalt have been measured in many parts of the Columbia plateau, and small areas were

mapped to show the relation of the basalt to adjacent formations. Problems concerning the stratigraphy, structure, and geomorphic history of the basalts constantly arose. Upon their interpretation commonly hinges the successful correlation of various volcanic-sedimentary assemblages. As the work progressed the need for additional detailed mapping in the Yakima-Ellensburg district to clarify some of the still unresolved problems, and to bring new light to those on which differences of interpretation had arisen, became essential. In 1948 the writer spent 3 months in the field mapping the Yakima East quadrangle (Pl. 1).

The Yakima East quadrangle was chosen because:

(1) It adjoins the Ellensburg quadrangle and so contains the eastward continuations of the units that Smith called the Yakima basalt, Ellensburg formation, and Wenas basalt.

(2) It contains two of the major water gaps cut by Yakima River across anticlinal ridges (Union Gap through Rattlesnake Ridge, and Roza Gap through Selah Butte Ridge). Furthermore, each ridge contains within the Yakima East quadrangle a much lower structural pass (Selah Springs Pass over Selah Butte Ridge, and Donald Pass over Rattlesnake Ridge) than the pass through which the water gaps were cut (Pl. 1).

(3) It lies only 4½ miles east of Kelley Hollow, the type locality of the Cascade peneplain, and also contains other areas where tilted Ellensburg beds and basalt have been eroded to a common surface.

(4) Construction work on the high-level Roza irrigation canal revealed hitherto undetected unconformities within the poorly exposed Ellensburg formation. Additional data on the Ellensburg also could be obtained from the logs of many water wells drilled in Moxee and Selah valleys.

Yakima Basalt

The Yakima basalt, as defined by Smith (1903a, p. 3), is exposed in four southeast-trending strips across the Yakima East quadrangle. These coincide with the crestal portions of the four anticlinal axes (Pl. 1).

The base of the Yakima basalt is not exposed in the Yakima East quadrangle. Basalt probably underlies the whole area to considerable depth. A well drilled in Union Gap penetrated 3800 feet of basalt without reaching its base. The bottom of this well, however, probably lies in the steeply dipping northern limb of this asymmetrical fold, and so the stratigraphic thickness penetrated by the well may be much less than 3800 feet. Above the curb of the well an additional 1050 feet of basalt is exposed on the walls of Union Gap.

Judging from the log of this and of other deep wells, the lower part of the Yakima basalt consists of massive flows with very few sedimentary intercalations. The upper 1500 feet of the basalt, well exposed in the numerous water gaps, contains many thin beds of sedimentary material.

In the northwest corner of the Yakima East quadrangle, 1300 feet of basalt, including the top of the formation, is well exposed on the walls of Roza Gap. The flows are, with one exception, the normal monotonous lava that characterizes the entire basalt plateau of eastern Washington. The average flow is 75–200 feet thick, with a scoriaceous upper portion grading into a rubbly top. Most flows show two-tier columnar jointing. The lower columns are generally 4–6 feet in diameter, whereas those developed from the upper cooling surface are less than half this size. In some flows the upper tier is replaced by an irregular hackly jointing that subdivides the lava into rough-sided blocks 4–18 inches in diameter. The lower half of some flows has a marked platy jointing at right angles to the columns. Along these platy joints the lava can be split into slabs a quarter of an inch to an inch thick.

Thin sections reveal an intersertal mat of monoclinic pyroxene and labradorite laths, with 10–25 per cent of interstitial glass. A few scattered grains of olivine, abundant tiny grains of magnetite, and irregular interstitial patches or rounded vesicle fillings of chlorophaeite are also present, though none of these constituents commonly comprises more than 1–2 per cent of the rock. In a few flows the chlorophaeite may reach 5 per cent or more.

The flows are generally nonporphyritic, but olivine, labradorite, or monoclinic pyroxene may occur as sparse phenocrysts. The normal pyroxene is pigeonite, but in flows containing pyroxene phenocrysts the center of the pheno-

cryst is almost invariably augite, zoned rather abruptly to pigeonite at the periphery. Where plagioclase is the porphyritic element, the phenocrysts are generally clustered in glomeroporphyritic clots.

The few chemical analyses of basalts from eastern Washington show a close resemblance to the "nonporphyritic central type" of the Mull authors (Bailey *et al.*, 1924, p. 16).

Sedimentary Intercalations

Lenses of micaceous silt, sandstone, and clay, with occasional conglomerate beds, are found between the flows at many localities in the upper part of the section. Residual soil zones were developed on the tops of some flows. One prominent soil zone, about 650 feet below the top of the Yakima basalt, is characterized by abundant fossil wood, including trunks and rooted stumps of large trees.

The most interesting and widespread sedimentary intercalation is a thin layer of freshwater diatomite, 6–10 feet thick, which grades upward into 5–15 feet of micaceous and quartz-rich siltstone and clay with paper-thin stratification. In places a discontinuous cross-bedded layer of coarse pumiceous sandstone lies above this. At Roza Gap (Pl. 1) this assemblage of sediments forms a thin stratigraphic unit averaging about 20 feet thick.

The diatomite unit is not confined to the Roza Gap area. It also crops out on the north side of Umtanum Ridge in Sections 34, 35, and 36, T. 15 N., R. 20 E., but is so poorly exposed that it could be mapped only in Section 34 (Pl. 1). Immediately north of this locality, however, Mackin (1947) found the diatomite over an extensive area in Squaw Valley (Badger Pocket quadrangle). Here the pure diatomite layer reaches a maximum thickness of 17 feet and has been mined. It also appears on the north side of Mount Baldy and in Roza valley. As Mackin (1947) notes, this widespread diatomite layer records the former presence of a shallow but extensive lake.

The diatomite rests directly on the surface of a distinctive basalt flow, and the two together form a good horizon marker. The flow is about 150 feet thick. In most places it is composed of three distinct layers. The upper 30 feet, immediately below the diatomite, is scoriaceous basalt, but the bubbles, instead of being uniformly distributed as in most flows, are strung out in irregular streaks and vary greatly in size and shape. In places the largest bubbles, 1–4 inches in diameter, have peculiar shapes with arched roofs and flat floors. This scoriaceous upper part also contains a few scattered phenocrysts.

Below this vesicular portion the flow changes abruptly to 30 feet of highly porphyritic, streaky lava. The phenocrysts are clustered in abundant glomeroporphyritic clots up to 1½ inches in diameter. In most places this distinctive porphyritic zone lies just above the center of the flow, but it shows local variations in thickness and position. The porphyritic zone grades downward into normal massive basalt containing scattered clots of feldspar, and characterized especially by many small interstitial patches of chlorophaeite.

The flow that overlies the diatomite layer is also slightly porphyritic, but it lacks the distinctive three zones of the flow beneath. It ranges from 100 to over 170 feet in thickness. Its basal portion is coarsely columnar, transected by horizontal zones of platy jointing. The upper 50 feet contains large and small amygdules filled with chlorophaeite and opal. At Roza Gap it shows no palagonitic or pillowed facies (Fuller, 1931), indicating that it advanced over dry land after the diatomite lake had been filled or drained.

Contact between the Yakima Basalt and the Ellensburg Formation

The top of the flow that overlies the diatomite was apparently selected by Smith as the top of the Yakima basalt and the base of the Ellensburg formation when he mapped the adjacent Wenas valley part of the Ellensburg quadrangle. Between this flow and the Wenas basalt lies a variable thickness of dominantly sedimentary materials usually referred to as the sub-Wenas part of the Ellensburg formation. The sub-Wenas beds are well exposed in cuts made for Roza Canal just south of the tunnel through Selah Butte Ridge (Table 1).

The beds in this section vary in thickness and lithology when traced laterally. Across Yakima River to the east they are well exposed in the high cliffs of Roza Gap. Here they maintain

TABLE 1.—SECTION ALONG ROZA CANAL AND TUNNEL, SOUTH FLANK OF ROZA GAP

Feet	
	ELLENSBURG FORMATION
10	Wenas basalt flow—columnar basalt, 2 foot columns in lower part grading into large compound columns near top
68	Mostly covered, float of tuffaceous sandstone and siltstone
75	Granule conglomerate, coarse sandstone, and silty pumiceous sandstone; one well-consolidated sandstone bed 30 feet thick, 25 feet above base
60	Interstratified conglomerate and coarse sandstone; conglomerate in 3–8 foot beds, sandstone in ½–3 foot beds, but increasing in abundance and thickness upward; pebbles in conglomerates chiefly andesite, some basalt near base of unit
2	Sandstone, and sandy granule conglomerate, strongly cross-bedded
4	Andesite cobble conglomerate; pebbles average 1½ inches but range up to 6 inches in diameter; pebbles are overwhelmingly andesitic, a few of acidic plutonic porphyries, quartzite, chert, and scoriaceous basalt
49	Basalt flow; highly weathered in upper part, contains numerous sandstone dikes from the overlying sandstone
40	Cross-bedded sandstone and siltstone; several thin layers of quartz-rich micaceous silts, but most of the sand is andesitic debris
	YAKIMA BASALT
60	Basalt flow; lower, coarsely columnar platy phase rests directly on diatomaceous silt; platy jointing restricted to lower part of basal tier of columns; slightly porphyritic, with small plagioclase phenocrysts clustered into sparse clots; no truly scoriaceous zone at top, though abundant vesicles in the upper 4 feet, and scattered vesicles filled with chlorophaeite and opal extend to 50 feet
17	Diatomite layer; 6 feet of nearly pure diatomite resting directly on flow surface, succeeded upward by 11 feet of diatomaceous silt, clay and sand; directly under the overlying basalt flow there is a thin layer of silt with abundant fragments of carbonized plants
33	Basalt flow; in most places shows three characteristic layers; the central one is highly porphyritic, the upper one contains large arched vesicles

about the same aggregate thickness, but vary rapidly in lithology from the measured section along Roza Canal. Eastward along the north wall of the canyon of Selah Creek the sedimentary section thins rapidly. In a little over 3 miles the entire section of sediments is cut out, and the Wenas basalt rests directly on the Yakima flows. Smith's map of the Ellensburg quadrangle shows a similar thinning and cutting out of the sub-Wenas part of the Ellensburg formation westward up the valley of Wenas Creek.

Approximately the same section of sediments is exposed beneath the Wenas basalt on the north side of Yakima Ridge in Sec. 6, T. 13 N., R. 19 E. The thick flow that appears beneath the diatomite at Roza Gap is present and can be recognized by its characteristic porphyritic center and the streaky zone of arched vesicles at the top. But here the diatomite layer is missing. Its position is taken by a mass of pillow lava and palagonite about 30 feet thick. The pillow lava is succeeded by a thick flow of basalt with columnar and platy jointing probably the same flow that covers the diatomite layer at Roza Gap. There are no sediments between any of these flows. However, the pillow lava, when traced to the east, acquires a matrix of palagonite, and sparse fragments of diatomite can be found in the palagonite.

Across Yakima Ridge the pillow lava-palagonite complex is well exposed in the steeply dipping southern limb of the anticline. But here the subaqueous lava is intimately mixed with and overlain by sediments—chiefly micaceous and sandy siltstones, but with some diatomaceous material and even local conglomerate beds. The pillowed flow, palagonite, and associated sediments are succeeded by a massive flow that appears to have been erupted on dry land, and then, in Sec. 8, T. 13 N., R. 19 E., by 160 feet of strongly cross-bedded pumiceous sandstone interlayered with thin conglomerate lenses and beds of micaceous siltstone. The conglomerate beds are chiefly andesitic debris, but some of the basal beds contain many pebbles of quartzite, acidic plutonic porphyries, granophyre, chert, vein quartz, phyllite, greenstone, and basalt. These sand-

stones and conglomerates are in turn overlain by the Wenas basalt flow.

Both the layers of sediment and the Wenas basalt pinch out eastward along the flanks of Yakima Ridge (Pl. 1). East of Kittitas Canyon the Yakima basalt contains only thin discontinuous layers of sediment. Near the east border of the quadrangle a porphyritic flow, believed to be the same as that beneath the diatomite layer at Roza Gap, is covered by at least four massive flows of basalt. This suggests that the diatomite layer, and perhaps the entire sub-Wenas section of sediments, is replaced eastward by basalt flows which did not extend as far west as Roza Gap. These flows probably dammed the lake in which the diatomite was deposited.

Correlation of flows and associated sediments between Yakima Ridge and Rattlesnake Ridge, the next major anticline to the south, is on a wholly insecure basis. The Wenas basalt did not extend over Rattlesnake Ridge. The porphyritic flow that underlies the diatomite at Roza Gap has not been definitely recognized on Rattlesnake Ridge, but it may be the poorly exposed porphyritic material about 300 feet beneath the top of the lava sequence. Micaceous silts and pebble beds containing nonandesitic material are scarcer and thinner in the basal part of the Ellensburg section on Rattlesnake Ridge than in sections to the north, indicating that the Yakima-Ellensburg contact may have been drawn (Pl. 1) at a higher stratigraphic level on Rattlesnake Ridge than in the northern areas. Local variations arise, however; quartzite and chert-bearing conglomerates are common east of Donald Pass on Rattlesnake Ridge.

From these relations it is obvious that the contact between any one basalt flow and an overlying sedimentary bed cannot serve as a workable horizon for defining the top of the Yakima basalt and the base of the Ellensburg formation throughout the entire area of the quadrangle. Such a boundary is of only local extent and cannot be traced far in the field. In general the sedimentary parts of the section thin and pinch out between successively younger flows when traced to the east. Thus the sub-Wenas part of the Ellensburg formation has been mapped in the Roza Gap area, but its equivalents in time are probably the uppermost lava flows mapped as Yakima basalt along the east edge of the quadrangle. Hence in a broader sense the entire lower part of the Ellensburg formation can be considered as a marginal sedimentary facies of the Yakima basalt flows.

Restudy of selected parts of the Ellensburg quadrangle shows that Smith was beset with the same difficulty in his attempts to draw the boundary between the Yakima basalt and the Ellensburg formation. Although he obviously picked the top of the flow that overlies the diatomite as the formational contact when he mapped Wenas valley, there are parts of this area where he drew the boundary at the top of the 49 foot flow (Table 1) that lies a little higher in the section. Farther north in a part of the valley of Roza Creek he selected a basalt-sediment contact that is at a much lower stratigraphic level. Here the diatomite layer and its overlying flows have locally been included within the Ellensburg formation, whereas in Wenas valley they occupy a part of the map that is shown as Yakima basalt. In general Smith tended to select successively higher flows for the formational boundary in proceeding from northwest to southeast across the Ellensburg quadrangle. The same stepping up of the boundary has undoubtedly occurred in mapping the Yakima East quadrangle (Pl. 1).

Physical Conditions, Yakima-Early Ellensburg Time

To sum up, volcanism and sedimentation prior to the outpouring of the Wenas basalt was characterized by slow spreading of basalt flows from the south and east. The margin of the basalt field was north and west of the Ellensburg quadrangle. Flows accumulated slowly; between most outpourings enough time elapsed to permit weathering of the basalt and growth of a heavy forest cover. The streams draining the highlands to the northwest were dammed by the advancing flows and spread out in shallow lakes along the periphery of the volcanic field. Succeeding flows poured into these lakes, forming pillow lava-palagonite complexes. These palagonitic and pillowed facies are much more abundant in the Ellensburg

quadrangle,[2] which lay closer to the lava margin, than they are in the Yakima East quadrangle. One large shallow lake became the site of deposition of a thin layer of diatomite, but most lakes not immediately overwhelmed with new lava were filled with micaceous and quartz-rich silts and sandstones, and with cross-bedded pebbly sandstones. In the lower part of the section the pebbles consist mostly of plutonic, metamorphic, and volcanic rocks, but sediments composed of pumice lapilli, glass shards, and fragments of andesitic lava are increasingly abundant in the upper part of the section. Water-stratified andesitic debris dominates the history of deposition after the outpouring of the Wenas basalt.

Basalt Flows Interstratified with the Ellensburg Formation

Wenas flow.—Smith mapped and described the Wenas basalt, a prominent flow interstratified with the Ellensburg formation. The Wenas basalt continues eastward from Smith's area into the Yakima East quadrangle. It is about 100 feet thick where it enters the quadrangle, but thins rapidly to the east and ends about halfway across the quadrangle (Pl. 1). The steep rubbly end of the flow is well exposed near Selah Springs, and it may also be seen on the south flank of Yakima Ridge where the flow ends abruptly between sedimentary layers in Section 11, T. 13 N., R. 19 E. (Pl. 1). Petrographically the Wenas basalt is identical with sparsely porphyritic flows of the underlying Yakima basalt.

Selah Butte flow.—The Wenas basalt between Selah Butte and Selah Springs is surmounted by several small buttes eroded from the overlying Ellensburg formation. Four of these buttes are capped by remnants of a basalt flow. This flow, here called the Selah Butte flow, is a basalt tongue in the Ellensburg formation about 150 feet above the top of the Wenas basalt. The Selah Butte flow could not have extended far to the south or west, for the Ellensburg sequence is well exposed on either side of Yakima Ridge and in lower Wenas Creek, but the Selah Butte flow is missing at these localities.

Elephant Mountain flow.—In the southeastern corner of the quadrangle (Pl. 1) a much more extensive and better exposed basalt flow is interstratified with the Ellensburg formation at a still higher stratigraphic level than the Selah Butte flow. This flow crops out on both flanks of Elephant Mountain, the eastern continuation of Rattlesnake Ridge. It averages about 35 feet thick in the area mapped, but thickens eastward into a widespread lava sheet in the adjoining Black Rock Spring quadrangle.

Pipe vesicles in the base of the flow indicate that it advanced from the southeast. The flow ended after advancing about 3 miles into the southeastern corner of the Yakima East quadrangle. Near its termination it contains abundant spiracles and incipient pillowed facies indicating that it flowed over marshy ground or into a shallow lake, but throughout most of the area it is a normal subaerial flow. Petrographically it is identical with the Yakima basalt.

Post-Wenas Part of the Ellensburg Formation

The bulk of the Ellensburg formation, and especially that part stratigraphically higher than the Wenas basalt, consists of andesitic debris, mostly water-stratified pyroclastic material carried eastward by streams from the rapidly growing chain of explosive andesitic volcanoes to the west. Cross-bedded layers of pure pumice lapilli alternate with fine-grained vitric tuffs and lenses of andesitic gravel in a bewildering assemblage of interlacing beds and channel lenses, none of which can be traced far. (*See* the description of a typical stratigraphic section measured by Calkins; Smith, 1903a, p. 3.) Massive agglomerates and mud-flow breccias are locally interstratified with the prevailing torrentially bedded, tuffaceous sediments.

The whole assemblage is typical of the pumice-slurry floods that result when strong Vulcanian or Peléean explosions are followed by heavy rains that wash the light and loose coating of pyroclastic debris into adjacent streams.

[2] The yellow tuffs referred to by Smith (1903a, p. 3; 1903c, p. 17) at Bald Mountain, and elsewhere, are palagonite tuffs formed by extrusion of basalt into water, and not the products of pyroclastic eruptions. (*See* Fuller, 1931.)

This part of the Ellensburg formation is a huge compound fan or bahada slope spread out to the east of the growing volcanic chain.

Unconformities within the Ellensburg Formation

The strongly cross-bedded tuffaceous sands and granule conglomerates of the Ellensburg formation show cut-and-fill structures and abundant evidence of local lateral planation of earlier deposited fill while the formation was accumulating. Such features are so abundant that a somewhat similar but more significant kind of intraformational unconformity has escaped attention. In many places groups of beds of limited thickness and extent show angular discordance of 2°–10°. Both the overlying and underlying beds dip toward the center of the nearest synclinal basin.

The first bed above an unconformity of this kind is generally a thin conglomerate or pebbly sandstone containing at least a few basalt pebbles in addition to the ubiquitous pebbles of andesite. The basalt pebbles are less rounded and much less well sized than the andesitic ones. In places, coarse angular basalt boulders up to 2 feet in diameter are scattered sparsely in a 1- to 2-foot pebbly pumiceous sandstone with well-rounded pebbles of andesite a quarter of an inch to an inch in diameter. In a few places the conglomeratic bed above an unconformity is over 80 per cent basalt gravel, but generally basalt pebbles form less than 25 per cent, and the proportion may vary erratically.

Because the Ellensburg formation is poorly exposed it is seldom possible to trace these unconformities, but all evidence indicates that they are only local features. Superb cross sections of several of them were seen during the excavation work for the Roza Canal. For example, in Sec. 22, T. 13 N., R. 19 E., a 1-foot bed of mixed basaltic and andesitic gravel could be traced along the excavation for nearly half a mile. Beds of pumicite and tuffaceous sand below the gravel dip 5°–11° S.—toward the center of the adjacent Moxee basin. The overlying gravel and tuffaceous beds dip 2°–3° S.

The same relation—older beds dipping more steeply than beds above the unconformity, but both dipping toward the center of an adjacent basin—was seen at several other localities (Roza Canal, N.W. part Sec. 31, T. 13 N., R. 20 E.; Donald Pass, Sections 19 and 29, T. 12 N., R. 20 E.; S.W. part of Sec. 9, T. 12 N., R. 20 E.; Roza Canal, Sec. 16, T. 13 N., R. 19 E.; West edge Sec. 36, T. 14 N., R. 19 E.).

Most of these basalt gravels are only a few feet or even a few inches thick. A much thicker conglomerate containing abundant basalt cobbles lies in the northeastern part of the quadrangle and is so widespread that it is shown with a special symbol on the geologic map (Pl. 1). In composition and appearance this gravel resembles the coarse post-Ellensburg gravels, such as Smith's Cowiche gravel (Smith, 1903a, p. 4), which lie with marked unconformity upon the Ellensburg in some of the larger structural basins. The basalt conglomerate in the northeastern part of the Yakima East quadrangle, however, is interstratified in the Ellensburg and lies near the base of that formation.

South of Selah Creek in Sections 22, 23, and 24, T. 14 N., R. 20 E., the conglomerate dips 30°–35° N., and its base is well exposed in a series of scallops across a group of rounded hills. The surface that the conglomerate covers is a distinct unconformity; many thin tuffaceous beds in the underlying Ellensburg sediments are cut off at the contact. Truncation of beds against the base of the conglomerate is also clearly shown along the crest of the steep ridge north of Burbank Creek in Sec. 6, T. 14 N., R. 20 E.

On a larger scale there is also much variation in the stratigraphic position of the base of the conglomerate (Pl. 1). In Sec. 1, T. 13 N., R. 20 E., and again in Sec. 36, T. 15 N., R. 19 E., it rests directly on the surface of the Yakima basalt, but in the areas between it is separated by up to more than 200 feet of tuffaceous sediments. These differences in stratigraphic position are not entirely due to pre-conglomerate erosion, however; they are partly due to local nondeposition of some beds in the Ellensburg.

The interpretation of these basalt gravel tongues and related unconformities seems fairly obvious. The upper andesitic portion of the Ellensburg formation was deposited chiefly in basins that were being downwarped into synclines while the sediments were accumulat-

ing. Locally the rising anticlines between the basins were eroded, and the basaltic detritus spread as thin sheets into the accumulating pile of andesitic debris. Since warping and folding were affecting not only the basalts but also the newly deposited sediments on the floors of the synclines, the basalt gravels commonly are unconformable with the tuffaceous beds below. Also the basalt boulders, transported only a short distance from an adjacent rising anticline, are not so well sorted nor so well rounded as the associated andesitic pebbles which came from a more distant source. This interpretation also explains why the unconformities are more numerous at the margins of the basins than in their centers, and why beds of basalt gravel are more abundant in the upper part of the Ellensburg series, as Smith (1901, p. 21) had noted.

Thus the upper part of the Ellensburg formation provides a clear record of contemporaneous folding, deposition, and erosion. At first basalt flows spread slowly from the south and east. Together with the diatomaceous layers and micaceous silts deposited in marginal lakes, they built up the basalt plateau. Then pyroclastic debris, washed from a growing chain of explosive andesitic volcanoes to the west, accumulated rapidly in subsiding basins. Contemporaneous uprise of the anticlinal ridges invigorated the streams flowing down their flanks and contributed basalt gravel to the upbuilding and deforming pile of andesitic debris.

Structure

Anticlinal Folds

Three of the longest anticlinal ridges of central Washington cross the Yakima East quadrangle (Fig. 1). Umtanum Ridge and Rattlesnake Ridge, each approximately 100 miles in length, extend from the Columbia River to the Pliocene-Pleistocene volcanic cover of the Cascade Range. They probably continue much farther west but have not been traced in the young volcanic cover.

Yakima Ridge is a less continuous anticline, with local sags and en echelon offsets. With Cowiche Ridge, its western continuation, it is at least 60 miles long.

Curiously, Selah Butte Ridge, which is transected by the deepest and most spectacular water gap (Roza Gap) in the Yakima East quadrangle, is only a minor irregular fold between the major Umtanum and Yakima Ridge anticlines. The Selah Butte anticline plunges and dies out within 5 miles when traced westward into the Ellensburg quadrangle and extends less than 4 miles beyond the east edge of the Yakima East quadrangle. Its total length is about 25 miles.

The Selah Butte anticline is more complicated than its neighbors. It consists of a major fold with two branches that join it at an acute angle (Pl. 1). Its north flank is cut by a high-angle fault with about 200 feet maximum displacement. It is much less eroded than its neighbors; the Wenas basalt extends over its crest almost undissected except for the sharp notch of Roza gap. On the crest are several erosion remnants of the post-Wenas part of the Ellensburg formation—rocks which are unknown on the high crests of the other anticlinal ridges, though they locally appear in low structural gaps with complex structure such as Donald Pass on Rattlesnake Ridge. Patches of the basaltic conglomerate that crops out extensively in the northeastern part of the quadrangle are found high on the flanks of the fold. If this conglomerate was derived from erosion of the crestal parts of the adjacent Yakima and Umtanum folds, the area of the present Selah Butte anticline must have remained a low flat basin of deposition long after the adjoining Umtanum and Yakima folds had grown to considerable size and had been extensively scored by erosion.

Faults

No faults of consequence were noted in the Yakima East quadrangle, though many small breaks with 10–20 feet displacement were found. The steep fault on the north limb of the Selah Butte fold is large enough to show on Plate 1, but it is less than 5 miles long, and its maximum dip-slip displacement is probably less than 250 feet. A similar fault cuts the basalt on the south flank of Yakima Ridge in Sec. 10, T. 13 N., R. 19 E.

Selah Creek crosses Selah Butte Ridge along a small cross fault which is clearly visible where it displaces the Yakima basalt-Lower Ellens-

burg contact. Kittitas Canyon probably follows a similar fault, or zone of shear.

Deformation at Shallow Depths

Folding and faulting, as Smith (1903b, p. 175) has pointed out, must have occurred practically at the surface. How can brittle rocks like basalt fold with little, if any, superincumbent load? Part of the adjustment to folding has been by bedding-plane slip, as shown by the local smearing out and slickensiding of thin sedimentary beds and residual soils intercalated between the basalt sheets. Probably most of the movement has been accommodated by minor adjustments between the numerous joint planes of the lava. Columnar joint surfaces are locally slickened where they have been squeezed against one another on the flanks of folds. Many joint columns are broken and displaced along secondary fractures. Almost all grooves on slickensided joints trend in the "a" direction, but they may show great variation in plunge. Tilting of columns by rotation and by shear along original platy or secondarily developed joints is visible locally on the limbs of the folds.

Even in steeply tilted flows, however, these effects are minor, and most details of the primary joint pattern are still preserved.

GEOMORPHOLOGY

Surfaces Stripped to the Wenas and Yakima Basalts

Most of the Ellensburg sedimentary rocks are poorly consolidated, and some of the pumice lapilli tuffs and tuffaceous clays are unconsolidated. On the other hand, the massive basalt flows strongly resist erosion, although large swift-flowing rivers can deeply trench them by plucking and carrying away the individual joint blocks (Bretz, 1924). Over wide areas the soft Ellensburg sediments have been completely stripped from the resistant basalt by the normal processes of desert erosion, and the stripped surface corresponds closely with the structure of the underlying basalt.

Throughout most of Selah Butte Ridge the topographic surface corresponds almost exactly with the top of the Wenas basalt, but a few patches of Ellensburg sediment remain to show that the entire ridge was once covered with sediments. Similarly, the smooth rounded back of Elephant Mountain on Rattlesnake Ridge corresponds closely with the top of the highest flow of Yakima basalt as it emerges from beneath the Ellensburg sediments on either flank of the ridge. There are also extensive areas on Umtanum Ridge and on Yakima Ridge east of Kittitas Canyon where topographic surfaces coincide with the structure of the underlying flows, but the deeper dissection of these ridge tops and the absence of remnants of sedimentary rocks make it uncertain whether they were ever buried beneath the Ellensburg.

Erosion Surfaces Discordant to Structure

In contrast to the stripped surfaces that correspond closely with stratigraphic surfaces of the lavas, there are in the Yakima East quadrangle many remnants of smooth erosion surfaces that cut the Ellensburg sediments and associated flows at an angle. These discordant surfaces are especially common along the margins of the larger synclinal basins, particularly of those basins that contain extensive Ellensburg and younger sedimentary deposits (Pl. 2, fig. 1). These discordant surfaces also occur as fragmentary, partially eroded remnants high on the flanks of some of the anticlinal ridges (Fig. 2; Fig. 3; Pl. 2). In the Yakima East quadrangle they are best developed on either side of Yakima Ridge (Fig. 2; Pl. 1). The surfaces slope basinward, away from the adjacent anticlinal axis. Two or more truncat-

PLATE 2.—EROSION SURFACES DISCORDANT TO STRUCTURE

FIGURE 1.—PEDIMENT SURFACE CUTTING ELLENSBURG STRATA
North flank of Yakima Ridge.

FIGURE 2.—SURFACE OF THE "CASCADE PENEPLAIN"
At its type locality east of Kelley Hollow, Ellensburg quadrangle. Note the coarse basalt boulders strewn over the surface, and the abrupt junction of the surface with a steep scarp rising to Umtanum Ridge in the background.

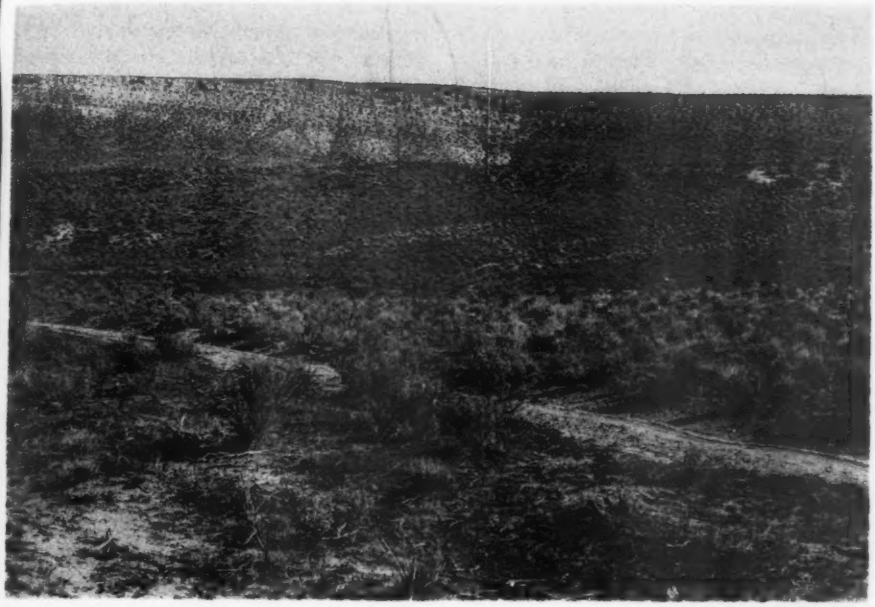

FIGURE 1

FIGURE 2

EROSION SURFACES DISCORDANT TO STRUCTURE

ing surfaces commonly form distinct steps on the flanks of an anticlinal fold. (See profiles, Fig. 2.) These surfaces bevel the underlying rocks to a smooth plane regardless of their structure (Pl. 2, fig. 1). Resistant basalt flows are truncated to the same plane as the soft Ellensburg strata.

A thin layer of basalt boulders covers most of the higher surfaces (Pl. 2, fig. 2), though on some it may be obscured by a younger coating of loess.

No individual truncating surface has been traced far; most are less than 5 square miles in area. When traced upslope nearly all terminate abruptly at the foot of a steep scarp scored by ravines from which the basalt boulders were delivered. (*See* profiles, Fig. 2 and Pl. 2, fig. 2.)

Their terminations downslope are less uniform. The higher surfaces generally drop abruptly to a lower and less dissected surface of the same kind. However, the lowest member of such a series of steps generally does not end in a basinward-facing scarp. Some slope into the sediment fill of the adjacent basin and disappear into the minor unconformities covered with basalt gravel. Recent erosion has merely exhumed part of an old erosion surface over which Ellensburg sediments were formerly de-

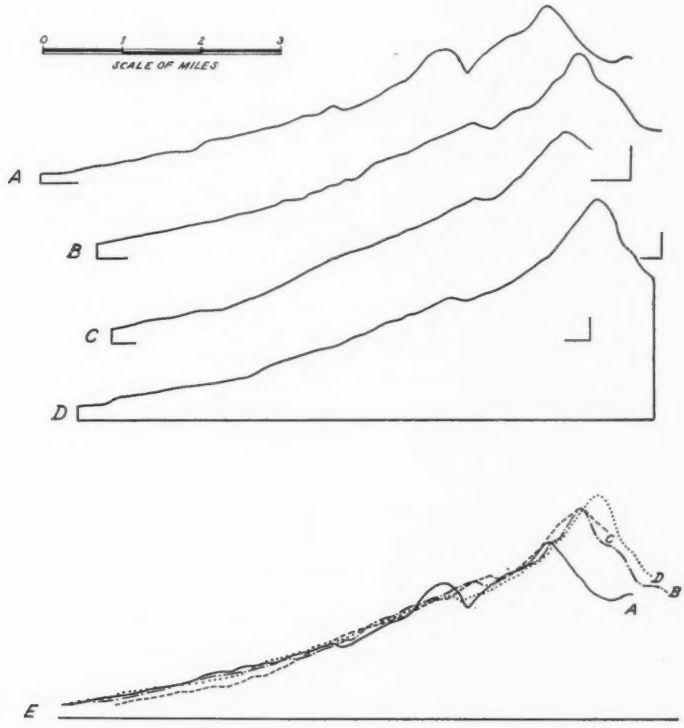

FIGURE 2.—PROFILES OF DISSECTED PEDIMENTS

South side of Yakima Ridge, east-central part of Yakima East quadrangle. All profiles are drawn with the vertical scale 5 times the horizontal scale.

A. Profile of flat-topped spur just west of Washout Gulch, and extending northward over the crest of Yakima Ridge

B. Profile of flat-topped spur east of Washout Gulch

C. Profile of flat-topped spur extending through the center of Sec. 26, T. 13 N., R. 20 E.

D. Profile of the flat-topped spur extending through the center of Sec. 25, T. 13 N., R. 20 E.

E. Profiles A, B, C, and D superimposed

posited. Much more commonly, however, the lowest surface grades basinward into a sheet of basaltic gravel with the form of an alluvial fan. Such gravel fans spread unconformably over the tilted Ellensburg strata of the adjacent basin.

Only small gravel sheets of this kind were found in the basins within the Yakima East quadrangle, but, in the much larger Kittitas Basin (also called the Ellensburg Valley) to the north, there are superlative examples of basaltic gravel fans that grade marginally into broad rock surfaces that cut tilted Ellensburg strata and associated basalt flows. These beveled rock surfaces in the Kittitas Basin are ordinary pediments like those found so commonly along the base of desert mountains in the southwestern United States. The higher flat surfaces that end basinward in a scarp, instead of grading into a gravel fan, are interpreted as uplifted pediments now being eroded. Below, new pediments are in process of forming.

Thus the flanks of the anticlinal ridges in central Washington show in numerous steplike pediment remnants the effects of a long and complicated process of erosional sculpturing under semiarid conditions. Some of the lowest pediments are forming today; they have low basinward slopes (1°–3°) and they grade downslope into alluvial fans of basaltic gravel. Behind them lie one or more higher steps whose original gentle tilts appear to have been steepened by renewed arching of the anticlinal fold. These are in various stages of dissection by consequent ravines that have worked rapidly headward up the tilted surface. The history recorded in these erosional land forms is the counterpart of that recorded by deposition in the adjacent synclinal troughs during slow gradual growth of the anticlines.

Type Locality of the "Cascade Peneplain"

The type locality for the "Cascade peneplain" of Smith is the spur just east of Kelley Hollow on the Ellensburg quadrangle, 4½ miles west of the edge of the Yakima East quadrangle (Smith, 1903c, p. 27). It lies on the south slope of Umtanum Ridge, at the approximate point where the shorter and younger Selah Butte fold merges and dies out against the flank of Umtanum Ridge.

The supposed peneplain remnant is a smooth surface, now tilted 2°–8° S. As Smith describes it (Smith, 1903c, p. 27):

> The plateau (remnant) is several hundred yards in width and over a mile in length, and preserves its even surface to the very brink of the steep-sided gulches that bound it on the east and west. The surface is thickly strewn with angular boulders of basalt, and there is not the slightest indication of the contact between the Yakima basalt and the overlying Ellensburg sandstone. On either side, however, in the walls of the gulches, the position of this contact can be accurately fixed and its dip seen to be 20°. Here, then, the planation was complete and the resultant lowland surface is perfectly preserved.

Smith's (1903c, Fig. 1) sketch of the beveled contact of the sandstone and basalt is reproduced as Figure 3. The boulder-strewn surface of the remnant is shown in Figure 2 of Plate 2.

Reinvestigation of this area confirms Smith's observations. There is no topographic break whatever where the supposed peneplain surface truncates the contact between the easily eroded tuffaceous sediments of the Ellensburg formation and the resistant basalt flow. But a number of features are incompatible with the interpretation of this surface as the remnant of a widespread peneplain formed by streams graded to sea level (Waters, 1939, p. 643–644).

The abundant angular basalt boulders (Pl. 2, fig. 2), some over 3 feet in diameter, scattered uniformly over the supposed peneplain surface both in areas underlain by basalt and those underlain by Ellensburg sedimentary rocks could not develop on a widespread peneplain surface formed by normal pluvial erosion. Such veneers of angular fragments are, however, characteristic of desert pediments over which "cloudburst" flash floods transport their coarse loads.

Another feature incompatible with the peneplain concept is that the Kelley Hollow remnant does not join smoothly with adjacent small erosion remnants that also transect the underlying rock structure. Instead it forms a distinct step, separated from both higher and lower surfaces by steep scarps (Pl. 2, fig. 2). This relation is well illustrated in Smith's sketch of the Kelley Hollow locality (Fig. 3). The foreground in Smith's sketch shows a

second flat surface, veneered with basalt boulders like the higher peneplain remnant, but separated from it by a steep scarp. Both are discordant with the structure of the underlying soft sandstone to a common surface at Kelley Hollow did he embrace the peneplain concept. In 1900 Gilbert's and McGee's pioneering studies on desert processes of erosion had not

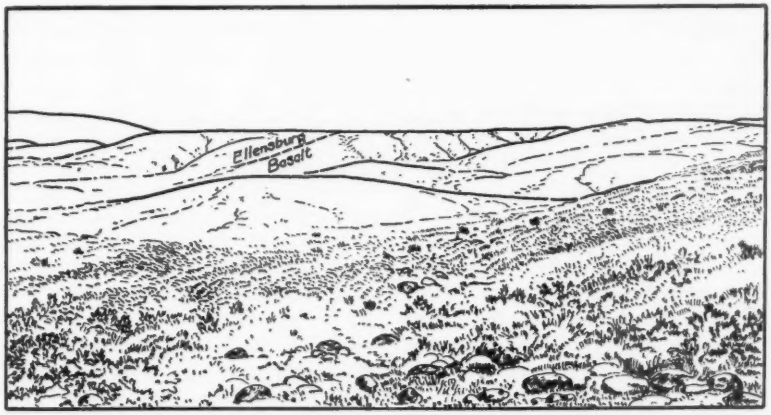

FIGURE 3.—SPUR EAST OF KELLEY HOLLOW, TYPE LOCALITY OF THE "CASCADE PENEPLAIN"
Redrawn from G. O. Smith (1903, p. 27, Fig. 1)
Note truncation of Ellensburg and basalt by the supposed peneplain and, in the foreground, a lower flat surface that also transects the rock structure.

rocks. The lower surface can be traced over a much larger area than the upper surface; remnants of it are particularly wide spread in a narrow belt paralleling Wenas Creek west of Kelley Hollow for about 3 miles.

Thus, the supposed peneplain surface, like the steps on the flanks of Yakima Ridge, appears to be the remnant of a pediment formed during the gradual rise of the anticlinal ridge. The important point is that it is a local feature, formed by the interplay of synchronous uplift and erosion during the rise of the anticlinal ridge, and does not record two orogenic episodes separated by a period of peneplanation between.

Russell (1893) and Willis (1903), inspired by the successful demonstration of widespread peneplanation in the Appalachian region by Hayes, Campbell, and Davis, brought the concept of the peneplain to the Cascade Mountains and the Columbia plateaus. Willis (1903, p. 48–49) credits Smith with "well maintained skepticism" of the peneplain concept during the course of their field work. (*See also* Smith, 1903c, p. 24–26.) Only after Smith's discovery of the truncation of both basalt and reached the stage of refinement to which Davis and others had brought the peneplain concept. Smith's interpretations were made without benefit of modern ideas of desert erosion; he knew the concept of the peneplain, but not that of the pediment. Had he been armed with this additional knowledge it seems certain that he would not have relinquished his skepticism of the peneplain concept.

Antecedent Yakima River and Columbia River

Smith's and Calkins' conclusion that Yakima River maintained its course across the growing anticlines is supported by the field work in the Yakima East quadrangle. The river crosses Selah Butte Ridge in a spectacular water gap 1900 feet deep. Six miles to the east at Selah Springs (Pl. 1) there is a structural gap 800 feet lower. By detouring only 2½ miles to the west the river could also have crossed Yakima Ridge in a low pass. Similarly the river did not use the low structural gap at Donald Pass (Pl. 1) on Rattlesnake Ridge, but cut through more than 1000 feet of basalt to cross over the ridge in the

deep slot called Union Gap 4½ miles farther west.

Flint (1938a, p. 226) suggested that Wallula Gap, where Columbia River crosses the Horse Heaven uplift (Fig. 1), is a low structural col that the Columbia overspilled and downcut after having been deflected by uplift from a former course farther northwest. Even here, however, the evidence does not favor such an interpretation. The rise of the Horse Heaven fold to its present height without simultaneous breaching of the ridge at Wallula Gap would have impounded an enormous lake at least 1000 feet deep in the Pasco Basin. Flint (1938a, p. 226) interpreted the Ringold sediments of Pleistocene age as the fill formed in this lake. Such a lake, however, would have left distinct traces of its margin in wave-cut cliffs, wave-built fills, and hanging deltas like those so conspicuously developed along the shores of Lake Bonneville as it lowered its outlet at Red Rock Pass. No such features are seen upstream from Wallula Gap, either at the level of the top of the gap or at the level of the top of the Ringold formation. Flint (1938b, p. 501) noted the absence of such features in a later paper.

Moreover, although the Ringold formation contains thinly stratified clays, silts, and diatomite layers that were doubtless deposited in lakes, these lakes appear to have been shallow, and to have shifted position. Their deposits are interstratified with ripple-marked sands and with typically river-bedded sediments. Merriam and Buwalda (1917, p. 263), who named the formation, considered it to be of flood-plain origin. McKnight (E. T. McKnight, 1923, The White Bluffs formation of the Columbia, Unpublished thesis, University of Washington) studied the formation near White Bluffs and concluded that the lithology and fossil evidence favored a river origin of most of the beds, though the presence of a thin layer of travertine suggests the presence of a shallow lake during a part of the period of deposition.

In answer to these objections, Flint (Personal communication, June 7, 1954) suggested that uplift of the Horse Heaven anticline to the west may have occurred so slowly that the river merely slackened instead of ponding and the Ringold fill may have been deposited about as rapidly as the anticline rose. After building up the basin to the level of the top of Wallula Gap, the river escaped over the anticline, simultaneously abandoning its former position through Satus Pass 80 miles west. This hypothesis explains the character of the Ringold sediments better, but is unacceptable because it would mean that all the sedimentary fill supposedly deposited between the top of Wallula Gap (elevation 1450 feet) and the surface of the Ringold flats (elevation 910 feet) must have been removed without leaving a trace in the many protected sinuous canyon embayments. Also the fill should have extended continuously between the top of Wallula Gap and the floor of Satus Pass which is now 3149 feet above the sea. No remnants of such a fill are found at these levels in the Yakima-Toppenish region.

How and when, then, did the Columbia become entrenched at Wallula Gap? There is good evidence that it was approximately in this position during late Ellensburg time. Tuffaceous andesitic sediments 400–500 feet thick, and locally capped with one or more flows of Yakima basalt, are widespread on the Horse Heaven plateau, especially between Roosevelt and Bickleton. The headwaters of Glade Creek are cut in gently tilted tuffaceous sands and silts. These deposits of andesitic debris were clearly derived from volcanoes to the west. Much thicker deposits of andesitic sediments fill the basin north of the Horse Heaven fold. They dip steeply in a well-exposed section on the north limb of the anticline south of Mabton. Similar deformed tuffaceous strata in the eastern part of the Rattlesnake Hills and at Saddle Mountain pass unconformably beneath the horizontal Ringold strata. Deposition of these prevailingly andesitic sediments in this position requires eastward-flowing streams that headed in the volcanic highland on the west. It also means that the south-flowing Columbia River could not have been flowing through Satus Pass, for in this position it would be between the tuffaceous deposits and their source of supply. Instead it must already have been somewhere east of the site of deposition, perhaps pushed there by the growing fans of water-stratified andesitic debris themselves.

Additional evidence that the Columbia has long been active in the vicinity of Wallula Gap is afforded by the structure of the gap. Two basalt flows appear on the east side of the gap

(in the hills which rise to 1750 feet about 2½ miles east of the rim of the gap) but have been removed by erosion from the crest of the fold west of the gap. This indicates that the river did not suddenly arrive on the site and quickly entrench itself, but must have shifted slowly down the plunge of the anticline removing some basalt from the axis during its shift.

Diversion of Columbia River

Warren (1941a; 1941b) advanced the interesting hypothesis that Columbia River once flowed from Sentinel Gap southwestward via Sunnyside, Satus Pass, and Goldendale to Hood River, but was diverted to Wallula Gap, 80 miles to the east, by the rise of the Horse Heaven fold (*see* Fig. 1). Most of the relevant field data to test this hypothesis lies in areas other than the Yakima East quadrangle. The following notes are based in part on detailed study of the Satus Pass region, but mainly on reconnaissance observations supplemented by published works of earlier writers.

Warren's chief argument concerns the distribution of a quartzite-bearing conglomerate that lies on the Yakima basalt. He believed this conglomerate was restricted to a narrow belt along the supposed former course of the Columbia (Warren, 1941b, Fig. 1, p. 210), and that it was deposited by the Columbia during its occupancy of this western course. He identified the conglomerate with the Hood River conglomerate of Buwalda and Moore (1930) on the basis of lithology, and though he regarded it as contemporaneous with the Ellensburg formation, he stated (Warren, 1941b, p. 213) that quartzite pebbles are not found in the Ellensburg. He thought the Ellensburg formation consisted only of volcanic debris deposited by east-flowing streams, whereas the "Hood River conglomerate" was laid down by an ancestral Columbia that carried metamorphic and plutonic rocks to the area from the crystalline complex north and east of the lava plateau.

These conclusions presuppose that the quartzite-bearing conglomerate is restricted to a relatively narrow zone closely coincident with the supposed course of the Columbia. However, quartzite-bearing conglomerates, as well as quartz-rich micaceous silts and sands derived from plutonic and metamorphic rocks, are widespread as a thin discontinuous veneer throughout south-central Washington and even into Oregon (Piper, 1932, p. 127). They are the dominant sediments in the basal beds of the Ellensburg formation in the Yakima East quadrangle. Indeed, Warren (1941a, p. 120) cited the occurrence of a conglomerate of "Hood River type" on the south flank of Elephant Mountain. They also occur far to the north, west, and east; for example, in the basal beds of the Ellensburg formation in the Kittitas basin; interbedded with the basalt on Saddle Mountain both east and west of Sentinel Gap (Calkins, 1905, p. 34); and on the Horse Heaven plateau far to the east of Satus Pass (Waring, 1913, p. 20).

The quartzite-bearing conglomerate is, in fact, coincident with the lower part of the Ellensburg formation, and the field evidence strongly favors the conclusions of Calkins (1905), Waring (1913), Buwalda and Moore (1930, p. 20–21), Piper (1932, p. 127), and others that it forms the basal beds of this formation, and grades both upward and laterally into the dominantly pyroclastic debris that forms the bulk of the formation.

On the other hand, quartzite-bearing conglomerate does not appear along parts of the linear strip which Warren (1941b, Fig. 1, p. 210) marks as the supposed former course of Columbia River. One vital area is the floor of Satus Pass. Here quartzite pebbles are conspicuously absent. According to Warren, Satus Pass is the wind gap left when Columbia River was defeated by rise of the Horse Heaven fold. The deposit in the pass is well displayed in deep road cuts along Highway U. S. 97. For eight-tenths of a mile north of the marker at the summit of the pass almost continuous road cuts 10–50 feet high expose coarse stream deposits. The material is chiefly angular to subrounded pebbles and cobbles 1–6 inches in diameter. The pebbles are almost 100 per cent basalt—the only exceptions noted were two pebbles of hypersthene andesite and one of caliche. Near the base of the deposit, however, a lens of torrentially bedded light-colored sand about 15 feet thick consists of fresh pumice lapilli and andesitic sand, mixed with basaltic debris. The pumice and andesite pebbles are fresh, similar to those in the recent pumice blanket that surrounds the volcanic cones of

Mount Saint Helens and Mount Adams to the west. Careful search of these road cuts revealed no pebbles of quartzite, or of any metamorphic or plutonic rock.

The same kind of gravel extends southward from Status Pass for several miles along the underfit valley of Klickitat Creek. Apparently Satus Pass is not the wind gap of a former Columbia River, but the site where the headwaters of Klickitat Creek were captured by a short branch of Satus Creek which flows down the steep northern limb of the fold. The axis of the Horse Heaven anticline is about 2 miles north of the present summit of the pass. Eight-tenths of a mile north of the summit, but still south of the anticlinal axis, a stream whose valley is topographically similar to that of Satus Pass and the head of Klickitat Creek enters the pass from the west. On reaching the pass, however, this stream does not follow the open valley to the south but turns north and descends precipitately through a rocky gorge across the anticlinal axis into Shenando Creek,[3] a tributary of Satus Creek.

Although the quartzite-bearing conglomerate does not occur at Satus Pass, it does appear about 4 miles south near Brooks Memorial Park. From here it can be traced southward along the valley of Klickitat Creek nearly to Goldendale. The conglomerate lies on the Yakima basalt and is tilted southward with it. Away from the valley of Klickitat Creek, however, the conglomerate is nearly everywhere concealed beneath much younger olivine-rich basalts erupted from Simcoe Mountain and from many other Quaternary lava cones near Goldendale. Indeed, the quartzite-bearing gravels owe their preservation largely to protection from erosion by this lava cap. Klickitat Creek, in its southward course from Satus Pass to Goldendale, has cut through these young basalt flows into the gravel. The quartzitic gravels are especially well exposed in many deep road cuts along U. S. 97 in the area 5–15 miles south of Satus Pass. In some of these road cuts the cap of olivine basalt truncates the gravel unconformably.

[3] The gorge and junction with Shenando Creek can be seen on the south edge of the White Swan topographic sheet, but unfortunately the site of capture and the valley of Klickitat Creek lie just off the White Swan sheet in the topographically unmapped quadrange to the south.

Since the quartzite-bearing gravel dips south, its zone of outcrop trends east-west, practically at right angles to the trend of Warren's ancestral Columbia. If the gravel ever extended over the top of the Horse Heaven anticline, it was eroded from the crestal area before outpouring of the olivine basalts, and before the cutting of the Satus Pass wind gap. The quartzitic gravel can be traced far to the east along the south flank of the fold. It is well developed at Bickleton, 20 miles east of Satus Pass, as Waring (1913, p. 21) noted. It is also exposed in the headwaters of Glade Creek, still farther east, and on the steeply dipping north flank of the fold south of Mabton. Scattered quartzite pebbles, but not a definite conglomerate bed, have also been found beneath the thick mantle of loess 2½ miles west of the brink of Wallula Gap, approximately 75 miles east of Satus Pass.

Scattered outcrops indicate that the quartzite-bearing conglomerate also extends far west of the Satus Pass-Goldendale line. Indeed the Hood River conglomerate at its type locality may be a remnant. In much of the region west of the Satus Pass-Goldendale area, however, the conglomerate is buried under Quaternary olivine basalt. These olivine-rich flows were erupted from local centers, and are a part of a great volcanic field of Pliocene to Recent olivine-rich basalt that extends along the east base of the Cascade Range from southern Washington to northern California. Petrographically they are similar to the "Porphyritic Central type" of the Mull authors (Bailey *et al.*, 1924) and are quite distinct from the Yakima basalt. Warren (1941a, p. 117, 120) commented upon the marked variations in the basalts, but appears not to have noted the unconformable relation of the olivine-rich flows to the quartzite-bearing conglomerate, and to have confused them with the monotonous Yakima basalt.

Thus, reconnaissance, supplemented by the published work of others, suggests the following sequence of events in place of that proposed by Warren: During the later stages of the accumulation of the Yakima basalt an ancestral Columbia River may have followed the approximate boundary between the upbuilding lava plain and the highlands of older rocks on the west and north. Sediments were deposited along this margin by the ancestral Columbia

and by tributary streams draining the highlands on the west. During this period the ancestral Columbia may have shifted widely.

Eventually andesitic volcanoes in the highlands to the west erupted explosively and showered the headwaters of the eastward-flowing streams with pyroclastic debris. This clogged them with pumice slurry floods and greatly accelerated deposition. A great compound fan of water-stratified volcanic debris grew eastward from the new volcanic highland, pushing the ancestral Columbia River far to the east across the basalt plain. Synchronous subsidence in the Yakima and Pasco basins may have assisted in this shift to the east.

Still later, flows of olivine-rich basalt were erupted from local centers in the Simcoe Mountains west of Satus Pass, in the basin of Tieton River, and at many other points along the east slope of the Cascades. They filled valleys eroded in the Yakima basalt and Ellensburg formation, and deeply buried these formations in the western part of the Horse Heaven plateau.

Summary and Conclusions

(1) Below the contact mapped by Smith as the top of the Yakima basalt several thin sedimentary beds and ancient soil zones are intercalated with the basalt flows. These sediments show the same lithologic variation as the lower part of the Ellensburg formation. In places they are so numerous that the exact position of the Yakima-Ellensburg contact is a matter of arbitrary choice. Smith's contact is not at the same stratigraphic level on different anticlinal ridges even within the Ellensburg quadrangle. In the Yakima East quadrangle the contact shown on Plate 1 may be stratigraphically different on Rattlesnake Ridge from that on Yakima and Umtanum ridges.

(2) The lower part of the Ellensburg formation contains several basalt flows in addition to the Wenas basalt. These flows increase in number toward the east. At one locality, however, the section of Ellensburg sediments beneath the Wenas basalt thins and pinches out so that the Wenas basalt rests directly on the Yakima basalt.

(3) The lower 100–300 feet of the Ellensburg formation, and also the sedimentary rocks interstratified in the upper part of the Yakima basalt, contain abundant debris derived from metamorphic and plutonic rocks. They also show evidence of having accumulated slowly in shallow lakes, ponds, and river flood plains.

On the other hand, the upper part of the formation, 1000–1600 feet thick in the Ellensburg and Yakima East quadrangles, consists chiefly of sediments of pyroclastic derivation which show evidence of rapid accumulation. They are composed of torrentially stratified layers of pumice lapilli and ash, andesitic gravel, and tuffaceous clays and silts. Here and there are discontinuous beds of coarse basalt gravel seemingly derived from rising anticlines in the Yakima basalt. These lenses of basalt gravel are more abundant in the upper part of the Ellensburg formation.

(4) Minor unconformities, with angular discordances of 2°–10° are common in the Ellensburg formation. Lack of exposures limits tracing, but they are probably of only local extent. The first bed above an unconformity is generally a basalt gravel or a pebbly sandstone containing at least a few cobbles of basalt. The unconformities are more common on the flanks of the synclinal basins than toward their centers, and are more common in the upper part of the Ellensburg series than near its base. They record deformation contemporaneous with the filling of the basin by andesitic debris, and mark sites where local accessions of basaltic cobbles were washed into the basin from the adjacent rising anticlines.

(5) The erosion surface at Kelley Hollow is a tilted pediment formed on the flank of the growing Umtanum fold, not a remnant of a widespread peneplain. Within the Yakima East quadrangle several similar fragments of dissected pediments, uplifted to various levels, record stages in the slow and somewhat discontinuous growth of the Yakima Ridge fold. Thus the evidence suggests one long period of deformation instead of two periods separated by peneplanation.

(6) Smith's and Calkins' conclusion that the prominent ridges are anticlines, not fault blocks,[4] is strongly confirmed. Small faults

[4] The writer is unable to agree with Hodge (1931) that the south side of the Horse Heaven uplift is a great fault scarp. Considerable reconnaissance in the steep canyons that cut the uplift revealed only minor faults, and in most places the basalt

occur, but they are minor subsidiary features. The majority of those seen by the writer are antithetic faults, which lower the center of the anticline instead of adding to the displacement on its limbs. A notable exception is the Tygh Ridge anticline in northern Oregon whose southern limb passes into a normal fault.

(7) The new mapping supports Smith's and Calkins' announcement that the water gaps across the ridges in the Yakima-Ellensburg area were cut as the Yakima River maintained its course across the growing anticlines.

(8) Diversion of a hypothetical ancestral Columbia River from a possible former position across the western part of the Horse Heaven uplift was due to the rapid eastward growth of a complex bahada slope of andesitic debris, not to defeat of Columbia River at Satus Pass by rise of the Horse Heaven fold as Warren believed. Nor do the field observations here reported support Flint's idea that Wallula Gap was cut by a Columbia River which overspilled this divide after being ponded by uplift to the northwest.

References Cited

Bailey, E. B., *et al.*, 1924, Tertiary and post-Tertiary geology of Mull, Loch Aline, and Oban: Geol. Survey Scotland, Memoirs, 445 p.

Berry, E. W., 1931, A Miocene flora from Grand Coulee, Washington: U. S. Geol. Survey Prof. Paper 170C, p. 31–42.

Bretz, J. H., 1924, The Dalles type of river channel: Jour. Geology, v. 32, p. 139–149.

Buwalda, J. P., and Moore, B. N., 1930, The Dalles and Hood River formations and the Columbia River gorge: Carnegie Inst. Wash. Pub. 404, p. 11–26.

Calkins, F. C., 1905, Geology and water resources of a portion of east central Washington: U. S. Geol. Survey Water-Supply Paper 118, 96 p.

Chappell, W. M., 1936, The effect of Miocene lavas on the course of Columbia River in central Washington· Jour. Geology, v. 44 p. 379–386.

Flint, R. F., 1938a, Summary of the late-Cenozoic geology of southeastern Washington: Am. Jour. Sci., v. 35, p. 223–230.

—— 1938b, Origin of the Cheney-Palouse scabland tract, Washington: Geol. Soc. America Bull., v. 49, p. 461–524.

Fuller, R. E., 1931, The aqueous chilling of basaltic lava on the Columbia River plateau: Am. Jour. Sci., v. 21, p. 281–300.

Hodge, E. T., 1931, Columbia River fault: Geol. Soc. America Bull., v. 42, p. 923–984.

Mackin, J. H., 1947, Diatomite deposits in eastern Washington (Abstract): Northwest Sci., v. 21, p. 33.

Merriam, J. C., 1901, A contribution to the geology of the John Day basin: Univ. Calif. Pub., Bull. Dept. Geol. Sci., v. 2, p. 269–314.

Merriam, J. C., and Buwalda, J. P., 1917, Age of the strata referred to the Ellensburg formation in the White Bluffs of the Columbia River: Univ. Calif. Pub., Bull. Geol. Sci., v. 10, p. 255–266.

Pardee, J. T., 1918, Geology and mineral deposits of the Colville Indian Reservation, Washington: U. S. Geol. Survey Bull. 677, 186 p.

Pardee, J. T., and Bryan, Kirk, 1926, Geology of the Latah formation in relation to the lavas of Columbia Plateau near Spokane, Washington: U. S. Geol. Survey Prof. Paper 140A, 16 p.

Piper, A. M., 1932, Geology and ground-water resources of The Dalles region, Oregon: U. S. Geol. Survey Water-Supply Paper 659B, p. 107–189.

Russell, I. C., 1893, A geological reconnaissance in central Washington: U. S. Geol. Survey Bull. 108, 108 p.

Smith, G. O., 1901, Geology and water resources of a portion of Yakima County, Washington: U. S. Geol. Survey Water-Supply Paper 55, 68 p.

——1903a, Ellensburg Folio: U. S. Geol. Survey Geol. Atlas, folio 86.

——1903b, Anticlinal mountain ridges in central Washington: Jour. Geology, v. 11, p. 166–177.

——1903c, Geology and physiography of central Washington: U. S. Geol. Survey Prof. Paper 19, p. 9–39.

——1904, Mount Stuart Folio: U. S. Geol. Survey Geol. Atlas, folio 106.

Waring, G. A., 1913, Geology and water resources of a portion of south-central Washington: U. S. Geol. Survey Water-Supply Paper 316, 46 p.

Warren, C. R., 1941a, Course of Columbia River in southern central Washington: Am. Jour. Sci., v. 239, p. 106–127.

——1941b, The Hood River conglomerate in Washington: Am. Jour. Sci., v. 239, p. 209–232.

Waters, A. C., 1939, Resurrected erosion surface in central Washington: Geol. Soc. America Bull., v. 50, p. 635–660.

Willis, Bailey, 1887, Changes in river courses in Washington Territory due to glaciation: U. S. Geol. Survey Bull. 40, 10 p.

——1903, Physiography and deformation of the Wenatchee-Chelan district, Cascade Range: U. S. Geol. Survey Prof. Paper 19, p. 41–101.

——1939, Discussion of "Resurrected erosion surface in central Washington": Geol. Soc. America Bull., v. 50, p. 658–659.

sequence continues unbroken across the line Hodge draws as a fault. The material at the top of the Maryhill grade cited by Hodge (1931, Fig. 13, p. 948) as gouge separated by sheared basalt is merely steeply dipping beds of the ordinary andesitic clay so commonly interstratified with the basalt.

The Johns Hopkins University, Baltimore 18, Maryland

Manuscript Received by the Secretary of the Society, April 5, 1954

Project Grant 383-41

BULLETIN OF THE GEOLOGICAL SOCIETY OF AMERICA
VOL. 66, PP. 685-698, 3 FIGS. JUNE 1955

LOG OF THE SENIGON WELL, SOUTHERN QUEBEC

BY T. H. CLARK AND ISLES STRACHAN

ABSTRACT

In 1942 a well was drilled to a depth of 2296 feet 40 miles south of Montreal. Black shale predominated down to 2090 feet, and the lowest 206 feet consisted of Trenton limestone. Examination of the graptolites and other fossils allows a correlation with the known Montreal section. The Trenton-Utica boundary occurs midway in the shales, and the limestone below is correlated with the St. Michel member of the Montreal formation. The stratigraphic units are uniformly thicker here than at Montreal, presumably because they were deposited within the limits of the Appalachian geosyncline. Because mere reference to graptolite species would not suffice, descriptions of many found in the core are given.

CONTENTS

TEXT

	Page
Introduction	685
Acknowledgments	686
Lithologic and paleontologic correlation	686
Limestone	686
Shale	688
Interpretation of the lithologic record	688
Interpretation of the paleontologic record	688
Conclusion	689
Graptolites of the Senigon core	689
Introduction	689
Stratigraphy	689
Paleontology	692
References cited	697

ILLUSTRATIONS

Figure	Page
1. Map of the Lacolle quadrangle, Southern Quebec	686
2. Correlation chart of the Senigon Well core	687
3. Graptolites from the Senigon core	694

TABLES

Table	Page
1. Ranges of all recognizable fossils in the Senigon Well core	690
2. Ranges of described graptolite species	692

INTRODUCTION

In 1942 a well was drilled to a depth of 2296 feet near Noyan, 20 miles south of St. John's, Quebec, 40 miles south of Montreal, and 4 miles north of the International Boundary. The sparse rock exposures of the surrounding area indicate that the region is underlain by essentially horizontal black shales, whose age might, from lithologic evidence alone, be either Trenton (Stony Point) or Utica (Iberville). Because fossils are very scarce the boundary between those two formations is not easily determined. Figure 1 (modified from Clark and McGerrigle, 1936, p. 666) shows both the position of the well and the assumed geological boundaries.

Below 34 feet of overburden, dark shales and sandstones continue for 2090 feet, thence passing into typical Middle Trenton limestone. That 2090 feet of shale should overlie Trenton limestone is not exceptional, but because no such thickness of Utica shale has been measured either from surface exposures or from well logs, much of this black shale probably belongs to formations higher or lower than the Utica. Succeeding the Utica is the lower Lorraine, which is in many places indistinguishable from the Utica, except where diagnostic fossils occur. And because shale deposition started in Trenton time, some, if not much, of the Trenton beds may be lithologically indistinguishable from the Utica.

The core from this well, therefore, offered a means of determining how much of the black shale belongs to each of the three formations. The ranges of any identifiable Trenton, Utica,

and Lorraine fossils was another expected result. Preliminary examination showed many graptolites, and it was hoped that, even in a ¾ inch core, an identifiable graptolite stipe might be preserved. Accordingly, after appropriate samples had been laid aside, the whole core was broken up into discs from 1/16 inch to ¼ inch thick (facilitated by easy splitting and a near horizontality of bedding) to extract the fossils. At least 150,000 discs were examined, involving more than a quarter of a million surfaces. The vast majority of these were barren. Two thirds of all fossils culled were graptolites; almost all the rest were brachiopods and trilobites.

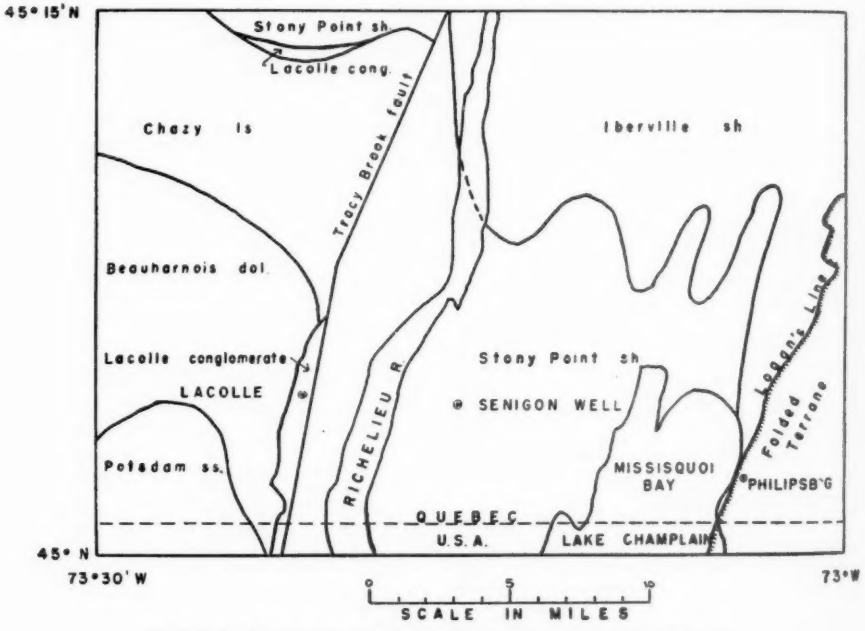

FIGURE 1.—MAP OF THE LACOLLE QUADRANGLE, SOUTHERN QUEBEC
To show location of the Senigon Well

ACKNOWLEDGMENTS

The work of separating the fossiliferous surfaces from the rest of the core was admirably carried out by Mr. Charles Dawson, whose enthusiasm and sharp eyes proved invaluable. For assistance in logging the core I am grateful to Miss Helena Phillips and Miss Mary Frederick for many hours of help in recording lithologic data.

The possible results were so important that the senior author proposed to Dr. O. M. B. Bulman that he undertake the work upon the graptolites, and, in 1947, all such fossils were sent to the Sedgwick Museum, Cambridge University, where they have been examined, under Dr. Bulman's supervision, by the junior author, to whom sole credit is due for all parts of this paper dealing with graptolites.

Publication was by permission of the Department of Mines of Quebec.

LITHOLOGIC AND PALEONTOLOGIC CORRELATION

Limestone

The rock below 2124 feet consists mostly of beds of nearly pure, very finely crystalline limestone alternating with dark calcareous shale. In only a few places does the limestone exceed 6 inches in thickness, or the shale beds 2 inches.

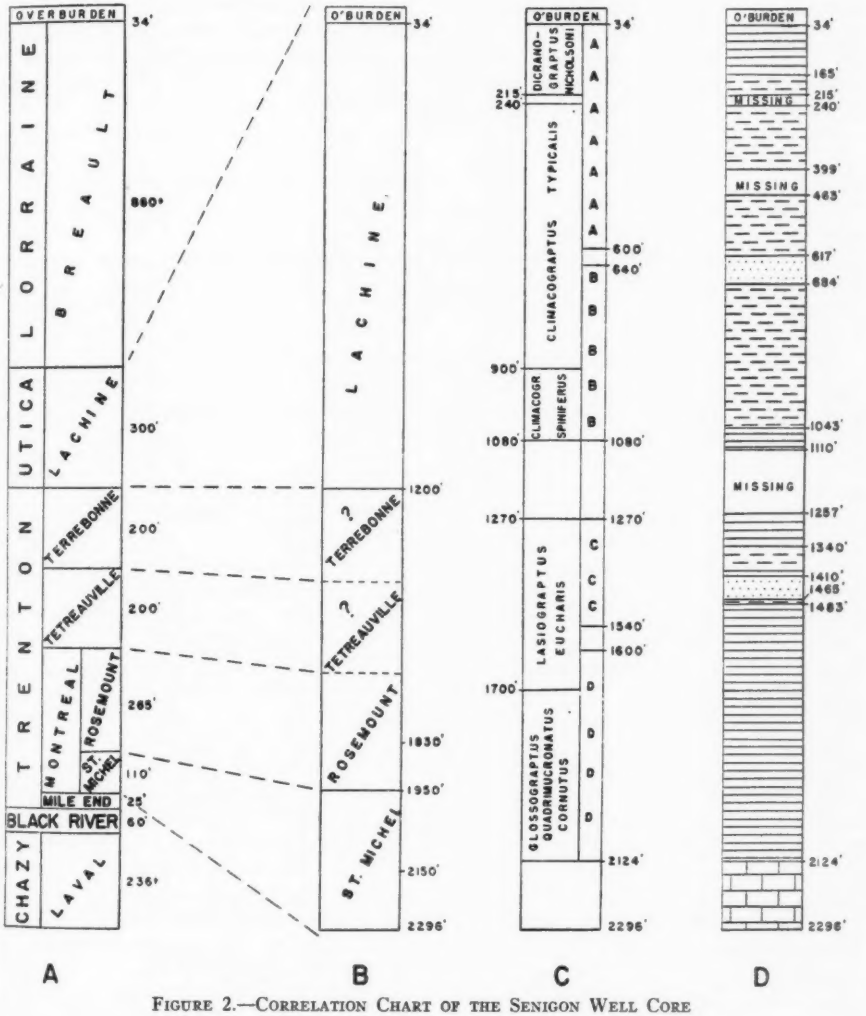

FIGURE 2.—CORRELATION CHART OF THE SENIGON WELL CORE

The limestone is gray in the upper part becoming black towards the bottom of the hole, where, for 46 feet, it is equalled in amount by dark calcareous and noncalcareous shales. In all this it resembles the Montreal formation (Clark, 1952, p. 65; equivalent to Kay's Sherman Fall) at Montreal, and differs markedly from the overlying Tetreauville or the underlying Mile End limestones. The limestone in the Senigon Well is correlated with the St. Michel limestone of the Montreal formation in the Montreal area. (*See* Fig. 2.) The presence, between horizons 2140 and 2160, of *Cryptolithus tesselatus*, *Schizotreta ottawaensis*, and *Triplecia nuclea* (all restricted to the St. Michel in the Montreal area) in limestones similar to those which continue to the bottom of the hole, means that drilling probably stopped within the St. Michel limestone. It further indicates that the St. Michel limestone beds are thicker here (172 feet) than at Montreal, where they are estimated (Clark, 1952, p. 75) at 100–120 feet

thick. Moreover, *Cryptolithus tesselatus* occurs also in shale between horizons 1950 and 1960. This indicates that shales, at least up to that horizon, were deposited in St. Michel time, and gives a total minimum thickness of 346 feet.

Shales

The shales are, with few exceptions, calcareous, and in half a dozen horizons are replaced by a few inches of limestone. At a dozen horizons there are thin bands of pyrite, up to ¼ inch thick. No part of the core has a petroleum-like odor.

Most of the shales are micaceous, some abundantly so. In logging the core particular attention was paid to hardness as tested by a steel point. This was taken to indicate the relative proportion of kaolin and quartz. A "soft" shale would probably be composed largely of kaolin, and so would effectively seal in oil or gas, whereas a "hard" shale, in reality a super-fine sandstone composed largely of minute particles of quartz would confine the oil but might in time allow movement of gas. In general the softer the shale the darker its color, and *vice versa*. The commonest designations in the detailed record of the log are "soft black shale" and "hard gray shale".

Interpretation of the Lithologic Record

During much of St. Michel time this region was subjected to the same calcareous sedimentation that occurred over the rest of southern Quebec, with an abundant benthos recorded in the limestone beds and both benthonic and pelagic elements recorded in the shales. Towards the end of St. Michel time mud was transported in greater amounts from the rising highlands to the east, smothering almost completely the calcareous-shelled organisms. Accumulation of calcareous pelagic tests, together with small-scale precipitation of $CaCO_3$ and probable deposition of fine, shelly sea-borne material, account for the slight and variable calcareous content of the shale. Probably decomposition products from the land were transferred into the sea, thus permitting the initial abundance of soft kaolin-rich shale immediately overlying or even interbedded with the limestone. Continued, perhaps slightly increased, uplift caused intensified weathering and transport, and was responsible for the harder quartz-rich shales and the fine-grained sandstones. A return to the earlier conditions resulted in the soft shales of the upper 131 feet, thus completing a major depositional cycle (soft shale, hard shale, sandstone, hard shale, soft shale), within which there occurs a minor cycle from 1483 to 1340.

Interpretation of the Paleontologic Record

The limestones belong to the St. Michel member of the Montreal formation of middle Trenton time. Between 2150 and 2124 feet a gradation by intercalation from limestone to black shale indicates continuous deposition during and beyond the end of St. Michel time. The Rosemount and succeeding Trenton formations are represented by undetermined thicknesses of shale. *Cryptolithus tesselatus* was found in shale just below 1950 feet, and because that fossil is confined to the lower part of the St. Michel member in the Montreal area, the horizon 1950 is used as the dividing line between the St. Michel and the Rosemount members, though it might be slightly higher (Fig. 2).

The next break in faunal continuity comes about 1940 feet, where the common Trenton brachiopods *Dalmanella rogata*, *Sowerbyella sericea*, and *Rafinesquina* spp. disappear. These bottom-living forms were outlasted by migrant trilobites of Trenton aspect, such as *Isotelus gigas* and *Calymene senaria*, which persist up to 1830 feet. This is also the highest horizon for crinoid stems (with one exception) and *Zygospira recurvirostris*, and is the upper limit of the normal open-water Trenton fauna surviving in an unfavorable muddy environment. However, this does not imply that no higher beds were deposited in Trenton time. The evidence furnished by the benthos is incomplete. The pelagic graptolite fauna, however, indicates that the break between Trenton and Utica graptolites comes somewhere within the 1110–1257 hiatus. Below this lie the *Glossograptus quadrimucronatus cornutus* and the *Lasiograptus eucharis* zones, whereas above it there are elements of three zones—that of *Climacograptus spiniferus* below, succeeded by *C. typicalis*, and, in the uppermost 166 feet of the core, the zone of *Dicranograptus nicholsoni*. Analysis of the

graptolite fauna, therefore, allows the Trenton-Utica time boundary to be pushed higher than the lithological differences or the evidence from other fossils dictate.

Conclusion

The results from the three types of evidence are shown in Figure 2. The differences in thickness of the St. Michel and the Utica in the Montreal and in the Senigon Well successions is significant. The great thickness of the St. Michel limestone in the Senigon Well might result in part from the disappearance not far south of Montreal of the Mile End formation (92 feet thick at Joliette, 40 miles northeast of Montreal; 25 feet thick at Montreal) where the St. Michel takes part of its place. The Senigon Well locality was closer by several miles to the geosyncline, and doubtlessly was affected by the general downsinking more than was Montreal which was supported by a stable shelf. This applies to the much greater difference between the two Utica accumulations, even if the 300-foot estimate of the thickness of the Montreal Utica should be doubled (Clark, 1952, p. 79). Marine geosynclinal sedimentation depends upon both subsidence and continuance of supply, and this latter factor, so prominent throughout the Paleozoic in the Appalachian region, is one of the most cogent, if not compelling, evidences in favor of the so called Appalachia, currently in some disrepute among sland-arcologists.

Graptolites of the Senigon Core

Introduction

Graptolites are fairly abundant throughout the core. With few exceptions they are poorly preserved. The rocks range from a hard black mudstone, in which the graptolites are preserved as thin films or in places as pyrite casts, to almost pure limestone, in which the graptolites are small broken fragments. No thin-bedded fissile "graptolite shales" were found among the core-discs.

Because the diameter of the core is small, complete rhabdosomes are rare, and the usually poor state of preservation makes identification at lower than generic level uncertain. The hardness of the matrix has also made it difficult to clean up specimens which were only partly exposed, but enough can be identified to give a general idea of the fauna and its stratigraphic position.

Stratigraphy

On the evidence of the graptolite fauna alone the core has been divided into four levels, each separated by a break of 50 or more feet. The fauna of each of these is given in Table 2.

The characteristic species of the upper half of the core (down to 1080 feet) are *Climacograptus spiniferus* and *C. typicalis*, with *Dicranograptus* cf. *nicholsoni* confined almost to the topmost 200 feet. The lower half of the core (below 1270 feet) is characterised by *Diplograptus* cf. *molestus* associated with *Lasiograptus* and *Neurograptus*. The common orthograptids appear throughout the core and those represented by only one or two specimens are of little stratigraphic importance.

Five of Ruedemann's zones of the New York Ordovician seem to be represented. The uppermost 200 feet could represent his zone of *Dicranograptus nicholsoni*, from 200 feet–900 feet his zone of *Climacograptus typicalis*, from 900 feet–1080 feet the zone of *C. spiniferus*, from 1270 feet–1700 feet the zone of *Lasiograptus eucharis*, and below 1700 feet his zone of *Glossograptus quadrimucronatus cornutus*.

The value of these zones for regional correlation is questionable, for example, *C. typicalis* ranges throughout the upper half of the core, occurring with *D.* cf. *nicholsoni* at the top, and *C. spiniferus* is not confined between the limits given above. The other correlations rest on the identification of a few specimens of each diagnostic species and must not be forced to fit any preconceived ideas.

It is obvious, however, that the core is to be correlated with at least part of the given horizons—with the upper part of the Canajoharie shale and the lower part of the Utica shale as defined by Ruedemann (1947, p. 52). A study of Kay's paper on the Trenton Group (1937) allows a correlation of the core with the upper part (Denmark member) of his Sherman Fall formation and with the lower (Hallowell) member of the succeeding Cobourg formation. Correlation with the European succession is much

TABLE 1.—RANGES OF ALL RECOGNIZABLE FOSSILS IN THE SENIGON WELL CORE

	0– 40	40– 80	80– 120	120– 160	160– 200	200– 240	240– 280	280– 320	320– 360	360– 400	400– 440	440– 480	480– 520	520– 560	560– 600	600– 640	640– 680	680– 720	720– 760	760– 800	800– 840	840– 880	880– 920	920– 960	960–1000	1000–1040	1040–1080	1080–1120	1120–1160	1160–1200	1200–1240	1240–1280	1280–1320	1320–1360	1360–1400	1400–1440	1440–1480	1480–1520	1520–1560	1560–1600	1600–1640	1640–1680	1680–1720	1720–1760	1760–1800	1800–1840	1840–1880	1880–1920	1920–1960	1960–2000	2000–2040	2040–2080	2080–2120	2120–2160	2160–2200	2200–2240	2240–2280	2280–3000
Conularia sp.																																																							
Serpulites sp.																																																								
Hyolithes sp.																																																								
Crinoid stems																																																								
Prasopora sp.																																																								
Bryozoa, miscellaneous																																																								
Trematis terminalis																																																								
Schizotreta ottawaensis																																																								
Lingula spp.																																																								
Leptobolus insignis	×		×		×		×											×		×		×		×	×	×	×					×			×			×																	
Platystrophia uniplicata																																×						×																	
Sowerbyella sericea																																																								
Dalmanella rogata																																																								
Rafinesquina alternata																																																								
R. spp.																																																								
Triplecia nuclea																																																								
Zygospira recurvirostris																																																								
Gastropods																																																							
Pelecypods																																																							
Geisonoceras tenuifilum																																	×																						
Isotelus sp.																																																							
Ceraurus pleurexanthemus																																																							
Calymene senaria																																	×																						
Cryptolithus tesselatus																																																							
Triarthrus ?eatoni	×					×												×				×	×									×	×						×	×																
Leperditia? sp.																										×								×				×	×																
Bythocypris cylindrica																										×												×																	
Lepidocoleus jamesi																										×																													
Conodont																										×																													

TABLE 1.—*Continued*

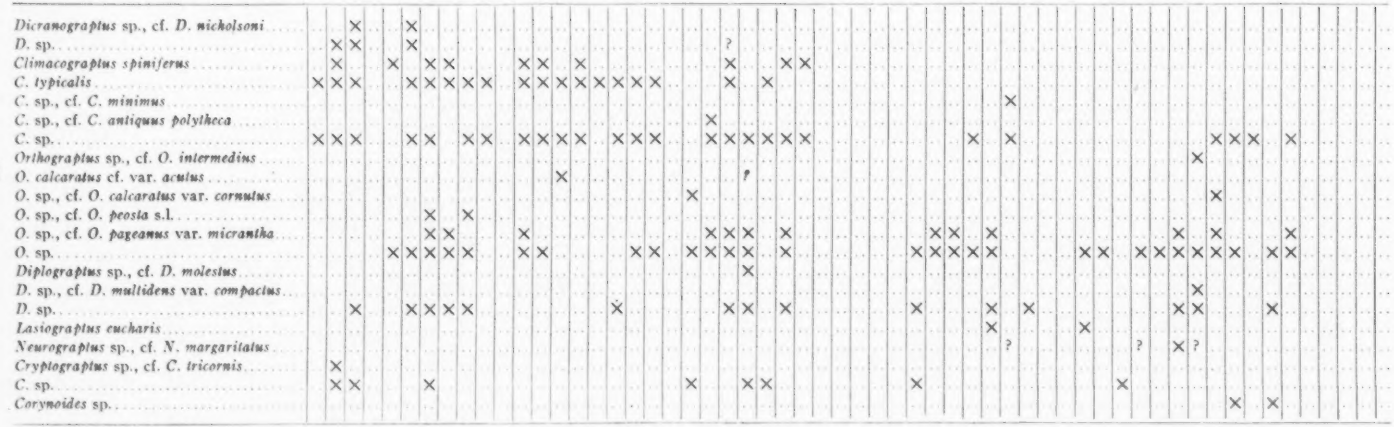
Dicranograptus sp., cf. D. nicholsoni
D. sp.
Climacograptus spiniferus
C. typicalis
C. sp., cf. C. minimus
C. sp., cf. C. antiquus polytheca
C. sp.
Orthograptus sp., cf. O. intermedius
O. calcaratus cf. var. acutus
O. sp., cf. O. calcaratus var. cornutus
O. sp., cf. O. peosia s.l.
O. sp., cf. O. pageanus var. micrantha
O. sp.
Diplograptus sp., cf. D. molestus
D. sp., cf. D. multidens var. compactus
D. sp.
Lasiograptus eucharis
Neurograptus sp., cf. N. margaritatus
Cryptograptus sp., cf. C. tricornis
C. sp.
Corynoides sp.

more difficult since the graptolites, particularly in the upper part, belong to the American province and many are not known to appear in European deposits. A correlation with a horizon about that of *Dicranograptus clingani* is the most that can be attempted at present, though the occurrence of *Diplograptus molestus* in the core allows a slightly lower horizon for the lower part of the core.

TABLE 2.—RANGES OF DESCRIBED GRAPTOLITE SPECIES

	Level A 0 ft. to 600 ft.	Level B 640 ft. to 1080 ft.	Level C 1270 ft. to 1540 ft.	Level D 1600 ft. to 2300 ft.
Dicranograptus cf. *nicholsoni* Hopk.	X	....	....	....
Climacograptus spiniferus Rued.	X	XC	....	....
C. typicalis Hall.	XC	XC	....	....
C. cf. *antiquus* var. *polytheca* Rued.	....	X	....	....
C. cf. *minimus* (Carr.)	....	....	X	....
Orthograptus calcaratus cf. var. *acutus* E. & W.	X	....	....	?X
O. cf. *calcaratus* var. *cornutus* (Rued.)	....	X	....	X
O. cf. *intermedius* Elles and Wood	....	....	....	X
O. cf. *peosta* (Hall) sensu lato.	XC	....	....	....
O. cf. *pageanus* var. *micrantha* E. & W.	X	X	X	X
Diplograptus cf. *molestus* Thors.	....	....	....	XC
D. cf. *multidens* var. *compactus* E. & W.	....	....	....	X
Lasiograptus eucharis (Hall)	....	....	X	X
Neurograptus cf. *margaritatus* (Lapw.)	....	....	....	X
Cryptograptus cf. *tricornis* (Carr.)	X	X	?X	X
Corynoides sp.	....	....	....	X

X indicates that species occurs.
XC indicates that species is common.

Paleontology

The following descriptions are intended to give some idea of the basis of the identifications, and are not meant to be definitive. They are necessary because no critical descriptions of any American graptolites have been published since 1907. The fossil lists alone would be useless without detailed descriptions and figures, particularly where an author has not had access to type material for comparison. The synonymies have been reduced to a minimum, and, except as otherwise indicated, full synonymies will be found in Ruedemann 1947.

Dicranograptus cf. *nicholsoni* Hopkinson

(Fig. 3g, h)

Fragments of a dicranograptid occur at various levels in the core down to about 200 feet and perhaps again at 910 feet. Most of the dozen specimens are biserial portions with forking characteristic of the genus, and the few isolated fragments of uniserial stipes similar to Figure 3h are placed in this group.

Thecae are of *D. nicholsoni* type with marked introversion and with spines on thecae of the biserial portion, which is 4–6 mm long and consists of 6–7 pairs of thecae. One specimen (Fig. 3h) shows straight uniserial stipes arising from the fork, so the specimens are probably referable to the type form of *D. nicholsoni* as described by Ruedemann rather than to varieties, such as *diapason* Gurley and *geniculatus* Rued., which show distinct change of growth direction in their stipes. In the typical form described by Elles and Wood, the biserial portion is normally longer (5–8 mm), and specimens from the core approach var. *minor* described by Bulman (1947, p. 41).

Climacograptus spiniferus Ruedemann

(Fig. 3d, f)

This species is represented in the core by more than 20 specimens at all levels down to about 1050 feet. Besides basal spines, it has a gradually broadening rhabdosome, widening from initial 0.5 mm to maximum of about 1.5

mm, and many thecae (15–11 in 10 mm), with their deep excavations occupying one third of both length and breadth of the rhabdosome.

Only one of the basal spines is derived from a theca (th1[1]), the other being the well-developed virgella. This arrangement is distinct from that in *C. bicornis*, and its later form *C. supernus*, where both basal spines are developed from thecae and the virgella can sometimes be seen as a small third spine. A similar development of virgella and first thecal spine is seen in *C. diplacanthus* Bulman (1932a) but that species is a larger form with fewer thecae per cm and smaller excavations.

Distal fragments of *C. spiniferus* have complete septum, missing in those of *C. typicalis*.

Climacograptus typicalis Hall

(Fig. 3a, b)

Specimens are abundant throughout the upper part of the core, down to 980 feet. Most seem to be of the type form described by Ruedemann, and the group is not subdivided here. Specimens have been analysed for thecal number and breadth, but no correlation with depth (and presumably with horizon) has been found. A few specimens show rather prominent mesial flanges or spines (Fig. 3b) but all other characteristics conform to the type. Ruedemann has distinguished two varieties of *C. typicalis* which show such spines. As concluded from his figures alone the specimens from the core are nearer var. *spinothecatus* Rued. than var. *crassimarginalis* Rued. and Decker.

Bullman (1932b) has described complete developmental series of *C. typicalis* so that characteristics of the species are well known. It can be easily distinguished from other climacograptids by the slender proximal end with a peculiarly bulbous first theca (Fig. 3a) and by extremely rapid widening of the rhabdosome from initial breadth of 0.5 mm to mature width, 2.0–2.4 mm in pyritised specimens, in a length of about 15 mm.

Climacograptus spp.

(Fig. 3e, j)

Several other species of *Climacograptus* occur throughout the core, particularly in the lower part, but cannot be satisfactorily assigned to any known species. Coarseness of matrix in some cases obscures the rhabdosome outline, though the thecae are obviously climacograptid. In only a few cases are proximal ends preserved; two are figured.

In Figure 3e the rhabdosome, particularly in the shape of proximal thecae, resembles *Climacograptus minimus* (Carr.), but in this species thecae number only 6–7 in the first 5 mm as against 8 in the specimen shown here.

In the other specimen figured (Fig. 3j) general form and size are those of *C. typicalis*, but here the first theca bears a prominent mesial spine not found in *C. typicalis* and it is very like some of those figured by Ruedemann as *C. antiquus* var. *polytheca*.

Orthograptus calcaratus cf. var. *acutus* E. and W.

(Fig. 3x)

1947 *Diplograptus* (*Orthograptus*) *calcaratus* var. *acutus*, Ruedemann, p. 399.

A single well-preserved specimen of the *O. calcaratus* group occurs at a depth of 539 feet. Thecae are not so everted as is usual in *O. calcaratus*, but there is a broad virgular tube not found in *O. truncatus*. In general form and in the absence of large basal spines, it approaches vars. *vulgatus* Lapw. MS and *acutus* Lapw. MS, but differs from them both in having 16–14 thecae per cm. In this respect it agrees closely with the copy of Lapworth's manuscript drawing of var. *acutus* given by Ruedemann (1947, Pl. 68, fig. 15) and should possibly be included in that variety although Elles and Wood, in their original description of the variety, give the thecal number as 12–9 per cm, and the specimen figured here does not show the characteristic widening of var. *acutus* Elles and Wood.

Two other specimens, at 955 feet and 2090 feet respectively, may also belong to this variety but they are not as well preserved as is the figured specimen.

Orthograptus cf. *calcaratus* var. *cornutus* (Ruedemann)

(Fig. 3m)

1947 *Glossograptus quadrimucronatus* var. *cornutus* Ruedemann, p. 445.

Two specimens are assigned to this variety from depths of 832 feet and 1931 feet. Both

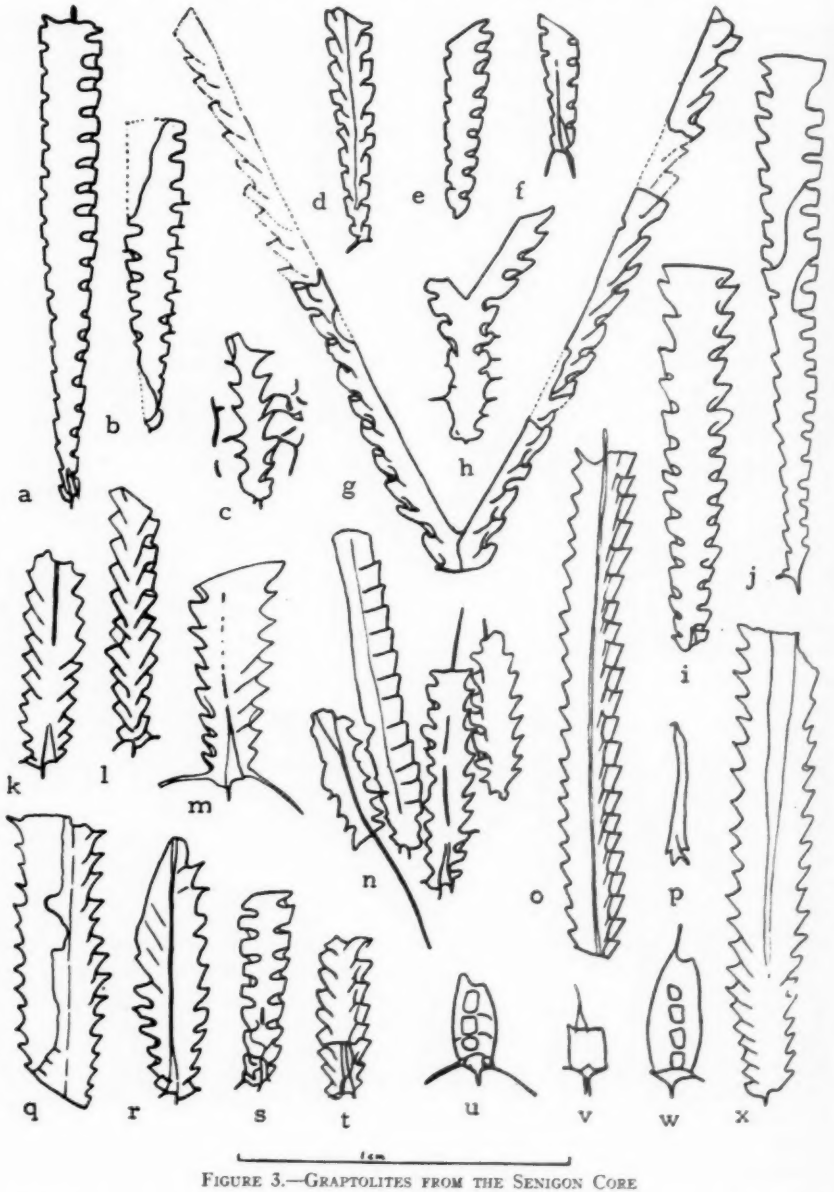

FIGURE 3.—GRAPTOLITES FROM THE SENIGON CORE

All figures ×5

a, b.—*Climacograptus typicalis* Hall. (1) Complete specimen in sub-scalariform view, 269 ft. (2) Specimen showing mesial spines, 81 ft.

c.—*Neurograptus* sp., cf. *N. margaritatus* (Lapw.), poorly preserved specimen with traces of lacinia. 1853 ft.

show long basal spines which have been regarded as characteristic of the variety but which also occur in *O. calcaratus* var. *tenuicornis* E. and W.

The figured specimen is better preserved than the other and looks much more like the *calcaratus* group of orthograptids than like the *quadrimucronatus* type to which Ruedemann refers the variety. This characteristic is also shown in the only figure given by Ruedemann which shows both the basal spines developed and the more distal thecae. Thecae in this figure number 7 in the first 5 mm as compared with 5 in 5 mm in var. *tenuicornis* and 7½–8 in 5 mm in specimens from the core. With increase in number of thecae per cm can be correlated rapid widening of the rhabdosome in the core specimens when compared with var. *tenuicornis* which has a relatively slender proximal end.

Orthograptus cf. *intermedius* Elles and Wood

(Fig. 3o)

1947 *Diplograptus* (*Orthograptus*) *truncatus* var. *intermedius* Ruedemann, p. 403.

Three specimens from between depths of 1904 feet and 1916 feet are tentatively assigned to this species. They are distinguished from other forms of the *truncatus* group in the core yb their remote thecae, numbering 14–10 in 10mm. The rhabdosome is also broader, reaching 2.5 mm in one specimen. The great length characteristic of the variety cannot be seen in the small core, but the specimens agree well with the original figure and description.

Orthopgraptus cf. *peosta* (Hall) sensu lato

(Fig. 3k, l)

1908 *Diplograptus peosta* Ruedemann, p. 372.

Among the orthograptid rhabdosomes found in the core, about a half dozen can be referred to this species. Most occur in the uppermost 300 feet of the core, but fragments of the same general type occur throughout.

The species belongs to the *O. truncatus* group characterised by straight thecae with simple apertures, but the number of thecae per cm (18–14 in core specimens) is much higher than that in the corresponding small British form, *O. truncatus* var. *socialis*.

Ruedemann (1908) figured several specimens as *Diplograptus peosta* and later (1925) erected several new species on variations shown by the *peosta* group. His descriptions differ greatly with his figures in breadth and thecal number, and it is impossible to assign the core specimens to any of his species. These small orthograptids are controversial, and in view of the poor preservation of the few specimens noted this group has not been reconsidered.

---

d, f.—*Climacograptus spiniferus* Ruedemann. (4) Typical specimen with complete septum, 467 ft. (6) Proximal end showing the sicula, 298 ft.

e.—*Climacograptus* sp., cf. *C. minimus* Carr., proximal portion in sub-scalariform view, 1497 ft.

g, h.—*Dicranograptus* sp., cf. *D. nicholsoni* Hopk. (7) Biserial portion, 81 ft. (8) Largest specimen with uniserial branches partly preserved as impression, 215 ft.

i.—*Dicranograptus multidens* var. *compactus* Elles and Wood, 1911 ft.

j.—*Climacograptus* sp., cf. *C. antiquus* var. *polytheca* Ruedemann, 897 ft.

k, l.—*Orthograptus* sp., cf. *O. peosta* (Hall) s.l. (11) Broader specimen showing sicula, 343 ft. (12) Typical specimen preserved in relief, 279 ft.

m.—*Orthograptus* sp., cf. *O. calcaratus* var. *cornutus* Rued., proximal end showing the sicula and the slender basal spines, 1931 ft.

n.—*Lasiograptus eucharis* (Hall), group of specimens, 1683 ft.

o.—*Orthograptus* sp., cf. *O. intermedius* Elles and Wood, slightly curved distal part of the rhabdosome showing uniform width, 1904, ft.

p.—*Corynoides* sp. ?Incomplete specimen, 1985 ft.

q, r.—*Orthograptus* sp., cf. *O. pageanus* var. *micranthus* Elles and Wood. (17) Broad distal fragment, partly as impression, 280 ft. (18) Proximal end showing sicula, 466 ft.

s, t.—*Diplograptus molestus* Thorslund. (19) Specimen partly in relief showing climacograptid thecae; 1644 ft. (20) Specimen in sub-scalariform view, 1929 ft.

u–w.—*Cryptograptus* sp., cf. *C. tricornis* (Carr.). (21) Specimen with long basal spines, 923 ft. (22) Young specimen showing sicula, 830 ft. (23) Largest specimen from core, 68 ft.

x.—*Orthograptus* sp., cf. *O. calcaratus* var *acutus* Elles and Wood, 539 ft.

Orthograptus cf. *pageanus* var. *micranthus* Elles and Wood

(Fig. 3q, r)

1907 *Orthograptus pageanus* var. *micranthus* Elles and Wood, p. 226.

A dozen or so specimens of a spined orthograptid with closely packed thecae have been found throughout the core. Most are distal fragments but a few proximal ends have been seen. The spines are not very long but are obvious as projections from the outer angles of thecal apertures. Thecae number 18–14 in 10 mm, and maximum observed breadth of the rhabdosome is 3 mm though the average breadth is rather less.

Closeness of the thecae puts these specimens into the *O. pageanus* group of spined orthograptids, and the breadth of only 2.5–3 mm agrees with that given for the variety *micranthus*. None of the many forms of *O. quadrimucronatus* approaches this high thecal number except var. *postremus* Ruedemann which may be a synonym of *O. pageanus* var. *micranthus*.

Diplograptus cf. *molestus* Thorslund

(Fig. 3s, t)

1947 *Diplograptus* (*Mesograptus*) *multidens* var. *diminutus* Ruedemann, p. 420.
1948 *Diplograptus molestus* Thorslund, p. 369.

A dozen or so specimens of a small diplograptid occur between 1640 feet and 1930 feet in the core. The specimens widen from about 1.0 mm to 1.6 mm in their length of 6–8 mm, and the thecae number 16–14 in 10 mm. The form is a diminutive *D. multidens*, as noted by Ruedemann for his variety, but the varietal name *diminutus* is preoccupied by *D. modestus* var. *diminutus* Elles and Wood 1907, and Ruedemann's variety appears to be synonymous with *D. molestus*, a name proposed by Thorslund for the form long known in Sweden as *Climacograptus rugosus*.

Diplograptus cf. *multidens* var. *compactus* Elles and Wood

(Fig. 3i)

1907 *Diplograptus* (*Mesograptus*) *multidens* var. *compactus* Elles and Wood, p. 262, Pl. XXXI, figs. 10a, c.

One of the diplograptids in the lowest part of the core is slightly larger than the preceding species and is close to *D. multidens* var. *compactus*. The figured specimen from 1911 feet is about 12 mm long and widens fairly rapidly from a breadth of 1 mm to a maximum of 2.5 mm. The proximal thecae are climacograptid in form, but distally the excavations become shallower and the thecae approach the orthograptid type. They number 15–12 in 10 mm. The specimen is not very well preserved and, though the sicula can be seen, there is little sign of spines on the basal thecae. General form and size, however, distinguish it from both *D. multidens* and *D. molestus* and it appears to be the form linking these two species.

Lasiograptus eucharis (Hall)

(Fig. 3n)

Several specimens, including what is probably a synrhabdosome of this form, occur in the core between 1464 feet and 1683 feet. Average breadth of the specimens is about 1.6 mm and thecae number 18–20 in 10 mm. The specimens agree well with most of those figured by Ruedemann, and a few traces of the lacinia have been seen. However, they show little sign of the amplexograptid thecae characteristic of *Lasiograptus*, s. str. as defined by Elles and Wood, but in view of their poor preservation the present generic reference is retained.

Neurograptus cf. *margaritatus* (Lapw.)

(Fig. 3c)

1908 *Lasiograptus* (*Neurograptus*) *margaritatus* Elles and Wood, p. 332.

Two poorly preserved specimens from a depth of 1853 feet are probably referable to this species. The thecae are of the simple orthograptid type with partially everted apertures, and the lacinia is well developed, both characteristics of *Neurograptus*. The small size of the specimens, with a breadth of only 1.3 mm exclusive of spines, together with closely packed thecae, 14 in 10 mm, indicates a reference to *N. margaritatus*.

Ruedemann (1947, p. 462), in discussing *Hallograptus*, with poorly developed or no lacinia, mentions that some of the North American

forms he referred to that genus may, with better material, be recognized as belonging to *Neurograptus*. The specimens described here agree with typical specimens of *Neurograptus* described by Elles and Wood and are quite distinct from British examples of *Hallograptus*.

Cryptograptus cf. *tricornis* (Carruthers)

(Fig. 3u, v, w)

Widely scattered specimens of a small *Cryptograptus* occur throughout most of the core. The longest has a length of only 4 mm; the breadth is usually 1.0–1.4 mm. None of the score or so of specimens shows the thecae well, and generic identification is based on sicular spines. The narrow rhabdosome suggests reference to *C. tricornis* s. str., but some may belong to mut. *insectiformis* Rued.

Corynoides sp.

(Fig. 3p)

Two small specimens of Corynoides occur at 1985 feet and 2050 feet but their preservation is too poor to allow specific determination.

References Cited

Bulman, O. M. B., 1932a, On the graptolites prepared by Holm, 1: Arkiv. Zoologi, Bd. 24A, no. 8.

—— 1932b, On the graptolites prepared by Holm, 2–5: Arkiv. Zoologi, Bd. 24A, no. 9.

—— 1944–1947, Caradoc (Balclatchie) Graptolites from limestones in Laggan Burn, Ayrshire: London, Palaeontogr. Soc. Mon.

Clark, T. H., 1952, Montreal Area, Laval and Lachine Map-areas: Que. Dept. Mines Geology Rept. 46, 150 p.

Clark, T. H., and McGerrigle, H. W., 1936, Lacolle Conglomerate: A new Ordovician formation in Quebec: Geol. Soc. America Bull., v. 47, p. 665–674.

Elles, G. L., and Wood, E. M. R., 1901–18, Monograph of British graptolites: London, Palaeontogr. Soc. Mon.

Kay, G. M., 1937, Stratigraphy of the Trenton Group: Geol. Soc. America Bull., v. 48, p. 233.

Ruedemann, R., 1908, Graptolites of New York: N. Y. State Mus. Mem. 11, Pt. 2.

—— 1925, The Utica and Lorraine formations of New York: Pt. II. Systematic Palaeontology: N. Y. State Mus. Bull. 262.

—— 1947, Graptolites of North America: Geol. Soc. Am. Mem. 19, 652 p.

Thorslund, P., 1948, The Chasmops Series of the Kullatorp Core: Bull. Geol. Inst. Upsala, v. 32, p. 343.

McGill University, Montreal; The University, Birmingham, England

Manuscript Received by the Secretary of the Society, April 5, 1954

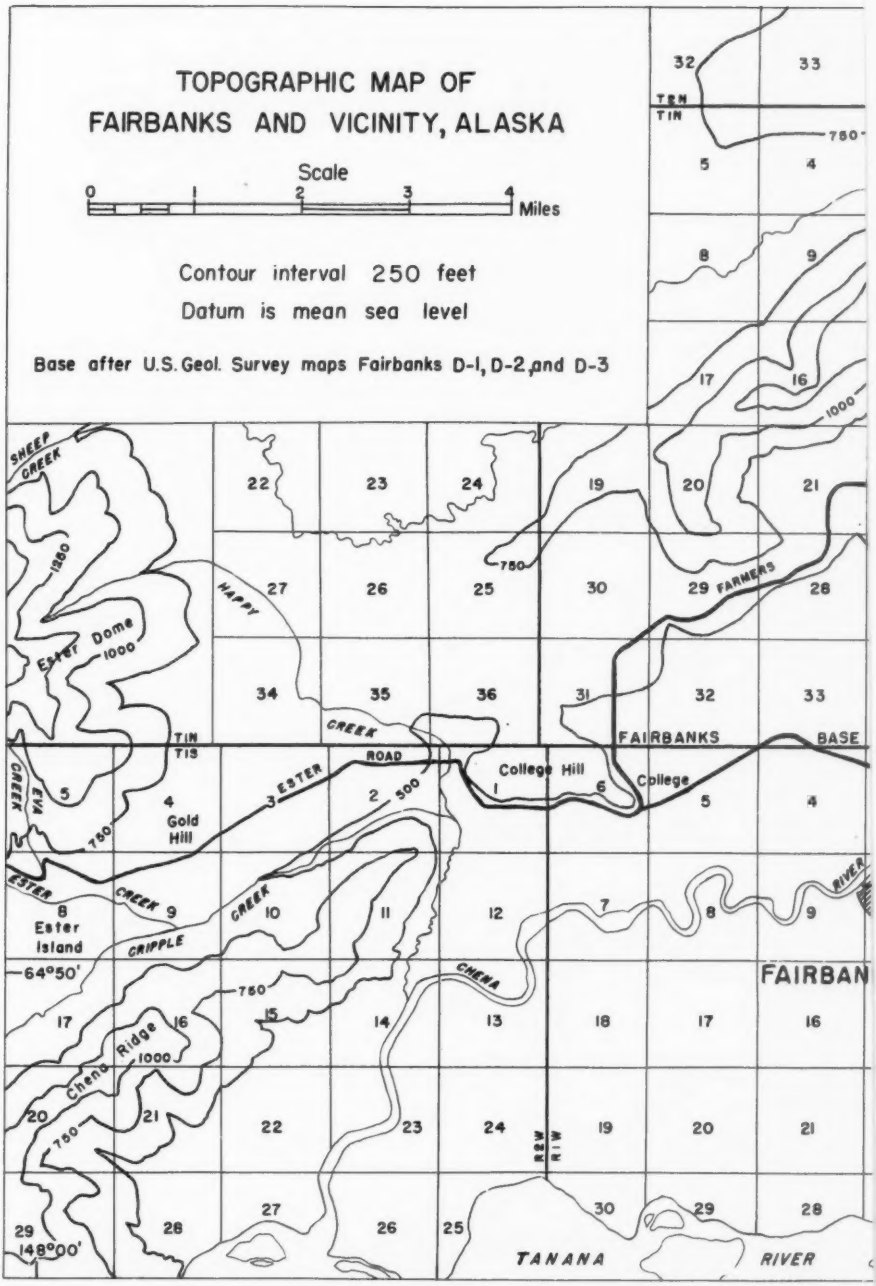

INDEX MAP OF FAIRB

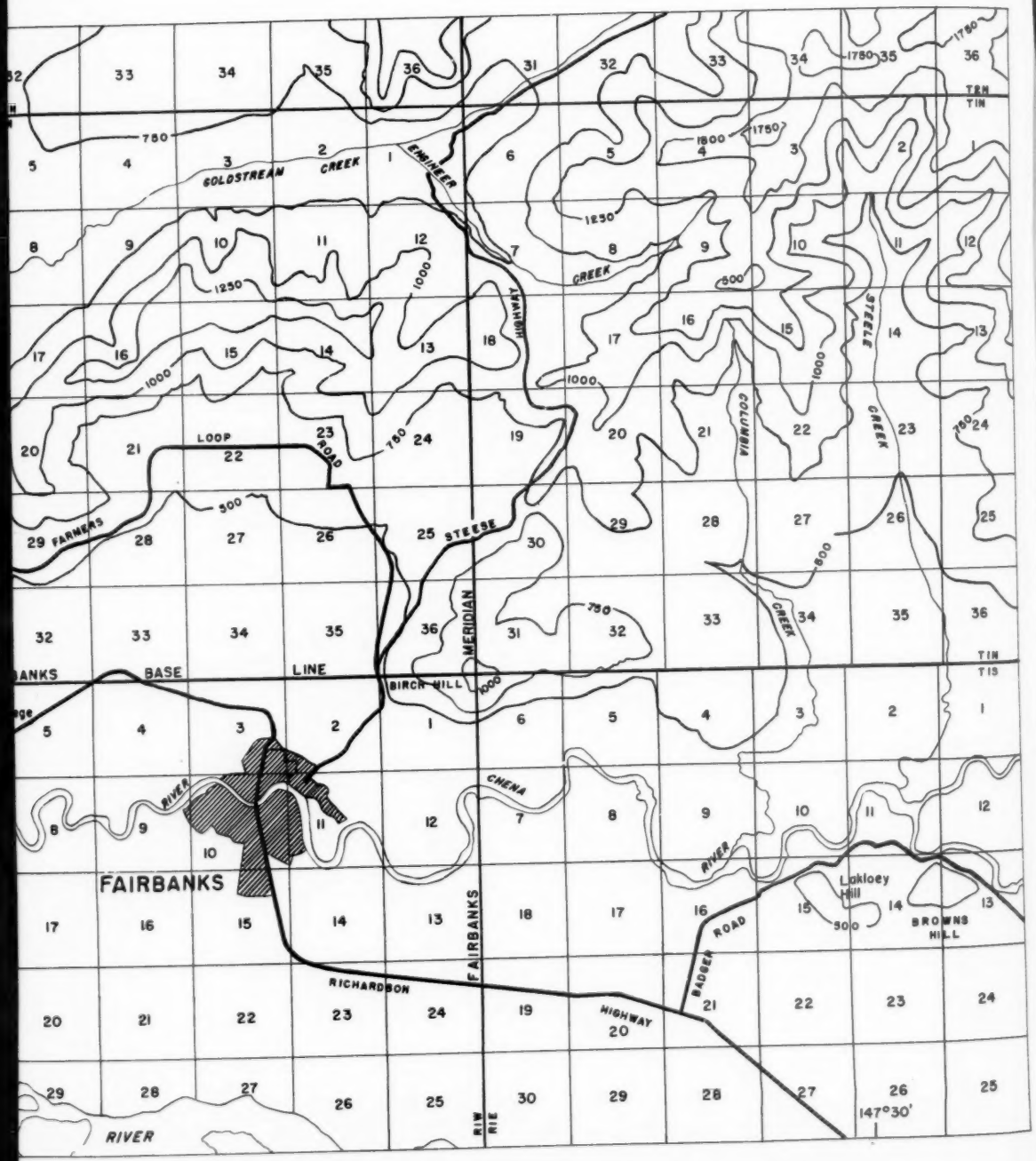

INDEX MAP OF FAIRBANKS AND VICINITY, ALASKA

BULLETIN OF THE GEOLOGICAL SOCIETY OF AMERICA
VOL. 67, PP. 699-724, 11 FIGS., 3 PLS. JUNE 1956

ORIGIN OF THE UPLAND SILT NEAR FAIRBANKS, ALASKA

BY TROY L. PÉWÉ

ABSTRACT

Silt mantles the upland slopes and ridge tops throughout the unglaciated interior of Alaska, reaching maximum thickness along the north side of the Tanana River Valley. The silt is probably loess deposited during glacial advances by south winds blowing from the glaciated Alaska Range across outwash plains in the Tanana Valley.

In the Fairbanks area, where it is best exposed, the upland silt is 1–80 feet thick on tops of low hills, 50–150 feet above the valley floor. It is 10–100 feet thick on middle slopes of higher hills and thins to a few feet on the higher slopes of ridges 800–2000 feet above the valley. Much silt has been reworked and moved by stream erosion into valley bottoms where it forms a fill 10–300 feet thick.

The upland silt is well sorted. The texture and mineral composition are uniform throughout the Yukon-Tanana upland, whether the silt overlies schist, chert, granite or basalt. The silt stands in sheer cliffs and is massive, showing little or no stratification.

During the past 50 years, fluviatile, marine, estuarine, lacustrine, residual, and eolian hypotheses have been proposed to explain the origin of the upland silt. The fluviatile marine and estuarine hypotheses never had strong support, but the lacustrine concept was popular in the early part of the century.

Most of the upland silt is considered to be wind blown, derived from glacial outwash because: (1) it occurs as a surficial mantle (2) it is lithologically independent of the underlying material, (3) stratification is indistinct or absent, (4) it is associated with sand dunes and ventifacts, (5) it contains fossils of air-breathing land animals, (6) the sorting and texture are similar to upper Mississippi Valley loess and wind-blown dust, (7) the grains are angular and relatively fresh, and (8) loess is being deposited in the region today.

CONTENTS

TEXT

	Page
Introduction	700
Acknowledgments	700
Physical setting	701
Physiography and geology	701
Climate	703
Distribution and thickness of upland silt	703
Color and texture	707
Mineral and chemical composition	709
Field relations	712
Fossils	714
Origin	714
General	714
Fluviatile hypothesis	714
Marine and estuarine hypotheses	715
Lacustrine hypothesis	715
Hypothesis of disintegration of local country rock	716
Eolian hypothesis	718
General	718
Field relations	718
Mechanical composition	721
Petrographic character	721
Summary of eolian hypothesis	722
Age and correlation	722
Conclusions	722
References cited	723

ILLUSTRATIONS

Figure		Page
1.	Index map of Alaska	701
2.	Landform map of Yukon-Tanana upland	702
3.	Climatic data for Fairbanks, Alaska	704
4.	Climatic data for Fairbanks, Alaska	705
5.	Map of immediate area of Fairbanks, Alaska	706
6.	Comparison of cumulative-frequency curves of upland silt in Yukon-Tanana upland	707
7.	Comparison of cumulative-frequency curves of upland silt in Yukon-Tanana upland	708
8.	Cumulative-frequency curves of upland silt from drill hole near the top of College Hill, Fairbanks, Alaska	708
9.	Cumulative-frequency curves of upland silt from Ester "Island" section	709
10.	Comparison of cumulative-frequency curves of upland silt from lithologically different hill tops near Fairbanks	719
11.	Comparison of cumulative-frequency curves of upland silt from Fairbanks, Alaska	721

Plate — Facing page

1. Index map of Fairbanks and vicinity, Alaska 699
2. Volcanic ash bed and upland silt 712
3. Linear ridges of upland silt 713

TABLES

Table — Page

1. Spot check of minerals, Yukon-Tanana upland, Alaska 710
2. Heavy-mineral analysis of upland silt from College Hill near Fairbanks, Alaska 710
3. Chemical analyses of silts from central Alaska 712

Introduction

Silt is the most widespread unconsolidated sediment in the interior of Alaska. A blanket a few inches thick covers most of central Alaska and is thickest near major rivers draining glaciated mountains. The greatest thickness is on the north side of the Tanana River Valley, best displayed at Fairbanks (Fig. 1) where thicknesses of more than 100 feet have been recorded. The upland silt is the parent material for most agricultural soil in the interior, and in many areas the silt serves as foundations for buildings and highways.

The upland silt of central Alaska has been studied since 1898 when Spurr (1898, p. 200–221) applied the name Yukon silts to the deposits in valleys of the Yukon and its tributaries. During the past 50 years workers in central Alaska have been concerned with its origin. Hypotheses suggested are fluviatile, marine, estuarine, lacustrine, residual, eolian, and combinations of two or more of these (Prindle, 1905, p. 25; 1909, p. 27; 1913, p. 50; Eakin, 1916, p. 55–61; 1918, p. 35–36; Mertie, 1917, p. 254; 1937a, p. 186–189; 1937b, p. 165–170; Harrington, 1918, p. 39; Bennett and Rice, 1919, p. 178–182; Wilkerson, 1932, p. 18–19; Dorsh, 1934, p. 4; Eardley, 1938, p. 317–336; Tuck, 1940, p. 1295–1310; Capps, 1940, p. 164–165; Taber, 1943, p. 1471–1479; 1953; p. 321–336; Péwé, 1950). Evidence is brought forth in the present paper to demonstrate that the upland silt is loess.

Although most early workers examined the silt only incidentally to their bedrock mapping, they did remark on its abundance. Eardley (1938) devoted considerable attention to the upland tan silt observed during a reconnaissance on the Tanana and Yukon rivers from Fairbanks to Holy Cross; Tuck (1940) examined the deposits at Fairbanks during placer gold operations. The most detailed study in the Fairbanks area was by Taber (1943) who examined sediments and frozen ground in central Alaska during the summer of 1935.

The present study is an outgrowth of the author's work in Alaska with the U. S. Geological Survey during the summers of 1946, 1947, 1948, and 1949. In order to understand fully the origin, distribution, and characteristics of the upland silt the writer studied the deposits in many places in the lower Yukon River Valley, Tanana River Valley, and Yukon-Tanana upland (Fig. 1). Most detailed studies, however, were concentrated in the Fairbanks area. Several hundred samples were collected, 112 mechanical analyses were made, and many samples were examined petrographically. Loess deposits were examined in midwestern and far-western States for comparison with the Alaskan silt.

Acknowledgments

Field work in connection with the program of the Alaska Terrain and Permafrost Section of the U. S. Geological Survey was supported in part by the Engineer Intelligence Division, Office of the Chief of Engineers, United States Army.

Mr. Roy Earling, formerly a vice-president of the United States Smelting, Refining, and Mining Co., generously made available records of subsurface materials and conditions. Mr. J. B. Metcalfe of the same Company discussed problems of the upland silt with the writer both in the field and in the office.

A. D. Howard of Stanford University, and several of the writer's associates on the U. S. Geological Survey, especially D. M. Hopkins, reviewed the manuscript and offered helpful suggestions pertaining to organization and content of the paper.

E. S. King, Jr., A. M. Gooding, D. R. Loftus, George Herman, and E. W. Marshall assisted in the field work. Mary Jean Péwé prepared

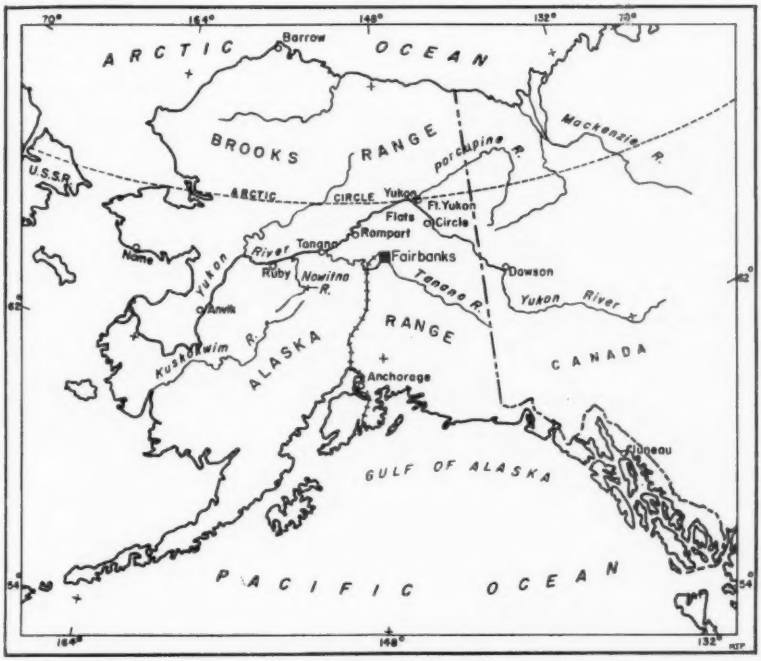

FIGURE 1.—INDEX MAP OF ALASKA

many of the illustrations, including compilation of Figures 3 and 4.

The writer is indebted to O. W. Geist, of the University of Alaska and American Museum of Natural History, for identification of vertebrate fossils and for his constant co-operation both in the field and in the office. J. D. Crawford, a vice-president of the United States Smelting, Refining, and Mining Co., and Ernest Wolff, research associate at the University of Alaska, kindly reviewed the manuscript.

Mechanical analyses of the 1947 silt samples (nos. 78–142) were made by the Permafrost Division of the St. Paul Office of the Corps of Engineers, United States Army, Fairbanks, Alaska. The Rock Island Office of the Corps of Engineers, United States Army, Rock Island, Illinois, analyzed the 1946, 1948, and 1949 silt samples.

Permanent grain mounts of 45 samples were made by Serah Johnson of the Geological Survey.

PHYSICAL SETTING

Physiography and Geology

Fairbanks, about 100 miles south of the Arctic Circle, is on the north side of the broad Tanana River Valley at the base of hills constituting part of the Yukon-Tanana upland, an east-west trending upland between the Yukon and Tanana rivers (Fig. 2). The upland is a maturely dissected area of accordant rounded ridges 2000–3000 feet in altitude. Scattered discontinuous groups of higher mountains project above the upland ridges to altitudes of of 5000–6000 feet. The upland is part of a large area of rolling country in central Alaska between the Brooks and Alaska ranges (Fig. 1).

The rounded ridges of the upland near Fairbanks have summits 1250–1800 feet above sea level. Local relief ranges from 50 to 700 feet. The bedrock is chiefly schist but includes local masses of basalt, quartz diorite, and granite.

South of the Yukon-Tanana upland lies the wide Tanana lowland, a sediment-filled trough between the upland on the north and the

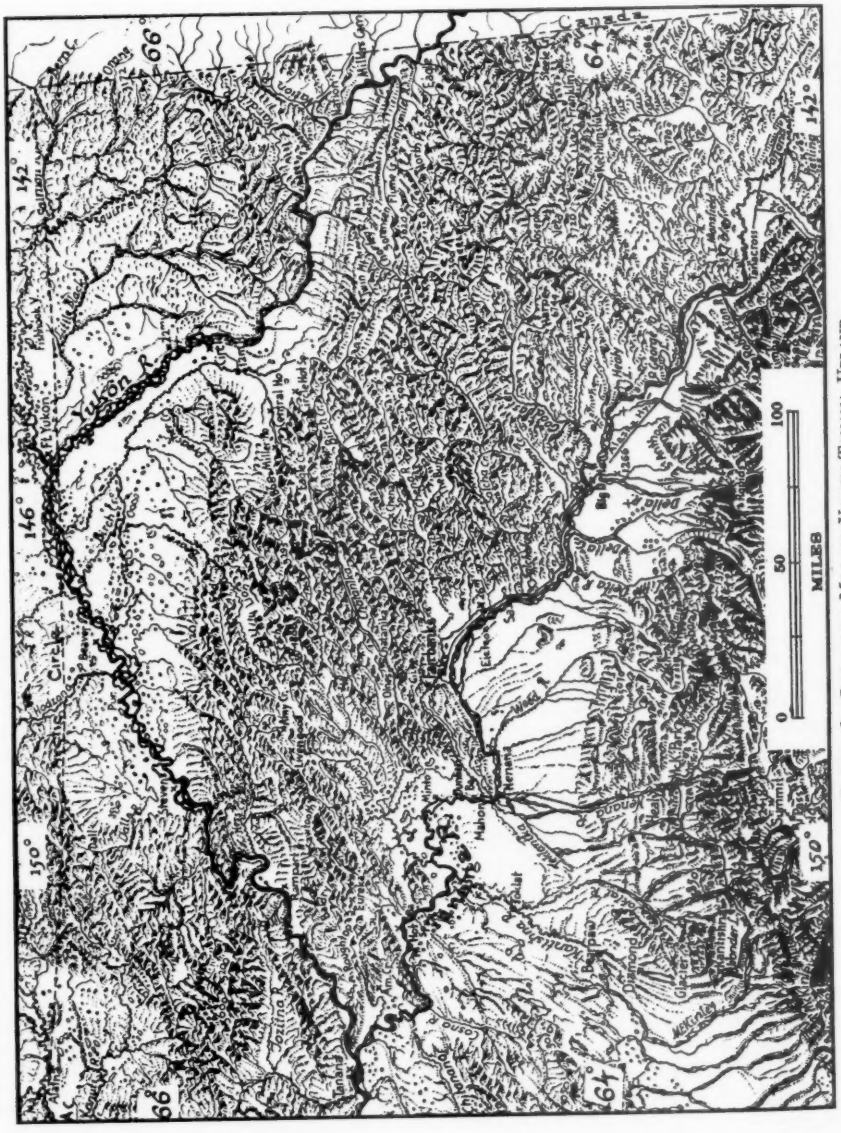

FIGURE 2.—LANDFORM MAP OF YUKON-TANANA UPLAND

Modified slightly from Erwin Raisz's Landform Map of Alaska, prepared for the Quartermaster Corps, U. S. Army, 1948. Reproduced courtesy of Dr. Erwin Raisz, Cambridge, Mass.

towering Alaska Range on the south. Huge alluvial fans extend northward from altitudes of about 1000 feet at the foot of the mountains to altitudes of about 450 feet at Fairbanks (Fig. 2).

The Tanana River flows along the north edge of the lowland and cuts the most on the north bank from its mouth to a point about 100 miles upstream from Fairbanks. This is the result of the result of the dumping of a great deal of material into the Tanana Valley from the Alaska Range on the south, although it may be in part ascribed to the effect of the earth's rotation (Farrell's law) (Eakin, 1910).

Central Alaska has not been glaciated, except in small local mountain masses, but glaciers from the Brooks Range on the north, the Alaska Range on the south, and the Yukon Plateau (Bostock, 1948, map 922A) on the east almost surrounded the interior of Alaska during times of glacial maxima. Glaciers from the Alaska Range probably approached within 50 miles of the Fairbanks area (Capps, 1932, Pl. 1; Péwé, 1952a, p. 1289). During the glacial advances, the heavily loaded rivers deposited several hundred feet of sand and gravel in the Tanana and Yukon valleys. Aggradation of the trunk valleys raised base level and caused tributaries from the unglaciated Yukon-Tanana upland to aggrade their lower valleys. More than 300 feet of sediment was deposited in creek valleys of the upland in the vicinity of Fairbanks.

The writer believes the upland silt was deposited, for the most part, during periods of glacial expansion by winds blowing from the outwash plains in the trunk valleys. The silt on the ridges and hill slopes interfingers with layers of black muck, generally perennially frozen, in the valley bottoms (Péwé, 1954, p. 342). The muck represents upland silt that has been retransported from the hill slopes by rill wash, creep. and stream action (Péwé, 1948, p. 10), incorporating much organic debris, including many vertebrate remains.

In a few places two stratigraphic units can be recognized in the silt, separated by a layer of muck. Where the muck is lacking, however, it has not been possible to subdivide the upland silt; consequently, the upland silt is treated as a single unit in this discussion.

FIGURE 2.—LANDFORM MAP OF YUKON-TANANA UPLAND
Modified slightly from Erwin Raisz's Landform Map of Alaska, prepared for the Quartermaster Corps, U. S. Army, 1948. Reproduced courtesy of Dr. Erwin Raisz, Cambridge, Mass.

Climate

The Fairbanks area has a continental climate, characterized by an extreme range between summer and winter temperatures (Fig. 3). The absolute minimum recorded temperature is −66°F.; the absolute maximum is 99°F. The mean annual number of days with freezing temperatures is 233, and freezing temperatures have been reported every month except July (U. S. Weather Bureau, 1943).

The mean annual precipitation is 11.7 inches (Fig. 4). Thunderstorms occur during the summer, but most precipitation falls in light showers. Sixty-three per cent of the annual precipitation falls from May through September.

The wind regimen in central Alaska is, in general, composed of a long, relatively calm winter period from September to May and a short, slightly windy summer period from June to August. A 10-year record at Fairbanks (U. S. Weather Bureau, 1943) indicates that the prevailing surface-wind direction for winter is north to northeast, and the summer direction is south to southwest. The average wind velocity in winter is about 3.5–4 mph, and in summer it is about 6 mph. The annual mean wind velocity at Fairbanks is 4.9 mph. High winds occur but are uncommon; about one gale is recorded yearly. The percentage of calms for the winter period is 6.3, and for the summer period 3.3.

A local exception to the general wind pattern of central Alaska exists at Big Delta (Fig. 2), 70 miles southeast of Fairbanks, where strong south to southeast winds (30–100 mph) occur both winter and summer.

Distribution and Thickness of Upland Silt

Silt is widespread in central Alaska and thickest near major rivers draining glaciated areas. It is especially thick along the north side of the Tanana River Valley where it flanks the middle and upper parts of the hills, and blankets the tops of many ridges and hills, especially those less than 1000 feet above sea level. Along the middle Yukon and Tanana rivers, it caps most bluffs less than 800 feet above the river.

In general, it is thickest in the valley bottoms and on lower slopes, thinning out on the higher

slopes (Fig. 5), attaining thicknesses of almost 100 feet on the middle slopes and as much as 300 feet in valley bottoms where it has accumulated chiefly as muck.

more than 10 feet on top of Lakloey Hill (Pl. 1) about 150 feet above the flood plain, at an altitude of approximately 600 feet. The silt may be thicker on these two hilltops, for bed-

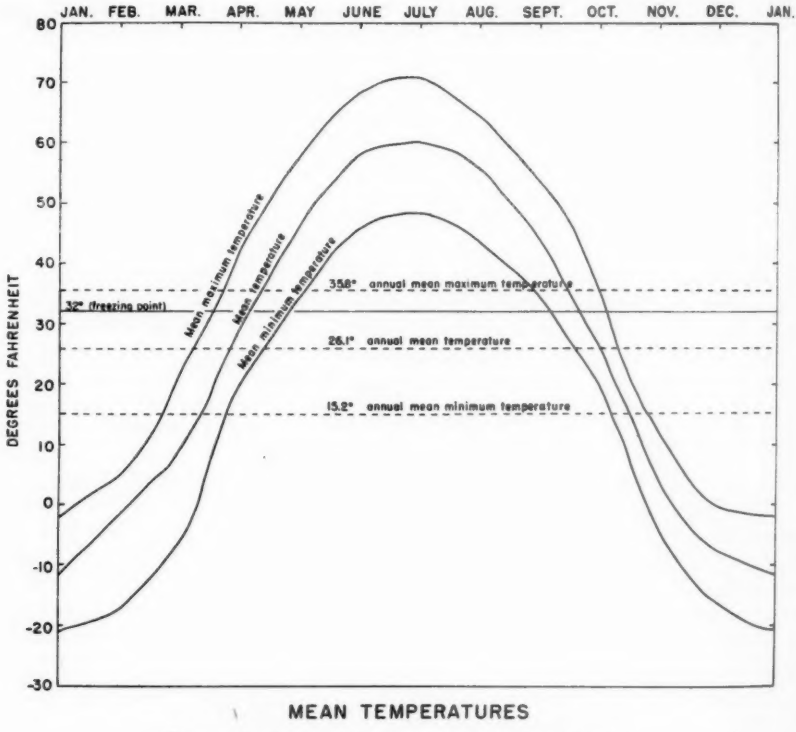

FIGURE 3.—CLIMATIC DATA FOR FAIRBANKS, ALASKA

Drilling has revealed an 180-foot accumulation of silt at the lower end of a spur of Ester Dome between Ester and Cripple creeks (Pl. 1, sec. 8, T. 1 S., R. 2 W.). This thickness includes no muck. Inasmuch as this deposit lies in a broad bedrock valley, part of the material may have been retransported from higher elevations on Ester Dome.

Hilltops are probably the only places where the original thickness has not been supplemented by slope wash and where the total original thickness can be approximated, modified only by that amount removed by erosion. Hand-augering revealed more than 4 feet on top of Browns Hill (Pl. 1) about 200 feet above the flood plain, at an altitude of 650 feet, and

rock was not encountered at either locality. A well drilled in 1947 near the top of College Hill (Fig. 5) (sec. 6, T. 1 S., R. 1 W.) penetrated 80 feet of dry tan upland silt before reaching shattered bedrock at approximately 470 feet above sea level—only 20 feet above the level of the present flood plain of the Chena River. On top of Gold Hill at an altitude of approximately 700 feet or about 250 feet above the flood plain, prospect drilling in sec. 3, T. 1 S., R. 2 W., revealed 150 feet of dry upland silt overlying auriferous gravels.

The upper limit of the upland silt has long been a problem. Eakin (1916, p. 67–70) and J. B. Dorsh (1934, p. 4, Unpub. thesis, Univ. Alaska) suggest that the silt does not occu

above 1200 feet. In the Fairbanks area, however, tan silt is found above this altitude, and no sharply defined upper limit has been observed. A few inches of upland silt was found on the commonly than at high altitudes away from the rivers, and it is more common on flat uplands at high altitudes than on summits of sharp, steep ridges at the same level.

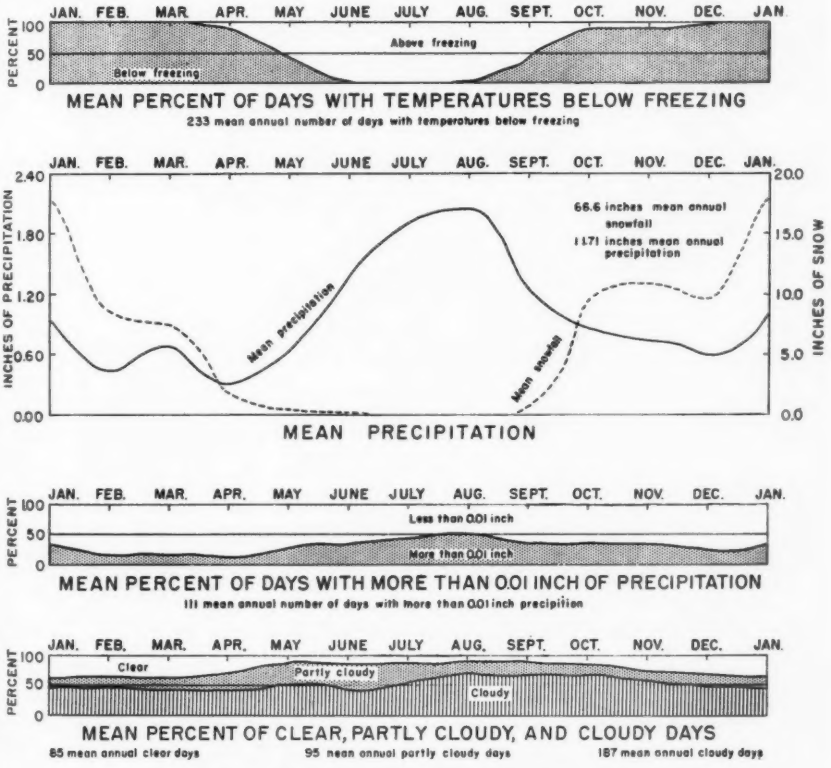

FIGURE 4.—CLIMATIC DATA FOR FAIRBANKS, ALASKA

top of the west end of Birch Hill at an elevation of about 1050 feet above sea level. The wide crest of Chena Ridge (Pl. 1), extending northeast through most of T. 1 S., R. 2 W., at an altitude of approximately 1200 feet locally bears a cover of more than 4 feet. Only an inch or two overlies bedrock at an elevation of 1600 feet on a spur of Ester Dome between upper Happy and upper Sheep creeks (Pl. 1), but, on the top of the 200–300-foot wide ridge at the head of Steele Creek (Pl. 1), 3½ feet of tan silt overlies weathered granite at altitudes of 1500–1800 feet. These observations suggest that there is no sharp upper termination of the upland silt. It occurs at high altitudes near rivers more

Detailed measurements of loess thickness over a large area, similar to those made in Illinois by G. D. Smith (1942), and in Iowa by Davidson and Handy (1952), have not yet been made in the Yukon-Tanana upland. Generally speaking, however, the upland silt and the related muck accumulations are thickest near the Tanana River in the Fairbanks area (Fig. 5) and thin to the north. Near the Tanana River low hills are capped by more than 100 feet, and higher ridges have 3–10 feet. Lower slopes are mantled by as much as 100 feet of silt, and valley bottoms have accumulations of muck up to 300 feet thick. To the north and northeast, away from the river, much less

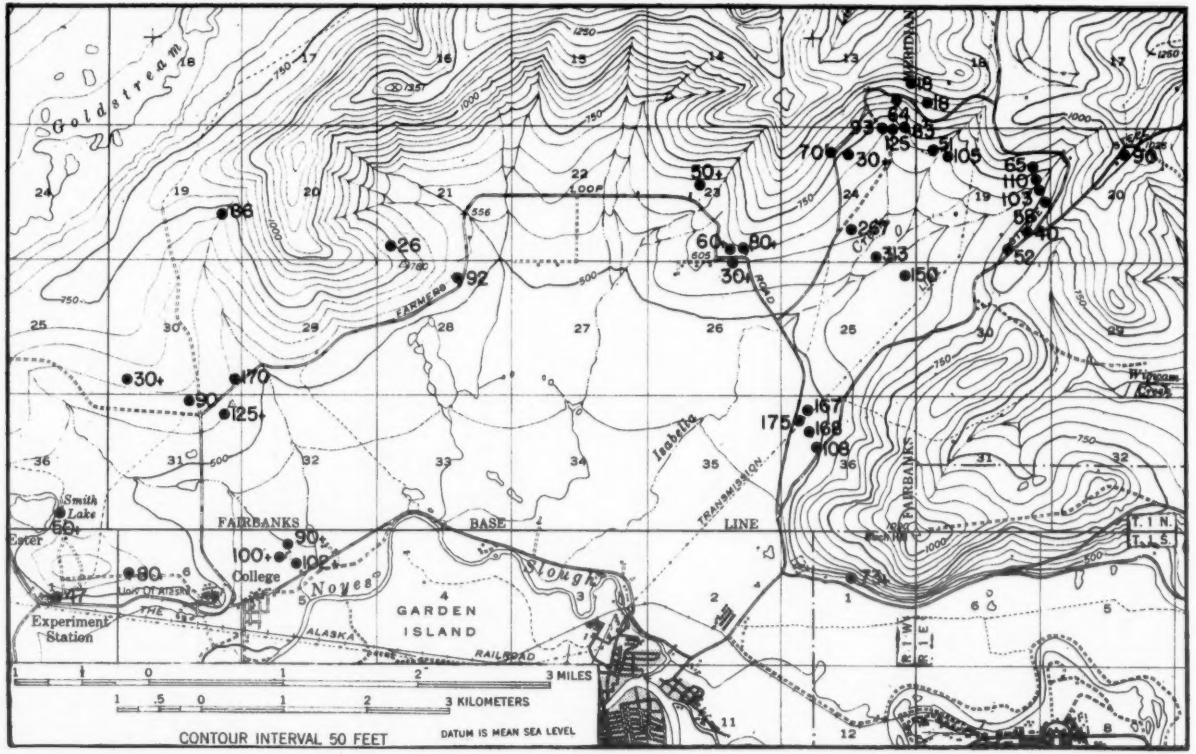

FIGURE 5.—MAP OF IMMEDIATE AREA OF FAIRBANKS, ALASKA

Showing thickness of silt

●30 = thickness of silt in feet over bedrock or gravel

●80+ = minimum thickness of silt in feet; base of silt not reached

land silt blankets the low ridge tops. No tails are available for thicknesses of silt on gher crests and slopes, but placer gold-mining erations reveal that thicknesses of muck,

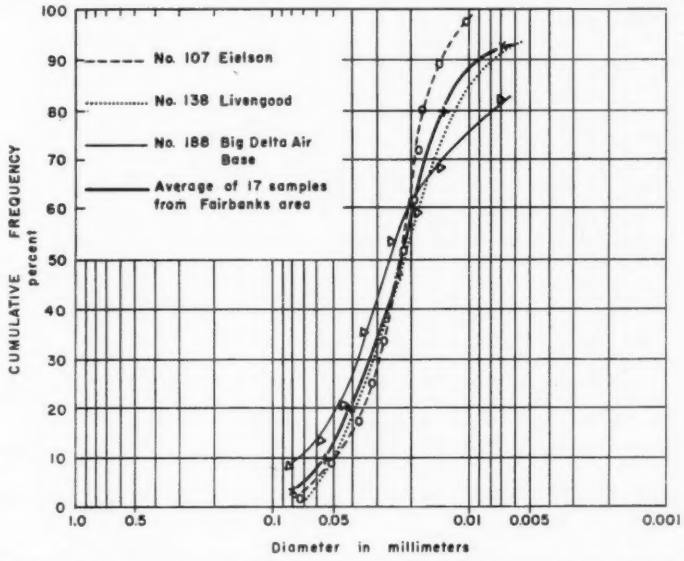

FIGURE 6.—COMPARISON OF CUMULATIVE-FREQUENCY CURVES OF UPLAND SILT IN YUKON-TANANA UPLAND

Showing average cumulative-frequency curve of 17 samples of upland silt from Fairbanks area, Alaska

ich are dependent upon silt abundance, pe, rainfall, and length of period of accumu- ion, are only 5–50 feet in the creek bottoms r Chatanika, Circle Hot Springs, and Chena rings (Fig. 2). North of Fairbanks these posits are thinner. This probably reflects a nner original upland silt layer because the es here are as steep, the rainfall is the same less, and the muck is the same age as near rbanks.

COLOR AND TEXTURE

ommonly the unfrozen upland silt is tan, lough grayish tan is not rare; when wet or en it is brown. In many localities thin, ix, carbonaceous layers and iron-stained nds are present.

The silt is well sorted. A composite plot of 17 mechanical analyses collected near Fairbanks reveals that the sediment is composed of 13 per cent very fine sand, 81 per cent silt, and 6 per cent clay (Figs. 6, 7).[1] As the clay content is low, the material has little plasticity.

The mechanical composition varies little with areal extent or depth. Comparison of cumulative-frequency curves of samples collected from various places in the Yukon-Tanana upland (Fig. 2) reveals that the texture of the tan silt is remarkably uniform (Figs. 6, 7). Vertical uniformity is demonstrated by mechanical analyses of samples taken at 10-foot intervals in an 80-foot churn-drill hole near the top of College Hill. The cumulative-frequency curves are almost identical and show that the sediment retains its uniform texture almost to bedrock (Fig. 8).

Upland silt on hillslopes includes small percentages of coarse material, consisting of resistant, spherical, marcasite concretions, 1–3 inches in diameter, many soft, tubular, iron concretions ½–1 inch long and ⅛–¼ inch in diameter, and angular schist fragments ½–1½ inches in diameter. The schist fragments are

[1] In this report the U. S. Department of Agriculture's classification is used: clay, .005–.0002 mm; silt, .05–.005 mm; very fine sand, .10–.05 mm.

Showing thickness of silt
●30 = thickness of silt in feet over bedrock or gravel
●80+ = minimum thickness of silt in feet; base of silt not reached

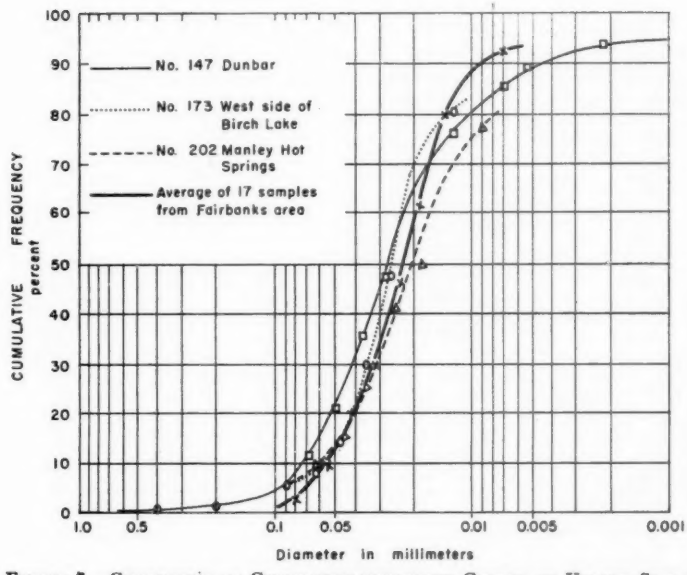

FIGURE 7.—COMPARISON OF CUMULATIVE-FREQUENCY CURVES OF UPLAND SILT IN YUKON-TANANA UPLAND

Showing average cumulative-frequency curve of 17 samples of upland silt from Fairbanks area, Alaska

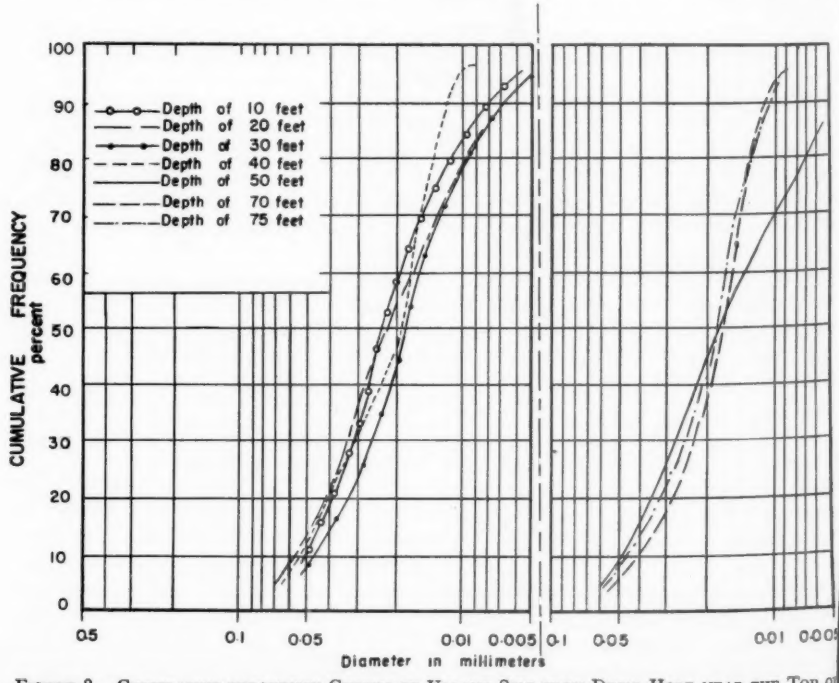

FIGURE 8.—CUMULATIVE-FREQUENCY CURVES OF UPLAND SILT FROM DRILL HOLE NEAR THE TOP OF COLLEGE HILL, FAIRBANKS, ALASKA

oncentrated near bedrock. They are not wind-aceted and probably have been incorporated nto the silt from the underlying shattered bed-ock by frost action. In some places these silt thickness may have been increased by retransportation of hillside silt. The east face of the cut exposes an almost vertical section of 180 feet, the Ester "Island" section (Pl. 1).

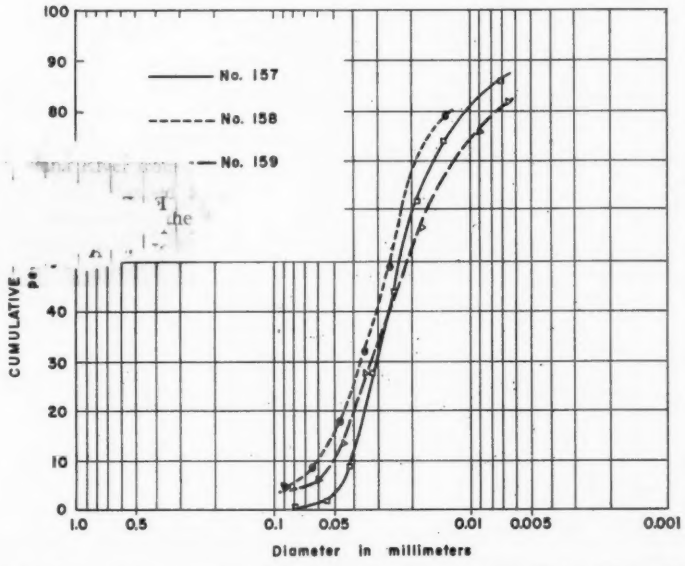

FIGURE 9.—CUMULATIVE-FREQUENCY CURVES OF UPLAND SILT FROM ESTER "ISLAND" SECTION
Between Ester and Cripple creeks, near Fairbanks, Alaska

fragments probably originated upslope, where shattered bedrock is exposed and is subject to downslope movement.

On the extreme east side of sec. 22, T. 1 N., R. 1 E., at an altitude of 750 feet, a section of upland silt was exposed in a well dug 32.3 feet to bedrock. A layer 1–2 inches thick of angular schist pieces an inch in diameter occurred 2 feet above bedrock, and many schist fragments half an inch in diameter were scattered through the silt 6 or 7 inches above bedrock. Coarse rock fragments are lacking higher in the well.

On the south side of Gold Hill placer gold mining exposed a 202-foot section of upland silt. It has little coarse material except for angular schist fragments 1–2 inches in diameter in a layer near the base 4–6 inches thick.

One of the largest and best exposures in the Fairbanks area occurs in a placer gold mining cut between Ester and Cripple creeks in sec. 8, T. 1 S., R. 2 W. The cut transects a silt spur which covers a broad bedrock valley, and the

The section is composed entirely of uniform-textured silt in spite of slight color variations. Cumulative-frequency curves of mechanical analyses of samples nos. 157, 158, and 159 from this section are strikingly similar (Fig. 9) and also similar to those of silt from the upland (Figs. 6, 7). Three horizontal light-gray layers are faintly visible in this exposure. The layers occur at 93, 142, and 150 feet respectively from the top of the section and are respectively 3.5, 1, and 15 feet thick. The uppermost layer forms a ledge in the cliff. Mineralogical and size-grade analyses (nos. 157, 158) reveal no differences between the gray silt and tan upland silt.

MINERAL AND CHEMICAL COMPOSITION

Several representative samples of the upland silt were prepared in permanent mounts for mineralogic analysis. Other samples were separated in acetylene tetrabromide, and permanent mounts were prepared for both the heavy and the fine fractions.

TABLE 1.—SPOT CHECK OF MINERALS PRESENT IN SILT SAMPLES FROM THE WESTERN PART OF THE YUKON-TANANA UPLAND, ALASKA

By Marie L. Lindberg, U. S. Geological Survey.

Number	Location	Anatase	Calcite	Chlorite	Chloritoid	Clinozoisite	Epidote	Feldspar*	Garnet	Glaucophane	Hornblende	Hypersthene	Muscovite	Opaque	Quartz	Rutile	Sphene	Tourmaline	Tremolite	Zircon
102	Birch Hill, Fairbanks	..	F	F	F	F	..	A	F	..	F	..	F	F	A	..	..	F	..	F
113	Browns Hill, Fairbanks	..	..	F	F	..	F	A	F	..	F	..	F	F	A	..	..	F	..	F
115	Lakloey Hill, Fairbanks	..	..	F	..	F	F	N	F	..	F	F	N	F	A	F	F			
138	Livengood Creek	..	F	F	..	..	F	A	F	..	F	F								
173	West side Birch Lake†	..	..	F	F	F	F	N	F	..	F	..								
201	Eva Creek, Fairbanks	..	..	F	F	..	..	N	F	..	F	F								
202	Manley Hot Springs	F	..	F	F	F	F	A	F	F	F	..	F	F	A	F	F	..	..	
215	Head of Steele Creek	..	..	F	F	F	F	N	F	..	F	F	N	F	A	F	F	F	..	F

A, abundant; *N*, numerous; *F*, few.

* Very altered grains of low index assumed to be altered feldspar.

† Péwé reports glass shards of volcanic ash in this sample. For mechanical analyses of samples *see* Figures 6, 7, 10. Because of fineness of silts, list of minerals present not considered exhaustive.

TABLE 2.—HEAVY-MINERAL ANALYSIS OF UPLAND SILT FROM COLLEGE HILL NEAR FAIRBANKS, ALASKA*

Mineral	Numerical Frequency in percentages
Opaque minerals†	37.0
Zoisite	10.3
Hornblende	10.1
Garnet**	9.6
Epidote	7.2
Unknown fragments	6.0
Clinozoisite	3.8
Augite	3.1
Sphene	3.1
Tourmaline	2.8
Hypersthene	2.6
Zircon	1.9
Apatite	1.4
Rutile	.7
Enstatite	.2
Tremolite	.2

* Separation made with acetylene tetrabromide; permanent mount made in canada balsam; 415 grains counted.

† Approximately 70 per cent magnetite and ilmenite.

** All isotropic grains listed as garnet.

Petrographic examination reveals that the grains are angular and fresh though slightly iron-stained. The mineralogy of the silt is uniform (Table 1). Typical samples contain abundant quartz, considerable muscovite, and feldspar, and less calcite, chlorite, chloritoid, clinozoisite, epidote, garnet, hornblende, opaque minerals, rutile, tourmaline, and zircon (Tables 1, 2).

The minerals in the silt are present in the schist of the Alaska Range and the Yukon-Tanana upland. This similarity in mineral composition was cited by Taber (1943, p. 1481) as evidence that the silt originated by weathering of the schist in place. However, there are several areas within 100 miles of Fairbanks where upland silt of this same mineral composition overlies rocks other than schist.

Tan silt rests on granite on a hilltop 1800 feet above sea level at the head of Steele Creek (Pl. 1, sec. 35, T. 2 N., R. 1 E.). Because it covers the crest, it cannot have been derived from schist at a higher altitude. Petrographic examination shows minerals foreign to the underlying bedrock. The granite consists principally of microcline, orthoclase, and quartz with smaller amounts of biotite, muscovite, and

plagioclase, and minor amounts of zircon, sphene, and allanite. There is little hornblende in the granite (Prindle and Katz, 1913, p. 70). No amphiboles were seen in the thin section examined by the writer. The silt contains, in addition to abundant quartz, feldspar, and muscovite, considerable hornblende, as well as chlorite, chloritoid, clinozoisite, epidote, garnet, hypersthene, rutile, sphene, tourmaline, and zircon (Table 1, sample 215).

On the west side of Birch Lake,[2] 50 miles up the Tanana River from Fairbanks, a hill of granite has been mapped by Mertie (1937a, Pl. 1). As exposed along the Richardson Highway, the slopes of this hill are covered with tan silt in sharp contact with porphyritic biotite granite. The granite is mostly quartz, orthoclase, and biotite, with minor oligoclase, apatite, chlorite, hornblende, and zircon. In addition to much quartz, feldspar, and muscovite, the overlying silt contains volcanic glass, chlorite, chloritoid, clinozoisite, epidote, garnet, hornblende, rutile, tourmaline, and zircon (Table 1, sample 102). Many of these minerals did not come from the underlying granite.

Upland silt at an elevation of about 1200 feet above sea level near the divide between Livengood and Hess creeks, 6 miles east of the village of Livengood (Fig. 2), contains calcite, chlorite, epidote, feldspar, garnet, hornblende, hypersthene, muscovite, quartz, tremolite, and zircon (Table 1, sample 138). The bedrock in this and surrounding hills is chert with small interbedded lenses of silicified limestone (Mertie, 1917, Pl. 13). Most of the minerals in the silt could not have been derived from the local bedrock.

Thick deposits of tan silt overlie biotite granite adjacent to the Tanana River at Manley Hot Springs, about 90 miles west of Fairbanks (Fig. 2). The rock consists essentially of quartz, potash feldspar (orthoclase and microcline), oligoclase, and biotite, with accessory iron minerals, zircon, muscovite, and tourmaline (Waters, 1934, p. 229). Petrographic examination of a sample of the upland silt from a road cut about 300 feet south of the Bath House reveals quartz and feldspar with lesser amounts of anatase, chlorite, chloritoid, clinozoisite, epidote, garnet, glaucophane, hornblende, muscovite, rutile, sphene, and zircon (Table 1, sample 202). The granite lacks many of these minerals.

Browns Hill and Lakloey Hill are isolated, silt-covered, bedrock knobs that rise above the flood plain of the Chena-Tanana River system near Fairbanks (Pl. 1). Both hills are composed of basalt. Overlying the basalt on the south side of these hills is unstratified tan silt, which contains the following minerals: chlorite, chloritoid, clinozoisite, epidote, feldspar, garnet, hornblende, hypersthene, muscovite, quartz, rutile, sphene, tourmaline, tremolite, and zircon (Table 1, samples 113 and 115). This silt could not have been derived from the underlying basalt.

These hills also consist in part of quartz-mica schist. The top of Browns Hill is only a few feet higher than the basalt outcrop, but the lack of exposures makes it impossible to determine whether the summits are underlain by schist or basalt. It is unlikely that silt derived from schist farther upslope washed down over the basalt, but, until excavations are made, any examples of lithologic independence must be considered inconclusive.

Chemical analyses show that the silt is locally calcareous but otherwise nearly constant in chemical composition over large areas (Table 3). No mineralogic analyses are available for the underlying quartz-mica schist bedrock, but Taber (1943, p. 1479–1481) shows that the chemical composition of the silt is similar to glacial flour derived from quartz-mica schist bedrock beneath the Castner Glacier (Table 3) which drains to the Delta River; thus the average composition of the silt is similar to the average composition of the schist.

In a few areas, however, these differ sharply in chemical composition. In an attempt to develop methods of geochemical prospecting in the Fairbanks area, specimens of weathered bedrock, upland silt free of rock fragments, and the vegetative mat were collected from auger holes in a mineralized area on the divide between Flume and Fox creeks, 12 miles northeast of Fairbanks (Matzko and Wedow, in preparation). The mineralized bedrock is overlain by

[2] Seven miles southeast of Salchaket Lake.

3–5 feet of upland silt. Chemical analyses of the weathered bedrock and silt containing bedrock fragments show 1000–8000 ppm of zinc and lead. The overlying upland silt, for the most part, contains only 30–50 ppm of zinc and lead. Fulton (1950, p. 654–670) shows that the upper 2 feet of residual soil over mineralized rock at Austinville, Virginia, where loess and glacial sediments are lacking, contains 800–1600 ppm of zinc. The lack of significant quantities of zinc and lead in the upland silt over the mineralized bedrock in the Flume-Fox Creek divide (3 miles north of mapped area, Pl. 1) suggests that the silt is transported.

TABLE 3.—CHEMICAL ANALYSES OF SILTS FROM CENTRAL ALASKA

Sample	In Per Cent			
	A	*B*	*C*	*D*
SiO_2	67.70	66.88	66.09	68.52
Al_2O_3	14.98	20.23	14.24	12.19
Fe_2O_3	5.97*	6.27*	4.15	3.05
FeO	—	—	1.71	2.27
TiO	0.70	0.58	0.91	0.86
CaO	3.30	2.58	2.32	2.60
MgO	1.18	2.11	1.94	2.14
Ma_2O	2.13	0.68	1.93	2.01†
K_2O	2.57	0.86	1.98	1.88†
MnO	Not det.	Not det.	0.08	0.08
P_2O_5	Not det.	Not det.	0.23	0.35
Loss on ignit.	3.71	5.40	Not det.	3.88
	102.24	105.59	95.58	99.83
H_2O	Not det.	Not det.	3.15	2.58
H_2O—	Not det.	Not det.	0.82	0.70
CO_2	Not det.	Not det.	0.02	0.06
Total C	Not det.	Not det.	Not det.	0.38

Analyses of samples *A* and *B* (Taber, 1943, Table 3, p. 1480), by students of University of South Carolina (Sample *A* is glacial rock flour from Castner Glacier on the Delta River, 50 miles south of Big Delta. Sample *B* near Steese Highway, 7 miles from Fairbanks).

Analysis of sample *C* by R. H. Stokes (Sample no. 158, Ester "Island", 10 miles west of Fairbanks).

Analysis of sample *D* by Israel and Charlotte Warshaw. Sample taken in frozen condition. Sample dried at 110°C and allowed to come to equilibrium with the moisture in the air before the complete analysis was made. (Sample no. 201, Eva Creek, 10 miles west of Fairbanks).

* Total iron is given as Fe_2O_3.

† Determined by S. M. Berthold with flame photometer.

FIELD RELATIONS

The upland silt overlies auriferous bench gravel and several bedrock types with a sharp contact. On lower slopes it is overlain by muck with a relatively sharp contact. In a placer

PLATE 2.—VOLCANIC ASH BED AND UPLAND SILT

FIGURE 1.—ESTER ASH BED IN UPLAND SILT

Exposed near base of Ester "Island" section between Ester and Cripple Creeks, near Fairbanks, Alaska (T.L.P., August 8, 1948)

FIGURE 2.—VERTICAL WALLS OF UPLAND SILT IN ROAD CUT ON SOUTHEAST END OF BIRCH HILL, FAIRBANKS, ALASKA

(T.L.P., Sept. 12, 1949)

FIGURE 1

FIGURE 2

VOLCANIC ASH BED AND UPLAND SILT

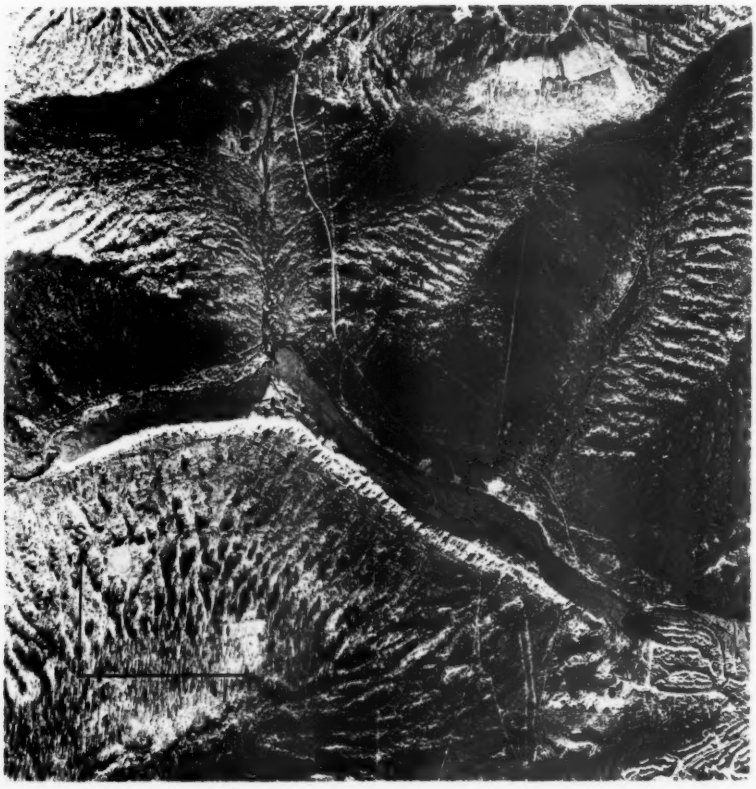

FIGURE 1

FIGURE 2

LINEAR RIDGES OF UPLAND SILT

mining cut on the south side of Gold Hill a muck layer 5 feet thick divides the loess into two deposits. Both bottom and top muck contacts are sharp. In this exposure the lower loess is 150 feet thick, and the upper loess is 15 feet thick.

The upland silt is massive, showing little or no stratification or jointing. Stratification is generally absent or indistinct in the uplands and upper slopes; however, near valley bottoms where some of it has been retransported, crude stratification is apparent. The faint stratification consists of iron-oxide-stained horizons, organic films, and vague color bandings of short lateral extent, and of volcanic-ash layers 10–100 feet long. In the Ester "Island" section the gray layers discussed previously create a weak gross stratification. In no instance does the faintly developed stratification resemble fluviatile or lacustrine bedding.

Several ash layers are interbedded with the upland silt. The gritty 6-inch-thick gray to white, pure glass (index 1.53) volcanic-ash layer (Pl. 2, fig. 1) near the base of the Ester "Island" section is distinctive and is here named the Ester ash bed from the adjacent Ester creek. It has sharp contacts with the silt both above and below. The same layer is exposed near the base of the 202-foot silt section of older loess on the south side of Gold Hill. An ash layer 3 inches thick, exposed in a road cut (Pl. 2, fig. 2) on Birch Hill in the NW¼ sec. 4, T. 1 S., R. 1 E., can be traced laterally for 100 feet and occurs 5 feet lower on the south side than on the north side. Deposition probably was on a sloping surface similar to the present one. These ash layers have sharp contacts with the silt both above and below and indicate old subaerial surfaces.

Detailed inspection of vertical faces of upland silt reveals minor folds and faults in the sediment. These structures are recognized where stratification is indicated by organic, iron-stained, or ash layers or where silt is frozen or wet and the differences in moisture content of certain horizons outline faint stratification. Minor folds, faults, and bedding are common in the upland silt but generally cannot be recognized because of uniform texture, composition, and color.

A conspicuous feature of the upland silt is its ability to stand in sheer cliffs. This is probably due to the angularity of the grains, and perhaps to strengthening by concretionary rods and tubes. As in the loess of the Mississippi Valley, vertical walls cut in the upland silt of the Fairbanks area stand for many years. Nearly vertical road-cut walls 20 feet high on Birch Hill had stood at least 5 years in 1949 (Pl. 2, fig. 2). The 180-foot cliff of silt at Ester "Island" is almost vertical except for minor slumping near the base; it has been standing since 1935. The well-sorted material is an excellent home for cliff swallows, which perforate the high silt cliffs with nest holes.

Jointing is common although no regional pattern was observed. In many places, iron staining has taken place along joints. The best jointing was observed near Engineer Creek where frozen upland silt was exposed in a high-level placer mining cut. Here a joint system, composed of two planes dipping 45°–60° from the surface, one to the north and one to the south, creates a mosaic of diamond-shaped blocks on the vertical wall. Clear ice has segregated in the joints.

Sharp, steep-walled gullies form in the upland silt today under favorable conditions. They are not common on undisturbed surfaces and are confined, for the most part, to areas of concentration of runoff such as below culverts, below breaks in placer mining water ditches, or where vegetation has been disturbed on steep slopes, as in cultivated fields.

PLATE 3.—LINEAR RIDGES OF UPLAND SILT

FIGURE 1.—VERTICAL AERIAL PHOTOGRAPH

Showing linear ridges carved from upland silt on upper slopes of hills near Fairbanks, Alaska. Boot-shaped excavation in valley bottom in center of photograph is placer gold mining cut on Engineer Creek. Black bar in lower left-hand corner of photograph represents 2,500 feet (Photograph by U. S. Air Force, Nov. 16, 1948).

FIGURE 2.—ROAD CUTS THROUGH LINEAR RIDGES OF UPLAND SILT

On south side of Birch Hill Fairbanks, Alaska (T.L.P., Aug. 28, 1947)

Old, slightly subdued parallel gullies are characteristic of most upper slopes underlain by loess (Pl. 3, fig. 1). The gullies are 30–50 feet deep and 300–600 feet long; the interfluves and gully bottoms are rounded and subdued (Pl. 3, fig. 2). In some instances the ridges of silt are separated into isolated, elongate, and round knobs of silt toward their lower ends (Pl. 3, fig. 1). Hills in the NW¼ sec. 28, T. 1 N., R. 1 W., both north and south of Farmers Loop road, are considered of such origin. Such mounds are not common in the Fairbanks area but are plentiful in the Dunbar area (Fig. 2) 30 miles to the west (Péwé, 1949, p. 3). The silt that eroded from the gullies was carried to creek valley bottoms where it now forms alluvial fans (Pl. 3, fig. 1).

The silt-blanketed hills in the Fairbanks area are not undergoing active gullying today except where human activity weakens the vegetative cover or concentrates runoff. The rounded gullies and ridges are relics of an ancient period of gully formation. If the rainfall were heavier or concentrated in summer storms or the silt less protected by vegetation, or the spring runoff more active, the material would be seriously gullied, and soon much of it would be removed from the hills. The rounded gullies must be relics of a past period when precipitation was greater or more intense, or the vegetation was thinner.

Fossils

Although vertebrate remains are abundant near Fairbanks, most specimens probably have come from retransported silt (muck) in creek bottoms and not from dry upland silt high on hillsides because: (1) most remains have been concentrated in valley bottoms by slope wash and mass movement of the mantle, and (2) exposures produced by placer mining in the creek valley bottoms are many times larger and more abundant than small exposures along isolated road cuts and active gullies on hillsides. Nevertheless, a few bones have been found in the unfrozen upland silt. A metatarsal and humerus of a fossil horse were found by Mr. Funk in 1948, on bedrock under 32.2 feet of upland silt at the bottom of a pit in the NE¼ sec. 22, T. 1 N., R. 1 E. The specimens are well preserved but not silicified. The top of the pit is 750 feet above sea level.

A well-preserved bison bone was found in tan silt in a road cut on the east side of Chena Ridge in the SE¼ sec. 11, T. 1 S., R. 2 W. An almost complete skeleton of a mammoth was found on the gravel at the base of the silt cliff at the Ester "Island" section at the time of excavation (Peter Maas, employee, United States Smelting, Refining, and Mining Co., oral communication, 1949). The bones were heavily iron-stained. Neither the silt nor the gravel was perennially frozen. The silt layer in which the mammoth was found contains marcasite concretions.

The writer knows of no land snails from the dry upland silt on the north side of the Tanana Valley. However, on the south side of the Tanana Valley lowland, he collected three species of land snails—*Succinea avara* Say, *Discus chronkhitei* (Newcomb), and *Euconulus fulvus alaskensis* Pilsbry[3] from Recent loess on a late Wisconsin end moraine along the east bank of the Delta River 30 miles south of the Tanana River (Fig. 2). These species are found in the loess of Kansas (Leonard, 1952, p. 8).

Origin

General

Hypotheses advanced to explain the origin of the tan silt include fluviatile, marine, estuarine, lacustrine, residual, and eolian, or combinations of these. The fluviatile, marine, and estuarine hypotheses have had little support, but the lacustrine concept was popular in the early part of the century. The eolian hypothesis was proposed relatively recently by Tuck (1940, p. 1304). The most recent and probably the most thorough analysis of the problem in the Fairbanks area was made by Stephen Taber (1943; 1953), who advanced the hypothesis that the silts were formed mainly by disintegration of local country rock.

Fluviatile Hypothesis

Although fluviatile silt is abundant on the flood plain of the Tanana and Chena rivers in

[3] Identified by T. C. Yen, U. S. National Museum, 1953.

the Fairbanks area and widespread on flood plains and terraces in the interior of Alaska in general, the tan silt of the upland is not considered fluviatile. Fluviatile silt is well stratified and cross-bedded, and individual beds are lens-like and fairly well sorted; but composite samples collected over large areas or through large vertical thicknesses are poorly sorted. The tan silt, however, is unstratified and uniform in texture. In addition it is difficult, in terms of the fluviatile hypothesis, to explain the existence within the upland silt of the undisturbed ash layers with sharp contacts above and below, the presence of as much as 80 feet of silt on hilltops 150 feet above river level, and a nearly continuous blanket over an irregular topography with 700 feet of relief. Remains of a fresh-water fauna should be found in the untransported material if it were fluviatile. No such fossils have been reported.

Marine and Estuarine Hypotheses

Harrington (1918, p. 39) attributed the high-level silt on the lower Yukon River, downstream from Anvik (Fig. 1), to inundation by an advancing sea. A marine origin may be plausible for this silt, which is close to the sea and confined to altitudes below 600 feet. However, Eardley (1938, p. 336) tentatively considers the high-level silt of the lower Yukon to be eolian.

A variation of the marine hypothesis is the estuarine hypothesis, which assumes inundation of interior Alaska by marine or brackish water, creating huge estuaries in the Yukon, Koyukuk, and Tanana river valleys. Submergence similar to that described in the marine hypothesis would be necessary, and such features as clay, mud cracks, ripple marks, and brackish-water fossils should be found. As under the marine hypothesis, the high-level silt in the Fairbanks area and vicinity cannot be accounted for in this way. This hypothesis may apply, however, to some low-level silt and sand of the lower Yukon and Koyukuk valleys.

To ascribe the upland silt to marine or estuarine origin would necessitate a rise in sea level or a subsidence of the land of about 1800 feet to inundate the interior of Alaska, because deposits are found at least up to this altitude. Deltas, shorelines, and beaches should be present if the water level were constant for a considerable time. The silt should be stratified and contain considerable clay, mud cracks, or ripple marks, and marine fossils, but none of these is present. The marine invasion required by this hypothesis is inconsistent with the Pleistocene history of interior Alaska. Thus it is highly improbable that the high-level silt in the interior of Alaska is marine.

Lacustrine Hypothesis

The lacustrine hypothesis was probably first advanced by Spurr in 1898 (p. 200–230), who considered some of his Yukon silts lacustrine. Prindle (1913, p. 50) extended the hypothesis to the upland silt of central Alaska. The lacustrine hypothesis received its strongest support from Eakin (1916, p. 73; 1918, p. 45) in the Yukon-Koyukuk areas. A. E. Glover (oral communication, 1947), former Territorial assayer at Fairbanks, and J. B. Dorsh (1934, unpub. thesis, Univ. Alaska, p. 4) advance the lacustrine hypothesis today.

The lacustrine hypothesis is considered unlikely because:

(1) A lake would require a barrier to impound the water. The vast inland lakes to which proponents of this idea refer are two lakes suggested by Eakin (1916, p. 73). He assumed the middle Yukon (upstream from Rampart) and its tributaries formerly flowed northeast up the valley of the Porcupine River to the Arctic Ocean. This drainage was supposed to have been blocked by glaciers in the area now occupied by the upper reaches of the Porcupine, and a huge lake formed in the Yukon Flats area (Fig. 2). This lake later was drained to the southwest by cutting through a bedrock constriction near Rampart. Another lake was created when the Tanana-Nowitna drainage, which was supposed to have flowed south into the Kuskokwim River basins, was blocked by glacier tongues extending northwest from the Alaska Range. Later this lake was drained by cutting through a bedrock ridge at Ruby (Fig. 1). The elevation of the surface of the lakes was thought to be about 1200 feet above sea level.

According to Brooks (1916, p. 8) and Capps (1932, Pl. 1) Wisconsin glaciers from the Alaska Range did not extend northward far enough to form the postulated dam across the Nowitna-Kuskokwim divide. The proposed ice

dam between the middle Porcupine and Mackenzie River drainages is not definitely established, and Brooks, in his dissenting introduction to Eakin's 1916 paper (p. 9), raises the question whether this scanty evidence of glaciation is sufficient "to justify the hypothesis of an ice barrier that ponded the waters over an area of 50,000 to 100,000 square miles." He questions the possibility that the stretch of the Yukon River between the Tanana River and the Yukon Flats was a watershed between the waters flowing southwest to the Kuskokwim and those flowing northeast to the Mackenzie. Brooks states (1916, p. 9) that the "character of the Yukon represents incised meanders, inherited from a previous drainage cycle, an explanation that seems to be in accord with the known facts." Wahrhaftig (1950) also assumes that the drainage was inherited from an earlier cycle.

The barrier that was supposed to impound the water to form the lake in the Tanana Valley is absent. Not only is the barrier for the Yukon Flats lake based on scanty evidence, but both past and present workers question Eakin's interpretation of the Rampart section of the Yukon River.

(2) Shore lines, wave-cut benches, and deltas should be present if the lake level remained constant for long. These features are lacking in the tan silt in the Fairbanks area.

(3) If the lacustrine origin were valid a definite upper limit would exist. Various workers assume that such a limit is found at an altitude of 1200 feet, but upland silt is found on ridges and hilltops at altitudes as high as 1750 or 1800 feet so that the upper limit is decidedly not clear cut.

(4) Lacustrine silt should be stratified and might even contain varves. The only stratification in the upland silt is due to isolated carbonaceous layers and iron-stained horizons and in many places is absent. No stratification like that commonly associated with lacustrine deposits is present.

At one location, running water transported hillside silt in suspension and deposited it in an artificial lake created by hydraulic mining. Later, when the lake was drained and the deposits partially removed, a 4-foot section of lacustrine silt was exposed. This lacustrine silt was finely laminated and in no way resembled the poorly stratified upland deposits.

(5) An appreciable amount of clay would be expected in the deposits of a large lake, particularly where sedimentation is from a schist terrain (Tuck, 1940, p. 1306). The average of 17 mechanical analyses (Fig. 6) of tan silt reveals that only about 5–10 per cent of the sediments is clay, and this does not occur in lenses or layers but is finely disseminated throughout.

(6) Lacustrine silts need bear no lithologic relation to the underlying deposits. This is true in many places in the Tanana and lower Yukon river valleys where the silt overlies schist, basalt, granite, gravel, slate, or sandstone. This would be true under the hypothesis of eolian origin, and also of the residual hypothesis if creep over variable bedrock had taken place.

(7) Some forms of life should have existed in the lake. To the writer's knowledge no lacustrine fossils have been found in the high-level dry upland silt. Fresh-water gastropods, pelecypods, and diatoms occur in the reworked material of the valley bottoms but not in the parent silt.

(8) Land fossils should be absent or scarce in lacustrine deposits unless (a) the lake were shallow, (b) carcasses floated out into the lake, or (c) carcasses were buried under an expanding lake. Considering the upland silt alone, land fossils are scarce. The fossils are fragmentary, and some show evidence of transportation.

(9) Mud cracks and ripple marks would be expected in lacustrine silts but are unknown.

Comparing the features to be expected for lacustrine origin with the observed facts, a striking discordance is noticeable. On the nine points considered all but two are unsupported in the field, and these two are of little value because the eolian hypothesis could account for the contrast of silt lithology and underlying bedrock, and the presence of land fossils. Therefore the lacustrine hypothesis alone cannot explain the origin of the tan upland silt near Fairbanks and in the middle Yukon and Tanana river valleys.

Hypothesis of Disintegration of Local Country Rock

A. S. Wilkerson in 1932 suggested that the silt was a product of slope wash after long con-

tinued disintegration. During the summer of 1935 Taber examined silt in the Fairbanks area and other parts of Alaska and in 1943 (p. 1473) presented "the hypothesis that the creek-valley silts have been formed chiefly by disintegration of local country rock, the products of weathering having been moved down the valley slopes by soil creep and slope wash and distributed over the valley floors by occasional floods." In 1953 he restated this belief. He does not limit this hypothesis to silt in creek bottoms, as he believes (1943, p. 1475) that silt at an elevation of 950 feet, 7 miles from Fairbanks on the Steese Highway (Sec. 18, T. 1 N., R. 1 E.) (Pl. 1), "is similar in origin to the other creek-valley silts of the district."

If the silts were formed by disintegration of local country rock, the following features would be expected:

(1) The minerals would be the same as in the underlying rock and would be present in about the same proportions allowing for differential resistance to weathering. In the Fairbanks area approximately 99 per cent of the bedrock is schist, and the mineral assemblage of the schist includes almost every mineral noted in the silt. Generally speaking, the minerals in the silt are similar to those in the schist in type and proportion.

Locally, however, typical upland silt overlies bedrock of granite, basalt, or chert, and contains minerals lacking in the bedrock. This may occur on hilltops where the silt could not have slumped from schist bedrock at higher altitudes. It is evident, therefore, that the silt in these localities did not come from the underlying or near-by bedrock.

(2) Sediment produced by rock disintegration would undoubtedly contain some large particles, especially of the more resistant minerals, but such resistant particles are scarce. However, in some localities, angular pieces of nonresistant mica schist up to 2 inches in diameter occur at the base of the silt, and perhaps such fragments were brought downslope by mass movement of the mantle. The proponents of the hypothesis state that as the residual material is transported downslope it is filtered through mosses to allow the fine sizes to pass, retaining the coarse sizes. Although this is possible, it is unlikely that this process is responsible for the sorting of such a tremendous amount of silt, with no great accumulation of coarse material anywhere. Certainly this activity seems unlikely on the relatively flat top of a hill where no creep takes place.

(3) If silt accumulated on the top of a hill through disintegration of underlying bedrock, the material should be finer and more weathered at the surface than it is closer to bedrock. This is not supported by examination of samples from the 80-foot-deep drill hole near the top of College Hill. Mechanical analyses of samples taken at depths of 10, 20, 30, 40, 50, 70, and 75 feet reveal (Fig. 8) the same size grade and sorting of the silt down to bedrock. Examination from top to bottom of a 10-foot section on the crest of Lakloey Hill reveals no change in size grade.

(4) Mechanical disintegration is probably the dominant process of bedrock weathering in sub-Arctic climates and depends largely on the action of alternate freezing and thawing. It is pertinent to inquire to what depth silt can accumulate by disintegration of bedrock in place before the silt blanket becomes thick enough to inhibit disintegration. On hillsides the silt may be removed as fast as it forms, but it would accumulate on flat hilltops and ridges. The depth of seasonal freeze and thaw of the ground in the Fairbanks area ranges from 4 to 8 feet, with deepest penetration in gravel and least penetration in silt. Under present climatic conditions, seasonal freeze and thaw of bedrock probably does not occur under a protective mantle of silt thicker than 4–6 feet. In past colder periods, seasonal penetration of frost probably was only slightly deeper in the nonperennially frozen ground. It is also true that, in the past, this well-drained silt may have been perennially frozen, but if no frequent alternation of freeze and thaw occurred, little disintegration would take place.

(5) Residual silt on a hilltop should contain no volcanic ash or carbonaceous layers or soil horizons if the material were formed by a progressive downward disintegration of the underlying bedrock. Sections of tan silt do reveal, however, undisturbed ash and carbonaceous layers.

In summary, although much silt has probably moved downslope by creep and slopewash, the

major portion of it did not originate through disintegration of the underlying bedrock. A comparison of the field observations with the relationships to be expected if the silt originated by disintegration reveals serious conflicts. None of the five points considered can be explained by the disintegration hypothesis. However, quite possibly disintegration of the schist has produced some silt in this area. Zeuner (1949, p. 24) has described some soils formed by frost-riving that have size-grade distribution and sorting of particles similar to loess.

Eolian Hypothesis

General.—Bennett and Rice (1919, p. 131–148), investigating the soils for agriculture possibilities, were impressed by the silt in the Fairbanks area and termed it the Fairbanks silt loam, a loessial soil. It resembles some of the loam soils derived from loess in the Mississippi Valley. Although they did not discuss the origin of the silt, this appears to be one of the first suggestions that it may be eolian. In succeeding years, Mertie (1937a; 1937b) and Capps (1940) referred to the silt as possibly eolian but no critical analyses of the sediments were made. In 1938 Eardley presented the result of his examination of silt along the middle and lower Yukon River from Tanana to Holy Cross and tentatively considered an eolian origin for the "tan loams" capping the bluffs. He also examined the tan silt in the Fairbanks area and classified it with his tan loam. In 1940, Tuck presented a clear discussion of the muck and silt in the Fairbanks area and concluded the silt was eolian. Crawford and Boswell (1948, p. 574) also think it is eolian.

After a study of the tan silt in various places in the interior of Alaska, including the glaciated area near Big Delta, the writer concluded that most of the upland silt originated by eolian activity and therefore is loess.

The expectable consequence of the eolian hypothesis falls into three groups: (1) field relations, (2) mechanical composition, and (3) petrographic character (H.T.U. Smith and Fraser, 1935).

(1) *Field relations.*—Important evidence in support of the eolian hypothesis is found in the field characteristics of the silt and in the relation of the material to the geologic and geographic surroundings.

TOPOGRAPHIC DISTRIBUTION: As clearly stated by Barbour (1930, p. 468), in reference to the loess of China, the mantle of loess "conforms closely to the general contouring of the buried pre-loess topography, filling up the gullies, covering minor depressions, lying deepest in the depressions and thinning-out up the flanking slopes of the higher ridges." The distribution of the tan silt in the Fairbanks area, as discussed earlier, is such that the deposit is thicker in the valley bottoms and thins upslope. On low hills a cover 4–80 feet is present and, at more than 1000 feet above sea level 700 feet above the flood plain, it is thin or absent except on flat ridges or in valley heads where it is found up to elevation of 1750–1800 feet, 1450–1500 feet above the flood plain. No definite upper limit exists; instead the silt thins irregularly upward.

INDEPENDENT LITHOLOGIC CHARACTER OF THE DEPOSIT: Wind-deposited material may differ mineralogically and texturally from the underlying material. This has long been a problem to those examining the silt in the Fairbanks area because the underlying schist easily decomposes to a clayey silt, which when transported by creep is somewhat similar to loess (Taber, 1943). Also the mineral content of this clayey silt derived by disintegration is similar to that of the loess because similar schists are widespread in the Alaska Range where loess would have originated as glacial flour. However, in the loess-blanketed regions just outside the Fairbanks area, the silt indiscriminately covers glacial till, granite, basalt, schist, and slate without change in its own mineralogical and chemical characteristics. This is borne out by petrographic study of samples from the following locations (Table 1): (1) Ridge at head of Steele Creek—silt over granite (2) Birch Lake—silt over granite (3) Livengood—silt over chert (4) Manley Hot Springs—silt over biotite granite and (5) Browns and Lakloey Hills—silt over basalt.

Near the Richardson Highway, about 12 miles south of the village of Big Delta (Fig. 2), tan silt overlies glacial moraine and coarse outwash gravel. Mechanical analysis of the silt reveals a sorting and size grade similar to the tan silt throughout the valley (Fig. 7). The fine

texture contrasts strongly with that of the underlying bouldery moraine and coarse outwash gravel.

Mechanical analyses of the silt from localities cited above reveal that the size grade and sorting are the same as those of the typical tan upland silt (Fig. 10).

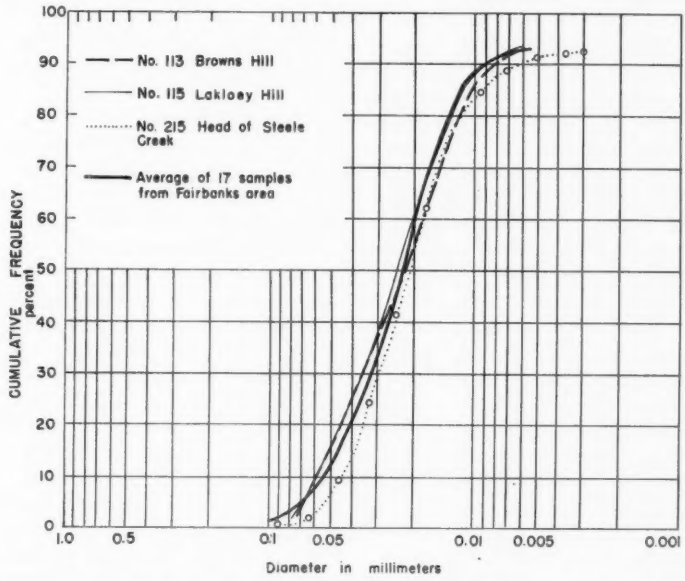

FIGURE 10.—COMPARISON OF CUMULATIVE-FREQUENCY CURVES OF UPLAND SILT FROM LITHOLOGICALLY DIFFERENT HILLTOPS NEAR FAIRBANKS

With average cumulative-frequency curve of 17 samples of upland silt from Fairbanks area, Alaska

DECREASE IN THICKNESS AWAY FROM SOURCE OF SUPPLY: The greatest thickness of upland silt on hilltops and muck in valley bottoms is near the Tanana River; to the north, away from the river, the upland silt on hilltops and the valley-bottom reworked silt becomes thinner.

ABSENCE OF DEFINITE STRATIFICATION: Absence of definite stratification is characteristic of loess and is a conspicuous feature of the upland silt. The only suggestion of stratification is that given by thin carbonaceous horizons, iron-stained horizons, or horizontal ash layers.

COLOR AND TEXTURE: Wind-deposited silt is generally light-colored unless stained by solutions or carbonaceous inclusions; the texture is usually uniform, and the clay component makes up less than 10 per cent of the sediment. These properties are also possessed by the upland silt of the Fairbanks area.

ASSOCIATION WITH OTHER EVIDENCE OF WIND ACTION: Smith and Fraser (1935, p 19) state that sand dunes and ventifacts may be expected near the source of material. Well-developed, vegetation-covered sand dunes occur along the north and northwest front of the Alaska Range from the Canadian border west into the Kuskokwim drainage. In the upper Tanana Valley the writer has observed from the air and seen on the ground an area of well-developed, vegetation-covered sand dunes extending southeast from the junction of Tok and Tanana rivers (Fig. 2) to the Alaska-Canada border.

Examination of the glaciated Big Delta area reveals sand dunes on the outwash plains and abundant ventifacts on the moraines. Ventifacts also occur on the north side of the Tanana River along the Richardson Highway about 20 miles west of the village of Big Delta, near the mouth of Shaw Creek (Fig. 2).

In the lower Tanana Valley the writer has

observed from the air poor- to well-preserved, forested sand dunes in the Minto Flats area and south of the Tanana River about 50 miles west of Nenana. Black (1951, Fig. 8) illustrates an extensive area of vegetation-covered dunes near McGrath in the upper Kuskokwim River Valley northwest of the Alaska Range.

Wind-blown silt is being deposited today in the upland north of the Tanana River (Péwé, 1951). At 1 p.m. on August 20, 1949, when a 14-mile-per-hour wind from the southeast was recorded at the Big Delta Air Force Base, a cloud of flood-plain silt was raised by the wind about 50–100 feet above the ground. An hour later the wind had increased in velocity to 30 miles per hour, and great clouds of grayish dust were transported by the wind from the flood plain. The writer noted from an airplane that the silt was carried to a relatively even level of 5000 feet above sea level, or 4000 feet above the ground, and was suspended over an area of about 300 square miles. The dust was so thick over this area that one could hardly see the ground from an altitude of 6000 feet

For the most part, the clouds of dust covered the area south of the Tanana River and west from the Delta River to Delta Creek; however, a few square miles north of the Tanana was blanketed, and some material was deposited on the upland where silt is at least 50 feet thick.

These observations support the hypothesis that the upland silt was carried by the wind from flood plains of glacial streams and deposited on adjacent flats and uplands. The velocity of 30 miles per hour compares favorably with the velocities of dust-bearing winds cited by Bryan (1927, p. 39–40) and Warn (1953, p. 70–71). Both the velocity of dust-bearing winds and maximum height to which dust was carried above the ground fit in well with Warn's (1952, p. 241) classification of blowing dust. These observations refute the statement of Taber (1943, p. 1500) that "little silt is carried to elevations of 1000 feet above the river, and the winds die out after travelling a short distance down the valley". He also states that winds could not have transported large quantities of silt across a major divide nearly 2000 feet above the river.

Contrary to Taber's statement (1953, p. 327–328), wind-blown dust is common in the Fairbanks area today, although it is not nearly so widespread as during major glacial advances. According to Dr. Ivar Skarland (written communication, June 27, 1950), chairman of the Anthropology department at the University of Alaska, "This spring, for nearly three weeks, there were clouds of dust in the air from Chena Bluffs to Big Delta". (Chena Bluffs are termed Chena Ridge in this report and are 6 miles west of Fairbanks.)

Skarland described wind-blown silt on the floor of an abandoned cabin at the mouth of Chena River, 6 miles southwest of Fairbanks (Pl. 1). He stated that the cabin was abandoned 4 or 5 years ago, and the only openings were two small windows and a door which faced the river. Although the cabin, which has now been washed away by the Tanana River's undercutting of the bank, was not above extremely high flood level, he believes the silt was not water laid. The sediment was not deposited evenly over the floor but was heaped up more than 4 inches thick on the side farthest from the openings, and only a trace of silt was present near the door. He wrote "I didn't actually measure the thickness of the material, but it must have averaged well over 2 inches if it had been spread out evenly over the whole floor."

Also, silt-covered papers and magazines on the floor had not been destroyed by water.

Skarland also stated that "... the main source [of the silt] seems to have been a series of bars across the Tanana, about one mile or more away."

FOSSILS OF AIR-BREATHING ANIMALS: Fossils of air-breathing animals could logically be expected in the silt if the material is eolian. Although most vertebrate fossils occur in muck, some have been found in upland silt. These fossils are by no means conclusive unless the silt-buried fossils occur on a hilltop. Otherwise the silt could have come downslope from disintegrating schist above and covered the bones.

No land snails have been found in the dry tan upland silt near Fairbanks; however, they have been found in upland silt 30 miles south of Big Delta. According to Russell (1944, p. 34), loess without land gastropods is to be regarded with suspicion. A factor to be considered, however, is the distribution of such gastropods. Gastropods probably do not occur uniformly in all

areas that receive wind-blown silt. Some loess of the upper Mississippi Valley contains no snails. Dr. T. C. Yen, paleontologist at the United States National Museum, Washington, D. C., reports that much loess of China and the Rhine Valley contains no terrestrial gastropods (oral communication, June 27, 1950).

(2) *Mechanical composition.*—If the material were loess the grain size and degree of sorting would be similar to that of wind-blown dust or volcanic ash which has been transpo ted a considerable distance (Udden, 1898, p. 31–60; Warn and Cox, 1951, p. 559), or silt known to be loess. Cumulative-frequency curves of mechanical analyses of wind-blown dust from Kansas (Swineford and Frye, 1945, p. 252) and Germany (Zeuner, 1949, p. 27) are similar to the average cumulative-frequency curve of the upland silt from the Fairbanks area (Fig. 11). Also the upland silt curve is similar to the curve of loess collected by the writer from the Mississippi Valley. The cumulative-frequency curve of a sample from the Ester ash bed also is strikingly similar to that of the upland silt (Fig. 11).

The great similarity of grain size and degree of sorting between the upland silt and the deposits of known eolian origin constitute a strong argument for the eolian hypothesis.

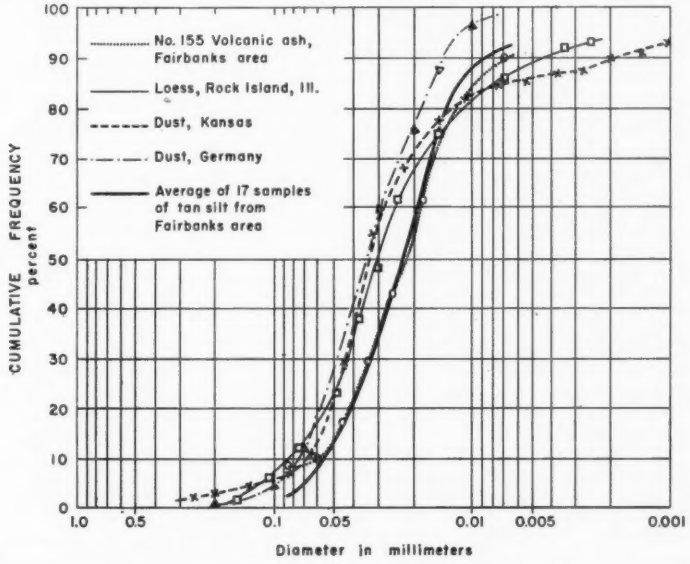

FIGURE 11.—COMPARISON OF CUMULATIVE-FREQUENCY CURVES OF UPLAND SILT FROM FAIRBANKS AREA

With cumulative-frequency curves of volcanic ash from Fairbanks area (Ester "Island" section), loess from Rock Island, Illinois, and modern wind-deposited dust from Germany (Zeuner, 1949, p. 27) and Kansas (Swineford and Frye, 1945, p. 252). Alaskan and Illinois samples collected by T. L. Péwé and analyzed by the Corps of Engineers, United States Army, Rock Island, Illinois.

(3) *Petrographic character.*—Angular grains are characteristic of loess (Twenhofel, 1932, p. 272) as well as other silts; the grains in the upland silt are relatively angular, especially the minerals of lighter specific gravity.

Smith and Fraser (1935, p. 20) point out that loess grains should be dominantly unweathered and clay minerals should be almost absent. The grains of the upland silt, except for some feldspars, are relatively fresh and unaltered although commonly iron-stained. However, degree of weathering would depend upon rate of deposition and age of the deposit.

Examination of the heavy fraction of an upland silt sample (no. 94) from near the top

of College Hill reveals a considerable content of several heavy minerals (Table 2). Taber (1943, p. 1490) argues that the upland silt cannot be loess because heavy minerals would be easily sorted out and left behind by wind or water transportation. However, loess from Iowa contains comparable percentages of heavy minerals (Kay and Graham, 1943, Figs. 20, 64, 65). It is significant in this connection that several heavy minerals present in silt over chert and basalt at Livengood and Browns Hill are lacking in the underlying bedrock.

Summary of eolian hypothesis.—Examination of the tan upland silt in the light of the eolian hypothesis reveals that the expectable consequences of this hypothesis are fully and reasonably supported by field and laboratory observations. It is, therefore, concluded that most of the high-level tan silt in the Fairbanks area and the Tanana and Middle Yukon river valley region is loess.

Age and Correlation

Glaciers have pushed northward repeatedly from the Alaska Range, and in Wisconsin time they advanced as far as the Tanana River between Big Delta and Tanacross (Fig. 2). During these glacial advances, braided silt-laden meltwater streams flowed over wide, vegetation-free flood plains and spread glacial flour over much of the 50-mile wide lowland south of Fairbanks. Strong south winds probably blew frequently off ice-clad mountains and picked up some of the silt on the flood plains and outwash plains, to redeposit it on the uplands to the north. The Yukon-Tanana upland, on the border of the glaciated area, was favorably located to receive much wind-blown silt.

Two or more periods of loess deposition are recorded in the upland silt near Fairbanks. During and after periods of loess deposition, part of the silt was frozen, thawed, eroded, and redeposited as muck in the valley bottoms (Péwé, 1952b, p. 1289–1290). These aspects of the late Quaternary period in the Fairbanks area are discussed more fully in a paper in preparation.

The oldest loess is the thickest and most extensive. Radiocarbon dating[4] of the muck layers interstratified with the loess layers indicates that the oldest loess is more than 30,000 years old (J. L. Kulp, Personal communication), and one of the younger loess deposits is younger than 4000 years (Kulp *et al.*, 1952, p. 412; Suess and Rubin, Personal communication).

The writer believes the prominent loess deposits in the Yukon-Tanana upland are correlative with prominent Wisconsin glacial advances recorded in many areas in Alaska, especially in the Alaska Range (Fernald, 1953; Wahrhaftig, 1953).

The major loess deposits perhaps are correlative with the Delta and Donnelly glaciations of the Big Delta area, 70 miles southeast of Fairbanks (Péwé *et al.*, 1953, p. 8–10).

Conclusions

Silt mantles the upland slopes and ridge tops throughout interior Alaska, reaching maximum thicknesses along the north side of the Tanana River Valley. It is best displayed at Fairbanks, where thicknesses of more than 100 feet have been recorded. The texture and mineral composition are uniform throughout the Yukon-Tanana upland, whether the silt overlies schist, chert, granite, or basalt. All the silt samples examined contain a high percentage of quartz and feldspar, and several samples contain considerable muscovite. All contain lesser amounts of chlorite, garnet, hornblende, and zircon, and most samples also contain a small amount of tourmaline, epidote, and chloritoid.

The silt is massive and has little or no stratification. Vertebrate fossils are rare, and no land snails have been found in the upland silt in the Fairbanks area.

Hypotheses advanced to explain the origin of the upland silt include fluviatile, marine, estuarine, lacustrine, residual, and eolian. The upland silt is not of fluviatile origin because (1) it is unstratified and contains no individual beds or lenses of other sediments, (2) it occurs as a nearly continuous blanket over an irregular topography with 700 feet of relief and is more

[4] Critical wood samples collected but not yet dated may modify the interpretation of the age of the loess.

than 1000 feet above the river, and (3) no freshwater fauna is present.

The marine and estuarine hypotheses are unlikely as a means of origin because of the absence of deltas, shore lines, beaches, clay, mud cracks, ripple marks, and marine or brackish-water fossils. Also, such an origin would necessitate a rise of sea level or a subsidence of the land about 1800 feet to inundate the interior of Alaska in late Pleistocene time, an inundation not borne out by any geologic evidence.

The lacustrine hypothesis for the origin of the upland silt in the interior of Alaska was strongly supported by Eakin (1916, p. 73; 1918, p. 45), but there are several reasons for believing this means of origin unlikely. No evidence supports the idea that glaciers from the Alaska and Brooks ranges blocked drainage of the Yukon and Tanana rivers to form huge lakes. No shore lines, wave-cut beaches, or deltas occur; neither are mud cracks, ripple marks, or freshwater fossils found in the upland silt. Neither stratification nor an appreciable amount of clay exists in the silt. No definite upper limit of the silt exists as expected under the lacustrine hypothesis.

The suggestion that the upland silt is a product of disintegration of local country rock was put forth by Taber in 1943 and restated in 1953. Examination of this hypothesis reveals: (1) the minerals in the silt are not everywhere similar to the underlying bedrock, (2) no large particles of more resistant minerals are present, (3) the silt does not become progressively coarse downward toward bedrock, (4) mechanical disintegration by alternate freezing and thawing could not produce 80 feet of silt on hilltops, and (5) the silt contains undisturbed volcanic ash and carbonaceous layers.

Evidence for eolian origin of the upland silt is as follows: (1) the silt occurs as a surficial mantle, (2) it is lithologically independent of the underlying material, (3) stratification is indistinct or absent, (4) it is associated with sand dunes and ventifacts, (5) it contains fossils of air-breathing land animals, (6) the sorting and texture are similar to loess and windblown dust of the Mississippi Valley area, (7) the grains are angular and relatively fresh, and (8) loess is being deposited in the region today.

Central Alaska has not been glaciated, except in small local mountain masses, but glaciers from the Brooks Range on the north, the Alaska Range on the south, and the Yukon Plateau (Bostock, 1948, map 922A) on the east almost surrounded the interior of Alaska during times of glacial maxima. Glaciers from the Alaska Range probably came within 50 miles of the Fairbanks area (Capps, 1932, Pl. 1; Péwé, 1952a). The upland silt is believed by the author to be loess and most of it was deposited during periods of glacial expansion by winds blowing across the unvegetated outwash plains and flood plains of glacial streams.

References Cited

Barbour, G. B., 1930, The loess problem of China: Geol. Mag., v. 67, p. 458–475.

Bennett, H. H., and Rice, T. D., 1919, Soil reconnaissance in Alaska, with an estimate of the agricultural possibilities: U. S. Dept. Agr. Bur. Soils Field Operations 1914, 16th Rept., p. 43–236.

Black, R. F., 1951, Eolian deposits of Alaska: Arctic, v. 4, p. 89–111.

Bostock, H. S., 1948, Physiography of the Canadian Cordillera, with special reference to the area north of the fifty-fifth parallel: Geol. Survey Canada Mem. 247, 106 p.

Brooks, A. H., 1916, Preface *in* Eakin, 1916, The Yukon-Koyukuk region, Alaska: U. S. Geol. Survey Bull. 631, p. 7–9.

Bryan, K., 1927, The "Palouse soil" problem: U. S. Geol. Survey Bull. 790-B, p. 21–45.

Capps, S. R., 1932, Glaciation in Alaska: U. S. Geol. Survey Prof. Paper 170, p. 1–8.

—— 1940, Geology of the Alaska Railroad region: U. S. Geol. Survey Bull. 907, 201 p.

Crawford, J. D., and Boswell, J. C., 1948, Dredging for gold in Alaska: Mining and Metallurgy, v. 29, p. 574–580.

Davidson, D. T., and Handy, R. L., 1952, Property variations in the Peorian loess of southwestern Iowa: Iowa Acad. Sci., v. 59, p. 248–265.

Eakin, H. M., 1910, The influence of the earth's rotation upon the lateral erosion of streams: Jour. Geology, v. 18, p. 435–447.

—— 1916, The Yukon-Koyukuk region, Alaska: U. S. Geol. Survey Bull. 631, 88 p.

—— 1918, The Cosna-Nowitna region, Alaska: U. S. Geol. Survey Bull. 667, 54 p.

Eardley, A. J., 1938, Unconsolidated sediments and topographic features of the lower Yukon Valley: Geol. Soc. American Bull., v. 49, p. 303–341.

Fernald, A. T., 1953, Multiple glaciation of the Alaska Range in the upper Kuskokwim region, Alaska: *in* Multiple glaciation in Alaska: a progress report, by T. L. Péwé *et al.*, U. S. Geol. Surv. Circ. 289, 13 p.

Fulton, R. B., 3d, 1950, Prospecting for zinc using semiquantitative chemical analyses of soils: Econ. Geology, v. 45, p. 654–670.

Harrington, G. L., 1918, The Anvik-Andreafski region, Alaska: U. S. Geol. Survey Bull. 683, 70 p.

Kay, G. F., and Graham, J. B., 1943, The Illinoian and post-Illinoian Pleistocene geology of Iowa: Iowa Geol. Survey, v. 38, p. 1–262.

Kulp, J. L., Tryon, L. E., Eckelman, W. R., and Snell, W. A., 1952, Lamont natural radiocarbon measurements II: Science, v. 116, p. 409–414.

Leonard, A. B., 1952, Illinoian and Wisconsinan molluscan faunas in Kansas: Univ. Kansas Paleont. Contrib., *Mollusca*, no. 4, 38 pages.

Matzko, J. J., and Wedow, Helmuth, Jr. (in preparation), Geochemical prospecting at an uraniferous galena deposit near Fox, Fairbanks district, east-central Alaska: U. S. Geol. Survey Bull.

Mertie, J. B., Jr., 1917, The gold placers of the Tolovana district, Alaska: U. S. Geol. Survey Bull. 662-D, p. 221–277.

—— 1937a, The Yukon-Tanana region, Alaska: U. S. Geol. Survey Bull. 872, 276 p.

—— 1937b, The Kaiyuh Hills, Alaska: U. S. Geol. Survey Bull. 868-D, p. 145–178.

Péwé, T. L., 1948, Permafrost investigations, Fairbanks area, Alaska: U. S. Geol. Survey in cooperation with Office Chief of Engineers, Permafrost Program Preliminary Rept., 16 p.

—— 1949, Preliminary report of permafrost investigations in the Dunbar area, Alaska: U. S. Geol. Survey Circ. 42, 3 p.

—— 1950, Origin of the upland silt in the Fairbanks area, Alaska (abstract): Geol. Soc. American Bull., v. 61, p. 1493.

—— 1951, An observation on wind-blown silt: Jour. Geology, v. 59, p. 399–401.

—— 1952a, Preliminary report of multiple glaciation in the Big Delta area, Alaska (abstract): Geol. Soc. America Bull., v. 63, p. 1289.

—— 1952b, Preliminary report on the late Quaternary history of the Fairbanks area, Alaska (abstract): Geol. Soc. American Bull., v. 63, p. 1289–90.

—— 1954, Effect of permafrost on cultivated fields, Fairbanks area, Alaska: U. S. Geol. Survey Bull. 989-f, p. 315–351.

Péwé, T. L., *et al.*, 1953, Multiple glaciation in Alaska: a progress report: U. S. Geol. Survey Circ. 289, 13 p.

Prindle, L. M., 1905, The gold placers of the Fortymile, Birch Creek and Fairbanks regions, Alaska: U. S. Geol. Survey Bull. 251, 89 p.

—— 1909, The Fortymile quadrangle, Yukon-Tanana region, Alaska: U. S. Geol. Survey Bull. 375, 52 p.

—— 1913, A geological reconnaissance of the Fairbanks Quadrangle, Alaska: U. S. Geol. Survey Bull. 525, 220 p.

Prindle, L. M., and Katz, F. J., 1913, Detailed description of the Fairbanks district: U. S. Geol. Survey Bull., 525, p. 59–152.

Russell, R. J., 1944, Lower Mississippi Valley loess: Geol. Soc. American Bull., v. 55, p. 1–40.

Smith, C. D., 1942, Illinois loess; variations in its properties and distribution: Univ. Illinois Bull. 490, p. 139–183.

Smith, H. T. U., and Fraser, H. J., 1935, Loess in the vicinity of Boston, Massachusetts: Am. Jour. Sci., 5th sec., v. 30, p. 16–32.

Spurr, J. E., 1898, Geology of the Yukon gold district, Alaska: U. S. Geol. Survey 18th Ann. Rept., p. 87–392.

Swineford, Ada, and Frye, J. C., 1945, A mechanical analysis of wind-blown dust compared with analyses of loess: Am. Jour. Sci., v. 243, p. 249–255.

Taber, Stephen, 1943, Perennially frozen ground in Alaska; its origin and history: Geol. Soc. American Bull., v. 54, p. 1433–1548.

—— 1953, Origin of Alaska silts: Am. Jour. Sci., v. 251, p. 321–336.

Tuck, Ralph, 1940, Origin of the muck-silt deposits at Fairbanks, Alaska: Geol. Soc. American Bull., v. 51, p. 1295–1310.

Twenhofel, W. H., 1932, Treatise on sedimentation: Baltimore, The Williams and Wilkins Co., 926 p.

Udden, J. A., 1898, The mechanical composition of wind deposits: Augustana Library Pub. no. 1, 69 p.

U. S. Weather Bureau, 1943, Climatic atlas for Alaska: Rept. 444 (229 p.) and supplement (72 p.) of the weather Information Branch, Headquarters, Army Air Forces.

Wahrhaftig, Clyde, 1950, Physiographic history of southern Alaska: a hypothesis (abstract): Geol. Soc. American Bull., v. 61, p. 1532.

—— 1953, Multiple glaciation of the Nenana River, Alaska: *in* Multiple glaciation in Alaska: a progress report, by T. L. Péwé, *et al.*, U. S. Geol. Survey Circ. 289, 13 p.

Warn, G. F., 1952, Some dust storm conditions of the southern High Plains: Am. Meteor. Soc. Bull. v. 33, p. 240–243.

—— 1953, Drought and dust on the plains: Weatherwise, v. 6, p. 67–71.

Warn, G. F., and Cox, W. H., 1951, A sedimentary study of dust storms in the vicinity of Lubbock, Texas: Am. Jour. Sci., v. 249, p. 553–568.

Waters, A. E., Jr., 1934, Placer concentrates of the Rampart and Hot Springs districts, Alaska: U. S. Geol. Survey Bull. 844-D, p. 227–246.

Wilkerson, A. S., 1932, Some frozen deposits in the gold fields of interior Alaska: A study of the Pleistocene deposits of Alaska: Am. Mus. Nat. History, Novitates 525, 22 p.

Zeuner, F. E., 1949, Frost soils on Mount Kenya, and the relation of frost soils to aeolian deposits: Jour. Soil Sci., v. 1, p. 20–30.

U.S. Geological Survey, Univ. of Alaska, Box 4004, College, Alaska

Manuscript Received by the Secretary of the Society September 8, 1953

Publication Authorized by the Director, U.S. Geological Survey

BULLETIN OF THE GEOLOGICAL SOCIETY OF AMERICA
VOL. 66, PP. 725-730, 1 FIG., 1 PL. JUNE 1955

DISCONFORMITY BETWEEN LOWER AND MIDDLE ORDOVICIAN SERIES AT DOUGLAS LAKE, TENNESSEE

BY JOSIAH BRIDGE[1]

ABSTRACT

Detailed mapping of exposed Ordovician strata on the shore of Douglas Lake, Tennessee, shows local relief of 140 feet on the post-Lower Ordovician erosion surface. Dolomite and chert conglomerates fill depressions on this surface. Disconformable relations at the base of the Middle Ordovician series are also known in the Appalachians south of Roanoke, Virginia, in central and eastern New York, and in many places throughout the world. This disconformity may be a reflection of a major orogenic episode.

CONTENTS

TEXT

	Page
Introduction	725
Field work and acknowledgments	725
Douglas Lake area	725
Mascot dolomite	727
Lenoir limestone	727
Strata above the Lenoir limestone	729
Significance of the disconformity	729
References cited	730

ILLUSTRATIONS

Figure	Page
1. Index map showing location of Douglas Lake area	726

Plate	Facing page
1. Geologic map and stratigraphic diagram of Lower and Middle Ordovician rocks exposed near Douglas Dam, Tennessee	730

INTRODUCTION

For many years it has been known, in a general way, that there is a stratigraphically important disconformity of considerable geographic extent at the base of rocks now classified as Middle Ordovician in eastern and central North America. This paper presents the results of recent observations on this disconformity in outcrops exposed during low-water stages along the north shore of Douglas Lake, Jefferson County, Tennessee (Fig. 1). These exposures, uncovered and washed by strong waves on an unprotected shore, reveal striking details of the contact between the Lower and the Middle Ordovician that is elsewhere concealed by surficial and residual materials.

FIELD WORK AND ACKNOWLEDGMENTS

These exposures were first observed in 1945, about 2 years after Douglas Dam was completed. In March 1952 a plane-table survey of the best-exposed part of the area, at a scale of 1 inch to 200 feet, was made with the assistance of J. M. Cattermole, Richard Van Horn, and William Keating of the United States Geological Survey.

DOUGLAS LAKE AREA

Douglas Lake, a reservoir of the Tennessee Valley Authority, occupies a broad, shallow syncline filled with Middle Ordovician shales (Athens or Sevier shale of older reports, using these terms in their broadest sense). Limestones immediately below the shales range from 105 to 115 feet in thickness and form the base of the Middle Ordovician series. Disconformably beneath them is the Mascot

[1]Deceased April 30, 1953. This paper has been prepared posthumously by R. B. Neuman, R. A. Laurence, Benjamin Gildersleeve, and J. M. Cattermole, from Bridge's notes and the manuscript of his paper, *The extent and significance of the post-Lower Ordovician unconformity*, delivered as the Presidential address before the Geological Society of Washington in December 1952. The illustrations were prepared for publication by Elinor Stromberg and Carolyn Bartlett.

dolomite, the highest formation of the Lower Ordovician series in eastern Tennessee. The Mascot dolomite is about 525 feet thick in this area, but only the upper 200 to 250 feet is exposed along the lake shore from the

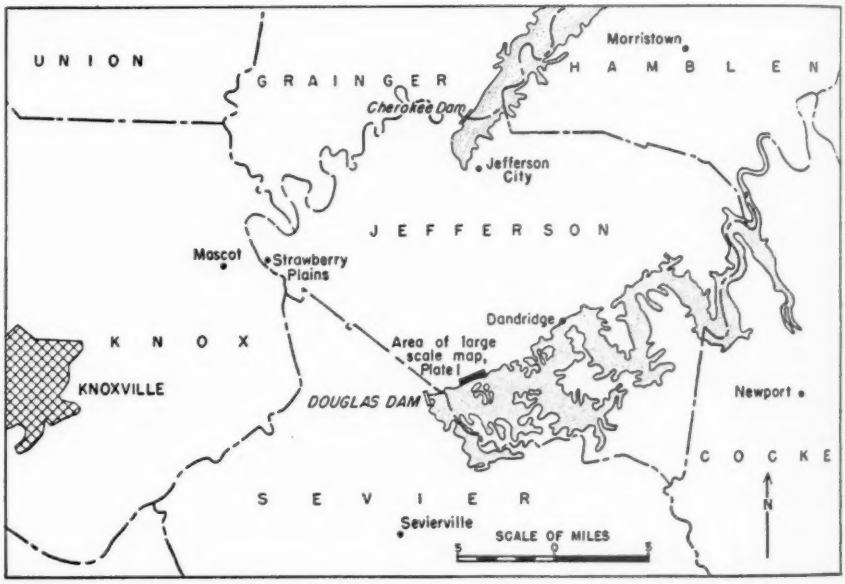

FIGURE 1.—INDEX MAP SHOWING LOCATION OF DOUGLAS LAKE AREA

vicinity of the dam northeastward for about 15 miles. The azimuth of the regional strike is about 70°, and the regional dip is 25°–35° SE.

The contact between the Lower and the Middle Ordovician rocks lies, for the most part, slightly below maximum lake level. It crosses the north shore of the reservoir about 1½ miles northeast of the dam. Prior to development of the reservoir, the contact was poorly exposed; its approximate position was located with difficulty between scattered outcrops of Lower and Middle Ordovician limestones.

The area mapped begins about 1½ miles northeast of Douglas Dam and extends along the north shore of Douglas Lake for about a mile. It is bounded on the northwest by State Highway 66 (relocated) and on the southeast by the lake. When the survey was made, the average lake level was 947 feet above sea level. Maximum lake level is 1002 feet above sea level, and the minimum low water level is 920 feet, but seldom is either extreme reached; the lake commonly fluctuates between about 990 feet and 930 feet. The area is usually well exposed only in midwinter, when lake level is below 950 feet.

The detailed mapping permitted tracing of several key beds in the Mascot dolomite across, or nearly across, the entire area; contacts of the overlying formations were similarly traced. Six sections were measured across the beds. Each section either started from a known bed in the upper part of the Mascot dolomite or passed through one. From these sections the thickness of the Mascot dolomite above a recognized horizon was computed to determine the amount of relief on the disconformable surface at the top of the Mascot and the thicknesses of the stratigraphic units above the disconformity.

The stratigraphic diagram (Pl. 1) combines the observations of the measured sections with the results of mapping and is a reconstructed section drawn parallel to the regional strike. On it certain key beds in the Mascot

dolomite are plotted as though they were horizontal, and the positions of other beds and of the water line at 947 and 1002 feet were adjusted to fit this projection. In order to show some very thin but significant units the vertical scale of the stratigraphic diagram is twice the horizontal scale. The oldest rocks, shown at the bottom of the diagram, crop out along the northern edge of the mapped area.

Mascot Dolomite

Several beds in the upper part of the Mascot dolomite are sufficiently distinctive to be easily traced and used as key horizons. Chief among these are individual beds (4–9 feet thick) of bright-blue very fine-grained to aphanitic limestone, which contrast sharply with the pale-gray fine-grained dolomites with which they are interbedded. Each bed appears to maintain its thickness through its exposed extent.

In this area the zone characterized by the gastropod operculum *Ceratopea ankylosa* Cullison lies near or at the top of the Mascot dolomite. The zone is 20–45 feet thick. Between beds of blue limestone at its base and top are light-gray fine-grained, in places cherty dolomite and one bed of blue limestone. In the western part of the area this zone is overlain by as much as 50 feet of unfossiliferous dolomite and limestone between sections 1 and 5 (Pl. 1), but from section 4 eastward the uppermost dolomite beds of the Mascot, the *C. ankylosa* zone, and a considerable thickness of the underlying dolomite beds are cut out by post-Early Ordovician erosion.

Beds of ribboned dolomite and limestone are interbedded with nondescript, fine-grained dolomite downward from about 95 feet below the top of the *C. ankylosa* zone. There are four such easily recognized lithologic units within the area, three of which were traced through most of its length.

At the eastern end of the area Middle Ordovician limestone rests on, and partly truncates, the uppermost ribboned dolomite and limestone unit, which lies approximately 95 feet below the top of the *C. ankylosa* zone. This, as well as other details observed in the measured sections, indicates that the maximum relief at the top of the Lower Ordovician is about 140 feet.

Two large depressions believed to be relic sinks and several smaller ones emphasize the disconformity at the top of the Mascot dolomite. One large sink is between sections 1 and 2, the other between 2 and 3 of Plate 1. The bottom of each is filled by 10–15 feet of rubble made up of blocks of Mascot dolomite, cemented by a dolomitic paste. The rubble of unoriented blocks grades upward into a more widespread chert-and-dolomite conglomerate. Some of the largest blocks within the rubble are 8 feet long and 2 feet thick. All the material appears to have been derived from the Mascot dolomite and to have been somewhat consolidated and recemented before deposition of the Middle Ordovician series. The beds on the western side of the western sink and on both sides of the other large sink dip gently inward toward the centers of the sinks. The unbroken beds of the Mascot dolomite beneath both sinks are slightly bowed downward. These features suggest solution below the sinks, resulting in slumping without much fracturing.

Lenoir Limestone

Douglas Lake member: The name Douglas Lake member is here proposed for beds overlying the Mascot dolomite and underlying the typical nodular member of the Lenoir limestone in this area. The type locality is in Jefferson County on the north shore of Douglas Lake, 1½ miles northeast of the Douglas Dam. The Douglas Lake member is composed of several rock types, including the rubble conglomerate in the sinks described above, chert conglomerate, and black dolomite.

The chert conglomerate overlies the rubble conglomerate in depressions on the upper surface of the Mascot dolomite and at other places forms the lower part of the Douglas Lake member. The rock is finely to coarsely conglomeratic, consisting of fragments of dark- and light-gray chert ranging from minute angular pieces to masses and nodules several inches in diameter, all clearly derived from chert horizons in the Mascot dolomite.

There are also a few angular fragments of Mascot dolomite ranging from small grains to cobbles about 4 inches in diameter, and a few blocks as much as 6 feet long and 1 foot thick. The chert weathers into high relief and is therefore the most conspicuous element in the conglomerate; the dolomite fragments weather at about the same rate as the matrix and enclosing rock and are best distinguished from them by orientation and color.

A fine paste of chert conglomerate fills fissures that follow joints and bedding planes in the Mascot dolomite. Patches of this material found 60 feet below the top of the Mascot dolomite give some idea of the amount of solution that took place prior to the deposition of the Middle Ordovician series. These filled fissures are most numerous near the filled sinks, but they have been found in nearly all parts of the area.

Black, fine-grained, thick-bedded dolomite forms the upper part of the Douglas Lake member in these exposures. Weathered surfaces are smooth and dark gray in contrast to the cross-hatched yellow weathered surfaces of the Mascot dolomite. The dolomite was a leveling unit, filling and smoothing the irregularities on the upper surface of the Mascot dolomite that remained after the deposition of the conglomerate. It has a maximum thickness of about 30 feet at the two large sinks. In measured sections the dolomite ranges from a feather edge (Pl. 1, sec. 6) to 15 feet (Pl. 1, secs. 1, 2, 3). It is absent, apparently by nondeposition, in the eastern end of the mapped area, but reappears about half a mile farther east and passes beneath alluvium in the vicinity of Shady Grove. The lowest dolomite beds bend into the sinks and other irregularities without noticeable fracturing. These dips are regarded as primary, differing from the centripetal dips in the Mascot dolomite which were caused by solution and slump.

The black dolomite grades upward almost imperceptibly into typical Lenoir limestone. The Douglas Lake member is therefore regarded as a discontinuous member of that formation. Similar non-fossiliferous, earthy dolomites have been found in the same stratigraphic position in other parts of eastern Tennessee and southwestern Virginia, but the relationships are not so clear elsewhere.

The dolomite beds of the Douglas Lake member are strikingly similar to unit A of the "33 beds" in the filled sink that was discovered in excavations for the foundation of Douglas Dam (Laurence, 1944); in fact, the western limit of the mapped area is only 1½ miles northeast of the dam. A careful search for fossils yielded only two small fragments of probable arachnid remains and a few linguloid brachiopods. No volcanic ash and none of the other distinctive lithologic types characteristic of the deposits filling the sink at the dam were found in the outcrop area. The beds here called the Douglas Lake member probably represent the continuation of the upper beds in the sink at the dam.

NODULAR LIMESTONE: Immediately above the Douglas Lake member is a dark-gray nodular, fine-grained, argillaceous limestone comparable to the typical Lenoir limestone. In the eastern part of the area, where the Douglas Lake member is missing, the lower 2 feet of these nodular beds contains small fragments of chert. This is the only place in the area where the nodular beds are conglomeratic. The exposures are separated from those farther west by an arm of the lake and by a cover of residuum. Consequently it is not known whether these beds are laterally contiguous with the Douglas Lake member or perhaps simply an inclusion of debris in the lowest beds of typical Lenoir lithology.

APHANITIC LIMESTONE: In the central part of the area, dove-gray nearly pure aphanitic limestone known as the Mosheim member of the Lenoir limestone occurs in two beds separated by a thin bed of nodular limestone. This thin bed contains several specimens of the gastropod *Maclurites magnus* Lesueur. At the eastern end of the area the aphanitic beds do not appear in the section; they are very probably replaced by the nodular beds of the Lenoir limestone. In the geologic studies that preceded the dam construction (Wedow and Laurence, 1943) Laurence (Personal communication) observed an outcrop of Mosheim in a creek bed, now flooded by the reservoir, about half way between sections 5 and 6 (Pl. 1). Exposures of Mosheim were also observed on the south side of the river, west of this area, but no Mosheim was present at the dam.

Strata Above the Lenoir Limestone

Succeeding the Lenoir limestone is 8–12 feet of shaly limestone superficially like the nodular limestone of the Lenoir. These upper beds are most shaly near the top of the unit and finally merge into a dark-blue pyritic limestone that weathers to a conspicuous rusty ledge. This shaly limestone and the pyritic bed are probably basal members of the overlying Athens shale. An undetermined thickness of Athens shale underlies the lake and crops out along its southern shore.

Significance of the Disconformity

The disconformity described here is not just a local feature; a disconformity at the base of the Middle Ordovician series has been reported in many places. It may be the reflection of a major orogenic episode. The extent of the disconformity has been realized only vaguely, and the evidence for it has never been adequately assembled and evaluated in a single report. Although the writer has collected much information about the contact between the Lower and the Middle Ordovician in central and eastern North America, the study is far from completion. Consequently only a brief summary of the significance of this break is presented here.

In Alabama the Attalla conglomerate near Birmingham (Butts, 1926, p. 120–121) is similar in stratigraphic position and composition to the Douglas Lake member. Munyan (1951, p. 54–60) described comparable rock in northwestern Georgia to which he applied the term Blackford formation. Rodgers (1953, p. 70, 78, 84, 87) described several localities in eastern Tennessee at which disconformable relations at this horizon were observed. The term Blackford member of the Cliffield formation (later raised to Blackford formation) was applied to clastic rocks disconformably overlying the Lower Ordovician dolomites in southwestern Virginia (Cooper and Prouty, 1943, p. 862; *see also* Butts, 1940, p. 126–127). There are no references to disconformable relations at this horizon between the latitudes of Roanoke, Virginia, and central New York; at least one author suggested that in places Middle Ordovician limestones overlie Lower Ordovician dolomites with a gradational contact (Neuman, 1951, p. 282–284).

The distribution of these reported occurrences of clastic rocks and apparent disconformable relations takes on greater interest when compared with information on subdivisions of the Lower Ordovician rocks. In parts of the Birmingham, Alabama, district, Middle Ordovician strata rest on Upper Cambrian rocks, and in adjacent sections they overlie various formations of Beekmantown age; a relief of about 1000 feet is indicated between these sections. In eastern Tennessee all known occurrences involve erosion of the Mascot dolomite—a minimum of 140 feet in the Douglas Lake area and 200 feet near Lee Valley (Rodgers and Kent, 1948, p. 32). In Virginia, near Pulaski, Middle Ordovician strata rest on different formations of Beekmantown age in the same strike valley, indicating relief on the upper surface of the Beekmantown dolomite of about 800 feet in 3 miles, and similar relations in Catawba Valley, near Marion and in the Burkes Garden area, have been reported (B. N. Cooper, Personal communication).

Farther north, in Warm Springs Valley, Allegheny and Bath counties, Virginia, along the western edge of the Valley and Ridge province, abundant fossils younger than any known in the Knox dolomite of Tennessee and southwest Virginia have been found. This indicates the presence of Lower Ordovician strata younger than any known in areas to the southwest. The thickness of these beds, and their relations to the overlying Middle Ordovician are not yet known. In central Pennsylvania the Lower Ordovician section is much thicker than in southern Virginia and eastern Tennessee, and most of this thickening appears to be due to the presence of younger strata to the north. Where these younger rocks crop out the contact between the Lower and the Middle Ordovician series is difficult to place, and some geologists believe it is gradational.

In central and eastern New York the disconformity is again evident. West of the Adirondack dome, in the Mohawk Valley, Middle Ordovician rocks, most of them considerably younger than the basal Middle Ordovician rocks of eastern Tennessee, locally

overlap Lower Ordovician rocks and rest on Upper Cambrian rocks.

This review applies to the relations between the Lower and the Middle Ordovician series in the Appalachians only. Similar relations, however, have been recognized in many places throughout the world. The interruption in deposition appears to have been very widespread, although in some areas it appears to have been of greater duration than in others, and possibly deposition was continuous in a few places. Thus, although the interruption to sedimentation was widespread, it certainly was not uniform in its time of occurrence or duration.

References Cited

Butts, Charles, 1926, Geology of Alabama, The Paleozoic rocks: Ala. Geol. Survey Spec. Rept. 14, p. 41–230.

—— 1940, Geology of the Appalachian Valley in Virginia: Va. Geol. Survey Bull. 52, 568 p.

Cooper, B. N., and Prouty, C. E., 1943, Stratigraphy of the lower Middle Ordovician of Tazewell County, Virginia: Geol. Soc. America Bull., v. 54, p. 819–886.

Laurence, R. A., 1944, An early Ordovician sinkhole deposit of volcanic ash and fossiliferous sediments in east Tennessee: Jour. Geology, v. 52, p. 235–249.

Munyan, A. C., 1951, Geology and mineral resources of the Dalton quadrangle, Georgia-Tennessee: Ga. Geol. Survey Bull. 57, 128 p.

Neuman, R. B., 1951, St. Paul group: A revision of the "Stones River" group of Maryland and adjacent states: Geol. Soc. America Bull., v. 62, p. 267–324.

Rodgers, John, 1953, Geologic map of east Tennessee, with explanatory text: Tenn. Div. Geology Bull. 58, 15 pl., 168 p.

Rodgers, John, and Kent, D. F., 1948, Stratigraphic section at Lee Valley, Hawkins County, Tenn.: Tenn. Div. Geology Bull. 55, 47 p.

Wedow, Helmuth, Jr., and Laurence, R. A., 1943, Geologic map and structure sections, Douglas project: Tenn. Valley Authority drawings.

Manuscript Received by the Secretary of the Society, October 11, 1954

Publication authorized by the Director, U.S. Geological Survey

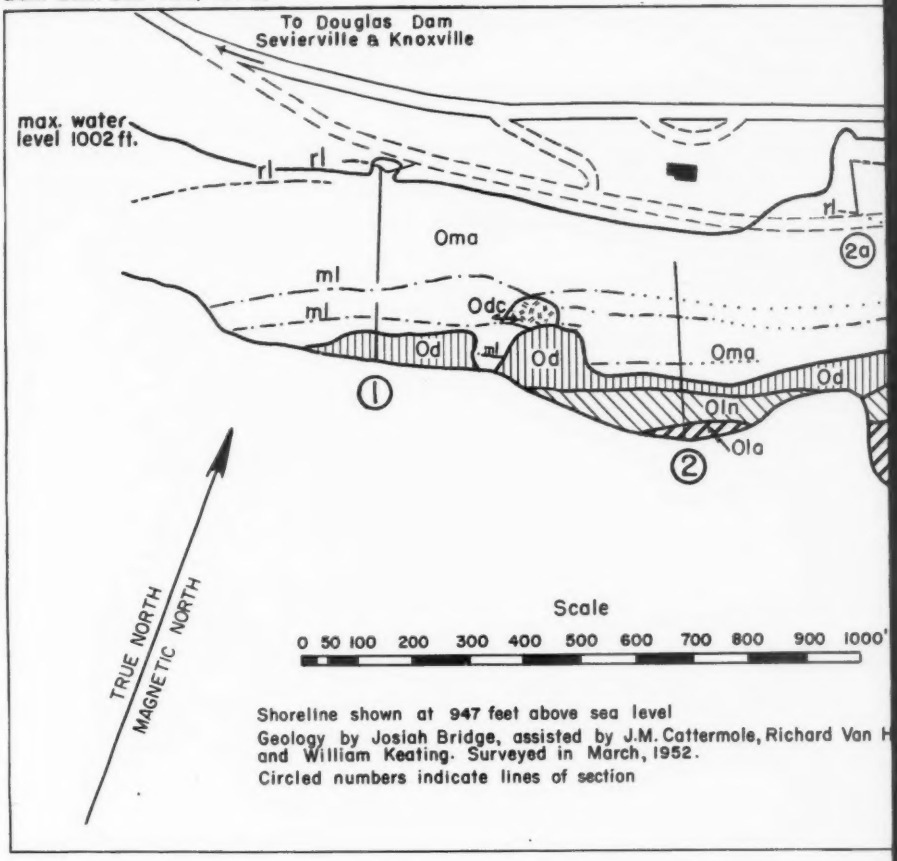

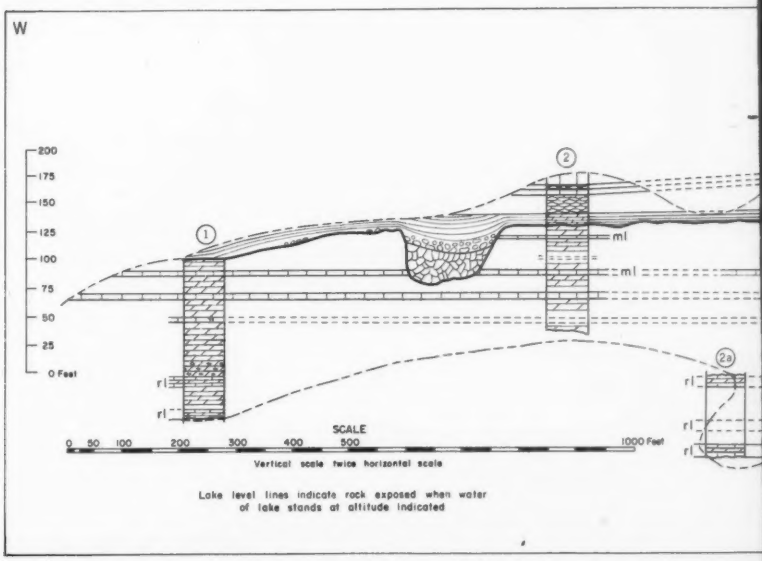

GEOLOGIC MAP AND STRA

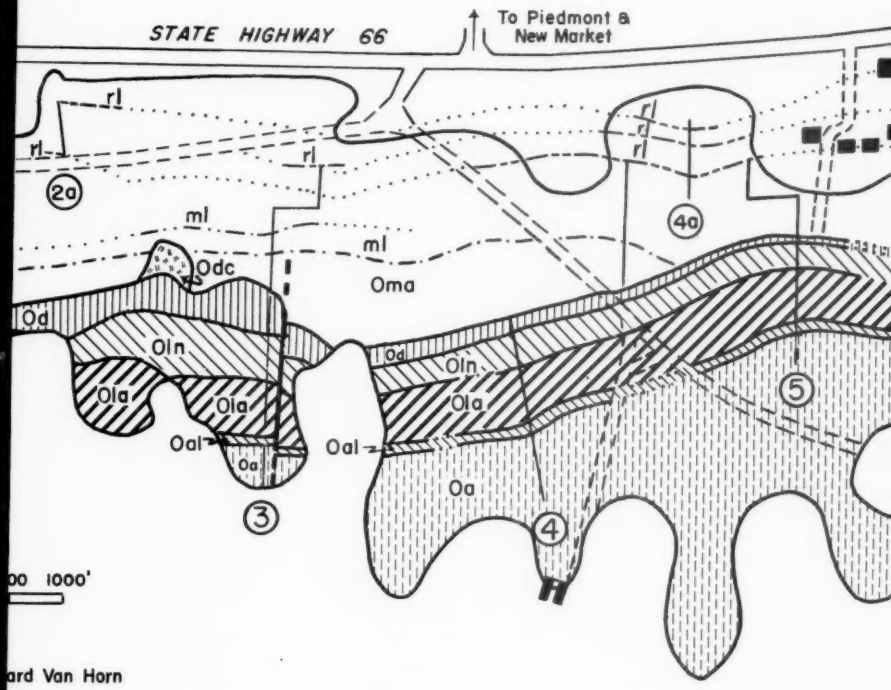

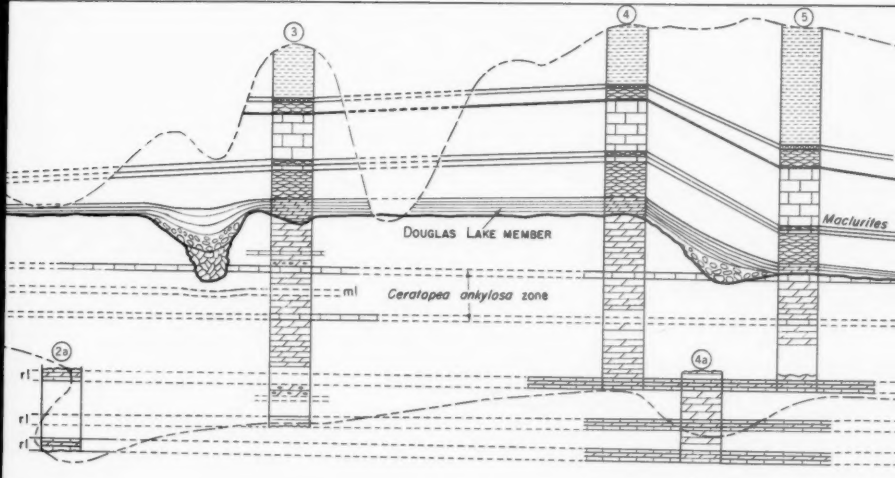

STRATIGRAPHIC DIAGRAM OF LOWER AND MIDDLE O

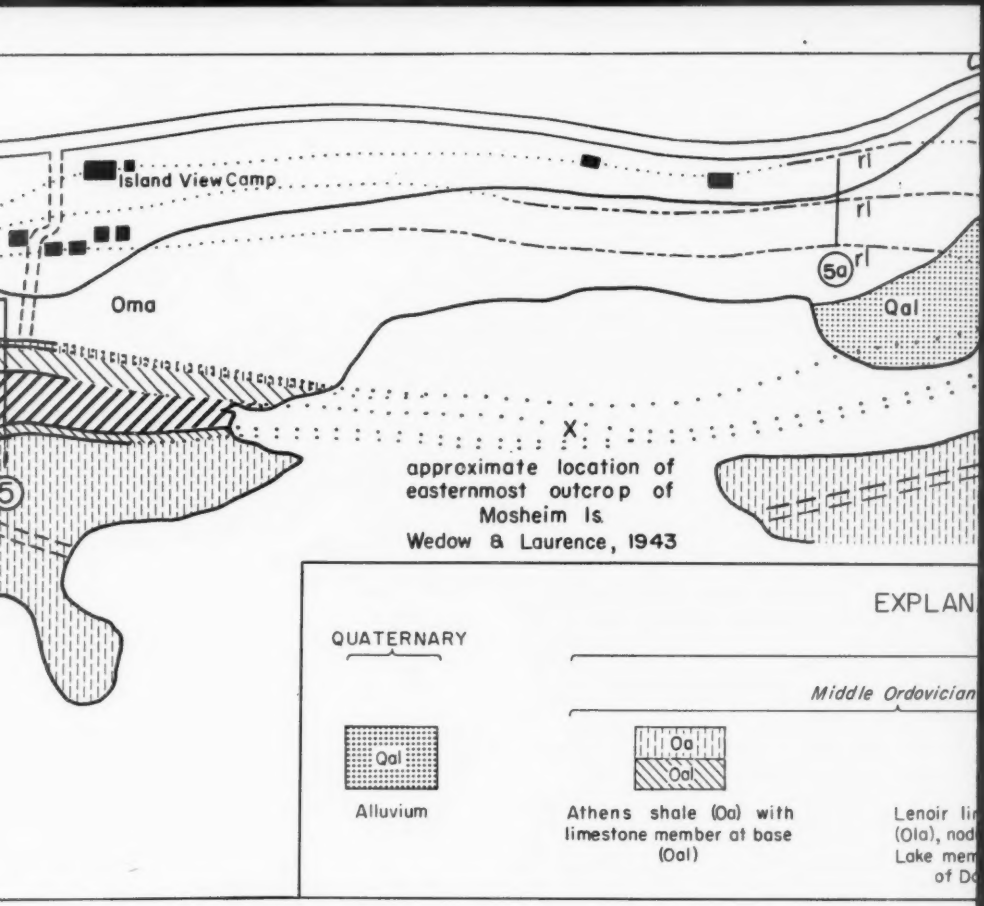

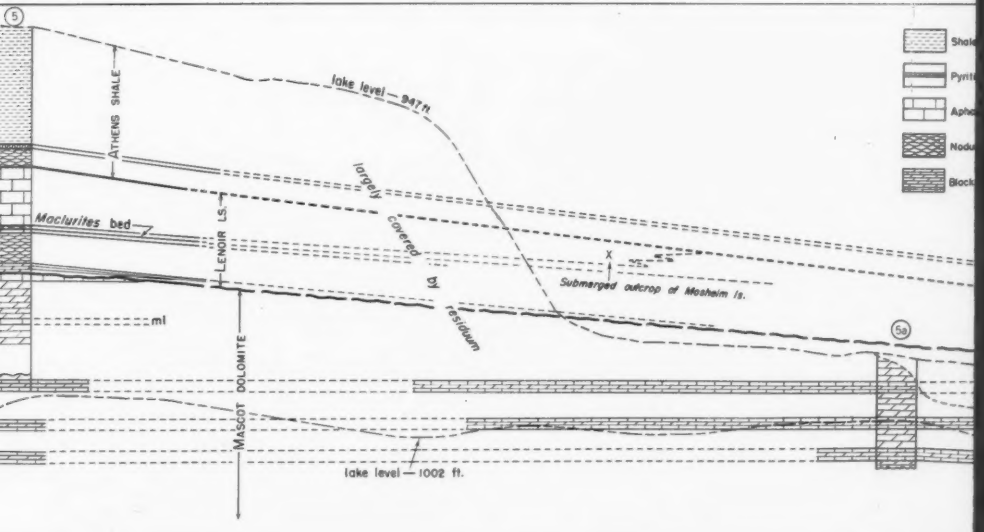

DDLE ORDOVICIAN ROCKS EXPOSED NEAR DOUGLAS DAM,

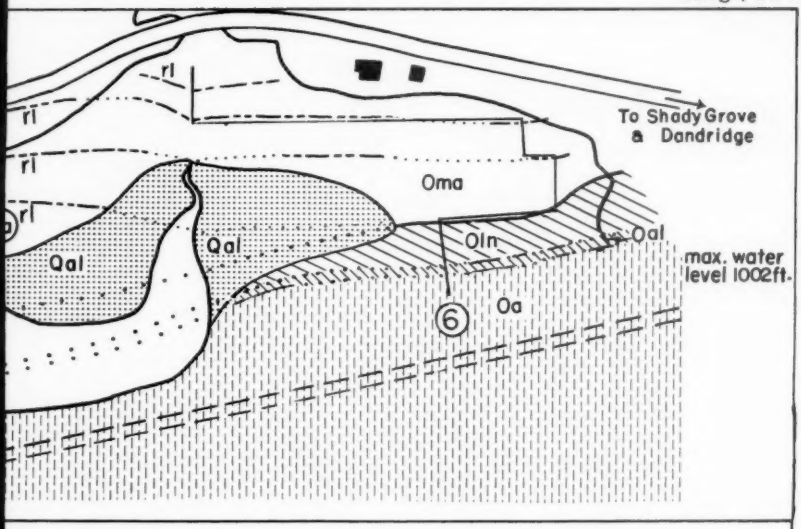

EXPLANATION

ORDOVICIAN

Middle Ordovician

Oln
Oda
Od
Odc

Lenoir limestone: Aphanitic limestone (Ola), nodular limestone (Oln), Douglas Lake member (Od), rubble conglomerate of Douglas Lake member (Odc)

Lower Ordovician

Oma

Mascot dolomite: gray dolomite with beds of ribboned limestone (rl) and massive limestone (ml)

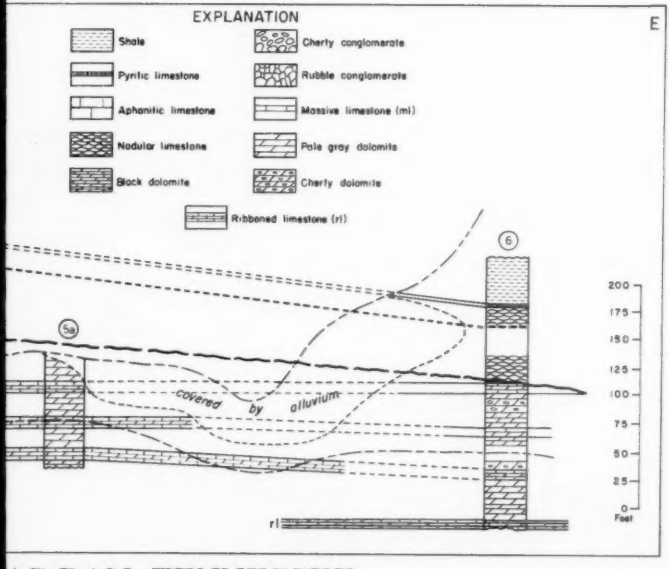

AS DAM, TENNESSEE

UM

VERTICAL AIRPHOTO OF O SHIMA VOLCANO, 1947

Outer slopes rise from coast to somma; cultivated in northwest corner in vicinity of coastal village of Motomura. Somma encloses caldera except northeast side; diameter 3 km. Central cone of Mihara Yama has crater floored with dark lava. Deep inner pit in shadow except for northeast side. Crater 800 m wide, pit 300 m wide.

BULLETIN OF THE GEOLOGICAL SOCIETY OF AMERICA
VOL. 66, PP. 731-762, 14 FIGS., 5 PLS. JUNE 1955

1950 AND 1951 ERUPTIONS OF MIHARA YAMA, O SHIMA VOLCANO, JAPAN

BY HELEN L. FOSTER AND ARNOLD C. MASON

ABSTRACT

Mihara Yama is the active central cone of O Shima Volcano on the island of O Shima, Tokyo Prefecture, Japan. The outer slopes of O Shima Volcano compose most of the island. Their crest is a somma, about 600 km in altitude and 3 km in diameter, which encloses a caldera. Mihara Yama rises from the southern part of the caldera to an altitude of 755 m. It is a truncated cone with a crater 800 m in diameter. Before the eruption in 1950 the crater contained an inner pit approximately 300 m in diameter and 165 m deep.

Mihara Yama erupted on July 16, 1950, after 10 years of quiescence. Activity continued until September 24. Eruption resumed on February 4, 1951, and continued until April 2, after which activity was intermittent until the eruption ceased on June 28.

In 1950 molten basalt was ejected explosively accompanied at times by flows. Two successive cinder cones formed from the accumulation of ejecta, some of which were hurled as high as 500 m. Lava filled the inner pit and crater, and a small amount overflowed into the caldera. About 52,000,000 metric tons of material was erupted.

In 1951 six successive small cones developed. Beginning February 21 the principal cone formed. Lava overflowing the crater rim solidified mostly as aa and covered nearly 2 square km of the caldera floor. The intermittent activity during the final 3 months consisted of nine brief periods of eruption, a few of which were relatively violent. Between eruptions and especially after the final eruption the crater floor subsided. In 1951 about 20,000,000 metric tons of material was erupted.

CONTENTS

TEXT

	Page
Introduction	732
Location	732
Acknowledgments	732
Geologic description	732
Regional geology	732
Earthquakes	733
General description	734
Volcanic activity in historic time	736
Structure	736
Summary of development	739
Petrology	740
Lava	740
Ejecta	741
Eruption of 1950	741
Condition before eruption	741
Beginning of activity	741
Explosive activity	741
Lava emission	743
Termination of eruption	744
Eruption of 1951	744
Renewal of eruption	744
Formation of principal vent	745
Lava flows	745
Intermittent activity and subsidences	747
Geophysical observations	750
Seismic activity	750
Geomagnetism	751
Gravity	752
Geochemical observations	752
Fumaroles	752
Volcanic gases	753
Sublimates	753
Physical measurements	754
1950 eruption	754
1951 eruption	754
Erupted material	755
Types of lava flows	755
Formation of pahoehoe	755
Formation of aa	756
Formation of modified types	757
Lava streams on slopes of Mihara Yama	758
Lamellar banding	759
Ejecta	759
References cited	760

ILLUSTRATIONS

Figure		Page
1.	Index map of O Shima and vicinity	733
2.	Map of O Shima prior to 1950 eruption	734
3.	Cross section of O Shima prior to 1950 eruption	735
4.	Map of Mihara Yama prior to 1950 eruption	735
5.	Cross section of Mihara Yama	742
6.	Sketch map of crater of Mihara Yama	743
7.	Surface explosive eruption of Mihara Yama	743
8.	Underground explosive eruption of Mihara Yama	743
9.	Cyclic outblast from small vent in 1951 eruption	745
10.	Map of Mihara Yama on April 20, 1951	746
11.	Maximum amplitude of tremors during 1950 eruption	750
12.	Maximum amplitude of tremors, February to April, 1951	750
13.	Maximum amplitude of tremors during period of intermittent eruption, April through June, 1951	751
14.	Magnetic declination on O Shima, 1951	751

Plate		Facing page
1.	Vertical air photo of O Shima Volcano, 1947	731
2.	Central cone, Mihara Yama	Following page 748
3.	Crater of Mihara Yama	
4.	Drawn-surface pahoehoe lava	
5.	Lava features	

TABLES

Table		Page
1.	Summary of eruptions in Izu Shichito, Japan	737
2.	Chemical analyses of O Shima lavas	740
3.	Analysis of condensate from gas issuing from driblet spire, Mihara Yama, March 1951	753
4.	Analyses of gas issuing from cracks in crater floor, Mihara Yama, March 1951	753
5.	Spectroscopic analyses of specimens from 1950 eruption, Mihara Yama	753
6.	Chemical analysis of white sublimate from 1950 eruption, Mihara Yama	754
7.	Viscosity of small lava stream on slope of Mihara Yama, 1951	755

INTRODUCTION

Location

Mihara Yama is the active central cone of O Shima Volcano on the island of O Shima, Tokyo Prefecture, Japan. O Shima (Big Island), also called Vries Island, after the Dutch navigator, stands at the entrance of Sagami Sea, and is 110 km south-southwest of Tokyo (Fig. 1).

Acknowledgments

A summary of studies by Japanese scientists is included, and acknowledgment is made of the information they furnished. Special thanks are due Dr. Seitaro Tsuboi, Geological Institute, Tokyo University; Dr. Hiromichi Tsuya, Dr. Takeshi Minakami, and Mr. Ryohei Morimoto of the Earthquake Research Institute, Tokyo University; Mr. Sadanori Murauchi, National Science Museum, Tokyo; Mr. Takeshi Kizawa, O Shima Meteorological Observatory; Mr. Akira Suwa, Central Meteorological Observatory, Tokyo; and Mr. Kinkiti Musya, formerly with Central Meteorological Observatory.

GEOLOGIC DESCRIPTION

Regional Geology

O Shima is the north end of the Izu Shichito (Izu Seven Islands), a chain of volcanic islands 200 km long (Fig. 1). These islands and the eastern side of the Izu Peninsula are a part of the Fuji volcanic zone, which continues northward across Honshu. On Honshu the zone coincides with the Fossa Magna, a graben largely filled by volcanic material from Pleistocene and Recent volcanoes, including Fuji San (Fuji Mountain: San and yama both mean mountain and are written with the same ideograph, but in Japan the mountain is called Fuji San, not Fujiyama).

The Izu Shichito is the north end of one of a pair of submarine ridges that extend south-southeast to 20°N. Farther south these ridges curve south-southwest to their termination at about 12°N. These ridges separate the basin of the Philippine Sea on the west from that of the Pacific Ocean. Paralleling them to the east is a nearly continuous foredeep, the Japan Trench, Bonin Trench, and Mariana Trench (Hess, 1948, Pl. 2).

The crests of the two ridges form other volcanic island chains south of the Izu Shichito—the Ogasawara Gunto (Bonin Islands), the Kazan Retto (Volcano Islands), and the Mariana Islands. The volcanoes of the Izu Shichito, the Kazan Retto, and the northern Mariana Islands were active in Pleistocene and Recent time, those of the Ogasawara Gunto and southern Mariana Islands in the Tertiary (Tsuya, 1937, p. 222). In the tropical Mariana

Islands coralline growth mantles much of the volcanic rock.

In the Izu Shichito the islands of O Shima, To Shima, Udone Shima, Miyake Jima, Mikura Jima, Hachijo Jima, and Ko Shima (O Shima group) are composed of basaltic rocks. Nii Jima, Shikine Jima, and Kozu Shima (Nii Jima group) are dacitic and rhyolitic (Fig. 1) (Tsuboi, 1920, p. 135).

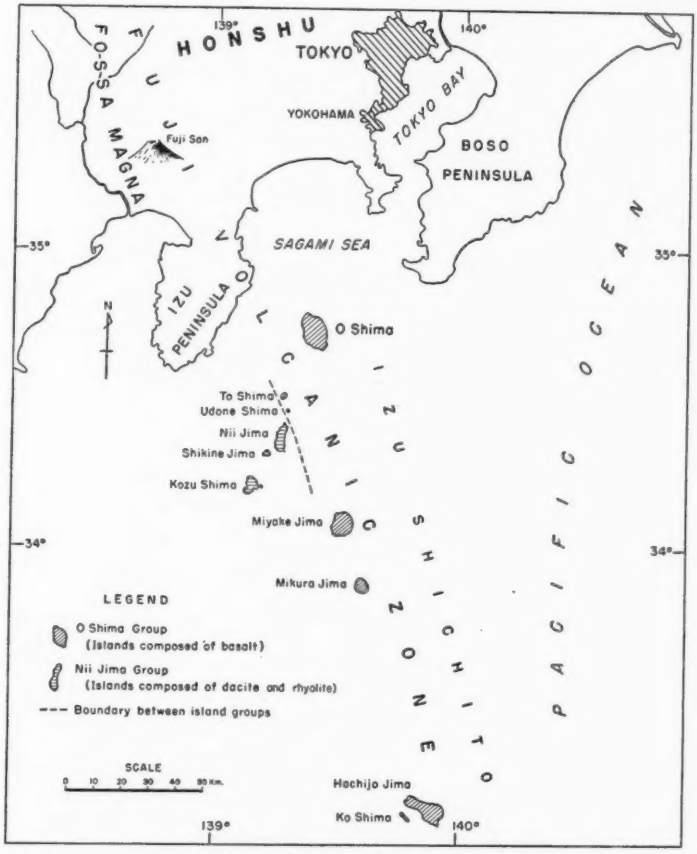

FIGURE 1.—INDEX MAP OF O SHIMA AND VICINITY

Earthquakes

Both volcanic and tectonic earthquakes occur in the area. The former are local, shallow, and of low intensity. On O Shima they accompany eruptions but may also occur at other times.

Many tectonic earthquakes occur in or near the area, although their foci are rarely beneath the islands. These earthquakes are of relatively low to moderate intensity, although an occasional quake may cause damage. The depths of their hypocenters range from only a few km to more than 500 km. From 1934 to 1939, for example, of 49 earthquakes in the area with hypocenters 100 km or deeper, 3 were between 100 and 200 km, 12 between 200 and 300 km, 16 between 300 and 400 km, 5 between 400 and 500 km, and 11 were reported merely as deep or quite deep. During the same period about 300 shallower quakes were recorded, a few of which may have been volcanic earthquakes (Musya, 1951b).

General Description

O Shima is about 13 km long, 8 km wide, and has an area of 103.8 square km. It is shaped like a parallelogram, with the long diagonal extending north-northwest. The coast line is relatively regular except for Habu Minato, an inlet at the southeastern corner of the island (Fig. 2). In most places cliffs border the shore.

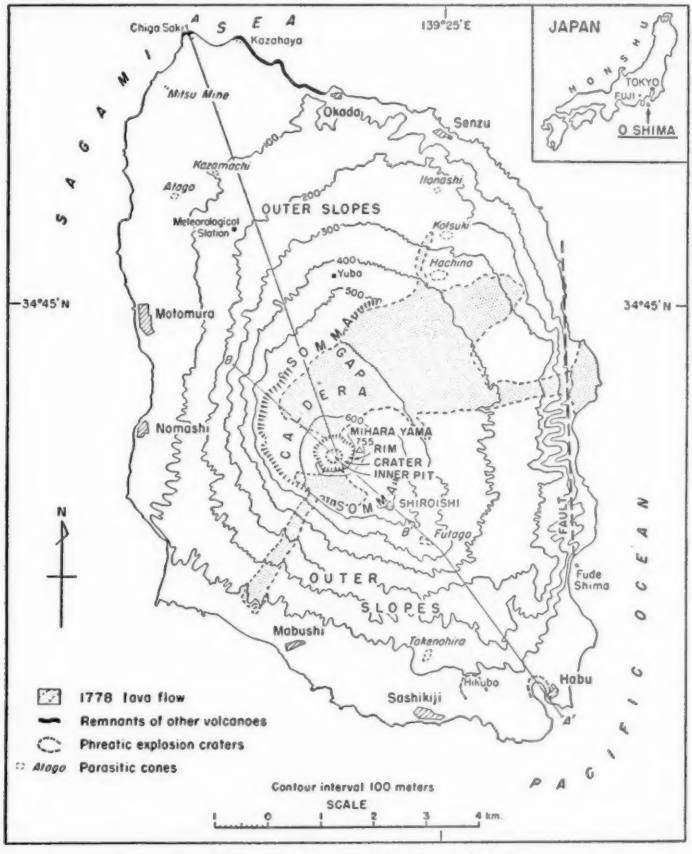

FIGURE 2.—MAP OF O SHIMA PRIOR TO 1950 ERUPTION

O Shima Volcano composes the entire island except along the north shore where there are small remnants of other volcanoes. Most of the area of O Shima Volcano consists of its outer slopes, which rise from the sea. These slopes have eight parasitic cones, and their slope steepens on the west side from about 5° near the shore to about 25° near the somma, and on the north and south sides from about 3° to about 22°. On the east side, from the top of coastal cliffs about 300 m high there is a rise of about 3° to the caldera floor.

The somma is about 3 km wide, and its altitude ranges from about 540 m at points on the north and west to 737 m at the peak of Shiroishi on the southeast. The bottom of the caldera is at approximately 530 m. It is a

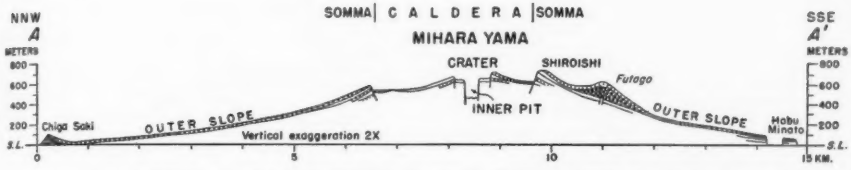

FIGURE 3.—CROSS SECTION OF O SHIMA PRIOR TO 1950 ERUPTION

O Shima volcano is composed of alternating layers of lava and ejecta. Mihara Yama, the central cone, is on south side of caldera. Shiroishi is highest point of somma. Futago is a parasitic cone. Habu Minato considered a phreatic explosion crater. Cliff at Chiga Saki is remnant of another volcano. Position of section shown on Figure 2.

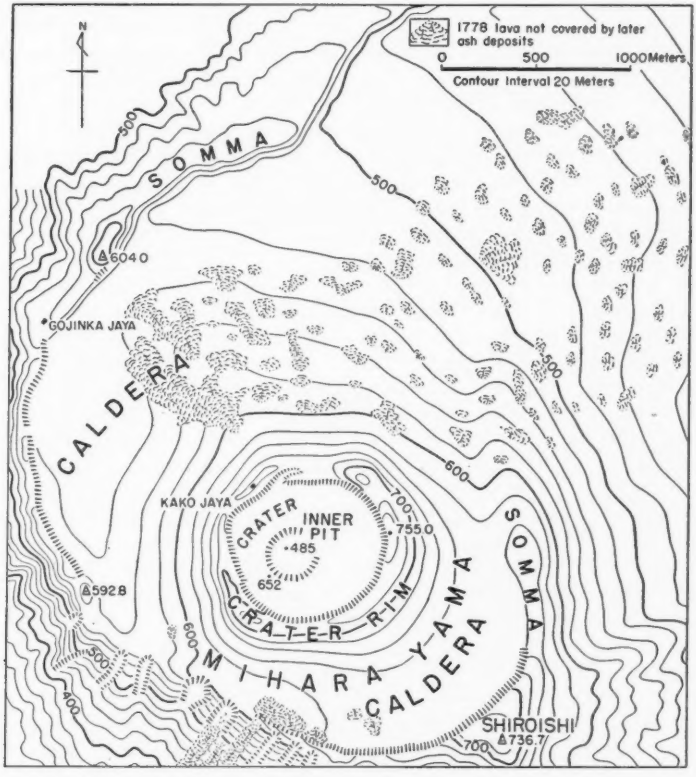

FIGURE 4.—MAP OF MIHARA YAMA PRIOR TO 1950 ERUPTION

nearly barren area called "sabaku" (barren or desert) (Pl. 1).

Mihara Yama rises in the south part of the caldera. Its name literally means "Three-field Mountain," but Mihara is believed to be a corruption of the word "mihora," which means sacred abyss. It is a truncated cone with barren, fairly smooth sides that slope about 8° near the base and about 35° near the top (Pl. 2, figs. 1, 2). The crater rim is about 800 m in diameter, and its altitude ranges from 675 m on the north side to 755 m on the east, the highest point on the island. Before the 1950 eruption the crater contained an inner pit (Figs. 3, 4).

Volcanic Activity in Historic Time

In the Izu Shichito about 75 eruptions have occurred during historic time; about 40 were eruptions of Mihara Yama (Table 1). Among major eruptions of Mihara Yama were those of 684, 1684, 1778, 1950, and 1951.

Structure of O Shima

O Shima consists of alternate layers of flows and ejecta. Most flows are only 3 or 4 m thick, and few are more than 15 m (Tsuboi, 1920, p. 13). The ejecta consist mostly of fragments erupted in the molten state, but some are shattered solidified rock. Most of the island is covered with ejecta from Mihara Yama.

The parasitic cones on the outer slopes are Atago, Kazamachi, and Mitsu Mine on the northwest; Itonashi, Kotsuki, and Hachino on the northeast; and Futago and Takenohira on the southeast (Fig. 2). They range from 20 to 250 m high, and the areas of their individual bases range from 18,000 to 950,000 square m (Tsuboi, 1920, p. 18). Itonashi, Kotsuki, and Hachino in the northeast are in an almost north-south line with Futago and Takenohira in the southeast, but others are not aligned.

Habu and Hikubo in the southeastern part of the island are probably phreatic explosion craters that resulted from the heating of ground water by magmatic intrusion (Fig. 2). Habu is a circular harbor about 275 m in diameter surrounded by a cliff about 50 m high except for a small outlet to the sea on the southeast side. Lava and ejecta similar to the material in the southeast slope of O Shima Volcano are exposed in southeastward-dipping layers (Tsuboi, 1920, p. 23).

Remnants of independent volcanoes form a a row of hills, including Chiga Saki and Kazahaya, with bold cliffs along the north coast west of Okada (Fig. 2). These volcanoes were separate islets that became connected as O Shima Volcano grew and its ejecta largely covered them (Tsuboi, 1920, p. 38–44). Their lavas differ from, and their beds are unconformable with those of O Shima Volcano.

The east side of O Shima rises precipitously for about 5 km north-south. A section of coastal cliff is interrupted where a flow from the 1778 eruption tumbled over it and formed a lava delta (Fig. 2). The escarpment presumably is the upthrown side of a north-striking fault which postdates the development of the outer slopes of O Shima Volcano as truncated layers of lava and ejecta are exposed in the cliff (Tsuboi, 1920, p. 16–18). The parasitic cones parallel the escarpment about 2 km to the west.

The somma where it encloses the caldera forms in places a cliff up to 50 m high, but elsewhere the mantle of younger volcanic ash and cinders rises without break from the floor of the caldera to the crest of the somma. The caldera was probably formed by subsidence or possibly by a combination of explosion and subsidence. However, no debris from an apex explosion are found on the somma rim. The gap in the caldera rim on the northeast side suggests more extensive collapse or, more likely, coalescence of two areas of collapse, for the north part of the caldera wall is composed of two arcs (Fig. 2).

The crater of Mihara Yama has had a complex history. A deep hole existed in the crater prior to the eruption of 1876–1877 when Naumann's cone formed at the bottom (Tsuboi, 1920, p. 32). During March to June in the 1912 eruption Naumann's cone was partly buried, and Nakamura's cone formed. In July this cone was destroyed, and in September and October Omori's cone formed. The altitude of the crater floor was about 615 m. In 1913 and 1914 these cones were buried, and several new small cones formed (Tsuboi, 1920, p. 35). The new floor of the crater was roughly level and had an altitude of about 650 m. The crater was encircled by cliffs 25–60 m high. The crater was little changed by a minor eruption in 1915.

After these eruptions the center of the crater began to subside. By 1923 the subsidence had formed an inner pit 100 m deep and more than 200 m in diameter. Subsidence continued intermittently, and in 1933 the inner pit reached its maximum size—about 400 m deep and 300 m wide (Nagata, 1941, p. 402).

The inner pit became famous because of the number of people who plunged into the abyss, believing that Mihara Yama was a sacred place in which they could find eternal rest. In 20 years the police recorded 1421 suicides and many others probably occurred unob-

TABLE 1.—SUMMARY OF ERUPTIONS IN IZU SHICHITO, JAPAN

O Shima		Other Izu Islands		Remarks
date		date	island	
680	Mar. 26			Explosive eruption
680	July 12			Heavy ash-fall
684	Nov. 29			Allusion that two lava flows reached the sea
		832	Kozu	Eruption
		838 Aug. 2	Near Kozu	Submarine eruption from August to October
856	Sept. 14			Ash reached Boso Peninsula
		886 July 3	Near Nii	Submarine eruption
1112	Nov. 18			Eruption lasted 2 weeks
		1154 Feb.	Miyake	Eruption
1338				Large falls of ash
1415	May 21			Sea water boiled; fish killed
1416	Sept 2			Eruption
1421	May 14			Sea water boiled; many fish killed
1442–43				Eruption
1469	Dec. 24	1469	Miyake	Eruption
		1487 Dec. 7	Hachijo	Eruption
		1518 Feb. to 1522	Hachijo	Long eruption
		1535 Mar.	Miyake	Eruption
		1595 Nov. 22	Miyake	Eruption
1600–01				Small eruptions
		1605 Oct. 27	Hachijo	Eruption
		1606	Near Hachijo	Island formed
1612–13				Small eruptions
1636–37				Small eruptions
1637	Aug. 26 to			Eruptions
1638	Feb			
		1643 Mar. 31	Miyake	Eruption of O Yama
		1652	Aoga	Eruption
		1670	Aoga	Eruption
1684	Mar. 31 to			Great activity between March 31 and
1690				April 11; two lava flows reached sea
1695	Apr. 12			Eruption
		1709 Apr. 23	Miyake	Eruption
		1712 Feb. 4	Miyake	Eruption
		1763 Aug. 17	Miyake	Eruption
		1777	Miyake	Possible eruption
1777	Aug. 31 to			Greatest activity began February
1778	Dec.			1778; on April 27 lava overflowed crater and eventually reached sea
1779				Explosions heard in Tokyo
		1780 July 19	Aoga	Eruption at Ikenosawa
		1781 May 4	Aoga	Eruption
		1783 Apr. 11	Aoga	Eruption
1783	Nov. 25			Ash-fall
1784				Eruption
		1785 Apr. 18	Aoga	Eruption

TABLE 1.—*Continued*

O Shima date	Other Izu Islands date	Other Izu Islands island	Remarks
1786			Explosions heard in Tokyo
1789 (?)			Abundant ash-fall
1803 Nov. 14			Ash fell in Tokyo
	1811 Jan. 27	Miyake	Eruption of O Yama
1822			Ash fell at intervals for 2 or 3 years
	1835 Nov. 11 to Nov. 29	Miyake	Eruption of O Yama
1837			Eruption
1846 (?)			Activity continued for 20 years
1870			Small eruption which lasted 4 days
	1874 July 3	Miyake	Eruption
1876 Dec. to 1877 Feb.			Lava emitted in crater; Naumann's cone formed
	1896	Bayonnaise Rocks	Submarine eruption
	1902 Aug. 7	Tori	Eruption
	1906	Bayonnaise Rocks	Submarine eruption
1910 Dec.			Eruption
1912 Feb. 23 to June 10			By April 10 bottom of crater covered with lava; Nakamura's cone formed; about 30 m of lava accumulated in crater
1912 July 27			Crater bottom subsided nearly 30 m and lava oozed from fissures; Nakamura's cone destroyed
1912 Sept. 16 to Oct. 29			Lava emitted; Omori's cone formed
1913 Jan. 14 to Jan. 24			Small cinder cones formed in crater bottom and lava emitted
1914 May 15			Lava emitted and small quantity of ash ejected; cinder cones in crater buried by lava.
	1915	Bayonnaise Rocks	Submarine eruption
1915 Oct. 14–16			Ash ejected in small quantities; largest eruption on October 16; no lava emitted
1922 Dec. 8–9			Lava erupted
1923 June 16–19			Ejecta thrown 50 m high
1928 Aug. 7–8			Small quantity of ash ejected
1933			Intermittent explosions and emission of lava in inner pit obscured by fumes; explosions violent on October 14.
1934			Minor explosive eruption; lava pond in inner pit; avalanches caused outblast of dark smoke on April 18.
	1934 May	Bayonnaise Rocks	Submarine eruption
1935 Apr. 26			Lava emitted on crater bottom
1938 Aug. 11			Between 6 and 7 a.m. lava in inner pit rose 35 m, then subsided; some lava ejected.

TABLE 1.—*Continued*

O Shima date	Other Izu Islands date	Other Izu Islands island	Remarks
1939 Aug. 9 to Sept. 16			Collapses occurred in inner-pit rim. On September 1 fissures developed in crater and ejecta erupted. On September 2 lava rose 40 m in bottom of inner pit. Lava masses several m in diameter hurled 30–40 m high and smaller pieces 100 to 120 m. On September 16 more lava emitted.
	1940 July 12 to Aug. 5	Miyake	Eruption
1940 Aug. 18 to Aug. 19			Large fissure opened in bottom of inner pit; bombs thrown 100 m high; on August 19 ejecta hurled 500 m high.
	1946	Bayonnaise Rocks	Submarine eruptions
1950 July 16 to Sept. 24			Continuous explosive eruption with frequent emission of lava, which beginning September 13 overflowed crater rim and accumulated in caldera.
1951 Feb. 4 to June 28			Continuous explosive eruption with frequent overflows of lava until April 2; thereafter eruption intermittent
	1952 Sept. to 1953	Bayonnaise Rocks (Myojin Reef)	Submarine eruptions began about September 17 and continued intermittently into 1953; ephemeral small volcanic islands

Sources: Tsuboi (1920), Musya (1941–1951), Omori (1915) (1918), and Nakamura (1915)

served. In 1934 while minor eruptions continued a Tokyo newspaper sponsored a descent by gondola into the inner pit by two reporters in an attempt to dispel this belief. They wore asbestos suits and masks and were lowered to a depth of 380 m, but dared not go lower because of blasts. This descent into a volcano pit surpassed the previous record of 245 m made by A. Kerner at Stromboli (Coleman, 1946, p. 152).

The inner pit began to fill after 1934. Lava emissions occurred in 1935, and in November 1936 the measured depth was only 290 m. After eruptions in 1938, 1939, and 1940 it was only about 180 m (Nagata, 1941, p. 402). Talus continued to accumulate until 1950 (Pl. 3, fig. 1).

Summary of Development

O Shima probably began to form by volcanic eruption in late Pleistocene or early Recent time. The first eruptions were submarine. Several small volcanoes developed to the north, became extinct, and were partly eroded by the sea. As O Shima Volcano grew, sufficient material was deposited to join these islets to O Shima. Faulting produced the escarpment along the eastern coast. Several minor eruptions on the outer slopes built small parasitic cones. At the southeast end of the island two phreatic explosions formed small craters. The caldera resulted from a major subsidence. Thereafter, renewal of eruption within the caldera area formed the central

cone of Mihara Yama, from which eruptions have continued intermittently.

TABLE 2.—CHEMICAL ANALYSES OF O SHIMA LAVAS

Per cent by weight

	1 Somma lava	2 Mihara 1778	3 Mihara 1912–14	4 Mihara 1950	5 Basalt mean
SiO_2	53.01	52.45	52.53	52.25	49.87
Al_2O_3	14.73	13.48	15.25	15.55	15.96
Fe_2O_3	3.38	4.60	2.69	2.92	5.47
FeO	9.42	10.02	10.57	10.22	6.47
MnO	0.34	0.31	0.24	.06	0.32
MgO	4.97	4.78	4.54	4.86	6.27
CaO	9.09	10.23	10.76	9.92	9.09
Na_2O	2.09	1.99	1.89	1.72	3.16
K_2O	0.44	0.52	0.43	0.39	1.55
TiO_2	1.03	1.39	0.74	1.57	1.38
P_2O_5	0.11	0.33	0.41	tr	0.46
ZrO_2	0.04	tr	tr	....	....
H_2O	1.22	....	....	0.71	....
	99.87	100.10	100.05	100.17	100.00

1. Somma lava. Location, south shore at east end of Sashikiji. Analyst, Ohashi (Tsuboi, 1920, p. 71).
2. Mihara Yama lava, 1778. Location, north foot of Mihara Yama. Analyst, I. Iwasaki (Iwasaki, 1935).
3. Mihara Yama lava, 1912–14. Location, northwest part of crater floor of Mihara Yama. Analyst, I. Iwasaki (Iwasaki, 1935).
4. Mihara Yama lava, 1950. Location, west foot of Mihara Yama. Analyst, G. Osaka (Minakami, 1951a, p. 9).
5. Basalt, mean value, computed by Daly (1914, p. 27).

PETROLOGY

Lava

Basaltic rocks compose O Shima (Tsuboi, 1920; Tsuya, 1937; Tsuya and Morimoto, 1951). The somma lava composing the older O Shima Volcano predominates. It is exposed in the somma cliffs, in ravines on the outer slopes, and in some sea cliffs. Most of it is a siliceous basalt with phenocrysts of calcic bytownite, small amounts of mafic minerals, small sparse crystals of olivine, and very little hypersthene and augite (Tsuboi, 1920, p. 68–70).

The lava consists of a black, porous, slaggy variety, a compact gray variety almost free from vesicles, and transitional forms. The groundmass of the black variety consists of labradorite prisms, pigeonite grains, small anhedra of magnetite, and interstitial glass that is colorless or brown from fine inclusions. The glass contains occult quartz. The nearly holocrystalline groundmass of the gray variety contains about equal amounts of felsic and mafic minerals. It consists of labradorite, pigeonite, euhedral magnetite, and a small amount of interstitial glass (Tsuboi, 1920, p. 67–72; Iwasaki, 1935). Because the lava is less siliceous and more femic than bandaite, Tsuboi applied the term "basaltic bandaite" (1920, p. 72). The ratio of iron to magnesium is high compared with the average basalt (Table 2).

Other types of lava also occur. A siliceous hypersthene basalt contains hypersthene phenocrysts in moderate quantity and minor augite and olivine. A siliceous hypersthene-augite basalt has both hypersthene and augite phenocrysts in moderate quantity but lacks olivine. A hypersthene-bearing augite-olivine basalt has augite, olivine, and some hypersthene phenocrysts, and a groundmass in which mafic minerals equal or exceed the felsic (Tsuboi, 1920, p. 73–79).

The lavas of the central cone, Mihara Yama, are considered one type. They are siliceous basalts in which the phenocrysts are chiefly calcic bytownite, with some hypersthene, augite, and magnetite. The phenocrysts compose 5–10 per cent of the rock volume. Those of plagioclase commonly are 2–3 mm long; the others are smaller. Olivine is absent. The groundmass is of two varieties comparable in color, texture, and composition to the two varieties in the somma lava, except that the plagioclase is typically sodic bytownite.

The lava of the central cone has slightly more lime, and less soda and magnesia, than that of the somma (Table 2). In the lava of the central cone olivine is absent, and the plagioclase of the groundmass is usually sodic bytownite, whereas in the somma lava small crystals of olivine are scattered thinly, and the plagioclase of the groundmass is labradorite. Although the lava of the central cone is a siliceous basalt like the somma "basaltic

bandaite," Tsuboi (1920, p. 87) called it "miharaite" because bytownite occurs instead of labradorite as the typical groundmass plagioclase.

The rocks of the remnant volcanoes exposed only along the west part of the north coast are also basalts. At Chiga Saki the hypersthene-augite-olivine-anorthite basalt has sodic bytownite as the plagioclase of the groundmass. At Kazahaya an olivine-bytownite basalt has sodic bytownite in the groundmass. East of Kazahaya an olivine-bytownite diabase has sodic bytownite in the groundmass (Tsuboi, 1920, p. 88–96).

Ejecta

Mihara Yama ejected volcanic dust, ash, sand, lapilli, bombs, blocks, and masses up to 5 m long. The volcanic ash and sand are black, red, and dark-brown fragments of glass and small crystals of bytownite. Most of the ash and sand originated from ejected lava (Tsuboi, 1920, p. 96–97). The lapilli, chiefly glassy and scoriaceous material that solidified in flight, commonly contain phenocrysts of bytownite. Relatively few are fragments of consolidated rocks. Bombs consist of material that solidified in flight and of ejecta that fell back into a crater pool, acquired a coating of lava, and were re-erupted. Some large masses are formed from lava that solidified in flight, and a few large blocks are fragments from solidified lava. Bombs and blocks occur on the surface only in the vicinity of Mihara Yama.

Chemically the ejecta are similar to the lava from Mihara Yama. However, like scoriaceous surface lava, ferric iron is increased (from about 2.9% to 3.5% or 4%) at the expense of ferrous iron (Tsuya *et al.*, 1952).

Eruption of 1950

Condition Before Eruption

Mihara Yama was quiescent for almost 10 years after its minor eruption on August 18–19, 1940. Only a few small fumaroles emitted steam from fissures along the south side of the crater wall. The rough floor of the crater, composed of red lava emitted in 1914, had open joints and lava blocks shoved over each other. Near the edge of the inner pit the red lava was plastered with scattered black clots of lava thrown from the bottom of the inner pit during the 1940 eruption.

The inner pit, approximately 300 m in diameter and 165 m deep, had nearly vertical walls (Fig. 5A; Pl. 3, fig. 1). At the bottom some talus had accumulated on the ejecta deposited during the 1940 eruption. Steam issued at times.

In May 1950 a reporter for the Tokyo Mainichi newspaper descended into the inner pit. He recorded an air temperature of 21.2°C at the bottom, compared with 16°C at the top. No unusual phenomena were observed (Kizawa, 1951a).

Beginning of Activity

The 1950 eruption commenced about 9:15 a.m. standard time (Zone I, 135°E., 12:15 a.m., G.C.T.) on July 16, without prior seismic or other warning. A dense fog prevented observation by people present at Kako Jaya (Crater Teahouse) on the northwestern rim of the crater. Rumblings were heard, and the Wiechert seismograph at the O Shima Meteorological Observatory began to record tremors (Kizawa, 1951b).

Eruption began from fissures in the south wall of the inner pit about 30 m below the rim (Murauchi, 1950). Incandescent material was violently ejected, with detonations heard at the coast, 7.5 km distant, and lava poured from the fissures. Several times in the first few days the explosion outlets in the wall of the inner pit shifted a few meters. As eruption continued, a well-defined vent resulted from rock breaking off the wall and from enlargement of fissures.

Explosive Activity

Explosive activity continued from July 16 until September 24. Explosions occurred at intervals of 3–20 seconds, most commonly of about 10 seconds. Ejecta ranged from ash to great masses of molten lava that in flight separated into pieces, some as large as 3 m long. Ejecta were thrown as high as 500 m. Pieces about 0.4 m in diameter were thrown the greatest distance horizontally; some landed 500 m from the vent.

Ejecta accumulated to form a divided cone, part on the inner pit floor and part perched 100 m higher on the south rim. By August 5 the two parts were joined, but the south side was still much higher. After August 7 slight changes 4 m below the low point in the rim. Large explosions threw up a sheet of lava, a part of which drenched the lower inner slopes of the cone and drained back into the pool. The lava often surged between explosions and over-

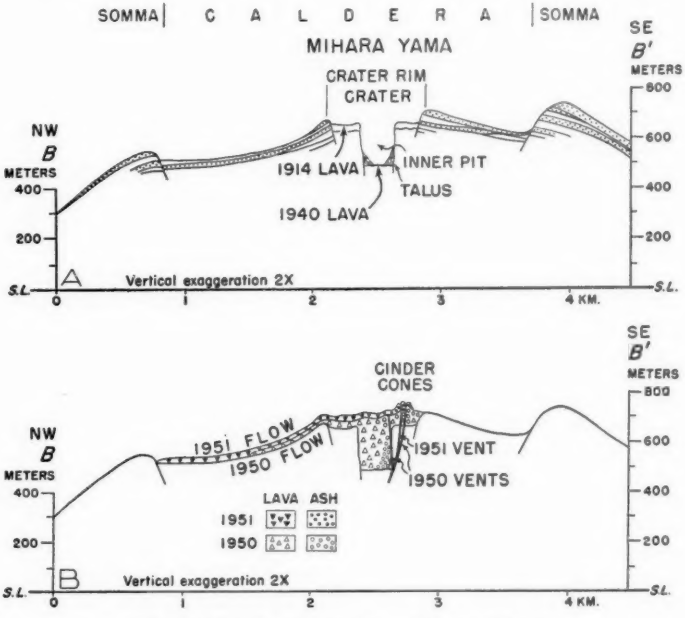

FIGURE 5.—CROSS SECTION OF MIHARA YAMA

A. Prior to 1950 eruption
B. After 1951 eruption but prior to subsidence in crater
Position of section shown in Figure 2

in the position of the vent added irregularities in the growth of the cinder cone. By August 15 the cone was about 50 m above the crater floor (Minakami, 1951a, p. 3).

A new vent developed on August 21 about 100 m south of the first cinder cone (Fig. 6). At first explosions continued undiminished at the older vent, but activity soon began to decrease and on August 23 ceased (Murauchi, 1950). By August 26 the new cone, the final 1950 cinder cone, was 40 m above its base at its highest point, the south side of its rim. At a low point on the northeast side, the rim was only about 25 m high. Molten lava in the crater of the cone formed a pool 18 m in diameter in which pieces of partly solidified lava floated. The surface of the pool was about 3 or flowed at the low point of the rim. The surface temperature of the pool was 800 to 900°C, but a maximum temperature of 1100°C was recorded for fresh inflows (Murauchi, 1950). The cone was 60 m high by September 1 and grew 10 m higher by the end of the eruption (Pl. 3, fig. 2).

The explosions were almost entirely magmatic resulting from the escape of gas (Bonney, 1899, Fig. 19), although occasionally strong explosions resulted from the rupture of rock barriers that confined high pressures. Bubbles of gas coalesce as larger bubbles rise faster and overtake smaller ones. Hence, after very large bubbles reach the surface, a short period of quiet usually follows. As the bubbles rise they expand at a geometric rate. Each time their

depth is halved the hydrostatic pressure of the lava column is halved. When the lava stands at the level of the ground surface, the bubbles reaching the surface are suddenly released from all except atmospheric pressure. Their explosive expansion throws out lava, which accumulates to form a cinder cone (Fig. 7). When hydrostatic pressure of the lava column increases, the lava overflows the low point of the cinder cone or, more commonly, escapes quietly as a flow from a side fissure. Despite the outpouring of lava, explosive activity usually continues undiminished, since the path of escape of the gas remains the same. Less commonly during eruption, the level of the lava is below the mouth of the vent. Underground explosions are not so strong as surface explosions because gas pressures within the confined duct exceed atmospheric pressure. Erupted lava hits the ceiling of any curved duct, and most drains back. Only small pieces that could be carried by the gas outblast reach the ground surface (Fig. 8).

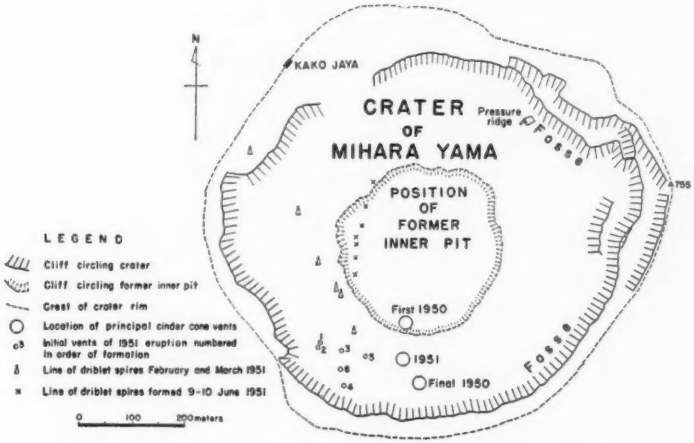

FIGURE 6.—SKETCH MAP OF CRATER OF MIHARA YAMA

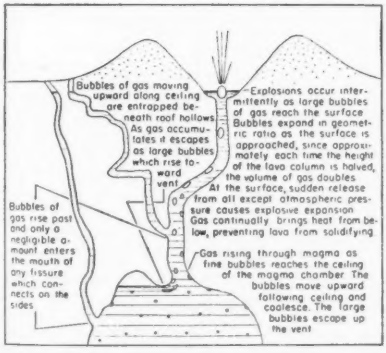
Bubbles of gas moving upward along ceiling are entrapped beneath roof hollows
As gas accumulates it escapes as large bubbles which rise toward vent
Explosions occur intermittently as large bubbles of gas reach the surface. Bubbles expand in geometric ratio as the surface is approached, since approximately each time the height of the lava column is halved, the volume of gas doubles
At the surface, sudden release from all except atmospheric pressure causes explosive expansion
Gas continually brings heat from below, preventing lava from solidifying
Bubbles of gas rise past and only a negligible amount enters the mouth of any fissure which connects on the sides
Gas rising through magma as fine bubbles reaches the ceiling of the magma chamber. The bubbles move upward following ceiling and coalesce. The large bubbles escape up the vent

FIGURE 7.—SURFACE EXPLOSIVE ERUPTION OF MIHARA YAMA

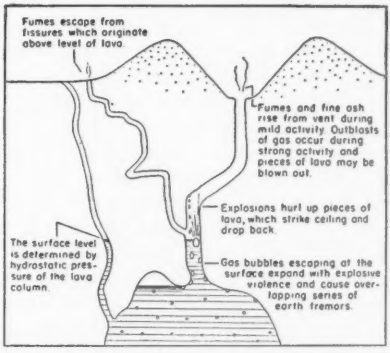
Fumes escape from fissures which originate above level of lava
Fumes and fine ash rise from vent during mild activity. Outblasts of gas occur during strong activity and pieces of lava may be blown out.
Explosions hurl up pieces of lava, which strike ceiling and drop back.
The surface level is determined by hydrostatic pressure of the lava column.
Gas bubbles escaping at the surface expand with explosive violence and cause overlapping series of earth tremors.

FIGURE 8.—UNDERGROUND EXPLOSIVE ERUPTION OF MIHARA YAMA

Lava Emission

Lava emerged the first day from the fissures where the eruption began, but by the next day lava from other openings began to accumulate at the bottom of the inner pit. The sources of

lava soon became concealed beneath accumulations of ejecta and flows. Most lava was emitted quietly from openings other than the explosion vents. After filling the inner pit, on August 15 lava overflowed onto the floor of the crater (Fig. 5B) (Minakami, 1951a, p. 2). The lava rose within the crater and on September 13 overflowed the lowest point of the rim about 150 m northeast of Kako Jaya and descended the slopes of Mihara Yama to the caldera floor. Within the next few days lava overflowed the crater rim at two other places, about 100 and 250 m southwest of the teahouse (Murauchi, 1950).

Termination of Eruption

On September 23 about 8:30 p.m. explosions suddenly ceased, and half a minute later a blast of gas, black with dust, shot upward several hundred meters. After the first blast, gas was emitted quietly, and large black billows ascended about 500 m before drifting southward. The black cloud presumably was formed from the expulsion of volcanic ash and dust that choked the vent after a drop in the level of the magma caused collapse. After a few minutes, explosions resumed.

Explosion ceased about 9 p.m., and after a pause a similar blast of gas was followed by quiet emission of black billows. Once more explosions resumed, but about 2 a.m. or 3 a.m. on September 24 eruption ceased.

Only a few bluish fumes and a sulfurous odor issued from the vent in the morning. The fumes within the orifice limited visibility to a depth of 2 m. The opening was 5 m by 3 m across, and its sides were solid. The inside slopes of the cone were rough and irregular, consisting partly of talus slopes of large clinkers and partly of steeper slopes of fused and compacted scoria. Where freshly exposed by slides, this scoria was red hot. Between the orifice and the bottom of the inside slopes a nearly level area about 2 m wide had been kept cleared of fragmental material by outblast from the vent. The rim of the cone was elliptical and about 12 m above the mouth of the vent. Its long diameter (east-west) was 60 m, and its short diameter 40 m. The outer slopes were loose clinkers at the angle of repose.

The cone was about 70 m high and only 2 m below the highest point on the island. Within 1 week, however, it subsided about 8 m (Takahashi, 1951). Slides from the inner slopes filled and concealed the vent. Concentric cracks on the rim formed as arcuate slices slumped inward. Lava emission ceased when explosive activity ended on September 24, although previously emitted lava continued to flow down the western slope of Mihara Yama for 4 days.

Eruption of 1951

Renewal of Eruption

Mihara Yama resumed eruption about 12:30 p.m. on February 4, 1951. The first new vent was on the crater floor about 200 m northwest of the final 1950 vent (Fig. 6) (Volcanological Subsection, 1951). Explosions were small, except for one about 12:50 p.m. of the first day, when ejecta were hurled more than 150 m high.

A second vent appeared on the morning of February 5 so close to the first that the accumulated scoria formed a single spatter cone a few meters high. About 5 p.m. a third vent formed about 40 m east of the first vents (Murauchi, 1951). These vents curved irregularly below their mouths and emitted blasts of hot gases that tossed up small amounts of molten lava. The ejecta were hurled only 5–10 m high and during stronger blasts a maximum of 50 m. The blasts lasted for 3 to 5 minutes, followed by 4 to 10 seconds of quiet.

The cyclic outblasts of gas may be explained by the presence of an enlargement in the duct leading from a magma reservoir to the surface (Fig. 9). The uniform gas flow during periods of emission suggests that the surface of the magma was near the top of a reservoir, allowing a steady release of gas. The expanding gas would throw up lava, most of which would fall back, but some pieces would be blown up the duct by the blast of the escaping gas. Pieces blown out of the vent would accumulate to form the small cinder cone. If an enlargement existed in the duct, however, many pieces would hit the ceiling and fall back. The material deflected from the ceiling, prevented from flowing down the duct by the continuous outblast, would accumulate around the mouth of the duct. After 3–5 minutes of accumulation,

the weight of the mass might be too great to be held back by the blast. While the accumulation drained down the duct the outblast would be stopped for 4–10 seconds.

A fourth vent, 70 m south of the third vent, on February 13 began to issue lava which flowed 100 m on the crater floor, but the outflow stopped after 1 day (Volcanological Subsection, 1951). Small clots of ejected lava formed a cinder cone. In the next few days a small fifth vent (Murauchi, 1951) formed 70 m northeast of the fourth vent, and a sixth about 30 m north (Fig. 6).

Lava began to well up at times through cracks near these vents, and eventually it covered the crater floor. After solidification of the lava, a large fissure extended from a point near the fifth vent northwestward about 400 m to the crater rim.

The several vents had common periods of minor explosive activity and lull, but the relative strength of the explosions shifted among them. None of their cones was more than 8 or 10 m high. These initial vents gradually became inactive after the appearance of the principal vent.

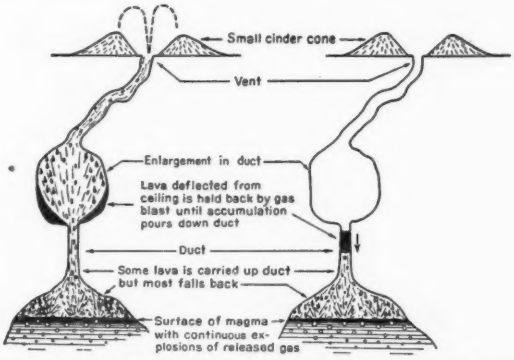
Small cinder cone
Vent
Enlargement in duct
Lava deflected from ceiling is held back by gas blast until accumulation pours down duct
Duct
Some lava is carried up duct but most falls back
Surface of magma with continuous explosions of released gas

FIGURE 9.—CYCLIC OUTBLAST FROM SMALL VENT IN 1951 ERUPTION

Formation of Principal Vent

The principal 1951 vent developed on February 21 as an elliptical cave-in on the north-northwest side of the final 1950 cinder cone (Fig. 6) (Suwa, 1951). Several small vents also appeared on the slope just below it, but these did not remain active long. Large explosions were common, and until the end of March the activity was comparable in magnitude to that of the 1950 eruption. The accumulation of ejecta from the principal 1951 vent resulted in a cinder cone compound with the final 1950 cone.

A row of driblet spires formed northwest of the principal vent on the crater floor above the long fissure (Fig. 6; Pl. 5, fig. 1). From their small vents nearly continuous blasts of hot gases issued, and occasionally clots of molten lava were plastered around the mouths of the vents or blown out and added to the exteriors of the spires. The spires were 3–6 m high. Small flows of lava oozed out of cracks in their lower parts and solidified as pahoehoe.

Lava Flows

Lava issued from various openings in the crater floor and on February 28 overflowed the west side of the crater rim to the floor of the caldera (Rikitake, 1951a). On March 1 the new lava reached as far as the tip of the longest 1950 lava flow on this side and continued beyond it (Figs. 5B, 10). The overflow on the rim widened and reached as far as Kako Jaya by March 9 (Suwa, 1951) and ignited the roof and timbers of the teahouse. The concrete walls withstood the flow, but lava entered through doors and windows, filled the interior, and poured out through openings on the opposite side. On March 17 lava crossed the caldera and reached the base of the somma

wall (Suwa, 1951). These flows are collectively known as the Kagamibata flow (Pl. 2, fig. 2).

Lava suddenly welled up in large volume at 9:55 p.m. on March 24 in the northwestern part of the crater. In a few seconds the lava spread over about 40,000 square m of the crater floor forming a pond, and then in a stream about 150 m wide cascaded over the west side of the crater rim at an estimated speed of 50 km per hour. It resembled flood waters as it cascaded over the rough surfaces of previous flows and on the caldera floor developed eddies at its margins. Meanwhile explosive eruptions at the cone continued unchanged. Lava continued to flow during the night, but the original stream blocked itself off and the flow shifted southward in a stream narrower than the original one. As a result of the higher outlet, the pond enlarged somewhat. On its west side a line of lava fountains spurted 5 or 6 m high.

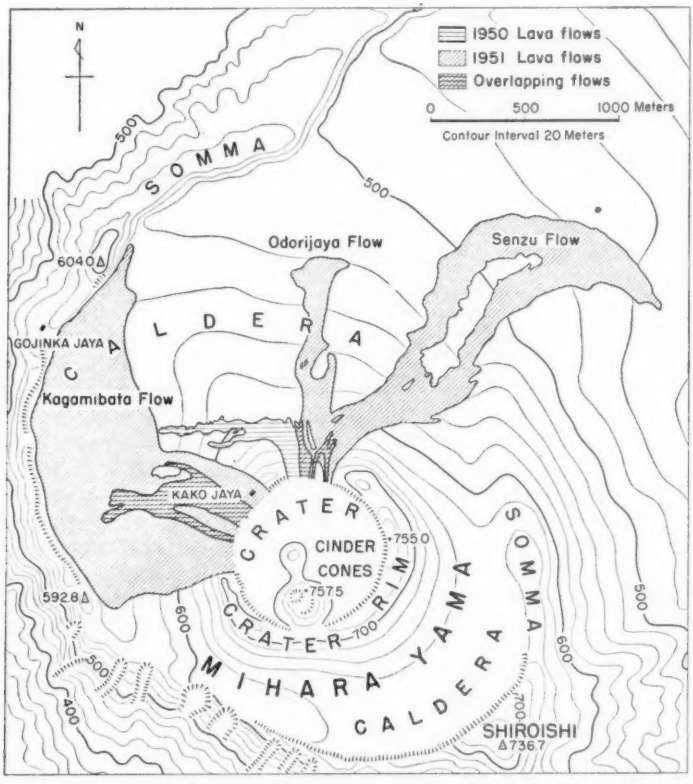

FIGURE 10.—MAP OF MIHARA YAMA ON APRIL 20, 1951

The 1951 cinder cone was at its maximum altitude, 757.5 m, but height reduced a few days later by partial collapse. Lava flows advanced no further although eruption continued intermittently until June 28.

Lava flowed over the north side of the crater rim on March 27 and 28 and formed the Odorijaya flow to the north and the larger Senzu flow to the northeast (Suwa, 1951). The Senzu flow was 2500 m long and averaged 250 m wide. Until March 30 it flowed through the gap in the somma in the same general direction as the principal flow in 1778 (Suwa, 1951).

Some of the feeding channels in the crater floor developed into a series of tunnels, a few more than 5 m wide. In one place in the north-

east part of the crater floor a pressure ridge (Shrock, 1948, p. 370) formed when the crust, which was about 45 cm thick, buckled up to form an inverted V having a base about 2.5 m and a height about 3 m (Fig. 6; Pl. 5, fig. 2). A medial wedge of fluid lava filled the space under the upbuckle, and some lava escaped through the ridge crack. As it solidified on the inclined sides it looked like stacked sandbags and festoons of rope. Later the wedge was drained, and the triangular hollow passage was left. Subsequent collapse at each end exposed the cross section.

A fosse was formed along the east periphery of the crater where the base of aa flows impinged on the crater wall. The sides of the fosse were made by the slope of the upper part of the aa front on one side and the inner slope of the crater wall on the other side. Both in 1950 and in 1951 several aa flows reached this part of the periphery of the crater, but the fosse persisted.

Intermittent Activity and Subsidences

The lava flows abated at the end of March, the lava pond cooled, and the principal vent stopped erupting on April 2. Thereafter the first of several major subsidences within the crater occurred. Fissures appeared, and slumping occurred on the inner and outer slopes of the cinder cone (Pl. 3, fig. 3). In the northwest part of the crater floor the subsidence was greatest and ranged from a few to about 20 m. The aligned driblet spires dropped with the floor and were tilted and broken. Four of the six initial vents disappeared. The welded lava lining the third vent stood as a spire above the subsided area, with an affixed shelf on one side consisting of an uncollapsed part of the crater floor. The fourth vent was south of the collapse.

From April until the end of the eruption on June 28 activity was intermittent. There were nine principal periods of eruption, lasting from less than an hour to a few days. Explosions occurred on the surface and underground (Figs. 7, 8). Parts of the crater floor and of the 1950 and 1951 cinder cones subsided between eruptions.

The most violent eruption during 1951 occurred during the first period, from the early morning of April 16 until April 19. Explosions regularly carried ejecta 250 m high, (Murauchi, 1951). Ejecta soon covered the fissures and began rebuilding the cone. The principal 1951 vent and the crater of the final 1950 cone were so near each other the rim directly between them was low because of slides. Material that fell in this vicinity either rolled back into the vent or partly filled the final 1950 crater. However, ejecta accumulating on the broader base at the two points where the rims separated formed the two highest points on the crater rim of the vent. The east point grew higher and for a few days after April 18 had an altitude of approximately 757.5 m, 2.5 m higher than the highest point of the island on the crater rim of Mihara Yama (Fig. 10) (Murauchi, 1951).

During the eruption of April 16–19 lava filled the area that had subsided in early April and formed two ponds, one about 150 by 50 m and the other about 140 by 90 m, and then advanced over other parts of the crater floor (Volcanological Subsection, 1951). It surrounded the spire left by the previous collapse, reached the level of the affixed shelf, and overflowed the crater rim on the west side, the last time lava overflowed the crater rim in 1951.

After 10 days, two more eruptions occurred only a few days apart. The first consisted of brief explosions between April 29 and May 3 (Suwa, 1951). The second lasted 30 hours on May 6–7. Lava fountained from two vents in the central part of the crater (Suwa, 1951), covered the eastern part of the crater floor, and circled in a stream northwestward at the periphery of the floor. The lava accumulated in the areas of collapse and raised the level of the crater floor, but never enough to overflow.

After a month of quiet a large eruption on June 9–10 lasted 27 hours (Murauchi, 1951). Lava filled the subsided areas. Seven driblet spires ranging from 1.5 to 5 m high extended north from the northwest side of the cinder cone (Fig. 6). In the same line and near the foot of some of the spires were several small lava pools ranging from 3–10 m across. In two of them lava fountains spurted 3–4 m high. Between June 14 and 22 four periods of activity lasted 13–21 hours each. Some individual explosions on June 14 and 21 were unusually large, and a few fragments were hurled as much as 500 m high. Air concussions were felt at a

weather station 40 km away on the mainland on June 21 (Suwa, 1951).

The final activity on June 27 and 28 was the second biggest of the 1951 eruption. It began about 3:45 p.m. and continued until noon the next day (Murauchi, 1951). Ejecta accumulated to a thickness of 5 m on the south rim of the final 1950 cinder cone, 150 m south-southeast of the vent. Masses of molten material up to 5 m long and 1 m wide, ellipsoidal bombs 0.5 m long, and splash bombs 0.35 m in diameter dropped on the crater rim 300 m west (Pl. 5, fig. 6). Some bombs were thrown over the western crater rim and halfway down the slope. At the foot of Mihara Yama 700 m west of the vent, 0.5 m of lapilli accumulated. Ash fell over the northern three-fourths of the island. At Motomura, 4.5 km northwest, the fall was so heavy the villagers carried parasols for protection. After June 28 eruption ceased, except for slight emission of fumes.

The subsequent subsidence was the largest in 18 years. The major subsidence occurred about July 1, but minor adjustments took place for several weeks thereafter. A crudely circular depression 150 m in diameter and 50 m deep formed in the area of the compound cone. Its sides consisted of the uncollapsed outer parts of the compound cone. The collapse engulfed material around and between the principal 1951 vent and the final 1950 vent. The collapse extended south within 80 m of the crater rim of Mihara Yama. At this point, part of the south side of the final 1950 cone was left as the highest point within the crater rim. On the north side the collapse was separated from a second area of subsidence by a

---

PLATE 2.—CENTRAL CONE, MIHARA YAMA

FIGURE 1.—MIHARA YAMA, SEPTEMBER 1950

Crest of low, truncated cone comprises crater rim. Highest point of island, 755 m altitude, on left (east) side on crater rim. Cinder cone within crater just visible above crater rim. From it rise steam and some ash. View south-southwest from somma.

FIGURE 2.—OBLIQUE AIRPHOTO OF MIHARA YAMA, MARCH 23, 1951

Somma largely encloses caldera, within which rises truncated cone of Mihara Yama, the crater filled with dark lava. Principal 1951 cinder cone on far (south) side where steam rises. Large Kagamibata flow advances north; smoke indicates burning brush—left of *X* which marks location of Gojinka Jaya on somma. Small flows to left formed in 1950. Shiroishi, highest point of somma, directly beyond Mihara Yama. Above it and slightly to right on coast is Habu Minato. View southeast. Asahi Shimbun photo.

PLATE 3.—CRATER OF MIHARA YAMA

FIGURE 1.—INNER PIT IN 1949

Inner pit near center of crater floor was 300 m wide and 165 m deep. Eruption in 1950 began from fissures on left side 30 m below crater floor and filled pit. Wisp of steam rises left of center from small fumarole at base of crater rim. View west-southwest.

FIGURE 2.—ERUPTION OF FINAL 1950 CINDER CONE, SEPTEMBER 23

Cone about 70 m high except where far left (south) slope overlaps crater rim. Heavy ash falls nearly conceal earlier lava flows on crater floor in foreground. View southwest from east side of crater rim.

FIGURE 3.—1951 CINDER CONE, APRIL 14

Partial collapse occurred in lull between end of period of continuous eruption and beginning of period of intermittent eruption. Slumping occurred inside cinder cone. Front left (northwest) slope slumped into depression in crater floor. Rough lava flow in foreground is an uncollapsed part of crater floor. View east-southeast from crater rim.

FIGURE 4.—COLLAPSE FOLLOWING 1951 ERUPTION

Floor of crater collapsed at site of pre-eruption inner pit, forming depression 250 m wide and 40 m deep. Beyond right side of picture another collapse occurred at site of principal 1951 cinder cone. View east, toward highest point of crater rim, 755 m altitude.

FIGURE 1

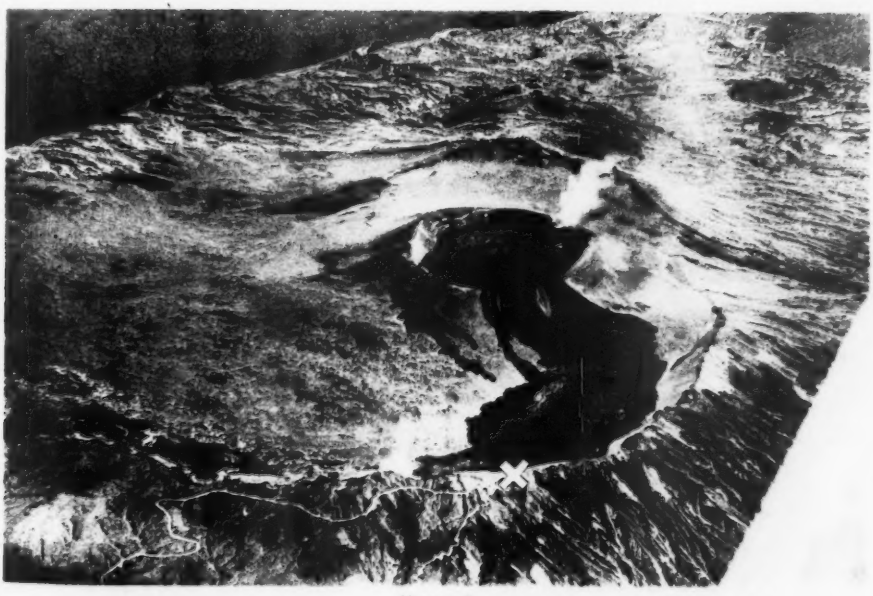

FIGURE 2

CENTRAL CONE, MIHARA YAMA

FIGURE 1

FIGURE 2

FIGURE 3

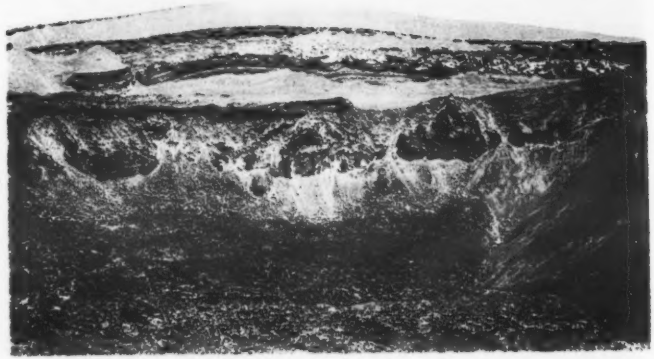

FIGURE 4

CRATER OF MIHARA YAMA

CRATER OF MIHARA YAMA

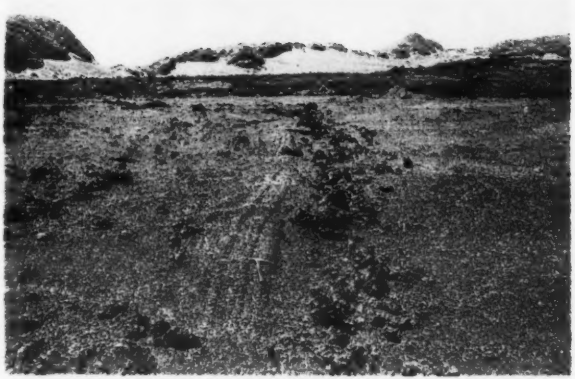

FIGURE 1

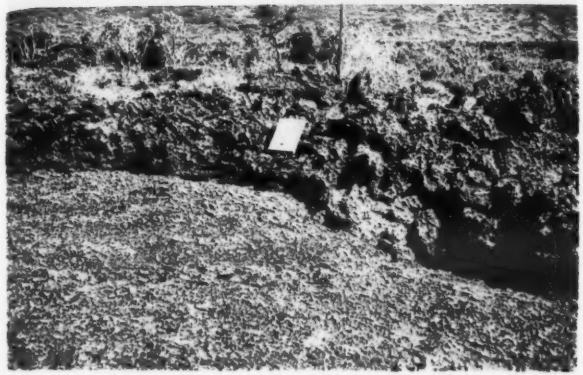

FIGURE 2

FIGURE 3

FIGURE 4

DRAWN-SURFACE PAHOEHOE LAVA

FIGURE 1

FIGURE 2

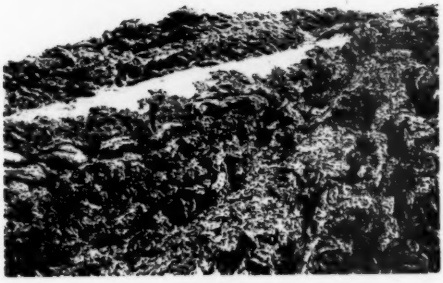

FIGURE 3

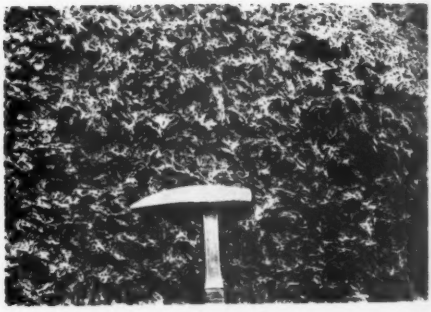

FIGURE 4

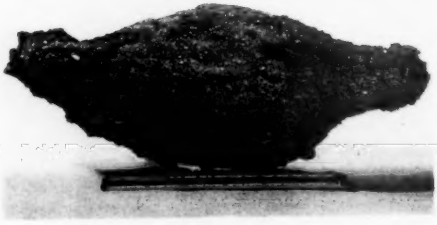

FIGURE 5

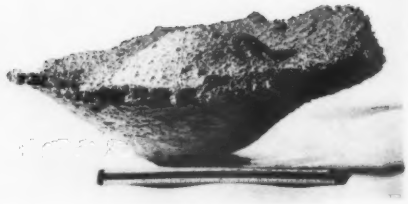

FIGURE 6

LAVA FEATURES

low jagged wall, a relic from slides accompanying the subsidences. This second depression had a diameter of 250 m and a depth of 40 m below the crater floor. It was located approximately in the position of the former inner pit (Pl. 3, fig. 4).

PLATE 4.—DRAWN-SURFACE PAHOEHOE LAVA

FIGURE 1.—LAVA FLOW WITH DRAWN SURFACE

Large areas of Kagamibata flow within caldera congealed with a drawn surface. Parallel ribs leading away from center foreground in direction of flow reflect shape of outlets through which lava was extruded. After surface hardened, extrusion of viscous lava through a crack formed line of aa fragments right of center. Subsequent ash fall partly conceals features. View north-northwest toward somma, on which Gojinka Jaya stands at low point of far right horizon.

FIGURE 2.—DRAWN AND AA LAVA SURFACES

After drawn-surface pahoehoe formed (foreground) near toe of Kagamibata flow, lava still flowing beneath became viscous enough to form aa upon exposure at margins of pahoehoe surface. Jointed marginal pieces of pahoehoe were plucked off by aa, resulting in abrupt transition between the two types. Field notebook rests on aa lava.

FIGURE 3.—CLOSE-UP OF DRAWN-SURFACE PAHOEHOE

As crust was forming on horizontal surface of flow, lava while still viscous was slowly drawn out by flow movement beneath it, forming stringy flakes in linear arrangement. Pencil 14 cm long.

FIGURE 4.—SLAB PAHOEHOE

Thin crust of drawn-surface pahoehoe formed, but after hardening it was broken and many fragments were upended by later underflow of more viscous lava. View of Kagamibata flow on caldera floor west-northwest toward somma.

PLATE 5.—LAVA FEATURES

FIGURE 1.—DRIBLET SPIRE

Row of spires formed in February 1951 on the crater floor along fissure (Fig. 6). Spire built by welding of pieces of molten lava occasionally tossed out by continuous outblast of gas. At base in foreground occasional small issues of lava solidified as skin pahoehoe in grotesque forms.

FIGURE 2.—PRESSURE RIDGE

Crust of lava flow on crater floor buckled up to form pressure ridge. Fluid lava beneath spurted out through crack on top and solidified on sides like stacked sandbags. After lava drained, hollow passage was left, exposed in cross section by partial collapse of ridge. View toward northeast crater rim, April 21, 1951 (Fig. 6).

FIGURE 3.—LAVA STREAM OVERFLOWING CRATER RIM

Most of time lava overflowed, streams were small. As bottom layer of small stream cooled, level of surface rose. Flow was about a meter above its surroundings, and confined in its channel by nearly vertical, self-built side wall only a few centimeters thick at ragged top. Stream flowed 2 m per second, and lava shot past gaps in side wall lower than surface of stream.

FIGURE 4.—UNDERSIDE OF CRUST OF DRAWN-SURFACE PAHOEHOE

As crust hardened, its soft underside was roughened both by drag as underflow dropped from contact with crust, and by pendants formed by drip of lava splashed up from underflow.

FIGURE 5.—SPINDLE-SHAPED BOMB

Separation of ribbon of lava in flight produced bombs with spindle ends drawn out to points of separation. Such bombs had a wobbly motion in flight; their points were not spiral and there was no indication of spinning. Upper scale 15 cm long.

FIGURE 6.—SPLASH BOMB

Ball of somewhat plastic lava, falling on loose ash and lapilli, splashed and conformed to its impact depression. This bomb landed on crater rim 300 m west of cinder cone on last day of eruption, June 28, 1951. Upper scale 15 cm long.

Geophysical Observations

Seismic Activity

A Wiechert horizontal- and vertical-motion seismograph is in operation at O Shima Meteorological Observatory, about 4.9 km north-northwest of Mihara Yama. No unusual seismic activity was recorded in the horizontal motion

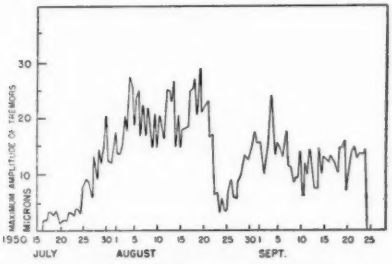

Figure 11.—Maximum Amplitude of Tremors During 1950 Eruption

Seismograph located at Meteorological Observatory, 4.9 km from eruption.

previous to the beginning of the 1950 eruption on July 16. For 2 months before the eruption the vertical motion recorded tremors so slight they were not interpreted as forewarnings (Kizawa, 1951b).

The Earthquake Research Institute installed a seismograph at Motomura on September 3, and a record was kept until the end of the 1951 eruption. Five other stations were temporarily occupied for short periods between September 3 and 23, 1950. These six stations and their distances from the crater vents were: (1) Kako Jaya on the west part of the crater rim, 0.6 km northwest; (2) Gojinka Jaya on the west part of the somma, 2.0 km northwest; (3) Yuba near the north part of the somma, 3.6 km north; (4) Motomura on the west coast, 4.6 km northwest; (5) Habu on the southeast coast, 5.8 km southeast; and (6) Okada on the north coast, 6.7 km north. The seismographs used were inverted pendulum type, which recorded the horizontal component of motion and were adapted to record acceleration (Minakami *et al.*, 1951).

Tremors recorded by the Wiechert seismograph at the Observatory were continuous during the 10 weeks of the 1950 eruption. Maximum amplitudes were recorded in those tremors having a period of about 0.6 second. For nearly a month the maximum amplitude for each day was near 20 microns, but a decrease to about 5 microns occurred between August 22 and 25 when activity shifted from the first to the final 1950 vent, although no decrease in total eruptive action was noted by

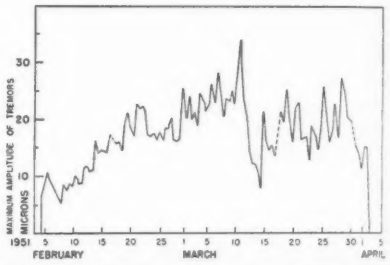

Figure 12.—Maximum Amplitude of Tremors, February to April, 1951

eye witnesses (Fig. 11). After 2 p.m. on September 23 the tremors decreased in amplitude, and after 4 p.m. on September 24 they could not be detected (Kizawa, 1951b).

At the six stations of the Earthquake Research Institute the maximum daily amplitudes differed little during the 3 weeks of observation in September, owing to the general similarity in the character of the eruption. The largest maximum amplitudes were recorded for tremors having a period of 0.6 second, as at the Observatory, and successively smaller maximum amplitudes were recorded for tremors having periods of 0.5, 0.4, 0.3, and 0.2 second. The largest amplitudes recorded at each of the six stations as measured in microns, all for tremors in the 0.6-second class, were: (6) 7; (5) 8; (4) 13; (3) 19; (2) 40; (1) 100. The geometric increase with approach to the crater vents, particularly for the nearest stations, indicates that the tremors originated within 300 m of the ground surface (Minakami *et al.*, 1951), presumably mostly from explosions near the top of the molten lava column.

During the 1951 eruption, tremors similar to those of 1950 were recorded by the Wiechert seismograph from the beginning of the eruption of February 4 to April 2, 1951 (Fig. 12). The maximum amplitude recorded during this

period was 34 microns on March 11. This figure was exceeded during four of the nine principal periods of intermittent activity that followed from April 16 to June 28 (Fig. 13). An amplitude of 54 microns was recorded during the eruption of April 16–19 (Kizawa,

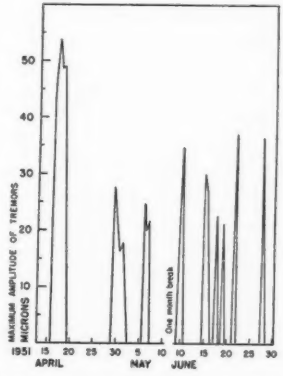

FIGURE 13.—MAXIMUM AMPLITUDE OF TREMORS DURING PERIOD OF INTERMITTENT ERUPTION, APRIL THROUGH JUNE 1951

1951b), the largest recorded at this station during either 1950 or 1951.

The frequency of explosions caused a complex overlapping of tremors on the seismograms, but the wave pattern of individual volcanic earthquakes could in some cases be distinguished. These were most apparent during the 1950 eruption; there were more than 50 on August 5, and 40 on August 8. On most days, however, there were less than 10. During the 1951 eruption, only 1 or 2 individual wave patterns per month were detectable (Kizawa, 1951b).

Geomagnetism

Two geomagnetic surveys had been conducted on O Shima prior to the 1950 eruption. In 1928 a magnetic dip survey was made. In 1936, three-component measurements were made with a magnetometer of the Japanese Hydrographic Department at 12 stations almost equidistant around the coast, and some measurements of dip only were made within the somma. Additionally, three-component measurements at four stations were made by the Hydrographic Department in 1913, 1933, and 1943 (Rikitake, 1951b, p. 161).

After eruption began three dip surveys were conducted, in July and September 1950 and in March 1951. Observations with a small earth

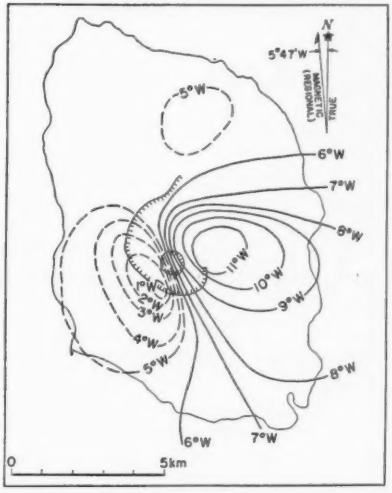

FIGURE 14.—MAGNETIC DECLINATION ON O SHIMA, 1951

Solid lines show local declinations greater than regional, dashed lines less.

inductor were taken at 36 stations on the island.

A three-component survey was also made at 10 stations in May 1951. A magnetometer of the Geographical Survey Institute was used having an accuracy of 0.1 second in declination and inclination and 1 gamma in horizontal intensity (Rikitake, 1951a).

The regional declination for the O Shima area in 1951 was 5°47′ W. In the vicinity of Mihara Yama there is considerable deflection. East of the crater the local declination is greater than the regional; the maximum is about 11°W. in the area 1 km east of the center of the crater. West of the crater the local declination is less than the regional; the minimum declination is about 1°W. in the area 1 km southwest of the center of the crater (Fig. 14). Within 3 km of Mihara Yama, the north needle is deflected toward a line passing through the center of the crater approximately

parallel to the regional declination (Rikitake, 1951c).

The regional magnetic dip in the vicinity of O Shima is 47°50′. Dip angles measured in 1950 on O Shima ranged from 46° to 56°. The largest anomalies were in the area of the somma (Rikitake, 1951b, p. 168–169). Between the July and September surveys of 1950, magnetic dips decreased all over the island; the largest decrease was 30′ in the vicinity of the crater. This decrease could be accounted for by loss of magnetism owing to rise of temperature in a mass having a mean radius of 2 km and a depth of 5.5 km (Rikitake, 1951b, p. 180).

A magnetometer recorded relative changes in declination from April 11 to July 17, 1951, at Nomashi, on the west coast, where the local declination is about 45′ less than the regional. From April 11 to May 12 declination decreased 5′. Continuous activity had stopped April 2, and during April 11 to May 12 there were three brief eruptions, the last on May 6–7. During the month of inactivity that followed, after declination decreased to a minimum on May 12, there was no change until June 1, when declination began to increase slowly until by June 15 it had increased 2′. Meanwhile sporadic eruptions resumed on June 9. From June 15 until the termination of eruption on June 28 declination remained constant. The decrease in westerly declination (an increase in deflection) at Nomashi may correspond to an increase in the magnetization of the rocks to the east underlying the volcano, consequent upon a thermal decrease associated with the decline in volcanism. The minor increase in declination associated with the renewal of sporadic outbursts may correspond to a decrease in magnetization consequent upon a thermal increase. Observations were insufficient to do more than suggest such a relationship (Rikitake *et al.*, 1951, p. 600–602).

Gravity

Four gravity surveys were made on O Shima between September 1950 and April 1951. The first was conducted from September 13 to 17, 1950, during eruptions; the second from November 21 to 26, 1950, when the volcano was quiescent; the third from February 20 to March 3, 1951, when eruption had resumed; and the fourth from April 9 to 13 during the period of intermittent activity. About 50 stations were occupied during each survey. Precise leveling was carried out in conjunction with the third and fourth surveys (Iida *et al.*, 1951).

Gravity anomalies (corrected) of the magnitude of 0.20 to 0.40 mgal were found. The anomalies were greater than could result from changes in elevation, although in some cases such changes accounted for a part of the anomaly. Likewise, the anomalies were much greater than instrumental and observational error, each of which was of the order of 0.01 mgal.

Gravity increased, in general, between the first and second surveys. The greatest change was in the area enclosed by the somma, where increases ranged from 0.17 to 0.58 mgal, and the largest was in the south part of the caldera. The greatest decrease was 0.41 mgal in the southwest part of the caldera.

Between the second and third surveys gravity decreased, especially in the south and east parts of the caldera and the adjacent area northeast outside the caldera (maximum decrease 0.17 mgal). Increases in the northwest part of the somma reached 0.04 mgal. The fourth survey showed a decrease in gravity; a maximum of 0.27 mgal was measured on the outside slope on the east side of the somma.

Geochemical Observations

Fumaroles

Fumaroles in the bottom of the inner pit, on the south and southwest sides of the crater, and at Yuba on the outer slopes 3.6 km north of the crater, showed no change prior to the 1950 eruption (Kizawa, 1951b). Presumably the steam originated from heating of meteoric waters.

The temperature of the steam in the inner pit in May 1950 was 54.6°C. The temperature of the fumaroles on the sides of the crater during April 1950 ranged from 41.0°C to 51.2°C, during May from 46.6°C to 53.0°C, during June from 45.2°C to 53.6°C, and during July from 46.8°C to 54.9°C. The eruption

caused no change except a fumarole situated south of the inner pit had a temperature of 43.8°C on July 4, 36.2°C on July 16 when the eruption began, and 66.9°C on July 24. Subsequently lava flows covered the fumaroles in the crater. At Yuba the steam temperature remained between 48.5°C and 49.5°C (Kizawa, 1951a).

TABLE 3.—ANALYSIS OF CONDENSATE FROM GAS ISSUING FROM DRIBLET SPIRE, MIHARA YAMA, MARCH 1951

(Iwasaki, 1951)

Grams per liter of condensate; ratio of condensate to gas not measured	
Fe	69.8
Cl^-	67.6
S	0.16
Si	0.090
Al	trace
SO_4^-	0.0
Ca, Mg, Ti	0.0

TABLE 4.—ANALYSES OF GAS ISSUING FROM CRACKS IN CRATER FLOOR, MIHARA YAMA, MARCH 1951

(Iwasaki, 1951)

Per cent by volume

	A	B	C
H_2	12.1	57.1	25.9
N_2	65.4	41.9	72.5
O_2	17.0	0.0	0.0
A	1.2	0.8	0.8
CO_2	4.3	0.2	0.8
	100.0	100.0	100.0

Samples A, B, and C taken in sequence from 3 separate cracks.

After eruption ceased, steam and sulfurous fumes issued from an area near the summit of the final 1950 cinder cone. On December 20, 1950, the temperature of this steam was 159.7°C (Kizawa, 1951a).

Volcanic Gases

Gases and sublimates were difficult to collect during the 1950 eruption. During the 1951 eruption, however, gas escaped from driblet spires beyond the range of most missles, and during the last 3 months activity was intermittent, permitting approach to other outlets of gas. Iwasaki collected gases from a driblet spire in 1951 and analyzed the condensate (Table 3). Some of the iron detected may have come from the pipe that was inserted into the orifice, but analyses of sublimates indicates iron in such gas (Iwasaki, 1951).

TABLE 5.—SPECTROSCOPIC ANALYSES OF SPECIMENS FROM 1950 ERUPTION, MIHARA YAMA

(Morimoto, Personal communication, 1951)

	A	B	C	D	E	F
Si	W	VS	....	VS	VS	VS
Al	....	M	....	VS	VS	VS
Fe	VW	VW	....	W	W	VS
Mg	W	S	M	....	M	S
Ca	VS	VS	S	M	VW	VS
Na	....	M	VS	M	VW	....
Sr	....	....	....	....	....	W
Mn	....	....	W	VW	....	S
Ti	....	....	....	....	....	S
P	....	M	....	....	....	....
Cu	....	....	VW	W	VW	....
V	....	....	....	....	....	W
Ba	....	....	VW	....	....	....

A	White crystalline sublimate
B and C	White, fine-grained sublimates
D	Yellowish subtransparent sublimate
E	Bluish incrustation on 1950 lava
F	Reddish-brown alteration product of 1950 lava by fumarolic action
VS	Very strong
S	Strong
M	Medium
W	Weak
VW	Very weak

Gas issuing from the crater floor was collected in a glass vacuum tube and analyzed with a mass analyzer (Table 4). A considerable admixture of air was indicated by the large amount of nitrogen. The radon content of these gases measured 1 to 3 mache (Iwasaki, 1951) (1 mache equals 3.6×10^{-16} curies per liter).

Sublimates

Sublimates collected around the 1951 fumaroles included gypsum, alum, hematite, mala-

chite, and several chlorides. Some bluish-green sublimates contained other copper compounds, some greenish-blue sublimates contained nickel and cobalt, and yellowish-brown sublimates contained iron compounds. Some sublimates were weakly radioactive. R. Morimoto (Personal communication, 1951) and associates made spectroscopic analyses of several sublimates and other specimens from the 1950 eruption (Table 5). The X-ray powder method on four specimens indicated the following minerals: Specimen A, contained gypsum; B, anhydrite; C, sodium and potassium chlorides; F, halloysite, anatase, and alunite. Specimen B was also chemically analyzed (Table 6).

TABLE 6.—CHEMICAL ANALYSIS OF WHITE SUBLIMATE FROM 1950 ERUPTION, MIHARA YAMA

(Morimoto, Personal communication, 1951)

	Per cent by weight
Si	18.07
Ca	31.19
Fe	trace
Mg	trace
SO_3	43.79
H_2O (+)	2.10
H_2O (−)	5.04
	100.19

K, Na, and Al not detected.

PHYSICAL MEASUREMENTS

1950 Eruption

Takahashi (1951) estimated that the 1950 flows and ejecta totaled 21,000,000 cubic m and weighed approximately 52,000,000 m tons. He estimated that 3,630,000 cubic m of material filled the inner pit; 12,210,000 cubic m more filled the crater; 4,220,000 cubic m composed the cinder cones; and 990,000 cubic m flowed over the crater rim. A density of 2.7 was used to calculate the weight of the material filling the inner pit and crater, 1.7 for the cinder cones, and 2.2 for the flows outside the crater because not so many of their voids were filled by subsequent flows.

Lava flows on the west side of Mihara Yama covered 0.11 square km, all of which was buried beneath the 1951 flows. On the north side 0.10 square km was covered, of which 0.03 square km was buried.

Temperature of the 1950 lava was measured by optical pyrometer and thermocouple. The highest temperature was 1246°C, measured by optical pyrometer, for lava outpouring in the inner pit (Morimoto and Ossaka, personal communication, 1952).

The viscosity of lava of undetermined temperature pouring from openings in the crater floor was estimated by Minakami (1951b, p. 3) at 1×10^3 poises. The viscosity of lava at 1,000°C and flowing at 10 cm/sec in a relatively small, narrow stream down a 30-degree slope of Mihara Yama was determined by Suwa (1951) to have been about 100×10^3 poises.

1951 Eruption

During the 1951 eruption, about 20,000,000 tons of lava was emitted (Suwa, 1951). Some of this filled subsided areas within the crater, but most overflowed the rim and congealed on the slopes of Mihara Yama and on the caldera floor. The Kagamibata flow covered 1.10 square km, the Odorijaya flow 0.16 square km, and the Senzu flow 0.60 square km, totalling 1.86 square km. As an area of 0.07 square km of the 1950 flows was not covered by the 1951 flows, the total area of the 1950 and 1951 flows outside the crater was 1.93 square km.

The maximum temperature recorded in 1951 was about 1200°C, for the surface of a lava pool (Suwa, 1951). The hot floods of lava that overflowed the crater rim briefly were not measured. In a stream small enough to be approached on the slope of Mihara Yama the viscosity increased rapidly from 5×10^3 poises to 200×10^3 poises when the lava cooled from 1125° to 1038°C (Table 7). At observation points 1 and 2, on the upper part of the slope of Mihara Yama, the temperatures of the lava at the surface and in the interior of the flow were almost the same. At points 3 and 4 lower down the slope, the temperature at the surface was about 10°C lower than in the interior.

The temperature of this flow at the point where it issued was estimated to be 1150°C, and the viscosity 1×10^3 poises (Minakami, 1951b).

TABLE 7.—VISCOSITY OF SMALL LAVA STREAM ON SLOPE OF MIHARA YAMA, 1951
(After Minakami, 1951b)

Point	Thickness of stream cm	Width cm	Velocity cm/sec	Slope degrees	Viscosity poises $\times 10^3$	Temp. °C
1	31	110	102	35	5	1125
2	50	160	35	27	20	1108
3	77	210	16	16	70	1083
4	130	250	8	11	200	1038

Points 1 to 4 in sequence from crater rim to near foot of slope.

ERUPTED MATERIAL

Types of Lava Flows

Lava emitted within the inner pit flowed only short distances and solidified as some form of pahoehoe. On the crater floor pahoehoe and some aa formed. On the steep slopes of Mihara Yama most flows solidified as aa, but there were small areas of pahoehoe. On the caldera floor most flows solidified as aa, but several solidified with a modified pahoehoe surface, and there were many small areas of pahoehoe.

The composition of flows was essentially the same, but different types of surfaces developed even from a single flow as a result of the conditions affecting the lava during its solidification. The principal factors observed on O Shima were the viscosity of the moving lava and the extent to which the lava, particularly that near the surface, moved during solidification. The viscosity was affected chiefly by temperature, but also by the amount of volatile matter. Movement of the lava was determined by viscosity, the gradient, the size of the flow, and obstructions.

Formation of Pahoehoe

Pahoehoe surfaces developed when a fairly smooth confining surface formed on relatively fluid lava and maintained its continuity during any subsequent deformation. Two types were common, crust pahoehoe and skin pahoehoe.

Crust pahoehoe formed on standing bodies of lava and on streams, particularly where slowed or pooled. Fluid lava, except when erupting or in turbulent flow, quickly formed a smooth surface, either horizontal in a pool or sloping in a stream. When the surface cooled sufficiently, a crust formed. Crust pahoehoe formed on large outpourings of lava where they became somewhat ponded before the surface congealed. Crusts were more likely to form on streams when the flow was steady and did not overrun the crust or leave it unsupported. When the crust while still viscous was dragged slightly by the lava stream it crinkled against itself and produced ropy structure, usually lobate as the center commonly advanced more than the sides. Crust pahoehoe usually did not form where stream flow was turbulent or swift, as on the steep slopes of Mihara Yama.

Hollows formed beneath the crust when the stream drained after the surface hardened, or when released gases were trapped beneath the crust. In a few places, draining left lava tubes. Trapped gas helped to protect the crust from the drag of the underlying stream; this was important when the stream became viscous. Trapped gases arched the centers of some crustal pieces before solidification was complete. The thickness of the crust depended upon the depth to which the lava had solidified before drainage occurred or gas bubbles became trapped. The crust in some places was left insufficiently supported and collapsed under its own weight or underfoot.

Skin pahoehoe formed from issues of hot, fluid lava when the chilled surface, in solidifying, preserved the shape resulting from the brief flow movement. At Mihara Yama, most such issues were small. Small spurts were emitted at intervals from conduits and from the base of driblet spires on the crater floor, and highly fluid lava escaped from streams coursing down the sides of Mihara Yama, from cracks leading from lava tubes, and from the molten interiors of some flows on the caldera floor. After emission the lava moved a short distance as its exposed surface cooled quickly

to form a thin skin. The skin either held the interior lava until it solidified, or contained it by stretching, or split and permitted a second emission. The skin thus momentarily acted as a pouch for the more fluid lava. A hollow was formed when the interior lava drained away while still sufficiently fluid to separate from the skin without dragging and breaking the skin. Cascade, ribbon, ropy, and other structures formed on surfaces of various gradients. Commonly the skin while viscous became wrinkled behind obstructions because of the pressure of the lava behind it. The skin hardened vitreous and brittle. The conditions which resulted in the formation of skin pahoehoe graded into those forming crust pahoehoe.

Pahoehoe lava was in general vesicular, particularly near the top of a flow where gas was trapped. As solidification proceeded, other bubbles became trapped at deeper levels, sometimes in a series of layers.

The formation of a pahoehoe crust on the surface of a moving stream of lava is comparable to a crust of ice forming over a running brook. The adherence of the ice to the firm margins prevents the crust from being carried away, since water (like very fluid lava) has little frictional drag. The water of a brook often drains after an ice cover forms, leaving a hollow (as beneath some pahoehoe surfaces). However, ice during its formation does not pass through a viscous stage, and the ice surface does not develop ropy and associated structures.

Formation of Aa

Aa surfaces formed on the margins of advancing flows in which the cooling lava reached its viscous stage without forming a confining crust, either because the incipient crust was carried away or engulfed by swift or turbulent stream flow, or because a flow had cooled sufficiently to become viscous before reaching the surface. As the lava cooled and crystallized, it became increasingly granular and viscous. A continuous crust formed less easily, because the increased viscosity both retarded the formation of a smooth surface and increased the drag from material flowing beneath the surface.

After viscosity reached a certain point, a smooth surface could no longer form, and pahoehoe could not develop. The increased flow friction in the body of the stream caused the even more viscous lava on the margins to be pushed, dragged, and separated into pieces. As differential movement separated pieces at the sides and top of a flow, the material connecting them to each other was drawn out at numerous points, broke, and formed strings, irregular protuberances, and jagged points of aa clinkers. Further slow movement of the viscous flow caused the clinkers to be shoved, rolled, overrun, and partly broken.

Streams of fresh fluid lava commonly passed beneath earlier surfaces. The type of surface which later formed depended upon the conditions prevailing during solidification. In the enclosed channel, the fresh lava might travel long distances yet remain sufficiently fluid to form pahoehoe upon exposure to the surface. Thus, from beneath a pahoehoe surface, lava might form either pahoehoe or aa. From beneath an aa surface, occasionally fluid lava poured out through cracks leading from the interior of the flow, and formed small pools or streams of pahoehoe alongside the aa flow. In such places pahoehoe had not formed from aa but from fluid lava in the interior of the flow. More commonly, however, the lava in the interior of an aa flow cooled slowly and increased in viscosity, and the margins advanced as an aa flow. Once a flow became aa, its surface of clinkers sustained aa development, as a confining crust could not form. As the lava in the interior approached any nonrigid margin already composed of clinkers, pieces separated with a clinker surface and were pushed, rolled, broken, and added to the flow. Aa could not develop so long as a flow was bounded by rigid margins, as by fused channel sides and a strong surface crust. However, occasionally aa formed beneath an older hollow crust when the surface of a later flow did not reach the bottom of the crust.

Flows that solidified on moderate gradients as aa had steep sides and fronts commonly 2–6 m high and a rough and furrowed top, surfaced with loose reddish-brown jagged clinkers. The clinkers commonly were 10–50 cm in diameter, but pieces were of all sizes up to

1 m in diameter. As a flow advanced, usually accompanied by crunching sounds, clinkers dropped off the face and fell to the toe. Flows that advanced over these, had a base of clinkers. Fragments breaking off aa fronts on the caldera floor, more than 1 km from the point of overflow on the crater rim, exposed red-hot lava into which a stick could be thrust, but which was sufficiently viscous that it only oozed out, forming aa clinkers within a few minutes. When flows reached the inner side of the somma and advanced up slopes of volcanic sands, the lava pushed up the loose sand and formed a ridge as much as 20–50 cm high.

The toes of aa flows fed by long streams advanced 20–100 cm per minute, but some flows fed by only small streams advanced only 1 cm per minute and less. After the feeding stream stopped, flows commonly continued for a few more days until the interior solidified.

Surface irregularities caused clinkers to appear more scoriaceous than the material actually was. Solidified aa was generally less vesicular than pahoehoe because it was stirred while cooling, and no continuous crust retarded gas escape. The amount of gas in the molten rock apparently was not significant in determining whether or not aa would form.

Aa fragments on the surface of a flow graded inward to rough aa surfaces of partly detached masses and then to the jointed, interior mass. The lava stream commonly consisted of thin bands differing slightly in vesicularity and amount of oxidation. The banding resulted from differential movement between thin layers, caused by differences in viscosity and flow friction. Entrapped gas bubbles were distorted, stretched, and finely divided. Beneath some aa surfaces, however, fresh inflows of fluid lava solidified in place without distortion of gas bubbles by such interlayer shearing. Hence, although the interior of aa flows tended to be distinctive, they were not necessarily so.

Typical aa flows were covered with clinkers. However, the surfaces of large areas of aa flows, particularly in the Kagamibata flows, consisted of the fragments of crusts that had been broken by underflows. Such crusts had formed over the large outpourings after they became pooled on the caldera floor. One section of a flow was surfaced predominantly with rectangular plates of crust, compressed so that pieces were pushed into near-vertical position. Another surface consisted predominantly of pieces of crust that were curled, presumably by deformation of the crust before it had hardened. Another consisted of bent and twisted pieces of ropy pahoehoe, which appeared to have formed at the periphery of a large flow, but which before fully solidifying had become deformed and broken by a subsequent flow.

Formation of Modified Types

Modified types of pahoehoe also formed. The most common had a drawn surface. Flows so wide their surfaces lacked side anchorage, and flows composed of lava somewhat viscous at emission, had their surface layer stretched during congelation by the drag from the more freely moving interior of the flows. The drawn-surface lava resembled pahoehoe for the surface was sufficiently fluid to form a fairly level continuous crust, but it was transitional to aa because during cooling the surface layer was dragged by lower layers and somewhat distorted. The drawn surfaces had barely attached, linear, stringy flakes, about 2 cm long and 0.5 cm wide (Pl. 4, fig. 3). Weathering soon caused crumbling of the looser flakes.

Some drawn surfaces also had long lines parallel to the direction of flow. Some lines were color differences, some resulted from differences in development of the flakes, and others were ribs and grooves (Pl. 4, fig. 1). The color differences resulted chiefly from differences in the amount of oxidation and the texture of the surface and were increased by weathering. Differences in development of the flakes were caused in part by slight differences in viscosity as the flakes formed. The ribs and grooves reflected the shape of outlets through which lava was extruded. These impressions are similar to those implanted on small aa extrusions known as "toothpaste aa" (Macdonald, 1953, p. 178).

The drawn surface was both formed and preserved by flow remaining lamellar until the lava solidified. As in pahoehoe crusts, hollows formed when gases became trapped beneath the crust or when the stream drained

after the crust had hardened sufficiently to support itself.

The underside of the crust of the drawn surface, as in some crust pahoehoe, commonly was rough because of irregularities left as the surface of the lava stream dropped from contact with it, and because of pendants (stalactites), hanging down about 1–5 cm, which were formed as a result of the drip of splashed lava (Pl. 5, fig. 4). Most such under surfaces had a thin red oxidized film. At depths of 5–10 cm within the crust some lens-shaped hollows up to 1 square m formed by the coalescence of trapped bubbles.

Beneath drawn surfaces the lava in many places solidified as solid rock with horizontal bands. The sequence beneath the surface was rather uniform over wide areas in the north part of the Kagamibata flow and consisted of a layer of black lava at the surface about 7 cm thick, a layer of grayish-brown lava about 5 cm thick, and a layer of purplish-gray lava about 5 cm thick. Beneath this were layers 10–100 cm thick ranging from reddish brown to dense black. Differences in fracturing of the various layers were revealed in large tension cracks up to 5 m deep. Black, fine-grained layers tended to have sharp fractures, whereas reddish-brown granular layers, both above and below a black layer, separated with a crumbly fracture surface.

Many collapses occurred in the area of drawn surfaces as a result of joints rendering the crust too weak to span the underlying hollows. In the Kagamibata flow some of the collapses were 25 m long, 15 m wide, and 5 m deep.

An isolated row of lava fragments formed here and there on top of the drawn surface where lava squeezed out through cracks. In some places the material curled out and looked like bulbous or ropy pahoehoe. In other places extrusion of more viscous lava formed a line of aa clinkers, which appeared incongruously isolated from other aa material (Pl. 4, fig. 1).

Drawn surfaces that could be traced toward the toe of a flow passed abruptly into aa surfaces, and in some places abrupt transition also occurred at the sides of a flow. Apparently at these margins jointed pieces of drawn-surface crust were plucked off as the under flow became more viscous, and these pieces were incorporated into the aa then forming (Pl. 4, fig. 2). Some drawn surfaces were fragmented by later flows, and the pieces became incorporated into the new flow as slab pahoehoe (Pl. 4, fig. 4). Some ropy pahoehoe crusts had drawn surfaces, as conditions that formed typical pahoehoe graded into conditions that formed the modified drawn surface.

The drawn surfaces produced when somewhat viscous lava was extruded could in some places be traced back to the point of emergence. Where the opening was between smooth joint faces or blocks of lava, a relatively smooth surface was produced. Irregularities in the opening left their imprint on the surfaces (Pl. 4, fig. 1).

In addition to stretching of the surface layer by faster movement of lower layers, the surface layer was stretched also when a flow was accelerated by an increase in gradient. As pieces of the surface layer were drawn out and separated, the material connecting them to each other stretched, broke, and formed roughly aligned, jagged points. The resultant surface pattern suggested superficially that the forward piece had advanced in the direction of the lava flow, but the lagging part had moved in the opposite direction. Such were only surface features. Like other drawn surfaces, at a depth of a few centimeters the crust solidified as a layer or layers of vesicular lava.

Drawn surfaces formed extensively within the crater and on all the flows, but particularly over large parts of the Kagamibata flow, where large outpourings of lava reached the caldera floor.

Another type of modified pahoehoe surface formed when pools of molten lava in the inner pit and in the crater solidified without significant linear flow movement, but with a moderately rough to rough surface and numerous trapped or broken bubbles, as a result of agitation resulting from inflows, thermal currents, escape of gas, and fall of ejecta. The lava cracked into large blocks by shrinkage during cooling, and some blocks subsided unevenly.

Lava Streams on Slopes of Mihara Yama

Large floods of lava poured down the side of Mihara Yama occasionally during 1951.

However, most of the time in 1950 and 1951 when lava overflowed the crater rim it formed small streams 1–4 m wide and 0.5–2 m thick. As the margins of a flow chilled and congealed, the channel became confined. The stream moved faster in the center than at the sides where there was frictional resistance. When the flow increased, or when its bottom cooled and its level was thus raised, overflow at the margins intermittently built up natural levees of lava.

A special type of natural levee developed from pulsating flows. The lava feeding some of the flows emerged from openings in the crater floor. Minor surges followed the periodic escape of large gas bubbles which while trapped in the concealed channel partly blocked the flow of lava. Such surges caused minor overflow along the sides of the exposed flow. Solidification of the overflow built up thin confining walls along sections of some streams. As the level of the flow was raised by solidification at the bottom, some flows became elevated as much as 1 m above their surroundings, yet were confined by nearly vertical sides only a few cm thick at the top (Pl. 5, fig. 3).

Pieces of crust, and blocks and smaller fragments torn from the sides, were carried by the streams down the slope. Most of them were suspended within the flow, as they differed little in density from molten lava. On steep slopes they commonly became engulfed within turbulent currents. Some blocks large enough to drag on the bottom of a flow protruded above the surface, giving a false impression of floating substantially emerged. Where bottom drag increased sufficiently, some of these blocks were rolled over by the pressure of the stream on their mid-part. The blocks impinged and collected at irregularities along the sides. By partly blocking the channel, in some places they caused overflow that contributed to the building of the natural levee of lava, and occasionally even caused a shift in the channel.

The occasional floods of lava that swept over the crater rim for brief periods overran earlier flows that stood in their path, both on the sides of Mihara Yama and on the caldera floor. The more usual small flows, however, were confined in channels or tunnels on the sides of Mihara Yama and commonly disappeared on the caldera floor beneath the accumulated cover of aa.

As a result of the diversity of flows, the lava left on the slopes of Mihara Yama was rough and jumbled. Aa was most common, but some cascade and other skin pahoehoe features formed from small spurts of fluid lava from streams on the slope.

Lamellar Banding

The flow of some lava streams was lamellar as a result of increasing frictional drag toward the margins where viscosity increased. Lamellae differed because of slight differences in vesicularity, in grain size, and in the extent of oxidation.

Ejecta

Most material was molten when ejected. Only that which fell close to the vent remained liquid in flight; the rest landed as solid or viscous material, depending upon the original temperature in the lava pool, the size of the mass, and the duration of flight. The motion imparted was mostly linear, and, although some masses were rotated or twisted, there was no spinning. Inequalities in force of emission between different parts of the same mass, differences in resistance to wind, slight rotation, and the whip effect at the peak of the trajectory when descent began caused erratic flight patterns, irregular folding and twisting, and splitting in flight. Larger masses were distorted more than were smaller pieces. Cooling during flight preserved some features, although delicate forms were broken upon impact.

Many of the lava bombs ejected had solid cores. Cored bombs formed most commonly when the cinder cone of a vent was large enough so that its inner slopes formed a substantial catchment area to funnel fragments of ejecta back toward the vent pool. In tumbling down the steep slopes, the fragments generally were somewhat rounded. When re-erupted, such pieces had a fresh coating of lava, which adhered to the firm core and was shaped during flight.

Ribbons of lava were commonly ejected from the surface of the pool. The ribbons broke into pieces as a result of differences in speed, direction, and momentum of the parts. Thicker

parts, which might or might not contain a solid core, became ellipsoidal, and their surface layer was drawn out at the two points of separation to form a spindle-shaped bomb. Quite commonly the tips of these points were curved as a consequence of flight through the air while still plastic, or as a result of the ribbon being curved at the time of separation. These points were never spiral, and there was no indication of spinning (Pl. 5, fig. 5).

A few bombs landed on ash or lapilli deposits while the surface lava was still sufficiently fluid to conform to the impact depression. The lava hardening in this form produced a splash bomb in which the spherical center appears embedded in a saucer (Pl. 5, fig. 6).

The ejecta forming the inner slopes of the cinder cones were commonly welded together, making a strong structure. The welding occurred because much of the material was relatively fluid when it landed, and pieces tended to cohere to each other. Faults and fissures formed in the welded material as a result of earthquakes and subsidence, but usually were soon concealed by later deposits.

References Cited

Bonney, T. G., 1899, Volcanoes: N. Y., G. P' Putnam's Sons, 351 p.

Coleman, Satis N., 1946, Volcanoes new and old: N. Y., John Day Co., 222 p.

Daly, Reginald, 1914, Igneous rocks and their origin: N. Y., McGraw-Hill Book Co., Inc., 563 p.

Hess, H. H., 1948, Major structural features of the western North Pacific, an interpretation of H. O. 5485, Bathymetric Chart, Korea to New Guinea; Geol. Soc. Am. Bull., v. 59, p. 417–446.

Iida, Kumiji, Hayakawa, Masami, and Katayose, Kuniyuki, 1951, Gravity change according to the eruption (In Japanese): Jour. Geography (Japan), v. 60, no. 3, p. 36–38.

Iwasaki, Iwaji, 1935, Geochemical study on the volcanoes in Japan (II): Chemical composition of lavas of Volcano O Shima, Izu: Chem. Soc. Japan Jour., v. 56, no. 12, p. 1511–1522.

—— 1951, Geochemical investigations of the volcano (In Japanese): Jour. Geography (Japan), v. 60, no. 3, p. 40–43.

Kizawa, Takashi, 1951a, Geophysical phenomena in volcanic activity (I) (In Japanese): Kenkyu Jiho (Jour. Meteorological Res.), v. 3, no. 7, p. 249–260.

—— 1951b, Volcanic tremor (In Japanese): Jour. Geography (Japan), v. 60, no. 3, p. 28–31.

Macdonald, Gordon A., 1953, Pahoehoe, aa, and block lava: Am. Jour. Sci., v. 251, p. 169–191.

Minakami, Takeshi, 1951a, 1. The eruption of Oo-sima during July-September, 1950: Report on the volcanic activities in Japan during 1948–1950, Tokyo, Science Council of Japan, p. 1–10.

—— 1951b, Volcanic tremors and the viscosity of fresh lava at various temperatures (In Japanese): Jour. Geography (Japan), v. 60, no. 3, p. 24–28.

Minakami, Takeshi, Miyazaki, Tsutomu, and Takahashi, Tomoko, 1951, The 1950–1951 eruption of Oo-sima and its seismometrical investigations (I): Tokyo Univ., Earthquake Res. Inst. Bull., v. 29, p. 360–381.

Murauchi, Sadanori, 1950, Recent eruption of the Volcano Miharayama, Oshima Island, Japan I (In Japanese): Natural Sci. and Mus., v. 17, no. 3, p. 1–13; II, v. 17, no. 4, p. 1–9.

—— 1951, Topographical changes inside the inner somma after the eruption of 1950 (In Japanese): Jour. Geography (Japan), v. 60, no. 3, p. 17–24.

Musya, Kinkiti, 1941–1951, Historical materials on earthquakes in Japan (In Japanese): 4 vols., Tokyo, Mainichi Shimbun Sha.

—— 1951b, Earthquakes that occurred in the Izu Islands, the Ogasawara Islands, and the Iwo Jima Group from January 1900 to May 1950: unpublished manuscript compiled from Geophysical Review, Central Meteorological Observatory, Tokyo; Seismological Data, July-Dec. 1948 and Jan.-June 1949, Central Meteorological Observatory, Tokyo; and List of Remarkable and Moderate Earthquakes from 1923 to 1949, Central Meteorological Observatory, Tokyo.

Nagata, Takesi, 1941, A geomagnetic study of the minor activities of Volcano Mihara, Oosima Island, August 1940: Tokyo Imp. Univ., Earthquake Res. Inst. Bull., v. 19, p. 402–410.

Nakamura, Seiji, 1915, History of eruptions of Mihara Yama, Izu O Shima: Repts. Imperial Earthquake Invest. Comm., no. 79, p. 38–56.

Omori, Fusakichi, 1915, Eruption of Izu-O Shima (In Japanese): Imperial Earthquake Invest. Comm. Repts., no. 81, p. 1–88.

—— 1918, Volcanic eruptions in Japan (In Japanese): Imperial Earthquake Invest. Comm. Repts., no. 86, p. 1–236.

Rikitake, Tsuneji, 1951a, The eruption of Mihara Yama in the province of Izu (In Japanese): Kagaku (Science), v. 21, no. 9, p. 476–482.

—— 1951b, The distribution of magnetic dip in Ooshima (Oosima) Island and its change that accompanied the eruption of Volcano Mihara, 1950: Tokyo Univ., Earthquake Res. Inst. Bull., v. 29, p. 161–181.

—— 1951c, Geomagnetic studies on Ooshima Island (In Japanese): Jour. Geography (Japan), v. 60, no. 3, p. 31–33.

Rikitake, Tsuneji, Yokoyama, Izumi, Okada, Atsushi, and Hishiyama, Yoneko, 1951, Geomagnetic studies of Volcano Mihara. The 3rd paper. (Magnetic survey and continuous observation of changes in geomagnetic declination.): Tokyo Univ., Earthquake Res. Inst. Bull., v. 29, p. 583–603.

Shrock, Robert R., 1948, Sequence in layered rocks: N. Y., McGraw-Hill Book Co., Inc., 507 p.

Suwa, Akira, 1951, The outline of the eruption and a review of the works of volcanologists

with reference to the eruption (In Japanese): Jour. Geography (Japan), v. 60, no. 3, p. 7–13.

Takahashi, Ryutaro, 1951, The activities in 1950, and the accompanying topographic changes (In Japanese): Jour. Geography (Japan), v. 60, no. 3, p. 14–17.

Tsuboi, Seitaro, 1920, Volcano Oshima, Idzu: Tokyo Imp. Univ., Coll. Sci. Jour., v. 43, article 6, p. 1–146.

Tsuya, Hiromichi, 1937, On the volcanism of the Huzi Volcanic Zone, with special reference to the geology and petrology of Idu and the Southern Islands: Tokyo Imp. Univ., Earthquake Res. Inst. Bull., v. 15, p. 215–357.

Tsuya, Hiromichi, and Morimoto, Ryohei, 1951, Petrography of the 1950 lavas of Oshima Volcano, Seven Izu Islands, Japan: Tokyo Univ., Earthquake Res. Inst. Bull., v. 29, p. 563–582.

Tsuya, H., Morimoto, R., and Ossaka, Joyo, 1952, Chemical composition of the 1951-lavas of Oshima volcano, Seven Izu Islands, Japan: Tokyo Univ., Earthquake Res. Inst. Bull., v. 30, p. 231–236.

Volcanological Subsection, Seismological Section, Central Meteorological Observatory of Japan, 1951, Preliminary report of the eruption of Mihara Yama (In Japanese): Sokko Jiho (Weather Service Bull.), v. 18, no. 12, p. 281–285.

MILITARY GEOLOGY BRANCH, U. S. GEOLOGICAL SURVEY, TOKYO, JAPAN (APO 500, SAN FRANCISCO, CALIF.); DEPT. OF GEOLOGY, UNIV. OF ILLINOIS, URBANA, ILL.

MANUSCRIPT RECEIVED BY THE SECRETARY OF THE SOCIETY, AUGUST 17, 1953

PUBLICATION AUTHORIZED BY THE DIRECTOR, U. S. GEOLOGICAL SURVEY

BULLETIN OF THE GEOLOGICAL SOCIETY OF AMERICA
VOL. 66, PP. 763-766, 2 FIGS. JUNE 1955

Short Notes

DIRECTION OF CURRENT FLOW IN SOME LOWER CAMBRIAN CLASTICS IN MARYLAND

By John C. Whitaker

Introduction

In recent years, the source area of the sediments filling the Appalachian geosyncline has been questioned. Dana (1890), Williams (1897), and Schuchert (1910) popularized the concept of an ancient crystalline land mass of Appalachia which lay to the east of the present continental margin and supplied detritus for the Appalachian geosyncline throughout the Paleozoic Era.

More recently, Kay (1947; 1951), Umbgrove (1947), and others have proposed the concept of marginal geosynclines and island arcs. In essence, they propose a two-fold division of the Appalachian trough into a miogeosyncline receiving detritus from a western cratonal source, and an adjacent eugeosyncline with detritus supplied from a volcanic archipelago lying approximately in the position of the present continental margin.

The purpose of this paper is three-fold: (1) it describes the use of the Schmidt equal-area net as a method to determine the attitude of cross-bedding before deformation; (2), it presents the results of a limited study in order to illustrate the suggested method; and (3) it urges further investigations of the source of sediments of the Appalachian geosyncline so that the two contrasting hypotheses may be evaluated.

Acknowledgments

The author is indebted to F. J. Pettijohn who originally suggested the problem and to Ernst Cloos and A. Paap who reviewed the manuscript and added many helpful suggestions.

Area Investigated

The lower Cambrian Weverton metaquartzite, exposed in the tightly folded belt of the Blue Ridge Province of Maryland and northern Virginia, has been investigated to determine the direction of the source area of these sediments (Fig. 1). The Weverton formation is part of a large blanket of clean, well-sorted, quartz sands (orthoquartzite) deposited during Cambrian time throughout most of the southern Appalachians. These sands are part of the larger clastic unit known as the Chilhowee group, representatives of which extend from Alabama to Pennsylvania. In the area investigated, the Weverton constitutes Catoctin, South, and Blue Ridge mountains.

Unfortunately, the Chilhowee group is poorly suited for a study intended to discover their direction (or directions) of source; this is so, simply because folding and erosion have left these strata exposed for only short distances across the trends of the folds. Under these conditions, the generally accepted criteria of lithologic and thickness variations over a wide area in order to determine the direction of the source of sedimentation is difficult to obtain.

A more direct approach to the problem is to systemetically measure the cross-bedding in order to determine the directions from which the currents have transported the sediments. This has been done in the Weverton sands in Maryland where it is exposed at South and Catoctin Mountains and Elk Ridge (Fig. 1).

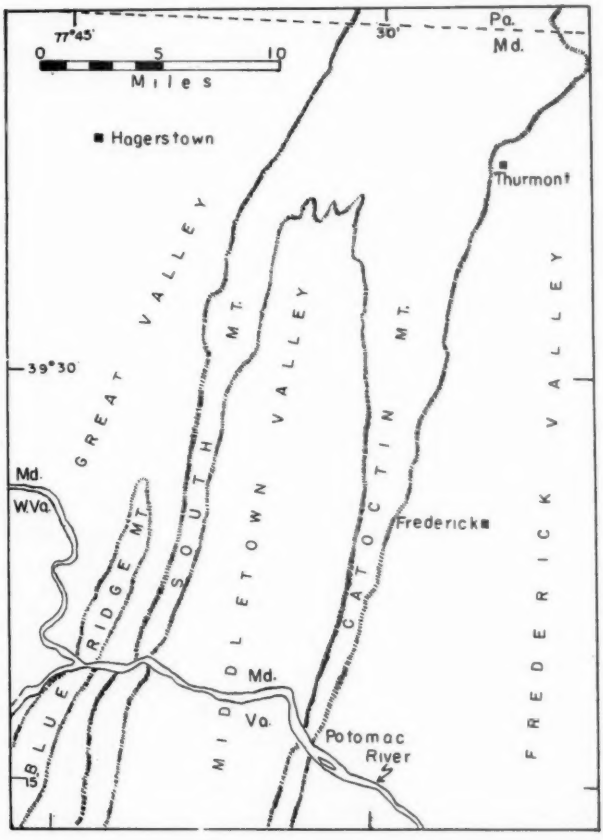

FIGURE 1.—INDEX MAP
Weverton exposures were investigated where the formation makes up Catoctin and South mountains and the portion of Blue Ridge Mountain (also termed Elk Ridge) north of the Potomac River

DESCRIPTION OF CROSS-BEDDING OF THE WEVERTON FORMATION

The terminology and classification of McKee and Weir (1953, p. 386) is used in the description of the cross-bedding.

The lower bounding surfaces of sets are planer surfaces of erosion and are, therefore, classified as *planar cross-stratification*. The shape of the cross-strata are *tubular* or *wedge*-shaped. The attitude of the cross-strata appear to be *non-plunging*, though the attitude of the axis can only rarely be inspected from two surfaces at right angles to each other. The cross-strata are asymmetric; their arching is *concave* or rarely *straight*. The dip of the cross-strata with respect to their corresponding strata is generally *low angle* (less than 20°), and the length of the cross-strata is always *small scale* (less than 1 foot).

METHOD EMPLOYED

The attitude of the strata and cross-strata may vary considerably, and therefore the strike and dip of both are recorded at each exposure. It is necessary to ascertain the attitude of the cross-strata at the time of deposition in order to determine the direction of current movement; this is achieved by various rotations employing the Schmidt equal-area projection. The pole of each stratum and its cor-

esponding cross-stratum are plotted. The tratum is then rotated to horizontal by using he strike of the stratum as the rotation axis. Such a rotation will alter the strike of the cross-stratum considerably unless the strike of both the stratum and cross-stratum happen to co-

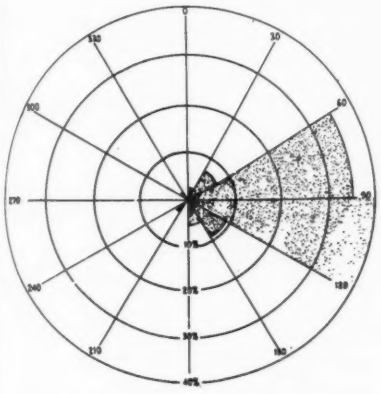

FIG. 2.—DIAGRAM SHOWING DIRECTION IN WHICH CURRENTS FLOWED

Compass divided into 12 parts: 40% from 90°–120°; 35% from 60°–90°; 9% from 120°–150°; 6% from 30°–60°; 5% from 150°–180°; 2% each from 0°–30° and from 210°–240°; 1% from 300°–330°.

incide. Once the stratum has been rotated to horizontal, the attitude of the pole of the cross-stratum represents its attitude prior to folding and therefore indicates the current direction. As it is the dip component of the cross-strata, rather than the actual amount of dip, that indicates the current direction, it is convenient to refer the results to a histogram showing the percentage of dips in the various directions (Fig. 2) so that the results of all the readings can be evaluated at a glance.

In areas, such as the arcuate trends of the Appalachians, this method involves some error. Arcuation in the Appalachians implies that crustal shortening has been more intense in areas of greatest degree of arcuation. Therefore, Appalachian sediments have not only been transported westward about subhorizontal rotation axes, but arcuation has produced some rotation of the sediments about vertical axes.

The general tectonic trend in Maryland is N. 15°–20°E. but swerves sharply to N.60°–70°E. in Pennsylvania. Thus, when the strikes of the strata are used for rotation axes employing the Schmidt equal-area net, there is no assurance that the resulting strikes of the cross-strata represent their original attitude prior to deformation. Because the amount of rotation about vertical axes resulting from arcuation is unknown, attempts to "pin point" the current directions become useless. As a result, only a generalized direction of current flow can be indicated in belts of strong arcuation.

The effect of the plunge of folds is also a factor. It is fitting and proper to rotate the cross-bed around the strike of the bedding proper if fold axes are horizontal. Neglect of plunge has the effect of increasing the "spread" or "scatter" of the observations but does not affect the mean value because the net plunge of all fold axes is zero.

CONCLUSIONS

Figure 2 shows the statistical results of the measurement of 136 cross-strata that have been rotated in the manner described. The results show that an overwhelming number of the readings indicate that the currents which transported the Weverton detritus came from the west. There seems to be no refinement of the direction beyond a general westerly component because of the limitations described above. Whether the assumption can be made that since the currents came from the west, therefore, the source of the Weverton sands was also from that direction awaits further work. The Weverton was studied for 55 miles along strike and 12 miles across the trends. Since folding may have caused crustal shortening as much as 50 per cent (Chamberlin, 1910; Cloos, 1940) the distance across the trend may represent as much as 24 miles before folding took place. Because this represents a fairly large area where the current direction is rather constant, the conclusion that these lower Cambrian sands have been swept eastward off the stable craton seems warranted.

FUTURE CONSIDERATIONS

Measurement of cross-strata in other periods of Appalachian clastic deposition to determine

the directions of current movement seems worth while. Similar investigations in the Tuscarora (Silurian), Oriskany (Devonian), and Pocono and Pottsville (Carbiniferous) sands should result in a framework of basic knowledge concerning the positions of source areas throughout Paleozoic time. Armed with this sort of information, we could more readily evaluate the hypothesis regarding the source of sedimentation and the tectonic history of the Appalachian geosyncline.

References Cited

Chamberlin, R. T., 1910, The Appalachian folds of Central Pennsylvania: Jour. Geology, v. 18, p. 228–250.

Cloos, E., 1940, Crustal shortening and axial divergence in the Appalachians of southeastern Pennsylvania and Maryland: Geol. Soc. America Bull., v. 51, p. 845–872.

Dana, J. D., 1890, Areas of continental progress in North America: Geol. Soc. America Bull., v. 1, p. 36–48.

Kay, M., 1947, Geosynclinal nomenclature and the craton: Am. Assoc. Petrol. Geologist Bull., v. 31, p. 1289–1293.

——, 1951, North American geosynclines: Geol. Soc. America Mem. 48, 143 p.

McKee, E. D., and Weir, G. W., 1953, Terminology for stratification and cross-stratification in sedimentary rocks: Geol. Soc. America Bull., v. 64, p. 381–390.

Schuchert, C., 1910, Paleogeography of North America: Geol. Soc. America Bull., v. 20, p. 427–606.

Umbgrove, J. H. F., 1947, The pulse of the earth: Martinus Nijhoff, 2d ed., 358 p.

Williams, H. S., 1897, On the southern Devonian formation: Am. Jour. Sci., v. 3, p. 393–403.

103 Churchwardens Rd., Baltimore, Md.

BULLETIN OF THE GEOLOGICAL SOCIETY OF AMERICA
VOL. 66, PP. 767-768 JUNE 1955

ANOMALOUS URANIUM-LEAD AGES

BY J. L. KULP AND W. R. ECKELMANN

In principle, the time of formation of a uranium mineral can be determined from one of the following isotopic ratios: Pb^{206}/U^{238}, Pb^{207}/U^{235}, or Pb^{207}/Pb^{206}. Since these ratios are affected in differing degrees and direction by various errors in measurement or geological alteration, the concurrence of ages obtained from these three ratios suggests a true absolute age. Actually for a large fraction of the mineral samples on which these ratios have been measured, the three isotopic ages do not agree (Nier, 1939); Nier *et al.*, 1941; Kerr and Kulp, 1952; Stieff *et al.*, 1953; Collins *et al.*, 1954; Kulp, Bate and Giletti, 1954). Since the uranium-lead decay is the primary basis of the absolute geological time scale (Holmes, 1947), and since it has been used to calibrate other methods (Wasserburg and Hayden, 1955), it is important to understand these anomalies.

In a recent paper, Kulp, Bate, and Broecker (1954) attempted to evaluate the factors that would produce the anomalous ages. It was concluded that uncertainties in the chemical and isotopic analyses and the physical constants were not a significant source of error. Except in the rare cases where the concentration of common lead in the total lead of a sample becomes large, the error in the correction for common lead is trivial. Radon leakage ranges from 0.01 per cent to 5 per cent in most minerals causing the 206/238 age to be low by this proportion for all minerals (*i.e.*, < 600 million years). For minerals older than 1000 million years the correction on the 207/206 age for radon leakage is generally unimportant. Five of about 50 samples for which uranium-lead ages have been published show the effect of recent oxidation and leaching. In these cases the 206/238 and 207/235 ages are higher than the 207/206 ages as expected for uranium removal. After a consideration of all these factors, many of the anomalous ages remain unexplained.

A single process that might produce the observed ages is that of the removal of lead from the uranium minerals at a time or times of recrystallization. Presumably this must occur at somewhat elevated temperatures and pressures in a neutral or reducing environment.

TABLE 1.—REPRESENTATIVE LAKE ATHABASCA PITCHBLENDE AGES
(Age in million years)*

Sample†	206/238	207/235	207/206
K-44	1315	1550	1860
K-45	1282	1490	1780
K-30	1005	1255	1650
K-53	220	395	1585
K-34	778	920	1300
K-48	254	321	820

* Probable errors caused by chemical and isotopic analysis are 1–2 per cent of the age increasing toward the younger samples.

† These samples are representative of the spread obtained in 24 samples.

Thermodynamically such removal is predicted since the lead ion does not fit in the uraninite lattice, but the rate of removal is apparently negligible at room temperature since specimens from some localities do not show this effect.

An unusual opportunity to study this hypothesis was presented by Dr. S. C. Robinson, Geological Survey of Canada, who submitted about 30 specimens of pitchblende and lead minerals from the Lake Athabasca uranium district. As can be seen from the representative samples of Table 1, a large spread in the apparent ages is obtained from the pitchblendes. The variation among samples from a single mine is as large as occurs in the entire district. These variations cannot be explained either by radon leakage or by the uncertainty of the isotopic composition of the lead in lead minerals which are intimately mixed with the pitchblende, since the leakage and the lead-mineral concentration are consistently small. The radiogenic-lead component of the lead minerals which are associated with the pitchblende appears to represent at least two distinct lead isotopic compositions (207/206 = 0.12 and

0.17) indicative of two periods of lead exsolution. If a single period of uranium deposition is involved, it must have occurred more than 1860 million years ago (Sample K-44), but less than 2000 million years ago. The upper limit is established by the 207/206 ratio of 0.12 for exsolved radiogenic lead. Also the last period of lead removal must have occurred less than 200 million years ago (Sample K-53).

Analysis of the data for all samples of the district indicates that the true age is 1900 ± 40 million years and that there must have been more than one period of lead exsolution. If there were only two periods of lead removal corresponding roughly to 150 ± 50 million years and 1200± 100 million years, all the apparent ages on all samples can be explained. This does not prove, however, that there were only two periods. Analyses of the Pb^{210} in these minerals show it to be in equilibrium with the U^{238}. Thus alteration is not occurring at present.

It is concluded that detailed study of the uranium and lead isotopic content of a district may make it possible to evaluate the time of deposition despite successive alterations. Further, some idea of the time or times of lead removal (thermal metamorphism?) may be obtained from the isotopic ratios. Except for young minerals, the 207/206 ratio gives a closer approximation to the true age than does the 206/238 and 207/235 ratios but remains a minimum. In extreme cases the 207/206 age may be less than half the true age. In general the 207/206 age can be assumed to be correct if accompanied by concurrent 206/238 and 207/235 ages.

The process of lead removal during the life of a radioactive mineral appears to be rather common particularly among the older samples. This concept is most useful in interpreting the earlier uranium-lead age determinations which have yielded anomalous results.

A full account of this research will be published. The authors are indebted to R. K. Wanless, R. J. Traill, W. S. Broecker, P. W. Gast, and G. L. Bate for helpful discussions.

This work was supported by the Research Division of the U. S. Atomic Energy Commission.

References Cited

Collins, C. B., Farquhar, R. M., and Russell, R. D., 1954, Isotopic constitution of radiogenic leads and the measurement of geological time: Geol. Soc. America Bull., v. 65, p. 1–21.

Holmes, A., 1947, The construction of a geological time-scale: Geol. Soc. Glasgow Trans., v. 21, p. 117–152.

Kerr, P. F., and Kulp, J. L., 1952, Pre-Cambrian uraninite, Sunshine Mine, Idaho: Science, v. 115, p. 86–88.

Kulp, J. L., Bate, G. L., and Broecker, 1954, Present status of the lead method of age determination: Am. Jour. Sci., v. 252, p. 345–364.

Kulp, J. L., Bate, G. L., and Giletti, B. J., 1954, New age determinations by the lead method N. Y. Acad. Sci. Ann., v. 60, art. 3, p. 509–520.

Nier, A. O., 1939, The isotopic constitution of radiogenic leads and the measurement of geological time. II: Phys. Rev., v. 55, p. 153–163.

Nier, A. O., Thompson, R. W., and Murphy, B. F., 1941, The isotopic constitution of lead and the measurement of geological time. III: Phys. Rev., v. 60, p. 112–116.

Stieff, L. R., Stern, T. W., and Milkey, R. G., 1953, A preliminary determination of the age of some Colorado Plateau uranium ores by the uranium-lead method: U. S. Geol. Survey, Trace Elements Inves. Rep. 268.

Wasserburg, G. J., and Hayden, R. J., in press, K^{40}/A^{40} dating: Geochim. et Cosmochim. Acta, v. 7, p. 51–60.

Lamont Geological Observatory, Palisades, New York

Lamont Geological Observatory Contribution No. 156

BULLETIN OF THE GEOLOGICAL SOCIETY OF AMERICA
VOL. 66, PP. 769-772, 3 FIGS., JUNE 1956

ADDITIONAL EVIDENCE OF VOLCANISM ON MARS

BY DEAN B. MCLAUGHLIN

Recently the author developed a hypothesis that attributes the dark markings of the Martian surface to volcanic ash deposited in elongated bands by the prevailing winds (McLaughlin, 1954a–1954d). The observational bases for this proposal are as follows: (1) The dark areas ("seas") are mainly in the south tropical zone and contain a number of bands oriented southeasterly. (2) These bands have tributary or terminal pointed "bays" on their north sides or northwest ends. (3) "Bays" north of the equator hook back, barblike, toward the northeast, while "bays" south of the equator do not. (4) Some of the strongest "canals" of the northern hemisphere trend northeasterly. (5) The pointed "bays" north of the equator connect with the bands to the south through a "flow pattern" that curves left on crossing the equator southward.

The systematic orientations suggested the trade winds, and the bands were interpreted as aeolian deposits. The strongest winds should occur during the southern hemisphere's summer, since the planet then passes perihelion. These winds would be of monsoon type, crossing the equator from north to south, thus producing the "flow pattern" which curves left in accord with the Coriolis effect of the planet's rotation. With the direction of flow thus established, the pointed bays were recognized as very local sources of large amounts of dark dust. Within the limits of terrestrial experience, only active volcanoes appear capable of producing such copious supplies of dust from tiny source areas.

This hypothesis accounts satisfactorily for the permanent dark regions, but it requires that the volcanoes be continuously and rather uniformly active. Most terrestrial volcanoes have relatively long intervals of quiescence between shorter phases of violent eruption. It is therefore important to determine whether any observations indicate intermittent volcanic activity on Mars.

Until within the past few decades, observation of the form of surface features of Mars depended almost wholly upon sketching of the planet as viewed with the telescope. This method is still superior for the very finest details, but gross features are now very well known as a result of photographic studies. For the record of changes, however, one must examine numerous old drawings. Considerable discrepancies are found between sketches made almost simultaneously by different observers. However, when several independent observers are in good agreement concerning a conspicuous feature, we can regard the record as reliable.

Changes on Mars were discussed critically by Flammarion (1892, p. 547–578). For our purposes, the later compilation by Antoniadi (1930) is more suitable, since it is more thorough and also includes better-established information. Antoniadi describes and traces the history of all features that had been mapped through 1929. The records of changes are scattered through the text but when brought together, form an impressive list. There are several striking examples of gradual encroachment of light-colored material upon dark areas. These strongly suggest aeolian deposition. Most relevant to the question of volcanism are several very prominent temporary dark markings that have appeared and later vanished. *Each of these had the form of a pointed "bay"* and, what is still more significant, *each showed a curvature consistent with the Coriolis effect of the planet's rotation*, if we assume that the vertex of the "bay" represents the source of material. Detailed discussion will be published in one of the astronomical journals. Here we shall briefly describe just two conspicuous examples.

These two markings appeared in the region of Solis Lacus, in 1877 and 1926, respectively (Fig. 1). The first, called Phasis, was certainly weak in 1862. Lockyer (1864, Pl. 2) did not record it at all, and only a trace of it is seen on sketches and maps by Kaiser (1872) made in 1862 and 1864. Dawes (1866) may have seen a faint trace of it in 1864. But it was noticed as a very strong feature by a number of observers in

FIGURES 1–3.—CHANGING APPEARANCE OF SOLIS LACUS REGION OF MARS

From drawings by Flammarion and Antoniadi. North is upward, opposite to usual astronomical convention.
(1) The dark horn-shaped feature at the left is Phasis, a temporary marking with left-hand curvature.
(2) "Normal" appearance of Solis Lacus region. Phasis is very faint. A strong dark spot, Phoenicis Lacus, is at or near position of vertex of Phasis in (1).
(3) The mis-shapen Solis Lacus, owing to a flaring and left-curving dark temporary marking, with vertex at a dark spot.

1877 (Flammarion, 1892, p. 253; Antoniadi 1930, p. 131, 138, 140, 162). It appeared as a dark horn-shaped area about 1000 km in length. Its vertex was a well-defined dark spot or "oasis," Phoenicis Lacus, at latitude 6°S. From there it trended southward, flaring and *curving left*, finally merging with the extensive southern dark "sea" at about Lat. 40°S. (Fig. 1). It was still prominent in 1879 and 1881, but was much diminished within a few years. A "canal" of very moderate strength is now intermittently visible in its position. Figure 2 shows the normal appearance of the region in recent years, with Phasis a mere streak, while in Figure 3, this "canal" is invisible. The writer (McLaughlin, 1954b, Pl. 12, figs. 10, 11) recorded a moderate shading there in 1939.

The observed changes suggest a great eruption in Phoenicis Lacus some time within a few years preceding 1877. The ash was caught by winds that crossed the equator southward and was deposited in the great horn-shaped area whose left-hand curvature shows the Coriolis effect. With cessation of activity, wind-borne light-colored dust from the reddish "deserts" eventually covered and obliterated Phasis, except for the fainter canal whose intermittent visibility suggests continuing mild activity.

The second case was more closely observed. The Solis Lacus region appeared normal in 1924 (Fig. 2). In 1926 Antoniadi (1930, p. 141) found it badly misshapen (Fig. 3). The distortion appears to have been produced by a flaring and curving dark marking whose vertex was a well-defined small "oasis" called Ius Lacus, almost on the equator. From there the dark area extended southward, flaring broadly and *curving sharply left* to pass over the normal Solis Lacus. The temporary feature endured until 1929 at least. By 1933, the appearance of the region was again normal (Antoniadi, 1933, p. 356).

In this case also, we can identify the locus of the eruption, and the curvature again reveals the Coriolis effect. The interpretation is so obviously parallel to that of Phasis that further comment appears to be unnecessary.

Other examples of temporary or intermittent markings of the same type are Cyclops (Antoniadi, 1930, p. 194), Hydaspis Sinus (p. 158), Gangis Sinus (p. 128), Tritonis Sinus (p. 174). Great changes have also affected certain canals whose curvature is consistent with Coriolis effect.

During the present century astronomers have tended to regard the dark coloration of the "seas" as due to vegetation. The clearly negative results of spectroscopic tests for chlorophyl (Millman, 1939; Kuiper, 1949, p. 339) seem not to have shaken this belief. Öpik (1950) argues that the relative permanence of the dark "seas" proves that they are covered by vegetation. Extensive dust storms are known to occur, and in a very short time the dark areas would be covered and obliterated by reddish dust, *if they were not renewed frequently*. Apparently he regarded the growth of vegetation as the most probable mechanism of renewal.

The forms of the markings, and especially of the temporary ones, appear practically fatal to the hypothesis that vegetation is the determining factor in the color contrasts. If the "seas" are covered by vegetation, why do they have the banded form, oriented with the trade winds that are demanded by meteorological physics? Why do they exhibit a curvature on crossing the equator? The agreement with the expected Coriolis deflection might occur by mere chance in a small percentage of cases. What can it mean when the agreement has practically no exception? In particular, why do the suddenly emerging temporary dark markings have their vertices at definite dark spots, flare out, and curve in the direction that agrees with that of the expected winds? The survival of any hypothesis must depend in large part on its ability to explain these facts. The volcanic hypothesis is conspicuously successful in accounting for them; the vegetation hypothesis does not appear competent to do so. The rapid disappearance of the temporary markings is eloquent testimony to the correctness of Öpik's suggestion that the permanent "seas" must be continually renewed. The volcanic mechanism of renewal makes no such drastic demands on our credulity as does the growth of vegetation under the rigorous conditions that exist on Mars.

The writer does not claim that living forms are absent from Mars. It is definitely asserted that the supposed evidence of vegetation has been based upon considerations too superficial to justify acceptance.

The amounts of ash required to produce the

observed changes do not appear excessive. The Phasis horn was typical, with an area of about 250,000 km². The thickness of ash can only be conjectured; it would probably range from meters very near the source to perhaps as little as 1 mm at 1000 km. An average thickness of 1 cm would give a total volume of 2.5 km³. Comparable and greater amounts have been calculated for terrestrial eruptions (Williams, 1941).

More important even than the total volume of ash is its distribution. The atmosphere of Mars is less dense than ours (pressure at the surface, about 80 mb), but gravity is only 38 per cent of the earth's. The transporting power of the Martian atmosphere may be fairly comparable with that of our own, especially at heights of several kilometers (since lower gravity results in less steep density gradient). On two occasions, ash from Vesuvius is reported to have fallen at Istanbul, 1200 km away (Phillips, 1869, p. 42, 48). In July 1953, ash from Mt. Spurr in Katmai National Monument fell a quarter of an inch thick at Anchorage, 400 km away (Muller *et al.*, 1954). However, we do not need to draw a conjectural parallel between Martian and terrestrial aeolian transportation. The vast dust clouds observed moving many hundreds of miles across the face of Mars (Antoniadi, 1930, p. 46; deVaucouleurs, 1951, p. 372–376) are ample proof of the transporting power of the Martian winds.

The temporary markings are attributed to great explosive eruptions, at least comparable with the greatest outbursts of Vesuvius, if not as violent as that of Krakatau. The more permanent dark areas may be accounted for by fairly continuous but relatively mild ("Strombolian") activity of the volcanoes at the points of the "bays." All things considered, Martian volcanism appears to be fairly comparable in magnitude with, but not to exceed appreciably, that on the earth at present. That its effects are so conspicuous on Mars is due to the absence or extreme weakness of processes that on earth operate powerfully and quickly obliterate thin falls of ash at great distances from their sources.

References Cited

Antoniadi, E. M., 1930, La Planéte Mars: Paris, Hermann et Cie.

——, 1933, La Planéte Mars en 1933: Soc. Ast. France Bull., v. 47, p. 343–361.

Dawes, W. R., 1866: Roy. Ast. Soc. Mem., v. 34, Pl. 2. (Note: There is no title.)

de Vaucouleurs, G., 1951, Physique de la planéte Mars: Paris, Michel.

Flammarion, C., 1892, La Planéte Mars: Paris, Gauthier-Villars.

Kaiser, F., 1872, Die bei den Oppositionen in den Jahren 1862 und 1864 angefertigten Abbildungen des Planeten Mars: Annallen der Sternwarte in Leiden, v. 3, p. 27–32, Pl. 1–3.

Kuiper, G. P., 1949, The atmospheres of the earth and planets: Univ. Chicago Press.

Lockyer, N., 1864, Observations on the planet Mars: Roy. Ast. Soc. Mem., v. 32: p. 179–191.

McLaughlin, D. B., 1954a, Volcanism and aeolian deposition on Mars: Geol. Soc. America Bull., v. 65, p. 715–717.

—— 1954b, Interpretation of some Martian features: Pub. Ast. Soc. Pacific, v. 66, p. 161–170.

—— 1954c, Wind patterns and volcanoes on Mars: Observatory, v. 74, p. 166–168.

—— 1954d, Further notes on Martian features: Pub. Ast. Soc. Pacific, v. 66, p. 221–229.

Millman, P. M., 1939, Is there vegetation on Mars?: Sky, v. 3, no. 10, p. 10–11.

Muller, E. H., Juhle, W., and Coulter, H. W., 1954, Current volcanic activity in Katmai National Monument: Science, v. 119: p. 319.

Öpik, E. J., 1950, Dust and the planets: Irish Ast. Jour., v. 1, p. 40–47.

Phillips, J., 1869, Vesuvius: Oxford, Clarendon Press, p. 42, 48.

Williams, H., 1941, Calderas and their origin: Univ. Calif. Dept. Geol. Sci. Bull., v. 25, p. 239–346.

THE OBSERVATORY OF THE UNIVERSITY OF MICHIGAN, ANN ARBOR, MICHIGAN

BULLETIN OF THE GEOLOGICAL SOCIETY OF AMERICA
VOL. 66, PP. 773-776, 1 FIG., 1 PL. JUNE 1955

SUBMARINE TOPOGRAPHY WEST OF MEXICO AND CENTRAL AMERICA

BY JOHN G. HEACOCK, JR., AND J. LAMAR WORZEL

A gravity survey was made in USS CHOPPER (SS 342) in March-April, 1949, to determine the gravity anomalies over the submarine trench which lies near the Pacific coast of Mexico and Central America. The soundings made along the track of the gravity survey were not adequate for making topographic corrections for the gravity values. All available data were used to construct a bathymetric chart. It is believed that this chart may be useful for other studies, and it is presented as Plate 1. In view of the scarcity of sounding data, and of the lack of modern soundings of high precision for use as a criterion for the reliability of the soundings on the various tracks, only a small fraction of the data was rejected, and the remainder was contoured as though it were reliable. This accounts for the obvious inaccuracy of much of the detail shown on the chart, particularly the tendency for contour lines to follow the ship's tracks in the area of low relief west of the trench.

The most interesting feature of the area surveyed is the trench which extends from 10° N., 86° W. off the coast of Costa Rica to about 20° N., 106° W. near Cape Corriente, Mexico. This trench has been called the Guatemala Trench and the Acapulco Trench by various authors, but it might well be more appropriate to call it the Middle America Trench. Only the part west of 99° W. longitude is shown in Plate 1. It is a question whether the Gulf of California is an extension of this trench. The trench is remarkably straight. Its axis is 50–100 miles off shore. The Guatemala Deep, where the sounding is about 3400 fathoms, is believed to be the deepest part of the trench. A depth of 2800 fathoms or more is found at all points along the length where data are available. On the landward side of the trench the average slope ranges from about 3° to 6°, on the seaward side from 1° to 3°, but in certain areas slopes as great as 35° are found. Between the edge of the continental shelf and the crest of the seaward wall, the trench is 40–60 miles wide. This trench is similar to those associated with island arcs in its relationship to shallow- and intermediate-depth earthquakes, and to volcanoes (Gutenberg and Richter, 1949, p. 35–38; von Wolff, 1929, p. 252–283). In the chart given by Gutenberg and Richter the intermediate-depth earthquake belt parallels the trench and has about the same longitudinal extent.

The trench most like this one follows the Pacific Coast of South America, and Wuenschel (in press) shows that it has free-air gravity anomalies of as great as −220 mgal along a belt displaced slightly landward from the axis of the trench.

A number of sections across the trench and across the neighboring Cocos Ridge (Fig. 1) were constructed from the contour map, not from individual lines of soundings as is usually done; hence the smaller details may in some cases be in question.

As other writers have pointed out, the continental shelf is only 10–20 miles wide north of the Gulf of Tehuantepec, and 30–60 miles wide south of it.

The Cocos Island Ridge is a broad ridge roughly 100 miles wide, rising to about the depth of 1000 fathoms, extending from the Panama-Costa Rica boundary southwest to Cocos Island. This ridge terminates the trench on the southeastern end. The Guatemala Basin, northwest of the Cocos Ridge, has a depth of 2000 to 2200 fathoms and borders the trench for about 500 miles. It is interesting to note that the Sigsbee Deep in the Gulf of Mexico, the low-lying Isthmus of Tehuantepec, the Guatemala Deep, and the Guatemala Basin are all in alignment.

The Albatross Rise forms the northwestern boundary of the Guatemala Basin. It rises to depths of 1600 to 1800 fathoms.

A number of conical peaks are shown on Plate 1. These are based on single soundings, and their shapes cannot be considered known.

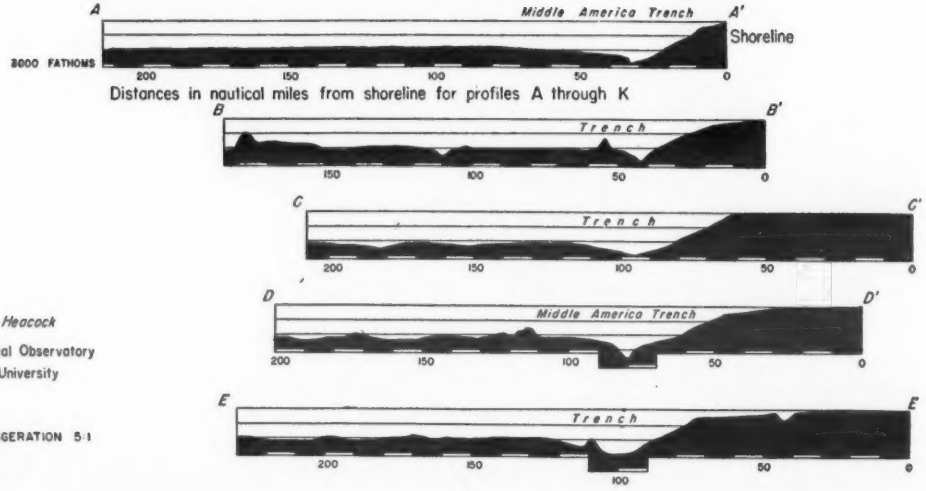

John G. Heacock

Lamont Geological Observatory
Columbia University

VERTICAL EXAGGERATION 5:1

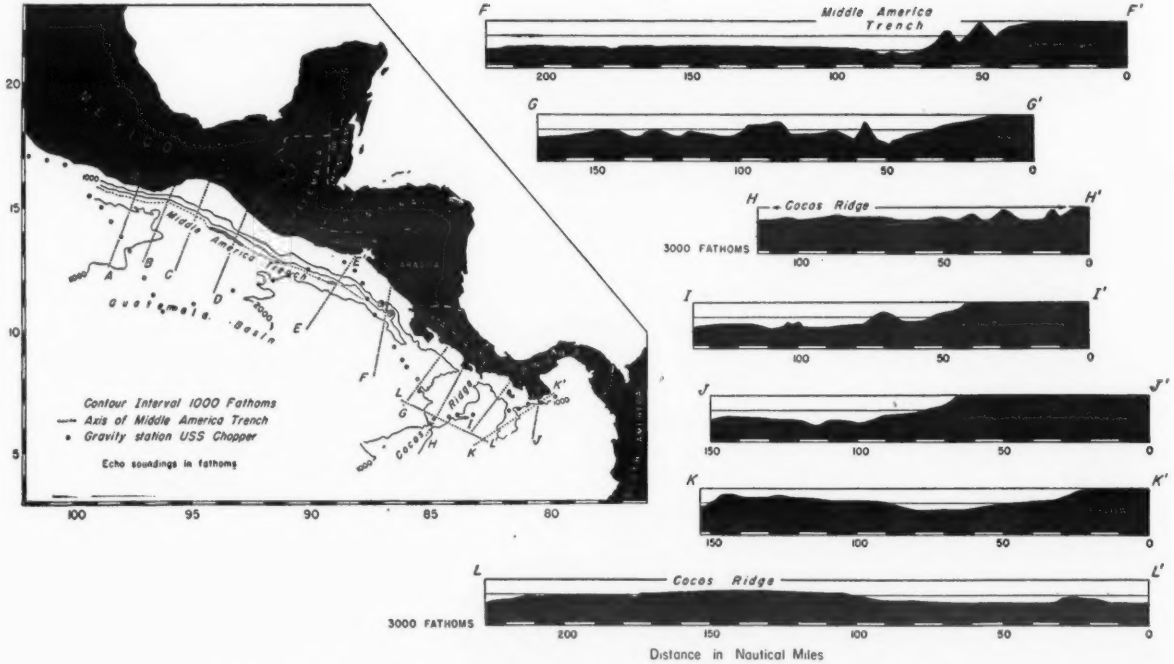

FIGURE 1.—TOPOGRAPHIC PROFILES, PACIFIC COAST, MEXICO AND CENTRAL AMERICA

A number of them lie in the trench and on its walls; the group at about 11° N., 87° W. is particularly notable.

ACKNOWLEDGMENTS

Thanks are expressed to the officers and men of the USS CHOPPER (SS 342), Commander John M. Bowers commanding, to Marie Tharp and Annette Trefzer for drafting the illustrations, to the Hydrographic Office of the U.S. Navy for data from their files, and to Bruce C. Heezen and Maurice Ewing for advice and assistance.

This project was carried out under Contract N6 onr 271 08 with the Office of Naval Research, Department of the Navy.

References Cited

Gutenberg, B. and Richter, C. F., 1949, Seismicity of the earth: Princeton Univ. Press, p. 1–273.

von Wolff, F., 1929, Der Vulkanismus: Stuttgart, Ferdinand Enke, v. 1, p. 1–711.

WUENSCHEL, P. C. (in press) Gravity measurements and their interpretation in South America between latitudes 15° and 33° south: Geol. Soc. America.

LAMONT GEOLOGICAL OBSERVATORY, PALISADES, N. Y.

LAMONT GEOLOGICAL OBSERVATORY CONTRIBUTION No. 147

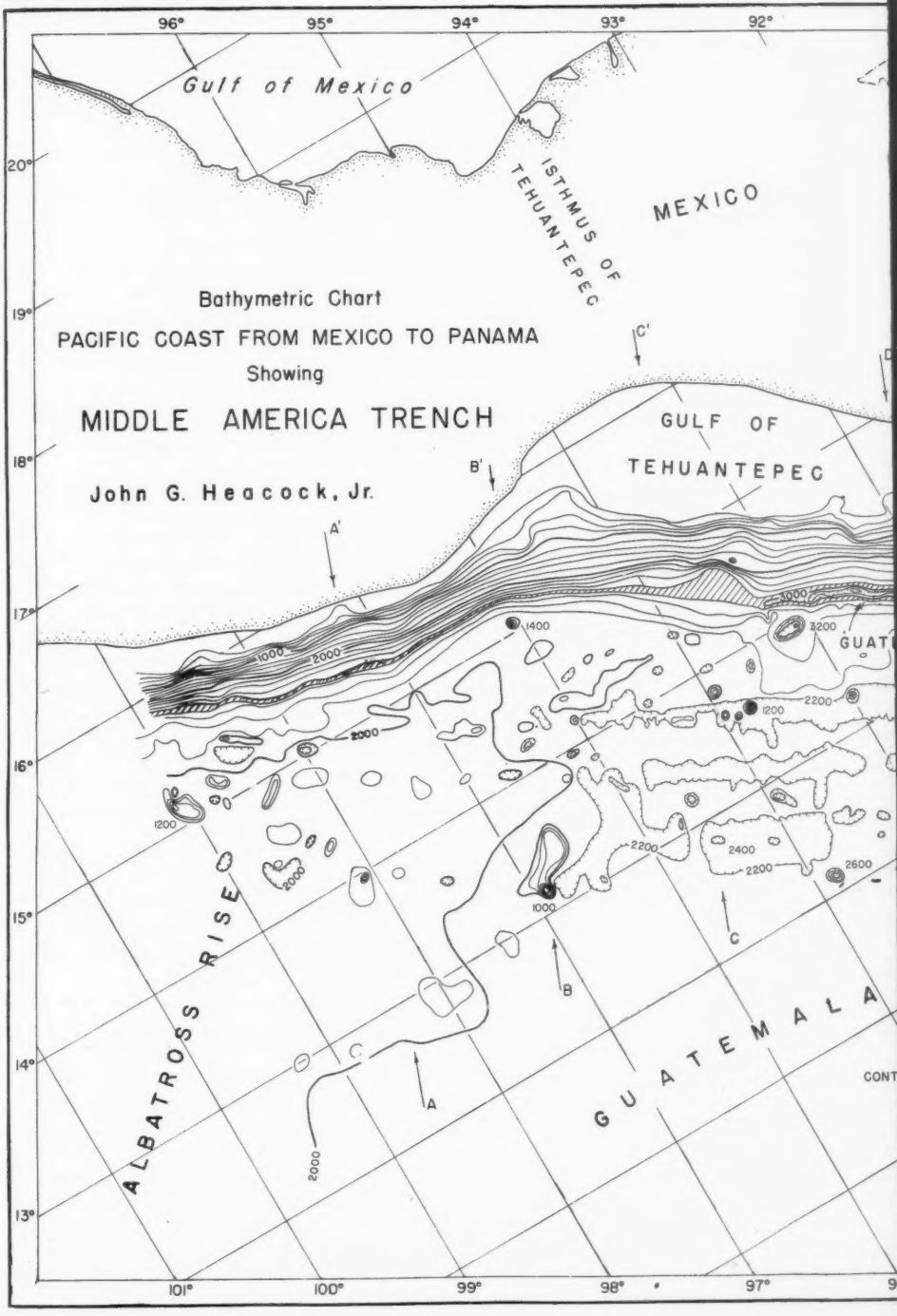
Gulf of Mexico
ISTHMUS OF TEHUANTEPEC
MEXICO
Bathymetric Chart
PACIFIC COAST FROM MEXICO TO PANAMA
Showing
MIDDLE AMERICA TRENCH
John G. Heacock, Jr.
GULF OF TEHUANTEPEC
ALBATROSS RISE
GUATEMALA
96°
95°
94°
93°
92°
20°
19°
18°
17°
16°
15°
14°
13°
101°
100°
99°
98°
97°
A'
B'
C'
A
B
C
1000
2000
1200
1400
2200
2400
2600
3000
3200

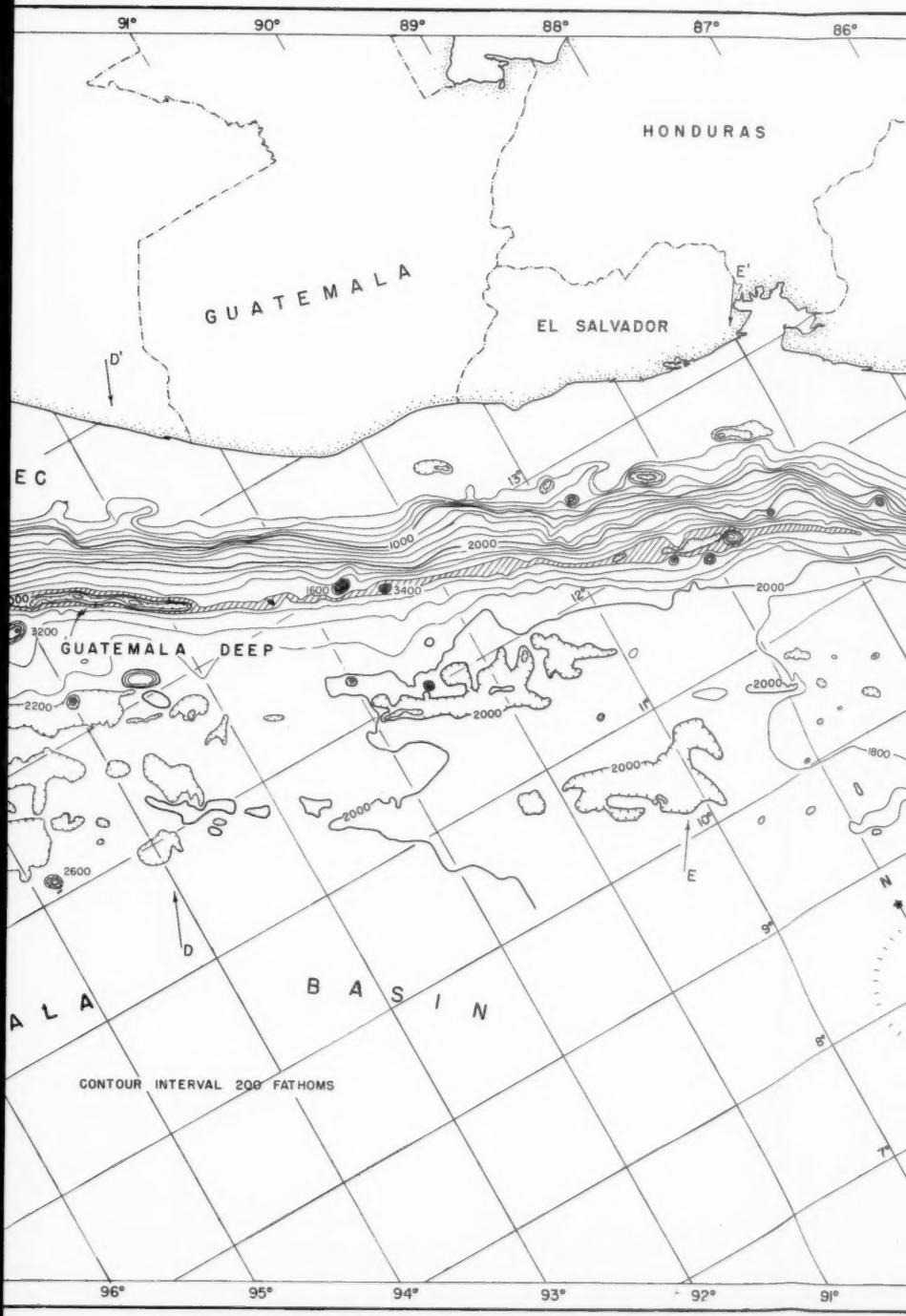

BATHYMETRIC CHART OF PACIFIC COAST FROM

Showing Middle America Trench

T FROM MEXICO TO PANAMA

a Trench

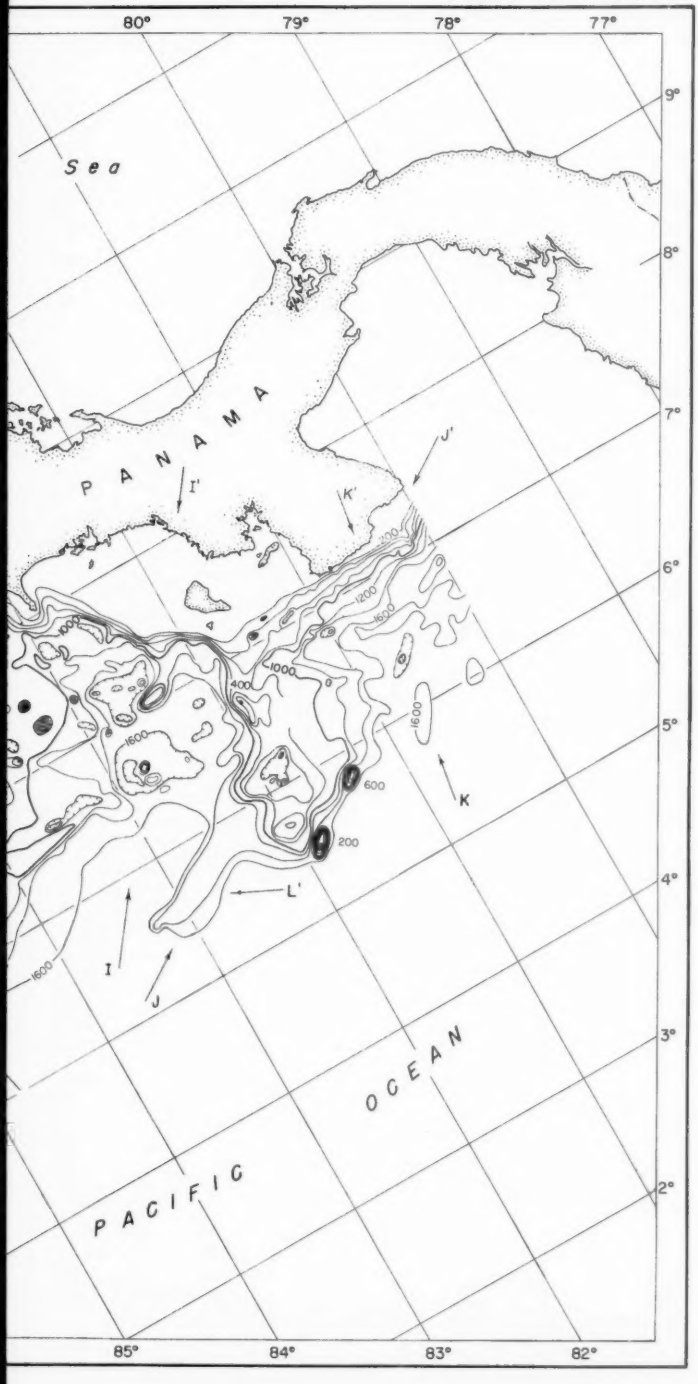
80°
79°
78°
77°
9°
8°
7°
6°
5°
4°
3°
2°
85°
84°
83°
82°
Sea
PANAMA
PACIFIC
OCEAN
I'
J'
K'
L'
I
J
K
200
400
600
800
1000
1200
1400
1600

BULLETIN OF THE GEOLOGICAL SOCIETY OF AMERICA
VOL. 66, PP. 777-782, 3 FIGS. JUNE 1955

GRAVITY ANOMALIES ASSOCIATED WITH SEAMOUNTS

BY G. LYNN SHURBET AND J. LAMAR WORZEL

Southeast of Cape Cod about 60 miles from the continental shelf there are several seamounts. Gravity measurements near two of them show free-air anomalies 30 to 90 mgal higher than values near by.

One seamount was investigated by Worzel and Northrop during ATLANTIS Cruise 173, in August 1951. It is located at 39° 50′ N, 66° 17′ W., about 60 miles from the 1000-fathom curve, where the depth is about 2100 fathoms. The seamount is named Retriever Peak, after one of the vessels used during investigations in a near-by part of the Gulf of Maine in 1951 (Drake *et al.*, 1954). Sounding profiles were made on seven tracks (Fig. 1) over the seamount to determine the configuration and minimum sounding. The navigation is based on two loran fixes, one about 2 hours before beginning the investigation, the other about 1-hour after completing the investigation. The absolute position of the seamount is probably accurate to within 2 miles. The maximum error in relative positions of the tracks is probably half a mile.

The soundings were recorded using an NMC-1 echo sounder adjusted to a sound velocity of 4800 ft/sec. The soundings have not been corrected for velocity variations in the water column or slope of the bottom.

Figure 1 shows that the minimum sounding obtained was slightly less than 1000 fathoms. The seamount has two peaks about 2 miles apart, and the base is more than 8 miles wide. The angle of maximum slope is at least 20°.

While the soundings were being made, C. L. Drake, on CARYN Cruise 25, took a bottom sample (core No. 4) with the piston corer (Fig. 1). David B. Ericson has examined this core and will publish a description and discussion. The core was taken at a depth of 980 fathoms, and it is 74 cm in length. According to Ericson its upper part is a fine well-sorted sand composed of about 52 per cent shells of Foraminifera, and 50 per cent quartz and other particles of nonbiogenous origin. At 40 cm there is a manganese oxide crust underlain by loose pebbles of igneous and metamorphic rocks. All this material has been transported. There is no trace of local volcanic activity. The fauna of the core is entirely Pleistocene. Currents have produced winnowing at some times and non-deposition at others.

On January 23, 1952, as a part of the program of gravity measurements at sea (Worzel and Ewing, 1950; 1952), the authors made gravity measurements in USS TORO (SS 422) at positions 39° 41′ N., 66° 05′ W. (station TO 6) and 39° 55′ N., 66° 13′ W. (station TO 7) (Figs. 1, 2). The free-air anomaly computed for station TO 6 is +16 mgal, the sounding 1865 fathoms. The free-air anomaly computed for station TO 7 is −3 mgal, the sounding 1920 fathoms. Previous data indicate a regional free-air anomaly for this area of about −30 ± 10 mgal.

During the gravity survey it was known that station TO 7 was only 6 miles north of Retriever Peak. The residual gravity anomaly of +27 mgal computed at that position was attributed to the excess mass of the seamount. Then the residual anomaly of +46 mgal computed for station TO 6, coupled with the fact that the sounding taken during that observation was about 400 fathoms less than the average depth in the area, led to the belief that station TO 6 was located on the flank of a seamount.

On April 23, 1952, USS TORO was again operating near station TO 6, and about 5 hours was available for the search of the area. A seamount was found about 4 miles east of station TO 6 at 39° 40′ N., 66° 00′ W. (Fig. 2) in an average ocean depth of 2250 fathoms. It is suggested that this seamount be name Picket Peak after the second vessel used in the Gulf of Maine survey of 1951 (Drake *et al.*, 1954).

Sounding profiles were made on eight tracks over the seamount to determine the configuration and minimum sounding. The tracks were plotted with a Dead Reckoning Tracer scaled at 1000 yards to the inch. Five loran fixes were

obtained during the investigation, and the absolute position of the seamount is probably accurate to within 1 mile. The maximum error in the relative positions of the tracks is probably half a mile.

the peak. A free-air anomaly of +58 mgal, or a residual anomaly of + 88 mgal, was computed for station TO 82.

Officer and Ewing (1954, p. 660) have reported about 12,000 feet of sediments at the

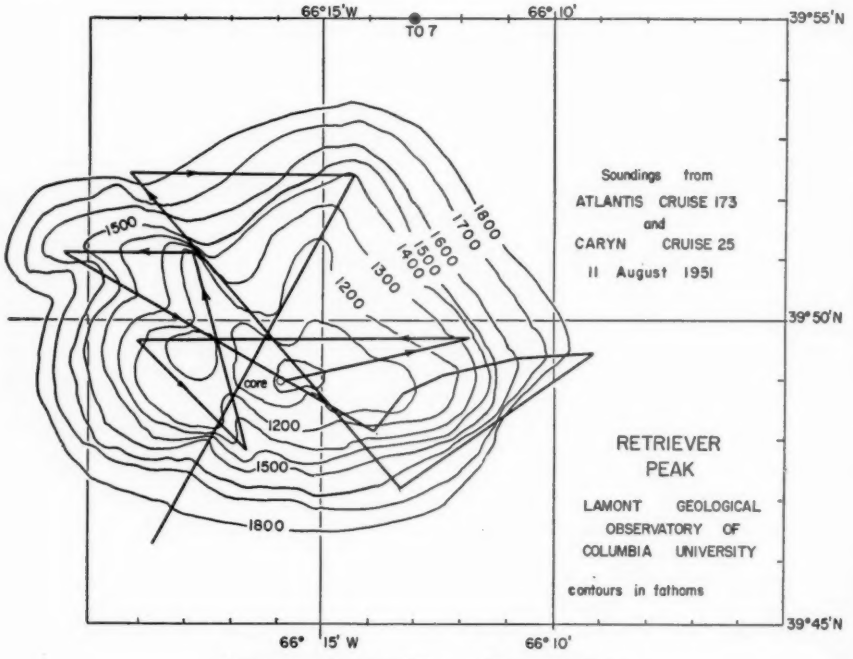

FIGURE 1.—CONTOUR MAP OF RETRIEVER PEAK

The soundings were taken visually with a standard NGA-1 echo sounder adjusted for a sound velocity of 4800 ft/sec. Corrections have not been applied to the soundings for velocity variations in the water column or for bottom slope.

The chart of Picket Peak shows that the minimum sounding obtained is slightly less than 1000 fathoms. The seamount has two peaks; however, the tracks are so oriented that the peaks are not well delineated. The seamount is slightly elongated along the northwest-southeast axis, and maximum slopes of at least 28° are found on the north side of the seamount.

Near the end of the sounding program another gravity observation, station TO 82, was made at 39° 41′ N., 66° 02′ W., 1.7 miles from

1000-fathom curve northwest from Picket Peak. The sediments thin slightly toward the southeast to about 10,000 feet near the 1700-fathom curve at 40° 22′ N., 66° 17′ W., about 40 miles north of Picket Peak. No data on sediment thickness nearer the seamount are available.

Figure 3 show the sections of these seamounts on east-west and north-south profiles. These profiles are approximated by the cylinders superimposed on the profiles (Fig. 3). At the bottom of the figure the computed anomaly curve for these cylinders (using 2.84 for the density of the rock in the seamount, 1.03 for the sea water, and 2.30 for the sediment after (Worzel and Shurbet, In press.)

The free-air anomalies for stations TO 6, TO 7, and TO 82 are plotted as circles on the scale of the computed curve. The residual anomalies

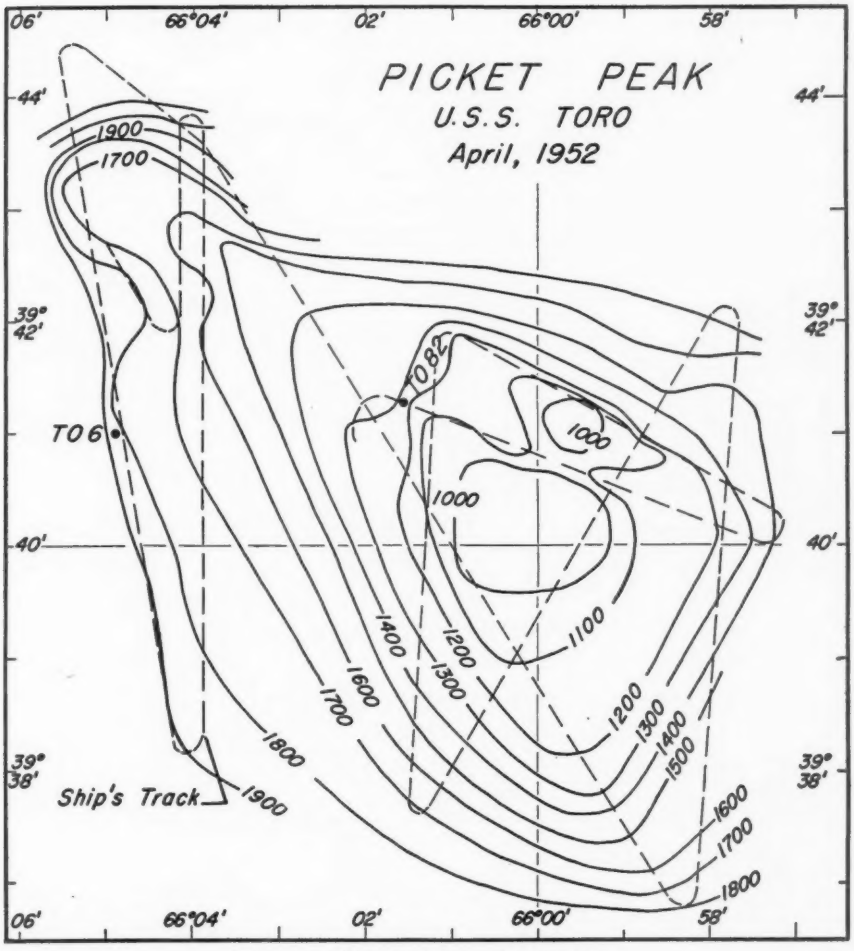

FIGURE 2.—CONTOUR MAP OF PICKET PEAK

are plotted as the triangular points. These points fall about 5 mgal below the computed curve. This excellent agreement is probably fortuitous since the regional anomaly is not known to better than about ± 10 mgal, since the slope corrections to the soundings would steepen the flanks of the seamounts, and since the estimates of the sedimentary thickness and subsediment shape have large probable errors. We can conclude that these peaks must be composed of rocks with density about 2.84 gm/cm³ if they are uncompensated loads on the crust, or of higher density if some compensation exists. The assumption of a substantially smaller cross section beneath the sediments would likewise require a density greater than 2.84 to explain the gravity anomaly. The assumption that the peaks have a thick sedimentary cover would also demand a higher density for the core. The seamounts are nearly circular and are part of a chain trending about northwest. They are probably volcanic peaks, as are all the peaks in the Atlantic Ocean over which magnetic profiles have been observed Heezen *et al.*, 1953, p. 29). The volcanism can be dated only as pre-Pleistocene from the

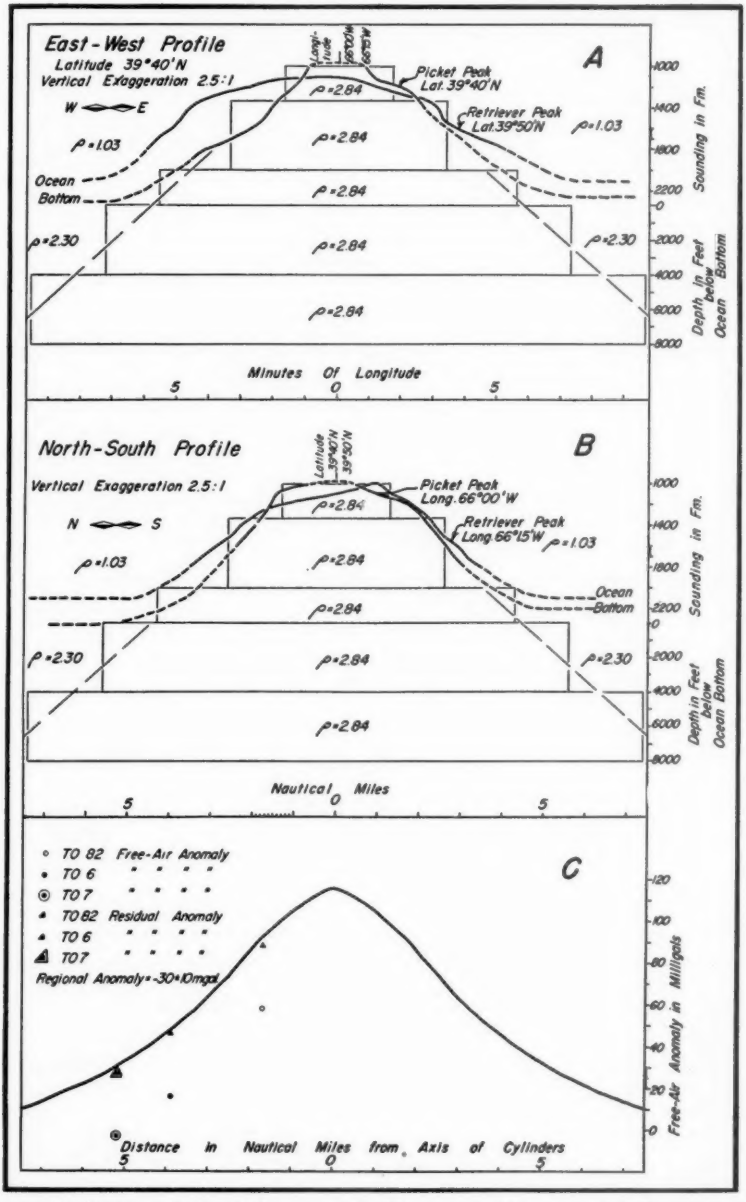

FIGURE 3.—PROFILES SHOWING ANOMALIES IN VICINITY OF RETRIEVER AND PICKET PEAKS

sediment sample. The evidence of strong currents capable of preventing deposition of sediments on peaks to depths of 1000 fathoms agrees with other results of coring and photography on other Atlantic seamounts (Tolstoy and Ewing, 1949; Heezen *et al.*, 1954).

We gratefully acknowledge the assistance of the officers and crews of USS TORO (SS 422), R. V. ATLANTIS, and R. V. CARYN, who made it possible to obtain the data. The contribution of the numerous members of the scientific parties is greatly appreciated. We thank Mr. David B. Ericson for permission to use his analysis of the core prior to its publication. This work was supported under contract N6 onr 271 Task Orders 8, 13, and 24 with the Office of Naval Research, Department of the Navy.

References Cited

Drake, C. L., Worzel, J. L., and Beckmann, W. C., 1954, Geophysical investigations in the emerged and submerged Atlantic coastal plain, Part IX: Gulf of Maine: Geol. Soc. America Bull., v. 65, p. 957–970.

Heezen, B. C., Ewing, M., and Miller, E. T., 1953, Trans-Atlantic profile of total magnetic intensity and topography, Dakar to Barbados: Deep-Sea Research, v. 1, p. 25–33.

Heezen, B. C., Ewing, M., Ericson, D. B., and Bentley, C. R., 1954, Flat-topped Atlantis, Cruiser, and Great Meteor Seamounts (Abstract): Geol. Soc. America Bull., v. 65, p. 1261.

Officer, C. B., Jr., and Ewing, M., 1954, Geophysical investigations in the emerged and submerged Atlantic coastal plain, Part VII: Continental shelf, continental slope, and continental rise south of Nova Scotia: Geol. Soc. America Bull., v. 65, p. 653–670.

Tolstoy, I., and Ewing, M., 1949, North Atlantic hydrography and the Mid-Atlantic Ridge: Geol. Soc. America Bull., v. 60, p. 1527–1540.

Worzel, J. L., and Ewing, M., 1950, Gravity measurements at sea, 1947: Am. Geophys. Union Trans., v. 31, no. 6.

—— 1952, Gravity measurements at sea, 1948, and 1949: Am. Geophys. Union Trans., v. 33, n. 3.

Worzel, J. L., and Shurbet, G. L., in press, Gravity interpretations from standard oceanic and continental crustal sections: Geol. Soc. America Special Paper 61, p. 87–100.

LAMONT GEOLOGICAL OBSERVATORY (COLUMBIA UNIVERSITY), PALISADES, N. Y.

LAMONT GEOLOGICAL OBSERVATORY CONTRIBUTION NO. 152

47. Mesozoic and Cenozoic Arcidae from the Pacific Slope of North America. P. W. Rinehart. 1943. 117 p., 15 pls., 3 figs. $1.50.
48. North American Pleospongia. V. J. Okulitch. 1943. 112 p., 19 figs. $1.50.
49. Ozarkian and Canadian Cephalopods. Part II: BreviconES. E. O. Ulrich, A. F. Foerste, and A. K. Miller. 1943. 240 p., 70 pls., 15 figs. $3.00.
50. Bibliography of Economic Geology of South America. J. T. Singewald, Jr. 1943. 159 p., $1.00.
56. Check List of California Tertiary Marine Mollusca. A. M. Keen and H. Bentson. 1944. 280 p., 4 figs. $2.25.
58. Ozarkian and Canadian Cephalopods. Part III. Longicones. E. O. Ulrich, A. F. Foerste, A. K. Miller, A. G. Unklesbay. 1944. 226 p., 68 pls., 9 figs. $3.00.
59. Upper Devonian Corals of the Mackenzie River Region, Canada. Stanley Smith. 1945. 126 p., 25 pls. $2.00.
60. Glacial Map of North America. By Committee on Glacial Map, R. F. Flint, *Chairman*. 1945. $2.00.

MEMOIRS

1. Stratigraphy of Western Newfoundland. Charles Schuchert and C. O. Dunbar. 1934. 123 p., 11 pls., 8 figs. $3.40.
2. Paleozoic Plankton of North America. Rudolf Ruedemann. 1934. 141 pp., 26 pls., 6 figs. $2.40.
3. Evolution of the Congo Basin. A. C. Veatch. 1935. 183 p., 10 pls., 8 figs. $2.10.
4. Geology in the Coastal Atlas of Western Algeria. R. van V. Anderson. 1936. 450 p., 19 pls., 2 figs. $4.20.
10. Radiolaria from the Kreyenhagen Formation near Los Banos, California. B. L. Clark and A. S. Campbell. 1945. 66 p., 7 pls. $1.20.
11. Mollusca of the Tertiary Formations of Northeastern Mexico. Julia Gardner. 1945. 332 p., 28 pls., 1 fig. $3.90.
12. Revision of the Upper Cambrian Fauna of New Jersey. B. F. Howell. 1945. 46 p., 8 pls. $1.00.
13. Pennsylvanian Geology of a Part of the Southern Appalachian Coal Field. H. R. Wanless. 1945. 162 p., 40 pls., 1 fig. $3.90.
14. Brachiopoda of the Independence Shale. M. A. Stainbrook. 1945. 76 p., 6 pls., 2 figs. $1.20.
16. Eocene Faunas from the Department of Bolivar, Colombia. B. L. Clark and J. W. Durham. 1946. 126 p., 28 pls., 1 fig. $2.10.
18. Lineation. A Critical Review and Annotated Bibliography. Ernst Cloos. 1946. 122 p., 10 pls., 15 figs. $1.80. Supplement (Literature for 1942–1952), self cover, 16 pages. 1953. 25 cents.
19. Graptolites of North America. Rudolf Ruedemann. 1947. 652 p., 92 pls., 1 fig. $9.00.
21. Origin and Development of Craters. T. A. Jaggar. 1947. 508 p., 87 pls., 14 figs. $6.00.
22. Reconnaissance Geology of Portions of Victoria Island and Adjacent Regions, Arctic Canada. A. L. Washburn. 1947. 142 p., 32 pls., 4 figs. $4.00.
23. Tertiary Nautiloids of the Americas. A. K. Miller. 1947. 234 p., 100 pls., 30 figs. $4.50.
25. Evolution of the Horse Brain. Tilly Edinger. 1948. 177 p., 4 pls., 24 figs. $2.00.
26. Bibliographic Index of Permian Invertebrates. C. C. Branson. 1948. 1049 p. $9.50.
27. Propagation of Sound in the Ocean. J. L. Worzel, Maurice Ewing, C. L. Pekeris. 1948. 205 p., 23 pls., 89 figs. $2.75.
28. Origin of Granite (Conference). James Gilluly, *Chairman*. 1948. 139 p., 13 pls., 5 figs. $1.80.
32. Stratigraphy and Fauna of the Agua Salada Group, State of Falcón, Venezuela. H. H. Renz. 1948. 219 p., 13 pls., 15 figs. $2.75.
33. Geology and Origin of South Park, Colorado. J. T. Stark *et al*. 1949. 188 p., 18 pls., 22 figs. $3.75.
34. Permian Crinoid Calceolispongia. Curt Teichert. 1949. 132 p., 26 pls., 24 figs. $2.50.
35. Geology of the Coast Ranges Immediately North of the San Francisco Bay Region, California. A. C. Weaver. 1949. 242 p., 14 pls., 2 figs. $6.50.
36. Geology of the Lake Titicaca Region, Peru and Bolivia. N. D. Newell. 1949. 111 p., 21 pls., 14 figs. $5.00.
37. Bibliography of Fossil Vertebrates, 1939–1943. C. L. Camp, S. P. Welles, and Morton Green. 1949. 371 p. $4.50.
38. Lower Cretaceous Stratigraphy in Southeastern Arizona. Alexander Stoyanow. 1949. 169 p., 27 pls., 2 figs. $2.50
39. Sedimentary Facies in Geologic History. C. R. Longwell, *Chairman*. 1949. 171 p. $1.75.
40. Revision of the Families and Genera of the Devonian Tetracorals. E. C. Stumm. 1949. 92 p., 25 pls. $2.00.
41. American Permian Nautiloids. A. K. Miller and Walter Youngquist. 1949. 218 p., 59 pls., 39 figs. $3.60.
42. Maquoketa Brachiopoda of Iowa. Y. Wang. 1950. 55 p., 12 pls. $1.40.
43. 1940 E. W. Scripps Cruise to Gulf of California. C. A. Anderson *et al*. 1950. 362 p., 65 pls., 28 figs. $6.50.
45. Interpretation of Ore Textures. E. S. Bastin. 1950. 101 p., 28 figs. $1.75.
46. Ecology of Foraminifera, Northwest Gulf of Mexico. Fred B. Phleger and Frances L. Parker. 1951. 132 p., 22 pls 33 figs. $2.75.
47. Interpretation of Aeromagnetic Maps. V. Vacquier *et al*. 1951. 151 p., 14 pls., 83 figs. $2.25.
48. North American Geosynclines. Marshall Kay. 1951. 143 p., 16 pls., 20 figs. $2.00.
49. Geologic Structure and Orogenic History of Venezuela. W. H. Bucher. 1952. 113 p., 5 figs. $1.50.
50. Deformation, Metamorphism and Mineralization in Gypsum-Anhydrite Cap Rock. Marcus Goldman. 1952. 169 p., 5 figs., 64 pls. $3.00.
51. Catalogue of the Cenozoic Plants of North America through 1950. Robert S. LaMotte. 1952. 381 p., 5 figs. $5.50.
52. Selected Petrogenic Relationships of Plagioclase. R. C. Emmons, *Editor*. 1953. 142 p., 38 figs., 16 pls. $2.00.
53. Paleozoic and Mesozoic Arachnida of Europe. Alexander Petrunkevitch. 1953. 128 p., 58 pls. $3.00.
54. Biostratigraphy of the Maqfi Section, Egypt. L. W. LeRoy. 1953. 73 p., 4 figs., 14 pls. $1.75.
55. Trilobites from the Lower Champlainian Formations of the Appalachian Valley. Byron N. Cooper. 1953. 68 p., 1 fig., 19 pls. $1.75.
56. North American and European Strophodontids: Morphology and Systematics. Alwyn Williams. 1953. 67 p., 5 figs., 13 pls. $1.50.
57. Bibliography of Fossil Vertebrates, 1944–1948. C. L. Camp *et al*. 1953. 465 p. $5.50.
58. Upper Paleozoic of Peru. N. D. Newell, John Chronic, and T. G. Roberts. 1953. 276 p., 44 pls., 43 figs. $4.00.
59. Silicified Middle Ordovician Trilobites. H. B. Whittington and W. R. Evitt II 1954. 137 p., 27 figs., 33 pls. $3.00.
60. Crystal Data. J. D. H. Donnay and Werner Nowacki. 1954. 719 p. $5.00.
61. Stratigraphy and History of the Moenkopi Formation of Triassic Age. E. D. McKee. 1954. 133 p., 19 figs., 12 pls. $3.00.
62. Ordovician Cephalopod Fauna of Baffin Island. A. K. Miller *et al*. 1954. 234 p., 20 figs., 63 pls. $4.75

Publications of The Geological Society of America

Publications may be purchased at indicated prices on order accompanied by remittance addressed to The Geological Society of America, 419 West 117 Street, New York 27, N. Y.

BULLETIN

Monthly, Advance subscription, $15 per year; separate numbers $1.50; back yearly volumes, as available: prior to 1935, $12.00 per volume; 1935–, $15.00 per volume. Ten-year indexes covering vols. 11–20, 31–40, 41–50, $1.50 per copy; covering vols. 51–60, $1.00 per copy.

PROCEEDINGS

Annually. Contains business of Annual Meeting, Reports of committees, and memorials. $1.50 per volume.

HISTORY

THE GEOLOGICAL SOCIETY OF AMERICA, 1888-1930. A Chapter in Earth Science History. By H. L. Fairchild. 1932. 232 p., 18 pls. $2.50.

BERKEY VOLUME

APPLICATION OF GEOLOGY TO ENGINEERING PRACTICE, Sidney Paige, *Chairman*, By 18 Authors (13 papers), 327 p. $2.75.

PENROSE VOLUME

LIFE AND LETTERS OF R. A. F. PENROSE, JR., H. R. Fairbanks and C. P. Berkey. 1952. 765 p. $4.00.

BIBLIOGRAPHY OF GEOLOGY EXCLUSIVE OF NORTH AMERICA

Annually, 1933-1940; biennially, 1941-1946; annually, 1947–. By Marie Siegrist, Marcia Lakeman, and Mary Grier. Vols. 1-8 inclusive, $2.50 per volume; Volume 9, $2.75; Volumes 10-12 out of stock; Volume 13, $3.25; Volume 14, $3.00; Volume 15, $3.00; Volume 16, $4.50; Volume 17, $5.75; Volume 18, $5.50.

SPECIAL COLORED MAPS

GLACIAL MAP OF NORTH AMERICA (Special Paper 60). By Committee on Glacial Map, R. F. Flint, *Chairman*. 1945. $2.00.

GEOLOGIC MAP OF SOUTH AMERICA. By South American Map Committee, A. I. Levorsen, *Chairman* 1950. $4.00.

GEOLOGIC-TECTONIC MAP OF VENEZUELA. By W. H. Bucher. 1950. $2.50.

TECTONIC MAP OF CANADA. By Geological Association of Canada. 1950. $1.50.

GEOLOGIC MAP OF NORTH AMERICA. Compiled by G. W. Stose. Reprinted 1951. $3.50.

PLEISTOCENE EOLIAN DEPOSITS OF THE UNITED STATES, ALASKA, AND PARTS OF CANADA. James Thorp and H. T. U. Smith *Cochairmen*. 1952. $3.00.

ROCK COLOR CHARTS

Prepared by Committee of National Research Council. $7.00 per set.

TREATISE ON INVERTEBRATE PALEONTOLOGY

Raymond C. Moore, *Editor*

Part D. PROTISTA 3 (Chiefly Radiolarians and Tintinnines). By A. S. Campbell and R. C. Moore. 1955. 195 p., 92 figs. $3.00.
Part E. ARCHAEOCYATHA AND PORIFERA. By V. J. Okulitch and M. W. de Laubenfels. 1955. 122 p., 88 figs. $3.00.
Part G. BRYOZOA. By Ray S. Bassler. 1954. 253 p., 175 figs. $3.00.

SPECIAL PAPERS

1. BIBLIOGRAPHY AND INDEX OF PALEOZOIC OSTRACODA. R. S. Bassler and Betty Kellett. 1934, 500 p., 24 figs. $3.00.
2. FOSSIL CRUSTACEA OF THE ATLANTIC AND GULF COASTAL PLAIN. M. J. Rathbun. 1935. 160 p., 26 pls., 2 figs. $1.50.
3. FOSSIL NON-MARINE MOLLUSCA OF NORTH AMERICA. Junius Henderson. 1935. 313 p. $2.10.
5. GEOLOGY OF SAINT JOHN, NEW BRUNSWICK. A. O. Hayes and B. F. Howell. 1937. 146 p., 9 pls., 4 figs. $1.50.
7. ATLANTIC SUBMARINE VALLEYS OF THE UNITED STATES AND THE CONGO SUBMARINE VALLEY. A. C. Veatch and Paul A. Smith. 1939. 101 p., 5 charts, 10 pls., 28 figs. $4.50.
9. FOSSIL SNAKES OF NORTH AMERICA. C. W. Gilmore. 1938. 96 p., 4 pls., 38 figs. $0.90.
11. GEOLOGY AND PALEONTOLOGY OF THE MINGAN ISLANDS, QUEBEC. W. H. Twenhofel. 1938. 132 p. 24 pls., 1 fig. $1.50.
12. TERTIARY FLORA FROM THE RIO PICHILEUFU, ARGENTINA. E. W. Berry. 1938. 149 p., 55 pls., 11 figs. $2.10.
13. OZARKIAN AND CANADIAN BRACHIOPODA. E. O. Ulrich and G. A. Cooper. 1938. 323 p. 53 pls., 14 figs. $3.90.
19. CAMBRIAN MEROSTOMATA. G. O. Raasch. 1939. 146 p., 21 pls., 14 figs. $1.50.
21. PALEONTOLOGY AND STRATIGRAPHY OF THE SILURIAN ROCKS OF THE PORT DANIEL-BLACK CAPE REGION, GASPE. S. A. Northrop. 1939. 302 p., 28 pls., 1 fig. $3.00.
3. BIBLIOGRAPHIC INDEX OF NORTH AMERICAN DEVONIAN CEPHALOPODA. E. M. Kindle and A. K. Miller. 1939. 179 p. $1.30.
7. BIBLIOGRAPHY OF FOSSIL VERTEBRATES. 1928-1933. C. L. Camp and V. L. VanderHoof. 1940. 503 p. $4.20.
28. REVIEW OF THE PELYCOSAURIA. A. S. Romer and L. I. Price. 1949. 538 p., 46 pls., 71 figs. $4.20.
29. PHACOPID TRILOBITES OF NORTH AMERICA. D. M. Delo. 1940. 135 p., 13 pls., $1.20.
33. NUMERICAL STRUCTURE FACTOR TABLES. M. J. Buerger. Reprinted 1953. 119 p., 4 figs. (Cloth bound) $1.50.
36. HANDBOOK OF PHYSICAL CONSTANTS. Edited by Francis Birch, *Chairman, et al.* 1942. 325 p., 19 figs. $1.70.
37. OZARKIAN AND CANADIAN CEPHALOPODS, PART I, NAUTILICONES. E. O. Ulrich, Aug. F. Foerste, A. K. Miller and W. M. Furnish. 1942. 157 p., 57 pls., 23 figs. $2.40.
38. TEREBRATULOID BRACHIOPODA OF THE SILURIAN AND DEVONIAN. P. E. Cloud Jr. 1942. 182 p., 26 pls., 17 figs. $1.80.
39. EOCENE RADIOLARIAN FAUNAS FROM THE MT. DIABLO AREA, CALIFORNIA. B. L. Clark and A. S. Campbell. 1942. 112 p., 9 pls., 5 figs. $1.00.
40. HADROSAURIAN DINOSAURS OF NORTH AMERICA. R. S. Lull and N. E. Wright. 1942, 242 p., 31 pls., 90 figs. $2.70.
42. BIBLIOGRAPHY OF FOSSIL VERTEBRATES, 1934-1938. C. L. Camp, D. N. Taylor, and S. P. Welles. 1942. 663 p. $5.70.
44. REVISION OF THE SUBORDERS, FAMILIES, AND GENERA OF THE SCLERACTINIA. T. W. Vaughan and J. W. Wells. 1943. 363 p., 51 pls., 39 figs. $3.90.
45. BIBLIOGRAPHIC AND FAUNAL INDEX OF PALEOZOIC PELMATOZOAN ECHINODERMS. R. S. Bassler and M. W. Moodey. 1943. 723 p. $5.70.

(Continued on inside back cover)

UNCLASSIFIED

INDEX TO VOLUME 66 (JANUARY–JUNE)*

Aa, O Shima volcano, Japan. By H. L. Foster and A. C. Mason ... 731
Aberdeen member (Blackhawk formation, Cretaceous) (new name), Book Cliffs, Utah-Colorado. By R. G. Young ... 177
Albation (in glaciers). By L. E. Nielsen ... 1
Accumulation (in glaciers). By L. E. Nielsen ... 1
†Additional evidence of volcanism on Mars. By D. B. McLaughlin ... 769
†Age determinations of some rocks from the Boulder batholith and other batholiths of western Montana. By R. W. Chapman, David Gottfried, and C. L. Waring ... 607
Alaska, Origin and character of the upland silt near Fairbanks. By T. L. Péwé ... 699
Analyses, Chemical
  Glendora volcanics, Los Angeles Basin, California. By J. S. Shelton ... 45
Analysis
  Chemical (method). By W. H. Dennen and W. C. Fowler ... 655
  Spectrographic (method). By W. H. Dennen and W. C. Fowler ... 655
—— of fracture patterns. By Ernst Cloos ... 241
†Anomalous uranium-lead ages. By J. L. Kulp and W. R. Eckelmann ... 767
Archean rocks
  Peridotites of Manpur, Singhbhum district, Bihar, and origin of associated asbestos deposits. By S. C. Chatterjee ... 91
Arkansas, Bibliography and index of literature on uranium and thorium and radioactive occurrences. By Margaret Cooper ... 257
Asbestos, Origin of deposits associated with peridotites of Manpur, Singhbhum district, Bihar. By S. C. Chatterjee ... 91
Ash falls, Provenience of. By C. S. Ross ... 427
Assimilation
  Trondhjemite batholith near Bidwell Bar, California. By R. R. Compton ... 9

Batholith near Bidwell Bar, California, Trondhjemite. By R. R. Compton ... 9
Bentonite beds, Provenience of. By C. S. Ross ... 427
Bibliography and index of literature on uranium and thorium and radioactive occurrences in U. S. Part 4: Arkansas, Iowa, Kansas, Louisiana, Minnesota, Missouri, Nebraska, North Dakota, Oklahoma, South Dakota, Texas. By Margaret Cooper ... 257
Bidwell Bar, California, Trondhjemite batholith near. By R. R. Compton ... 9
Biogeochemistry, Sampling in. By H. V. Warren *et al.* ... 229
BLOOMER, R. O., AND WERNER, H. J.: Geology of the Blue Ridge region in central Virginia ... 579
Blue Ridge region in central Virginia, Geology of. By R. O. Bloomer and H. J. Werner ... 579
Book Cliffs, Utah-Colorado, Sedimentary facies and intertonguing in the Upper Cretaceous of. By R. G. Young ... 177
Brewster County, Texas, Geology of Cathedral Mountain quadrangle. By W. N. McAnulty ... 531
BRIDGE, JOSIAH: Disconformity between Lower and Middle Ordovician series at Douglas Lake, Tennessee ... 725

California
  Glendora volcanic rocks, Los Angeles Basin. By J. S. Shelton ... 45
  Trondhjemite batholith near Bidwell Bar. By R. R. Compton ... 9
Cameo member (Price River formation, Cretaceous) (new name), Book Cliffs, Utah-Colorado. By R. G. Young ... 177
"Cascade peneplain" in south-central Washington. By A. C. Waters ... 663
Castlegate member (Price River formation, Cretaceous) (new name), Book Cliffs, Utah-Colorado. By R. G. Young ... 177
Cathedral Mountain quadrangle, Brewster County, Texas, Geology of. By W. N. McAnulty ... 531
Catoctin Mountain, Maryland and Virginia, Geology of. By J. C. Whitaker ... 435
†CHAPMAN, R. W., GOTTFRIED, DAVID, AND WARING, C. L.: Age determinations of some rocks from the Boulder batholith and other batholiths of western Montana ... 607
CHATTERJEE, S. C.: Peridotites of Manpur, Singhbhum district, Bihar, and origin of associated asbestos deposits ... 91
Chemical analyses
  Glendora volcanics, Los Angeles Basin, California. By J. S. Shelton ... 45
  Method. By W. H. Dennen and W. C. Fowler ... 655
CLARK, T. H., AND STRACHAN, ISLES: Log of the Senigon well, southern Quebec ... 685
Climate in Mexico, Pleistocene. By P. B. Sears and K. H. Clisby ... 521
CLISBY, K. H., AND SEARS, P. B.: Palynology in southern North America.
  Part III: Microfossil profiles under Mexico City correlated with the sedimentary profiles ... 511
—— (With P. B. SEARS): Palynology in southern North America.
  Part IV: Pleistocene climate in Mexico ... 521
CLOOS, ERNST: Experimental analysis of fracture patterns ... 241
Columbia River
  Geomorphology of south-central Washington, illustrated by the Yakima East quadrangle. By A. C. Waters ... 663
—— —— basalt in south-central Washington. By A. C. Waters ... 663
COMPTON, R. R.: Trondhjemite batholith near Bidwell Bar, California ... 9
Conglomerate of northeastern Ohio, Source of Sharon. By J. O. Fuller ... 159
Continental-slope topography in northwest Gulf of Mexico. By B. L. Gealy ... 203
COOPER, MARGARET: Bibliography and index of literature on uranium and thorium and radioactive occurrences in U. S. Part 4: Arkansas, Iowa, Kansas, Louisiana, Minnesota, Missouri, Nebraska, North Dakota, Oklahoma, South Dakota, Texas ... 257
Corcoran member (Price River formation, Cretaceous) (new name), Book Cliffs, Utah-Colorado. By R. G. Young ... 177
Cozzette member (Price River formation, Cretaceous) (new name), Book Cliffs, Utah-Colorado. By R. G. Young ... 177
Cretaceous
  Sedimentary facies and intertonguing of the Book Cliffs, Utah-Colorado. By R. G. Young ... 177
Cumberland Plateau, Tennessee, Low-angle overthrusting in. By R. G. Stearns ... 615

* Full titles of papers are in boldface type.
† Indicates Short Note.

Cyclic classification
Sedimentary facies and intertonguing in the Upper Cretaceous of the Book Cliffs, Utah-Colorado. By R. G. Young ... 177

DELAVAULT, R. E. (With H. V. WARREN AND J. A. C. FORTESCUE): Sampling in biogeochemistry ... 229
DENNEN, W. H., AND FOWLER, W. C.: Spectrographic analysis by use of mutual standard method ... 655
Desert member (Blackhawk formation, Cretaceous) (new name), Book Cliffs, Utah-Colorado. By R. G. Young ... 177
Devonian
Source of Sharon conglomerate of northeastern Ohio. By J. O. Fuller ... 159
Disconformity between Lower and Middle Ordovician series at Douglas Lake, Tennessee. By Josiah Bridge ... 725
†Discovery of *Sonoraspis* in Southern California. By Alexander Stoyanow and Takeo Susuki ... 467
Distribution of igneous rocks in space and time. By G. W. Tyrrell ... 405
Dollard, Saskatchewan, Drumlins with jointed boulders near. By W. O. Kupsch ... 327
Douglas Lake member (Ordovician) (new name), Tennessee. By Josiah Bridge ... 725
Drumlins with jointed boulders near Dollard, Saskatchewan. By W. O. Kupsch ... 327

†ECKELMANN, W. R. (With J. L. KULP): Anomalous uranium-lead ages ... 767
Economic geology
Geology of the Lima region, southwestern Montana and adjacent Idaho. By Robert Scholten *et al.* ... 345
†ENGLAND, J. L. (With O. F. TUTTLE): Preliminary report on the system SiO_2-H_2O ... 149
Equilibrium glaciers, Regimen and flow of ice in. By L. E. Nielsen ... 1
Experimental analysis of fracture patterns. By Ernst Cloos ... 241

†FAGERSTROM, J. A.: Unusual desiccation cracks in the Benwood limestone of eastern Ohio ... 339
Fairbanks, Alaska, Origin and character of the upland silt near. By T. L. Péwé ... 699
Farrer facies (Price River formation, Cretaceous) (new name), Book Cliffs, Utah-Colorado. By R. G. Young ... 177
Faulting
Experimental analysis of fracture patterns. By Ernst Cloos ... 241
Gulf of Mexico. By B. L. Gealy ... 203
Flow and regimen of ice in equilibrium glaciers. By L. E. Nielsen ... 1
FOREMAN, FRED: Palynology in southern North America. Part II: Study of two cores from lake sediments of the Mexico City Basin ... 475
FORTESCUE, J. A. C. (With H. V. WARREN AND R. E. DELAVAULT): Sampling in biogeochemistry ... 229
FOSTER, H. L., AND MASON, A. C.: 1950 and 1951 eruptions of Mihara Yama, O Shima volcano, Japan ... 731
FOWLER, W. C. (With W. H. DENNEN): Spectrographic analysis by use of mutual standard method ... 655
Fracture patterns, Experimental analysis of. By Ernst Cloos ... 241
FULLER, J. O.: Source of Sharon conglomerate of northeastern Ohio ... 159

GEALY, B. L.: Continental-slope topography in northwest Gulf of Mexico ... 203
Geology of Blue Ridge region in central Virginia. By R. O. Bloomer and H. J. Werner ... 579
—— —— **Cathedral Mountain quadrangle, Brewster County, Texas.** By W. N. McAnulty ... 531
—— —— **Catoctin Mountain, Maryland and Virginia.** By J. C. Whitaker ... 435
—— —— **Hanover quadrangle, New Hampshire-Vermont.** By J. B. Lyons ... 105
—— —— **Lima region, southwestern Montana and adjacent Idaho.** By Robert Scholten *et al.* ... 345
Geomorphology
Continental slope in northwest Gulf of Mexico. By B. L. Gealy ... 203
Geology of Lima region, southwestern Montana and adjacent Idaho. By Robert Scholten, K. A. Keenmon, and W. O. Kupsch ... 345
Low-angle overthrusting in the central Cumberland Plateau, Tennessee. By R. G. Stearns ... 615
—— **of south-central Washington, illustrated by the Yakima East quadrangle.** By A. C. Waters ... 663
Geophysics
1950 and 1951 eruptions of Mihara Yama, O Shima, Japan. By H. L. Foster and A. C. Mason ... 731
Glacial geology
Pleistocene geology of the southwestern Wind River Mountains, Wyoming. By G. W. Holmes and J. H. Moss ... 629
Glaciology
Drumlins with jointed boulders near Dollard, Saskatchewan. By W. O. Kupsch ... 327
Regimen and flow of equilibrium glaciers. By L. E. Nielsen ... 1
Glendora volcanic rocks, Los Angeles Basin, California. By J. S. Shelton ... 45
†GOLDBERG, E. D., AND INMAN, D. L.: Neutron-irradiated quartz as a tracer of sand movements ... 611
†GOTTFRIED, DAVID (With R. W. CHAPMAN AND C. L. WARING): Age determinations of some rocks from the Boulder batholith and other batholiths of western Montana ... 607
Graptolites
Log of the Senigon well, southern Quebec. By T. H. Clark and Isles Strachan ... 685
Grassy member (Blackhawk formation, Cretaceous) (new name) Book Cliffs, Utah-Colorado. By R. G. Young ... 177
†GRAY, H. H.: Thickness of bedding and parting in sedimentary rocks ... 147
Gulf of Mexico, Continental-slope topography in northwest. By B. L. Gealy ... 203

Hanover quadrangle, New Hampshire-Vermont, Geology of. By J. B. Lyons ... 105
†HEACOCK, J. G., JR., AND WORZEL, J. L.: Submarine topography west of Mexico and Central America ... 773
HOLMES, G. W., AND MOSS, J. H.: Pleistocene geology of the southwestern Wind River Mountains, Wyoming ... 629
†HONKALA, FRED S.: Selected bibliography of standard stratigraphic sections of North America ... 153
Hydrography
Continental-slope topography in northwest Gulf of Mexico. By B. L. Gealy ... 203

Ice in equilibrium glaciers, Regimen and flow of. By L. E. Nielsen ... 1
Idaho, Geology of Lima region. By Robert Scholten *et al.* ... 345
Igneous rocks
Cathedral Mountain quadrangle, Texas. By W. N. McAnulty ... 531
Catoctin Mountain, Maryland and Virginia. By J. C. Whitaker ... 435

Igneous rocks (*Continued*)
Distribution in space and time. By G. W. Tyrrell.... 405
Glendora volcanic rocks, Los Angeles Basin, California. By J. S. Shelton..... 45
Hanover quadrangle, New Hampshire-Vermont. By J. B. Lyons..... 105
Lima region, southwestern Montana and adjacent Idaho. By Robert Scholten *et al.*..... 345
Trondhjemite batholith near Bidwell Bar, California. By R. R. Compton..... 9
—— —— in space and time. By C. S. Ross..... 427
Index of literature on uranium and thorium and radioactive occurrences in the U. S. Part 4. By Margaret Cooper..... 257
†Inman, D. L. (With E. D. Goldberg): Neutron-irradiated quartz as a tracer of sand movements..... 611
Intertonguing (and sedimentary facies) in the Upper Cretaceous of the Book Cliffs, Utah-Colorado. By R. G. Young..... 177
Iowa, Bibliography and index of literature on uranium and thorium and radioactive occurrences in. By Margaret Cooper..... 257

Japan, 1950 and 1951 eruptions of Mihara Yama, O Shima volcano. By H. L. Foster and A. C. Mason..... 731
Jointed boulders in drumlins near Dollard, Saskatchewan. By W. O. Kupsch..... 327

Kansas, Bibliography and index of literature on uranium and thorium and radioactive occurrences in. By Margaret Cooper..... 257
Keenmon, K. A. (With Robert Scholten and W. O. Kupsch): Geology of the Lima region, southwestern Montana and adjacent Idaho..... 345
Kenilworth member (Blackhawk formation, Cretaceous) (new name), Book Cliffs, Utah-Colorado. By R. G. Young..... 177
Kettleman Hills, California
Experimental analysis of fracture patterns. By Ernst Cloos..... 241
Kindreds of igneous rocks. By G. W. Tyrrell..... 405
†Kulp, J. L., and Eckelmann, W. R.: Anomalous uranium-lead ages..... 767
Kupsch, W. O.: Drumlins with jointed boulders near Dollard, Saskatchewan..... 327
—— (With Robert Scholten and K. A. Keenmon): Geology of the Lima region, southwestern Montana and adjacent Idaho..... 345

Lacustrine sedimentation
Palynology in southern North America. Part II: Study of two cores from the lake sediments of the Mexico City Basin. By Fred Foreman..... 475
Landslides in Gulf of Mexico. By B. L. Gealy..... 203
†Late Keweenawan or early Cambrian glaciation in Upper Michigan. By R. C. Murray..... 341
Lima region, Montana and Idaho, Geology of. By Robert Scholten *et al.*..... 345
Literature on uranium and thorium and radioactive occurrences in the U. S. Part 4. By Margaret Cooper..... 257
Loess deposits in Alaska. By T. L. Péwé..... 699
Log of the Senigon well, southern Quebec. By T. H. Clark and Isles Strachan..... 685
Los Angeles Basin, California, Glendora volcanics in. By J. S. Shelton..... 45
Louisiana, Bibliography and index of literature on uranium and thorium and radioactive occurrences in. By Margaret Cooper..... 257
Low-angle overthrusting in the central Cumberland Plateau, Tennessee. By R. G. Stearns..... 615
Lyons, J. B.: Geology of Hanover quadrangle, New Hampshire-Vermont..... 105

Manpur, India, Peridotites and origin of associated asbestos deposits. By S. C. Chatterjee..... 91
Maryland, Geology of Catoctin Mountain. By J. C. Whitaker..... 435
Mason, A. C. (With H. L. Foster): 1950 and 1951 eruptions of Mihara Yama, O Shima volcano, Japan..... 731
Mathematics of equilibrium glaciers. By L. E. Nielsen.... 1
McAnulty, W. N.: Geology of Cathedral Mountain quadrangle, Brewster County, Texas..... 531
†McLaughlin, D. B.: Additional evidence of volcanism on Mars..... 769
Metamorphism
Catoctin Mountain, Maryland and Virginia. By J. C. Whitaker..... 435
Hanover quadrangle, New Hampshire-Vermont. By J. B. Lyons..... 105
Trondhjemite batholith near Bidwell Bar, California. By R. R. Compton..... 9
Mexico, Pleistocene climate in. By P. B. Sears and K. H. Clisby..... 521
Mexico City Basin, Study of two cores from the lake sediments of. By Fred Foreman..... 475
Microfossil profiles under Mexico City. By K. H. Clisby and P. B. Sears..... 511
Migmatites in trondhjemite batholith near Bidwell Bar, California. By R. R. Compton..... 9
Mineralogy
Peridotites of Manpur, Singhbhum district, Bihar, and origin of associated asbestos deposits. By S. C. Chatterjee..... 91
Minnesota, Bibliography and index of literature on uranium and thorium and radioactive occurrences in. By Margaret Cooper..... 257
Mississippi Trough; of Gulf of Mexico. By B. L. Gealy... 203
Missouri, Bibliography and index of literature on uranium and thorium and radioactive occurrences in. By Margaret Cooper..... 257
Montana, Geology of Lima region. By Robert Scholten *et al.*..... 345
Moraines
Pleistocene geology of the southwestern Wind River Mountains, Wyoming. By G. W. Holmes and J. H. Moss..... 629
Moss J. H. (With G. W. Holmes): Pleistocene geology of the southwestern Wind River Mountains, Wyoming.. 629
†Murray, R. C.: Late Keweenawan or early Cambrian glaciation in Upper Michigan..... 341

Nebraska, Bibliography and index of literature on uranium and thorium and radioactive occurrences in. By Margaret Cooper..... 257
Nielsen, L. E.: Regimen and flow of ice in equilibrium glaciers..... 1
Neslen facies (Price River formation, Cretaceous) (new name) Book Cliffs Utah-Colorado. By R. G. Young.. 177
†Neutron-irradiated quartz as a tracer of sand movements. By E. D. Goldberg and D. L. Inman..... 611
New Hampshire, Geology of Hanover quadrangle. By J. B. Lyons..... 105
1950 and 1951 eruptions of Mihara Yama, O Shima volcano, Japan. By H. L. Foster and A. C. Mason... 731
North Dakota, Bibliography and index of literature on uranium and thorium and radioactive occurrences in. By Margaret Cooper..... 257

O Shima volcano, 1950 and 1951 eruptions of Mihara Yama, Japan. By H. L. Foster and A. C. Mason..... 731
†Occurrence of *Chirotherium* in South America. By F. E. Peabody..... 239

Oceanography
Continental slope topography in northwest Gulf of Mexico. By B. L. Gealy ... 203
Ohio, Source of Sharon conglomerate of northeastern. By J. O. Fuller ... 159
Oklahoma, Bibliography and index of literature on uranium and thorium and radioactive occurrences in. By Margaret Cooper ... 257
Ordovician
Log of the Senigon well, southern Quebec. By T. H. Clark and Isles Strachan ... 685
—— series, Douglas Lake, Tennessee, Disconformity between Lower and Middle. By Josiah Bridge ... 725
Origin and character of the upland silt near Fairbanks, Alaska. By T. L. Péwé ... 699
Orthoquartzite
Source of Sharon conglomerate of northeastern Ohio. By J. O. Fuller ... 159

Pahoehoe, O Shima volcano, Japan. By H. L. Foster and A. C. Mason ... 731
†Paleoecological significance of the strontium-calcium ratio in fossils and sediments. By K. Turekian ... 155
Paleontology
Log of the Senigon well, southern Quebec. By T. H. Clark and Isles Strachan ... 685
Palynology in southern North America.
Introduction and acknowledgments. By P. B. Sears ... 471
Part II: Study of two cores from lake sediments of the Mexico City Basin. By Fred Foreman ... 475
Part III: Microfossil profiles under Mexico City correlated with the sedimentary profiles. By K. H. Clisby and P. B. Sears ... 511
Part IV: Pleistocene climate in Mexico. By P. B. Sears and K. H. Clisby ... 521
†Peabody F. E.: Occurrence of *Chirotherium* in South America ... 239
Pedlar formation (new name), Blue Ridge region, central Virginia. By R. O. Bloomer and H. J. Werner ... 579
Peridotites of Manpur, Singhbhum district, Bihar, and origin of associated asbestos deposits. By S. C. Chatterjee ... 91
Petrographic provinces. By G. W. Tyrrell ... 405
Petrography
Peridotites of Manpur, Singhbhum district, Bihar, and origin of associated asbestos deposits. By S. C. Chatterjee ... 91
Petroleum
Geology of the Lima region, southwestern Montana and adjacent Idaho. By Robert Scholten, K. A. Keenmon, and W. O. Kupsch ... 345
Petrology
Glendora volcanics, Los Angeles Basin, California. By J. S. Shelton ... 45
1950 and 1951 eruptions of Mihara Yama, O Shima volcano, Japan. By H. L. Foster and A. C. Mason ... 731
Peridotites of Manpur, Singhbhum district, Bihar, and origin of associated asbestos deposits. By S. C. Chatterjee ... 91
Troodhjemite batholith near Bidwell Bar, California. By R. R. Compton ... 9
Péwé, T. L.: Origin and character of the upland silt near Fairbanks, Alaska ... 699
†Pillar Falls mud flow and Shoshone Falls andesite near Twin Falls, Idaho. By H. T. Stearns ... 463
Pleistocene
Continental slope topography in northwest Gulf of Mexico. By B. L. Gealy ... 203
—— climate in Mexico. By P. B. Sears and K. H. Clisby ... 521
—— **geology of the southwestern Wind River Mountains, Wyoming.** By G. W. Holmes and J. H. Moss ... 629
Plutonic rocks
Distribution of igneous rocks in space and time. By G. W. Tyrrell ... 405
Pollen analysis
Palynology in southern North America. By P. B. Sears, K. H. Clisby, and Fred Foreman ... 471
†Preliminary report on the system SiO_2-H_2O. By O. F. Tuttle and J. L. England ... 149
Provenience of pyroclastic materials. By C. S. Ross ... 427
Pyroclastic materials, Provenience of. By C. S. Ross ... 427

Radioactivity
Bibliography and index of literature on uranium and thorium and radioactive occurrences in the U. S. Part 4. By Margaret Cooper ... 257
Regimen and flow of ice in equilibrium glaciers. By L. E. Nielsen ... 1
Rocky Mountains
Pleistocene geology of the southwestern Wind River Mountains, Wyoming. By G. W. Holmes and J. H. Moss ... 629
Ross, C. S.: Provenience of pyroclastic materials ... 427

Salt domes, Fractures above. By Ernst Cloos ... 241
Sampling in biogeochemistry. By H. V. Warren, R. E. Delavault, and J. A. C. Fortescue ... 229
San Andreas rift, California
Experimental analysis of fracture patterns. By Ernst Cloos ... 241
Saskatchewan, Drumlins with jointed boulders near Dollard. By W. O. Kupsch ... 327
Scale models
Experimental analysis of fracture patterns. By Ernst Cloos ... 241
Scholten, Robert, Keenmon K. A., and Kupsch W. O.: Geology of the Lima region, southwestern Montana and adjacent Idaho ... 345
Sears, P. B.: Palynology in southern North America. Introduction and acknowledgments ... 471
—— and Clisby, K. H.: Palynology in southern North America.
Part IV: Pleistocene climate in Mexico ... 521
—— (With K. H. Clisby): Palynology in southern North America.
Part III: Microfossil profiles under Mexico City correlated with the sedimentary profiles ... 511
Sediment flows in Gulf of Mexico. By B. L. Gealy ... 203
Sedimentary facies and intertonguing in the Upper Cretaceous of the Book Cliffs, Utah-Colorado. By R. G. Young ... 177
—— profiles, their correlation with microfossil profiles under Mexico City. By K. H. Clisby and P. B. Sears ... 511
Sedimentation
Continental slope topography in northwest Gulf of Mexico. By B. L. Gealy ... 203
Origin and character of the upland silt near Fairbanks, Alaska. By T. L. Péwé ... 699
Palynology in southern North America. Part II: Study of two cores from the lake sediments of the Mexico City Basin. By Fred Foreman ... 475
Sego member (Price River formation, Cretaceous) (new name), Book Cliffs, Utah-Colorado. By R. G. Young ... 177
Seismology
1950 and 1951 eruptions of Mihara Yama, O Shima volcano, Japan. By H. L. Foster and A. C. Mason ... 731
†Selected bibliography of standard stratigraphic sections of North America. By Fred S. Honkala ... 153
Serpentinization in peridotites of Manpur, Singhbhum district, Bihar. By S. C. Chatterjee ... 91
Shale
Log of the Senigon well, southern Quebec. By T. H. Clark and Isles Strachan ... 685

Sharon conglomerate of northeastern Ohio, Source of. By J. O. Fuller ... 159
SHELTON, J. S.: Glendora volcanic rocks, Los Angeles Basin, California ... 45
†SHURBET, G. L. (With J. L. WORZEL): Toro Seamount ... 465
Sigsbee Scarp of Gulf of Mexico. By B. L. Gealy ... 203
Silt near Fairbanks, Alaska, Origin and character of. By T. L. Péwé ... 699
Snowden member (new name), Blue Ridge region, central Virginia. By R. O. Bloomer and H. J. Werner ... 579
Source of Sharon conglomerate of northeastern Ohio. By J. O. Fuller ... 159
South Dakota, Bibliography and index of literature on uranium and thorium and radioactive occurrences in. By Margaret Cooper ... 257
Spectrographic analysis by use of mutual standard method. By W. H. Dennen and W. C. Fowler ... 655
Spring Canyon member (Blackhawk formation, Cretaceous) (new name), Book Cliffs, Utah-Colorado. By R. G. Young ... 177
†STEARNS, H. T.: Pillar Falls mud flow and Shoshone Falls andesite near Twin Falls, Idaho ... 463
STEARNS, R. G.: Low-angle overthrusting in the central Cumberland Plateau, Tennessee ... 615
Stoping
  Trondhjemite batholith near Bidwell Bar, California. By R. R. Compton ... 9
†STOYANOW, ALEXANDER, AND SUSUKI, TAKEO: Discovery of *Sonoraspis* in Southern California ... 467
STRACHAN ISLES (With T. H. CLARK): Log of the Senigon well, southern Quebec ... 685
Stratigraphy
  Blue Ridge region in central Virginia. By R. O. Bloomer and H. J. Werner ... 579
  Cathedral Mountain quadrangle, Texas. By W. N. McAnulty ... 531
  Catoctin Mountain, Maryland and Virginia. By J. C. Whitaker ... 435
  Disconformity between Lower and Middle Ordovician series at Douglas Lake, Tennessee. By Josiah Bridge ... 725
  Hanover quadrangle, New Hampshire-Vermont. By J. B. Lyons ... 105
  Lima region, southwestern Montana and adjacent Idaho. By Robert Scholten *et al.* ... 345
  Log of the Senigon well, southern Quebec. By T. H. Clark and Isles Strachan ... 685
  Origin and character of the upland silt near Fairbanks, Alaska. By T. L. Péwé ... 699
Structure
  Blue Ridge region, central Virginia. By R. O. Bloomer and H. J. Werner ... 579
  Cathedral Mountain quadrangle. By W. N. McAnulty ... 531
  Catoctin Mountain, Maryland and Virginia. By J. C. Whitaker ... 435
  Continental slope in northwest Gulf of Mexico. By B. L. Gealy ... 203
  Experimental analysis of fracture patterns. By Ernst Cloos ... 241
  Hanover quadrangle, New Hampshire-Vermont. By J. B. Lyons ... 105
  Lima region, southwestern Montana and adjacent Idaho. By Robert Scholten *et al.* ... 345
  Glendora volcanic rocks, Los Angeles Basin, California. By J. S. Shelton ... 45
  Low-angle overthrusting in the central Cumberland Plateau, Tennessee. By R. G. Stearns ... 615
  South-central Washington, illustrated by the Yakima East quadrangle. By A. C. Waters ... 663
Submarine canyons in Gulf of Mexico. By B. L. Gealy ... 203
†—— topography west of Mexico and Central America. By J. G. Heacock, Jr., and J. L. Worzel ... 773
Sunnyside member (Blackhawk formation, Cretaceous) (new name) Book Cliffs, Utah-Colorado. By R. G. Young ... 177
†SUSUKI, TAKEO (With ALEXANDER STOYANOW): Discovery of *Sonoraspis* in Southern California ... 467

Tectonics
  Distribution of igneous rocks in space and time. By G. W. Tyrrell ... 405
  Peridotites of Manpur, Singhbhum district, Bihar. By S. C. Chatterjee ... 91
Tennessee
  Disconformity between Lower and Middle Ordovician series. By Josiah Bridge ... 725
  Low-angle overthrusting in the central Cumberland Plateau. By R. G. Stearns ... 615
Texas
  Bibliography and index of literature on uranium and thorium and radioactive occurrences in. By Margaret Cooper ... 257
  Geology of Cathedral Mountain quadrangle, Brewster County. By W. N. McAnulty ... 531
†Thickness of bedding and parting in sedimentary rocks. By H. H. Gray ... 147
Thorium, Bibliography and index of literature on. Part 4. By Margaret Cooper ... 257
Topography in northwest Gulf of Mexico, Continental-slope. By B. L. Gealy ... 203
†Toro Seamount. By J. L. Worzel and G. L. Shurbet ... 465
Trans-Pecos Texas, Geology of Cathedral Mountain quadrangle. By W. N. McAnulty ... 531
Trondhjemite batholith near Bidwell Bar, California. By R. R. Compton ... 9
Tuffs, Provenience of. By C. S. Ross ... 427
Turbidity currents in Gulf of Mexico. By B. L. Gealy ... 203
†TUREKIAN, K.: Paleoecological significance of the strontium-calcium ratio in fossils and sediments ... 155
†TUTTLE, O. F., AND ENGLAND, J. L.: Preliminary report on the system SiO_2-H_2O ... 149
TYRRELL, G. W.: Distribution of igneous rocks in space and time ... 405

Ultrabasics of Manpur, Singhbhum district, Bihar. By S. C. Chatterjee ... 91
†Unusual desiccation cracks in the Benwood limestone of eastern Ohio. By J. A. Fagerstrom ... 339
Uranium, Bibliography and index of literature on. Part 4. By Margaret Cooper ... 257

"Vein quartz"
  Source of Sharon conglomerate of northeastern Ohio. By J. O. Fuller ... 159
Velocity of glacial flow
  Regimen and flow of ice in equilibrium glaciers. By L. E. Nielsen ... 1
Vermont, Geology of Hanover quadrangle. By J. B. Lyons 105
Virginia
  Geology of the Blue Ridge region. By R. O. Bloomer and H. J. Werner ... 579
  Geology of Catoctin Mountain. By J. C. Whitaker ... 435
Volcanic dust, Dispersal of. By C. S. Ross ... 427
—— rocks
  Distribution of igneous rocks in space and time. By G. W. Tyrrell ... 405
Volcanism
  Glendora volcanic rocks, Los Angeles Basin, California. By J. S. Shelton ... 45
Volcanology
  1950 and 1951 eruptions of Mihara Yama, O Shima volcano, Japan. By H. L. Foster and A. C. Mason. 731

†WARING, C. L. (With R. W. CHAPMAN AND DAVID GOTTFRIED): Age determinations of some rocks from the Boulder batholith and other batholiths of western Montana 607
WARREN, H. V., DELAVAULT, R. E., AND FORTESCUE, J. A. C.: Sampling in biogeochemistry 229
Washington, Geomorphology of south-central. By A. C. Waters 663
WATERS, A. C.: Geomorphology of south-central Washington, illustrated by the Yakima East quadrangle 663
WERNER, H. J. (With R. O. BLOOMER): Geology of the Blue Ridge region in central Virginia 579
†WHITAKER, J. C.: Direction of current flow in some Lower Cambrian clastics in Maryland 763
——: Geology of Catoctin Mountain, Maryland and Virginia 435
Wind River Mountains, Wyoming, Pleistocene geology of. By G. W. Holmes and J. H. Moss 629
†WORZEL, J. L., AND SHURBET, G. L.: Toro Seamount 465
†—— (With J. G. HEACOCK, JR.): Submarine topography west of Mexico and Central America 773
Wyoming, Pleistocene geology of the southwestern Wind River Mountains. By G. W. Holmes and J. H. Moss . 629

Yakima East quadrangle, Washington, Geomorphology of. By A. C. Waters 663
YOUNG, R. G.: Sedimentary facies and intertonguing in the Upper Cretaceous of the Book Cliffs, Utah-Colorado .. 177

V

U